

PREDICTION OF WAVE TRANSMISSION AND DAMAGE LEVEL OF TANDEM BREAKWATER USING SOFT COMPUTING TECHNIQUES

Thesis

**Submitted in partial fulfillment of the requirements for the degree of
DOCTOR OF PHILOSOPHY**

by

GEETHA KUNTOJI

(Reg. No: 123035 AM12F06)



**DEPARTMENT OF APPLIED MECHANICS AND HYDRAULICS
NATIONAL INSTITUTE OF TECHNOLOGY KARNATAKA,
SURATHKAL, MANGALURU – 575 025
DECEMBER 2017**

PREDICTION OF WAVE TRANSMISSION AND DAMAGE LEVEL OF TANDEM BREAKWATER USING SOFT COMPUTING TECHNIQUES

Thesis

**Submitted in partial fulfillment of the requirements for the degree of
DOCTOR OF PHILOSOPHY**

by

GEETHA KUNTOJI

(Reg. No: 123035 AM12F06)



**DEPARTMENT OF APPLIED MECHANICS AND HYDRAULICS
NATIONAL INSTITUTE OF TECHNOLOGY KARNATAKA,
SURATHKAL, MANGALURU – 575 025
AUGUST 2018**

DECLARATION

by the Ph.D. Research scholar

I hereby *declare* that the Research Thesis entitled “**Prediction of Wave Transmission and Damage Level of Tandem Breakwater using Soft Computing Techniques**” which is being submitted to the **National Institute of Technology Karnataka, Surathkal** in partial fulfilment of the requirements for the award of the Degree of **Doctor of Philosophy** in the **Department of Applied Mechanics and Hydraulics** is a *bonafide report of the research work carried out by me*. The material contained in this Research Thesis has not been submitted to any University or Institution for the award of any degree.

123035 AM12F06, GEETHA KUNTOJI

(Register Number, Name & Signature of the Research Scholar)

Department of Applied Mechanics and Hydraulics

National Institute of Technology Karnataka, Surathkal

Place: NITK-Surathkal

Date: 13th August 2018

C E R T I F I C A T E

This is to *certify* that the Research Thesis entitled “**Prediction of Wave Transmission and Damage Level of Tandem Breakwater using Soft Computing Techniques**” submitted by **Geetha Kuntoji** (Register Number: 123035 AM12F06) as the record of the research work carried out by her, is *accepted as the Research Thesis submission* in partial fulfilment of the requirements for the award of degree of **Doctor of Philosophy**.

Prof. Subba Rao
(Research Guide)

Dr. Manu
(Research Guide)

Prof. A Mahesha
(Chairman - DRPC)

**DEPARTMENT OF APPLIED MECHANICS AND HYDRAULICS
NATIONAL INSTITUTE OF TECHNOLOGY KARNATAKA, SURATHKAL,
MANGALURU – 575 025**

ACKNOWLEDGEMENTS

I express my deep sense of gratitude to my research supervisors Prof. Subba Rao and Dr. Manu, Professors Department Applied Mechanics and Hydraulics, NITK for their encouraging, logical and critical suggestions during this work. The interaction and the time spent during discussions are imprinted in my memory permanently. Only with their moral support and guidance, this research work could be completed and I could publish my work in international journals and conferences.

I would like to express my gratitude to the former Director of NITK, Surathkal, Prof. Swapan Bhattacharya, the former Director In-charge Prof. K. N. Lokesh and present Director Prof. Karanam Uma Maheshwar Rao for granting me the permission to use the institutional infrastructure facilities.

I am greatly indebted to Research Progress Assessment Committee members, Prof. Sitaram Nayak and Prof. Paresh. Chandra. Deka, for their critical evaluation and useful suggestions during the progress of the work. Also, I wish to extend my gratitude to Prof. Sukmol Mandal Adjunct Faculty, Applied Mechanics and Hydraulics Department, NITK Surathkal, for his support and encouragement and valuable suggestions.

I sincerely acknowledge the help and support of Prof. M. K. Nagaraj, Prof. Subba Rao and Prof. G. S. Dwarakish former Heads of the Department and Prof. Amai Mahesha, present Head of the Department of Applied Mechanics and Hydraulics, NITK, Surathkal, for permitting me to use the departmental computing and laboratory facilities and their continuous support in completing the work. I would like thank Dr. Pruthviraj U for providing me the lab with high configured system for my research work.

I express my deep sense of gratitude to the Research Scholar Mr. Sreedhara B M. who helped me in every manner and to successfully complete my research work. Mr. Eluru Nava Bharath Reddy, Mr. Jithin. J. S, Mr. Mohit. Babu and Mr. Karthik. S, M.Tech (MS) brothers of our own department also helped me to carry out my research work.

I sincerely acknowledge the help and support rendered by the faculty, staff and research scholars of the Department of Applied Mechanics & Hydraulics. I take this opportunity to thank Mr. B. Jagadish, former Foreman, and Mr. Balakrishna, Literary Assistant, Mr. Anil, Mr. Ananda Devadiga, Mr. Gopal Krishna, Mr. Padmanaba, Mr. Harish, Mr. Niranjana Ms.

Ashwini, Department of Applied Mechanics and Hydraulics, NITK, Surathkal and all the non-teaching staff for their support and help during the research work.

I sincerely acknowledge the help and support of all the Professors, Associate Professors, Assistant Professors and Teaching and non-teaching staff of Department of Applied Mechanics and Hydraulics, NITK, Surathkal, in completing the work.

Finally, I wish to express love and affection to my beloved Father Shri. Siddappa Kuntoji for his sacrifice and never ending support and Late Mother Smt. Somavva Kuntoji and Smt Lalitha. Kuntoji, for their constant love, care and blessings and my dearest beloved sisters Smt. Neelamma, Swetha and brothers Basavaraj Kuntoji, Raghavendra Kuntoji and Shrishail Kuntoji for their continuous love, support and all the sacrifices they had to make.

Geetha S. Kuntoji.

ABSTRACT

Tranquility condition inside the port and harbor has to be maintained for loading and unloading cargo and embarking and de-embarking passengers. To maintain calm condition inside the port and harbor, breakwater has to be constructed to dissipate energy of incoming waves. The alignment of the breakwater must be carefully considered after examining the predominant direction of approach of waves and winds, degree of protection required, magnitude and direction of littoral drift and the possible effect of these breakwaters on the shoreline. In general these studies are invariably conducted in a physical model test where various alternatives are studied and the final selection will be based on performance consistent with cost. Mathematical modeling of these complex interactions is difficult while physical modeling will be laborious and uneconomical. Hence soft computing techniques are employed in the present study.

Soft computing techniques, such as, Artificial Neural Network (ANN), Support Vector Machine (SVM), Adaptive Neuro-Fuzzy Inference System (ANFIS) and Particle Swarm Optimization (PSO) have been efficiently used for modeling coastal engineering problems. For developing soft computing models for predicting wave transmission and damage level of tandem breakwater, experimental data set by Rao et al. (2004) is collected from M. S. Lab of Applied Mechanics and Hydraulics Department, NITK Surathkal, India. They have conducted the study on the tandem breakwater subjected to regular waves in wave mechanics lab. These data sets are divided into two groups, one for training and other for testing. The input parameters, that influence the wave transmission (H_i/H_{tmax}) over a submerged reef and damage level (S) of conventional rubble mound breakwater of tandem breakwater are relative wave steepness (H_i/gT^2), the relative spacing (X/d), stability number ($H/\Delta D_{n50}$), relative crest widths (B/d), (B/L_o), relative crest height (h/d), relative submergence (F/H_i), relative water depth (d/gT^2), which are considered in the present study. The performance of the all models in the prediction of wave transmission and damage level is compared with the measured values using statistical measures, such as, Correlation Coefficient (CC), Root Mean Square Error (RMSE), Nash-Sutcliffe Efficiency (NSE) and Scatter Index (SI).

The ANN model is developed for prediction of wave transmission and damage level of tandem breakwater. Predictions of ANN(8-3-1) for wave transmission and ANN(8-5-1) for

damage level showed good performance compared with other ANN models with different hidden neurons for 100 epochs. It is observed that the CC_{test} of 0.99 and CC_{test} of 0.956 is obtained between predicted and observed wave transmission and damage levels respectively.

Further, to predict wave transmission and damage level of tandem breakwater, SVM model is developed. This technique works on structural risk minimization principle that has greater generalization ability and is superior to the empirical risk minimization principle as adopted in conventional neural network models. Support Vector Machines (SVM) are based on statistical learning theory. The basic idea of support vector machines is to map the original data set into a feature space with three dimensional through a non-linear mapping function and construct an optimal hyper-plane in new space. Four SVM models are constructed using four different kernel functions. In order to know the effectiveness of each kernel function in predicting wave transmission and damage level of tandem breakwater, SVM is trained by applying these kernel functions. Performance of SVM is based on the best setting between of SVM and kernel parameters. SVM model with radial basis kernel function gives CC_{test} of 0.965 for wave transmission and CC_{test} of 0.935 for damage level is considerably better than SVM models with other kernel functions.

Adaptive Neuro-Fuzzy Inference System (ANFIS) uses hybrid learning algorithm, which is more effective than the LMA approach used in ANN. ANFIS models with different membership functions namely Triangular-shaped built-in membership function (TRIMF), Trapezoidal-shaped built-in membership function (TRAPMF), Generalized bell-shaped built-in membership function (GBELLMF), and Gaussian curve built-in membership function (GAUSSMF) are developed to predict wave transmission and damage level of tandem breakwater. ANFIS model with GAUSSMF gave realistic prediction compared with the observed values with CC_{test} of 0.935 for wave transmission and CC_{test} of 0.875 for damage level. It is observed that the ANN models yield higher CC compared to ANFIS models.

However, it is noticed that ANN model in isolation cannot capture all data patterns easily. ANN models are developed with particle swarm optimization (PSO). PSO tuned ANN (PSO-ANN) model is developed to predict wave transmission and damage level of tandem breakwater. The performance of the PSO-ANN(8-3-1) model in the prediction of wave transmission gives CC_{test} of 0.879 and PSO-ANN(8-2-1) model gives CC_{test} of 0.589 for damage level compared with the measured values. PSO-ANN(8-3-1) and PSO-ANN(8-2-

1) models prediction are not matched well with observed values and performed poor compared to the all other hybrid models.

Further, PSO is applied to avoid over-fitting or under-fitting of the SVM model due to the improper selection of SVM and kernel parameters. SVM and kernel parameters are optimized using PSO optimization technique. PSO-SVM model is developed to predict wave transmission and damage level of tandem breakwater. The performance of the PSO-SVM model with polynomial kernel function gives CC_{test} of 0.984 for wave transmission prediction and PSO-SVM model with radial basis kernel function give CC_{test} of 0.941 for damage level compared with the measured values. The results are found to be reliable.

The different soft computing models namely ANN, SVM, ANFIS, PSO-ANN and PSO-SVM and results are compared in terms of CC, RMSE, SI and NSE. ANN performed well and showed good results compared to SVM models in prediction of wave transmission and damage level of tandem breakwater. PSO-SVM model performed better in both cases of wave transmission and damage level prediction compared to other hybrid models with higher CC, NSE and lower RMSE, and SI. PSO-SVM with polynomial kernel and PSO-SVM with radial basis kernel function give higher CC, NSE and lower RMSE, SI compared to all the Individual and hybrid soft computing models. Therefore, PSO-SVM model can be utilized as an alternate soft computing technique to provide accurate and reliable solution in prediction of the wave transmission and damage level of tandem breakwater.

Keywords: Tandem breakwater, Wave transmission, Damage level, Artificial Neural Network (ANN), Support Vector Machine (SVM), Adaptive Neuro-Fuzzy Inference System (ANFIS), Particle Swarm Optimization (PSO).

DESCRIPTION	PAGE NO:
ABSTRACT	i
CONTENTS	v
LIST OF PLATES	ix
LIST OF FIGURES	x
LIST OF TABLES	xiii
NOMENCLATURE	xv
ABBREVIATIONS	xvi
1 INTRODUCTION	
1.1 GENERAL BACKGROUND	1
1.2 ARTIFICIAL INTELLIGENCE	3
1.2.1 Artificial Neural Network (ANN)	3
1.2.2 Adaptive Neuro-Fuzzy Interface System (ANFIS)	4
1.2.3 Support Vector Machine (SVM)	4
1.2.4 Particle Swarm Optimization (PSO)	5
1.3 SCOPE OF THE PRESENT INVESTIGATIONS	5
1.4 ORGANIZATION OF THE THESIS	7
2 LITERATURE REVIEW	
2.1 GENERAL	9
2.2 STUDIES ON REVIEW OF BREAKWATER	10
2.2.1 Rubble Mound Breakwater	11
2.2.1.1 Stability of rubble mound breakwater	12
2.2.1.2 Damage of rubble mound breakwater	13
2.2.1.3 Failure of Breakwater	15
2.2.2 Submerged Reef	16
2.2.2.1 Stability of submerged reef	18
2.2.2.2 Crest width of submerged structure	21
2.2.2.3 Wave transmission over submerged reef	21
2.2.3 Protected Breakwater System	23
2.2.4 Tandem Breakwater System	28
2.3 REVIEW OF APPLICATIONS OF SOFT COMPUTING TECHNIQUES IN COASTAL ENGINEERING	30

2.3.1	Artificial Neural Network	30
2.3.2	Adaptive Neuro-Fuzzy Inference System	35
2.3.3	Support Vector Machines	36
2.3.4	Hybrid Artificial Intelligence Models	38
2.3.5	Summary of Literature	40
2.4	PROBLEM FORMULATION	42
2.5	RESEARCH OBJECTIVES	42
3	EXPERIMENTAL MODEL SETUP AND DATA USED	
3.1	GENERAL	44
3.2	EXPERIMENTAL SET-UP	46
3.2.1	Details of wave flume	46
3.2.1.1	Experimental Procedure	48
3.2.2	Data Collection and Interpretation	48
3.2.3	Normalization of data and consistency check	53
3.3	SUMMARY	55
4	RESEARCH METHODOLOGY AND MODEL DEVELOPMENT	
4.1	GENERAL	56
4.2	ARTIFICILA NEURAL NETWORK (ANN)	56
4.2.1	Feed-forward backpropagation network (FFBP)	56
4.2.2	Training a neural network	58
4.2.3	Levenberg-Marquardt (LM) method	59
4.2.4	Feed forward backpropagation neural network for wave transmission and damage level prediction of tandem breakwater	60
4.3	ADAPTIVE NEURO-FUZZY INFERENCE SYSTEM (ANFIS)	61
4.3.1	Architecture of ANFIS	61
4.4	SUPPORT VECTOR MACHINE REGRESSION (SVMR)	64
4.4.1	Theoretical background of SVMR	64
4.4.2	Support Vector Machine (SVM) Model Development	65
4.5	PARTICLE SWARM OPTIMIZATION (PSO)	70
4.5.1	PSO Algorithm and Rules	71
4.5.2	Proposed hybrid PSO-ANN and PSO-SVM models	72
4.5.3	Training PSO-ANN and PSO-SVM	72
4.5.3.1	The steps followed in PSO-ANN model development	73

4.5.3.2	The steps followed in PSO-SVM model development	75
4.6	MODEL PERFORMANCE CRITERIA	76
4.6.1	Root mean square error (RMSE)	77
4.6.2	Nash-Sutcliffe Efficiency (NSE)	77
4.6.3	Correlation Coefficient (CC)	78
4.6.4	Scatter Index (SI)	78
5	PERFORMANCE OF ANN AND SVM MODELS	
5.1	GENERAL	79
5.1.1	Performance of Artificial Neural Network (ANN) model for predicting transmitted wave height (H_t/H_{tmax})	80
5.1.2	Performance of ANN model in the prediction of damage level (S)	84
5.1.3	Summary of ANN Model results	88
5.2	PERFORMANCE OF SUPPORT VECTOR MACHINE (SVM) MODEL	88
5.2.1	The performance of the SVM model for predicting the wave transmission (H_t/H_{tmax})	88
5.2.2	The performance of the SVM model in predicting the damage level (S)	93
5.2.3	Summary of SVM model results	96
6	PERFORMANCE OF ANFIS, PSO-ANN AND PSO-SVM MODELS	
6.1	GENERAL	98
6.2	PERFORMANCE OF ADAPTIVE-NEURO FUZZY INFERENCE SYSTEM (ANFIS) MODEL	98
6.2.1	Simulation results of ANFIS Model for predicting wave transmission (H_t/H_{tmax})	99
6.2.2	Simulation results of ANFIS Model in predicting the damage level (S)	102
6.2.3	Summary of ANFIS model results	105
6.3	PERFORMANCE OF PSO-ANN MODEL FOR PREDICTING WAVE TRANSMISSION (H_t/H_{tmax}) AND DAMAGE LEVEL (S)	105
6.3.1	Summary of PSO-ANN model results	112
6.4	PERFORMANCE OF PSO-SVM MODEL FOR PREDICTION OF WAVE TRANSMISSION AND DAMAGE LEVEL OF TANDEM	112

BREAKWATER		
6.4.1	Simulation results of PSO-SVM model for predicting wave transmission (H_t/H_{tmax}) over submerged reef and damage level (S) of emerged breakwater of tandem breakwater	113
6.4.2	Simulation results of PSO-SVM model for predicting damage level (S) of Conventional rubble mound breakwater of tandem breakwater	118
6.4.3	Summary of PSO-SVM model results	123
6.5	COMPARISON OF PERFORMANCE OF BEST ANN, SVM, ANFIS, PSO-ANN AND PSO-SVM MODELS	123
6.5.1	Summary of best model results	129
7	SUMMARY AND CONCLUSIONS	
7.1	SUMMARY	130
7.2	CONCLUSIONS	131
7.3	RECOMMENDATIONS	133
7.4	LIMITATIONS OF PRESENT STUDY	133
7.5	SUGGESTIONS FOR FUTURE WORK	133
REFERENCES		
PUBLICATIONS		
RESUME		

LIST OF PLATES

Plate No:	Plate caption	Page No:
3.1	View of the experimental setup	47
3.2	View of wave flume with wave probes	48
3.3	View of wave flume with profiler	48
3.4	View of Conventional Rubble Mound Breakwater	50
3.5	View of Submerged Reef	52
3.6	View of protected breakwater	53
3.7	Top view of protected breakwater	53

LIST OF FIGURES

Fig. No:	Figure caption	Page No:
1.1	Tandem Breakwater	2
2.1	Evolution of Tandem Breakwater	9
2.2	Wave transmission coefficient (Van der Meer et al., 2005)	22
2.3	Submerged defenced reef	26
3.1(a)	Cross section of Tandem breakwater	46
3.1(b)	Schematic diagram of Regular wave flume setup with tandem breakwater	46
3.2(a)	Consistency of H_i/gT^2 , X/d , $H/\Delta D_{n50}$, B/d , B/L_o , h/d , F/H_i , d/gT^2 , and H_t/H_{tmax}	54
3.2(b)	Consistency of H_i/gT^2 , X/d , $H/\Delta D_{n50}$, B/d , B/L_o , h/d , F/H_i , d/gT^2 and S	55
4.1	Feed forward backpropagation network used in study	57
4.2	ANFIS structure used in the study	62
4.3	SVM architecture used in the study	65
4.4	The loss margin setting corresponds to one-dimensional linear SVM to D-dimensional nonlinear SVM	66
4.5	Separation, alignment and cohesion stage of PSO process respectively, (Craig Reynolds, 1986)	71
4.6	Flowchart of PSO-ANN used in the study	75
4.7	Flowchart of PSO-SVM used in the study	76
5.1	Scatter plots for ANN1 to ANN5 model for H_t/H_{tmax}	82
5.2	Box-Whisker plot for ANN1-ANN5 and observed model for H_t/H_{tmax}	83
5.3	Comparison of H_t/H_{tmax} predicted by ANN3 with observed values	83
5.4	Shows scatter plots of ANN1 to ANN5 models for S	86
5.5	Box-Whisker plot for ANN1-ANN5 and observed model for S	87
5.6	Comparison of damage level predicted by ANN5 model with	87

	observed values	
5.7	Scatter plots of predicted and observed H_t/H_{tmax} by SVM for different kernel functions	92
5.8	Box-Whisker plot of predicted and observed wave transmission by SVM	92
5.9	Comparison of wave transmission predicted by SVM with observed values	92
5.10	Scatter plots of S for SVM model for damage level with different kernel function	95
5.11	Box-Whisker plots of SVM model for damage level with different kernel function	95
5.12	Comparison of damage level predicted by SVM (RBF) with observed values	95
6.1	Scatter plots of predicted and observed H_t/H_{tmax} by ANFIS for different membership	101
6.2	Box-Whiskers plot of H_t/H_{tmax} for ANFIS model with different membership	101
6.3	Comparison of H_t/H_{tmax} predicted by ANFIS model with observed values	101
6.4	Scatter plots of predicted and observed S for ANFIS model with different membership functions	104
6.5	Box-Whiskers plot of S for ANFIS model with different membership functions	104
6.6	Comparison of damage level prediction by SVM (RBF) with observed values	105
6.7	Scatter plots of H_t/H_{tmax} by PSO-ANN model	108
6.8	Box-Whisker plot of wave transmission prediction by PSO-ANN with observed values	109
6.9	Comparison of wave transmission predicted by PSO-ANN3 with observed values	109
6.10	Scatter plots for S for PSO-ANN hybrid models	111
6.11	Box-Whisker plot of damage level prediction for different PSO-ANN models	111
6.12	Comparison of damage level predicted by PSO-ANN2 with observed values	112
6.13	Data fitting of models developed (linear kernel) for prediction of	114

	H_t/H_{tmax}	
6.14	Data fitting of models developed (polynomial kernel) for prediction of H_t/H_{tmax}	114
6.15	Data fitting of models developed (RBF kernel) for prediction of H_t/H_{tmax}	114
6.16	Scatter plots of PSO-SVM model for H_t/H_{tmax} with observed data	116
6.17	Box-Whiskers plot of H_t/H_{tmax} for PSO-SVM model	117
6.18	Comparison of PSO-SVM model (polynomial kernel) for predicting H_t/H_{tmax} with observed values	118
6.19	Data fitting of models developed (linear) for prediction of Damage level	119
6.20	Data fitting of models developed (polynomial) for prediction of damage level	119
6.21	Data fitting of models developed (RBF) for prediction of damage level	119
6.22	Scatter plots of damage level (S) prediction using SVM model with different kernel functions	121
6.23	Box-Whisker plots of damage level (S) for PSO-SVM model	122
6.24	Comparison of damage level predicted by PSO-SVM model (RBF) with observed values	123
6.25	Box-Whisker plot for wave transmission comparison of individual models	125
6.26	Comparison of ANN (8-3-1) and SVM (RBF) models for wave transmission	125
6.27	Box-Whisker plot for wave transmission comparison of hybrid models	126
6.28	Comparison of ANFIS (Gaussmf), PSO-ANN (8-3-1) and PSO-SVM (Polynomial) models for wave transmission	126
6.29	Box-Whisker plot for damage level comparison of individual models	127
6.30	Comparison of ANN (8-5-1) and SVM (RBF) models for damage level	128
6.31	Box-Whisker plot for damage levels comparison of hybrid models	128
6.32	Comparison of ANFIS (Gaussmf), PSO-ANN (8-2-1) and PSO-SVM (RBF) models for damage level	128

LIST OF TABLES

Table No:	Table caption	Page no:
2.1	Limits of damage level (S)	14
3.1	Model characteristics Conventional breakwater	49
3.2	Wave characteristics	50
3.3	Non-dimensional input parameters and their range used in the experiment	51
4.1	Data used for training and testing the SVMR models with input parameters	69
4.2	Different Kernel Functions	69
4.3	The range of parameters in the data set used for the training and testing phases of artificial intelligence models	73
5.1	Statistical parameter for ANN models for predicting H_t/H_{tmax}	80
5.2	Statistical results for ANN models for predicting damage level (S)	84
5.3	Optimal parameters for SVM models for predicting H_t/H_{tmax}	89
5.4	Statistical measure of SVM model simulation for different kernel functions	89
5.5	Optimal parameters for SVM models for predicting S	93
5.6	Statistical measures of SVM models for S prediction with different kernel functions	93
5.7	Comparison of ANN and SVM statistical measures	97
6.1	Statistical measure of ANFIS models for predicting wave transmission	99
6.2	Statistical measure of ANFIS models for prediction of damage level	103
6.3	Statistical parameters of PSO-ANN model predictions for H_t/H_{tmax}	106
6.4	Statistical parameters of PSO-ANN model predictions for damage level (S)	106
6.5	Optimal parameters for PSO-SVM models for predicting H_t/H_{tmax}	115
6.6	Statistical parameters for PSO-SVM models for predicting H_t/H_{tmax}	115
6.7	Optimal parameters for PSO-SVM models for predicting Damage level (S)	120

6.8	Statistical parameters for PSO-SVM models for predicting Damage level(S)	120
6.9	Comparing Statistical Measures of ANN, SVM, ANFIS, PSO-ANN and PSO-SVM Models for wave transmission (H_t/H_{tmax})	124
6.10	Comparing Statistical Measures of ANN, SVM, ANFIS, PSO-ANN and PSO-SVM Models for damage level (S)	127

NOMENCLATURE

K_{Δ}	: Armour unit weight
B	: Reef crest width
B/d	: Relative reef crest width
B/L_o	: Relative reef crest width
d	: Depth of water above sea bed
d/gT^2	: Depth parameter
D_{n50}	: Mean size diameter of armour unit
F	: Free board
F/H_i	: Relative reef submergence
h	: Reef height
h/d	: Relative reef crest height
H_i	: Incident wave height
H_s	: Significant wave height
H_t	: Transmitted wave height
H_{tmax}	: Maximum transmitted wave height
H_t/H_i	: Transmission coefficient (K_t)
H_o/gT^2	: Deepwater wave steepness
H_i/gT^2	: Incident wave steepness
$H_i/\Delta D_{n50}$: Hudson's stability number
K_t	: Transmission Coefficient
K_r	: Reflection Coefficient
L_o	: Deepwater wave length
S	: Damage level
T	: Wave Period
W_{50}	: Armour unit weight of reef
X	: Spacing between main breakwater and reef
X/d	: Relative reef spacing

ABBREVIATIONS

AI	: Artificial Intelligence
ANFIS	: Adaptive Neuro-Fuzzy Inference System
ANN	: Artificial Neural Network
BP	: Back-Propagation
CC	: Correlation Coefficient
ERM	: Empirical Risk Minimization
FFBP	: Feed-Forward Backpropagation Network
GASVMR	: Genetic Algorithm- Support Vector Machine Regression
GP	: Genetic Programming
GWL	: Ground Water Level
HIMMFPB	: Horizontally Interlaced Multilayer Moored Floating Pipe Breakwater
HWL	: High Water level
KPCA	: Kernel Principal Component Analysis
LW	: Low Water level
MLP	: Multi-Layer Perceptron
NN	: Neural Network
PSO	: Particle Swarm Optimization
RBF	: Radial Bias Function
RMSE	: Root Mean Square Error
S	: Damage level
SI	: Scatter Index
SVM	: Support Vector Machine
SVR	: Support Vector Regression
SWL	: Still Water Level
TBW	: Tandem Breakwater

CHAPTER 1

INTRODUCTION

1.1 GENERAL BACKGROUND

In Coastal Engineering, breakwaters are necessary for the protection of ports and harbours and economic growth of the country. Breakwaters are the hard solutions (Mani and Jayakumar, 1995; Kakinuma, 2003), which are widely constructed for the purpose of protecting vital installations on the coast and offshore. Breakwaters are barriers, either natural or artificial, that extend into the open water of a sea or a lake to break the force of the waves and provide calm water zone in a harbor. Natural breakwaters are offshore islands and promontories that shelter the shore from waves. Artificial breakwaters may be attached to the land or separated from it and are constructed in various shapes and sizes. They can be built of stones and rubble, of masonry, or of a combination of these. Since, sea waves have enormous amount of energy; the construction of structures to mitigate such energy is not easily accomplished. As these structures need a considerable amount of initial investment; they should be properly aligned, designed and constructed. Economic design of coastal structures, such as breakwaters, is of great importance in coastal and ocean engineering.

Various types of breakwaters are in use throughout the world. Research activities are in progress to study the performance characteristics of different types of breakwaters in order to recommend the most feasible one for a given prevailing environment.

Breakwaters are classified mainly as:

- Rubble mound or heap breakwaters
- Upright or vertical wall breakwaters
- Mound with superstructure or composite breakwaters
- Special type of breakwaters

Breakwaters are commonly used in protecting and maintaining tranquillity inside ports and harbours from wave action, in arresting the siltation near the river mouth and in protecting coastal areas and beaches. The main purpose of the breakwater is to dissipate wave energy approaching the coast. The effect of the waves on the

conventional rubble mound breakwater is decreased by placing a submerged reef on the seaside of the breakwater.

The continuous action of wave on the rubble mound breakwater will slowly affect its stability, which in turn degrades and transforms into an S-shaped profile with an extension at toe. The extended toe is then gets separated from the breakwater known as a submerged reef and is further placed on the sea side of the conventional breakwater. The resulting structure is a tandem breakwater (refer Fig.1.1).

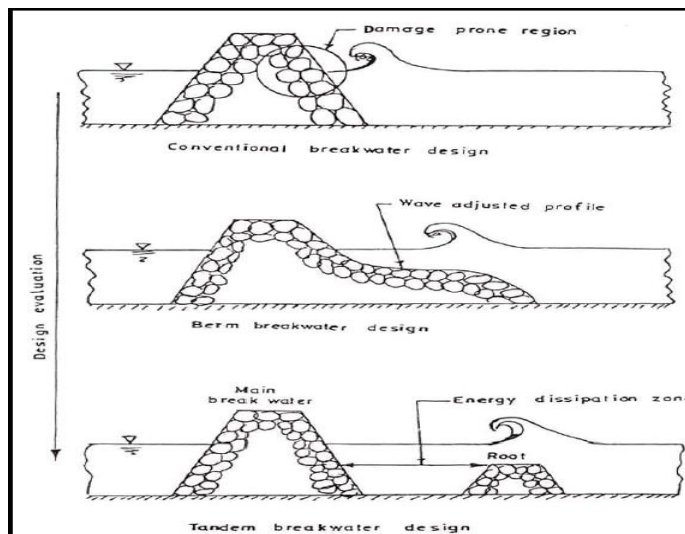


Fig. 1.1 The evolution of tandem breakwater

The detached submerged reef acts as a wave attenuator and reduces the wave impact on the conventional breakwater, minimizing the size of armour stones required for given conditions. It also helps in achieving the stability of structure, which eventually makes tandem breakwater as an economic and stable innovative type breakwater (Cox and Clark, 1992; Gadre et al., 1985; Shirlal and Rao, 2003). In India, the tandem breakwater concept was adopted for the rehabilitation of the damaged breakwater at Andaman and Nicobar Islands. The tandem breakwater may not always provide the least cost alternative, as section costs are strongly related to material costs and water depths. However, the tandem breakwater has offered significantly reduced design risk since high return period events such as large storm waves are reduced to a more manageable level, reducing the chance of catastrophic failure of the main breakwater in storm events outside the design envelope. Accurate prediction of wave transmission and damage level plays a key role in proper functioning of the tandem breakwater. The wave transmission and damage level of tandem breakwater can be directly

measured by conducting experiments in the laboratories whenever required. The experiments were conducted by Rao and Shirlal in 2004. In the present study the data is collected from the authors and an effort is made to employ the soft computing tools to predict the wave transmission over a submerged reef and damage of conventional rubble mound breakwater of tandem breakwater. As there is no simple mathematical model to predict the wave transmission and damage level of tandem breakwater. By putting light on the previous studies soft computing tools are applied as best alternate techniques successfully for predicting various parameters of different breakwaters. As it is very difficult to conduct the experiments all the times as the breakwaters are massive in size as well as expensive. If the experimental data is available, then using the data soft computing techniques are developed. Based on the fact that the physical modelling is laborious and expensive the present study is chosen. The various soft computing techniques are employed to predict the wave transmission and damage level of tandem breakwater. The techniques adopted in present study are described briefly in the following sections.

1.2 ARTIFICIAL INTELLIGENCE

In recent years, application of artificial intelligence (AI) techniques in modeling coastal processes like structure stability, damage level and wave transmission has received much attention from the researchers. AI algorithms provide explanation of an externally driven process without a need of complex physical models under similar site conditions. Literature reports use of AI methodologies like artificial neural network (ANN), adaptive neuro-fuzzy interface system (ANFIS) and support vector machine (SVM) and Particle Swarm Optimization (PSO) for predicting the transmitted wave height over submerged reef and damage level of emerged main conventional rubble mound breakwater.

1.2.1 Artificial Neural Network (ANN)

ANN is an information system, stimulating the ability of human brain to sort out patterns and learn from trial and error. ANN has an ability to extract relationships that exists within the data with which it is presented. This approach is faster, robust in noisy environments, flexible in the range of problems it can solve and highly adaptive

to the newer environments. Due to these established advantages, currently the ANN has numerous real world applications such as wave forecasting, hydrological processes like evapotranspiration, static stability processes of conventional coastal protective structures, image processing, speech processing, robotics, and stock market predictions. There has been research on its implementation in the system engineering related fields such as time series prediction, rule based control, etc. In recent years, ANN methods have been successfully applied to many studies in the field of coastal and ocean engineering.

1.2.2 Adaptive Neuro-Fuzzy Interface System (ANFIS)

Jang in 1993 proposed a method that used neural network learning algorithm for constructing a set of fuzzy if-then rules with appropriate membership functions from the stipulated input output pairs. An ANFIS model combines the transparent and linguistic representation of a fuzzy system with learning ability of ANN. This incorporates the generic advantages of artificial neural networks like massive parallelism, robustness, and learning in data-rich environments into the system. The modeling of imprecise and qualitative knowledge as well as the transmission of uncertainty is possible through the use of fuzzy logic. ANFIS comes with an additional benefit of being able to provide a set of rules on which the model is based.

1.2.3 Support Vector Machine (SVM)

Vapnik (1995) developed the foundation of support vector machines (SVM). SVM gained popularity due to many promising features like better empirical performance and providing globally optimal solutions. The formulation embodies structural risk minimization (SRM) principle, which has shown better performances than the empirical risk minimization principle (ERM), employed by conventional neural networks. SRM minimizes an upper bound on the expected risk, as opposed to ERM that minimizes the error on the training data. It is this difference, which equips SVM with a greater ability to generalize, thus, achieving the goal of statistical learning, which involves inequality constraints.

1.2.4 Particle Swarm Optimization (PSO)

Performance of any AI model largely depends on the user's understanding of the model, along with the quantity and quality of inputs presented to it. Tandem breakwater, like many other conventional coastal protective structures operate under a large range of independent input parameters with varying scale effects influencing its stable performance and as well structure stability, leading to a non-linear and non-stationary behavior of the dataset. AI models alone may not be able to cope with these characteristics of the dataset if, input and/or output data is not preprocessed. Furthermore, there is also a need for working towards enhancing the performance of these models. Use of hybrid models may help in increasing the accuracy of ANN and SVM models.

Particle Swarm Intelligence (Kennedy & Eberhart, 1995) first developed in the end of 1990s is being widely applied in many engineering fields, such as wave forecasting, damage level, wave transmission, signal process, image compression, pattern recognition, hydrology, earthquake investigation, etc. Since the last decade, PSO has become a popular technique for analyzing variations, wave parameters affecting the stability of coastal protective structures.

1.3 SCOPE OF THE PRESENT INVESTIGATIONS

In earlier decades, many researchers carried out experimental, theoretical and numerical investigations on breakwaters (Priest et al., 1964; Baird and Hall, 1984; Ergin et al., 1989; Van der Meer, 1996). Physical model studies on breakwaters involve several common assumptions applied in hydrodynamics which may not be accurate.

For decades, the breakwaters have been designed by conducting experiments on its stability through physical model studies, which are laborious and expensive (Hall and Kao, 1991; Van der Meer, 1992). Several researchers have carried out experimental, analytical and numerical studies on breakwaters in the past, but failed to give a simple mathematical model to predict the wave transmission over a submerged reef by considering all the boundary conditions. To understand the stability of tandem breakwater, a proper study of wave transmission over a submerged reef is essential.

Artificial neural networks and Support Vector Machines are effective and successful in solving various coastal engineering problems. ANN is trained using a set of data and once the model learns from the training data, predictions are done better (Mase, et al., 1995; Yagci et al., 2005; Kim et al., 2005) and also rating curve was established in hydrology (Sudheer and Jain, 2003). Support Vector Machines (SVM) has been used for the prediction of stability number of armour blocks of breakwaters (Balas, 2010) and also used to predict significant wave heights (Kim et al., 2011) and reservoir sedimentation and nearshore wave power (Garg and Jyotiprakash, 2013). Some of the hybrid techniques were used for the fundamental design of conventional rubble mound breakwaters and the results are found to be better compared to traditional designs (Van der Meer, 1985). The hybrid Genetic Algorithm based Support Vector Machine (GA-SVM) models are implemented for predicting wave transmission coefficient of horizontally interlaced multilayer moored floating pipe breakwater (Patil et al., 2012).

The soft computing models have also been used successfully for predicting damage levels, damage ratios and different coastal engineering problems (Hagan, 1994); Kennedy and Eberhart, 1995; Rao and Mandal, 2005; Mehmet, 2011; Zanaganah et al., 2009; Castro et al., 2011; Harish et al., 2012; Jian-Chuan et al., 2015).

Further, Harish et al. (2015) applied hybrid PSO-SVM to predict the damage level of the non-reshaped berm breakwater and it is found that the PSO-SVM method gave higher accuracy compared to other soft computing models. The PSO-ANN is applied for the Management of Groundwater Resources (Nagesh et al. 2013). Hadi et al. (2016) developed PSO-LM based ANN to predict transmitted wave height π -type floating breakwater and results states that the efficiency of this model was improved when compared with the empirical formulas. But, it is observed from literature that there are hardly any applications of ANN, SVM, ANFIS, PSO-ANN and PSO-SVM models to study the stability of tandem breakwaters. Hence, it is decided to investigate of the applicability of ANN, SVM, ANFIS, PSO-ANN and PSO-SVM modeling approach for predicting the transmitted wave height (H_t/H_{tmax}) over a submerged reef and damage level (S) of conventional rubble mound breakwater of tandem breakwater. For this purpose the experimental data set obtained by Rao and

Shirlal in 2004 on tandem breakwater using two dimensional wave flume of the Marine Structure laboratory, NITK Surathkal. The performance of the ANN, SVM, ANFIS, PSO-ANN and PSO-SVM are compared and the best model is selected based on statistical parameters.

1.4 ORGANIZATION OF THE THESIS

The thesis is presented in seven chapters.

- Chapter 1- Introduction: Introduction to breakwaters, classification of breakwaters. Further, it includes an introduction to breakwater failure and alternative solution, wave transmission and its damage level and scope of the present investigations has been discussed.
- Chapter 2- Literature review: The literature review on theoretical and analytical studies specifically related to submerged reef, conventional rubble mound breakwaters and tandem breakwaters, applications of soft computing techniques in coastal/ocean engineering, problem formulation and objectives of the present work have been discussed.
- Chapter 3- Experimental model setup and data used: Briefly explained features of the experimental model setup, experimental investigations carried out in the wave flume and the data used for developing soft computing models.
- Chapter 4- Research Methodology and Model Development: Discussed in detail theoretical background of research methods used in developed soft computing models to predict the wave transmission over submerged reef and damage level of conventional rubble mound breakwaters of a tandem breakwater, such as, ANN, SVM, ANFIS, PSO-ANN and PSO-SVM has been discussed.
- Chapter 5- Results of ANN and SVM models: The results obtained from the soft computing models, such as, ANN, SVM in prediction of wave transmission over submerged reef and damage level of conventional rubble mound breakwaters of a tandem breakwater are analyzed, discussed and interpreted. Also, the performance of these models is compared with each other.
- Chapter 6- Results of ANFIS, PSO-ANN and PSO-SVM: The results obtained from the hybrid soft computing models, such as, ANFIS, PSO-ANN and PSO-SVM in prediction of wave transmission over submerged reef and damage level of

conventional rubble mound breakwaters of a tandem breakwater are analyzed, discussed and interpreted. Also, the performance of these models is compared with each other.

- Chapter 7- Summary and Conclusions: Summary and Conclusions drawn based on the results of soft computing models and suggestions for future work have been presented.

The Appendix I consists of list of references, list of publications based on the present work, and a brief resume of the researcher.

LITERATURE REVIEW

2.1 GENERAL

The concept of the rubble mound breakwater and submerged reef breakwater, operating together as a single unit, is called the tandem breakwater. The reef serves to reflect and dissipate wave energy and induces wave breaking, hence, reducing impact of waves on main breakwater, which can then be designed with lighter armour units and may prove as economical. Fig. 2.1 shows the design evolution of the tandem breakwater system. According to Cox and Clark (1992), an efficient design of the tandem system relies on precise quantitative information regarding the hydraulic performance of the submerged reef breakwater and the wave transmission. Their results demonstrate the possible success of the concept. According to them, the reef breakwater has been successful in the substantial reduction of the wave loading on the main structure without damaging itself.

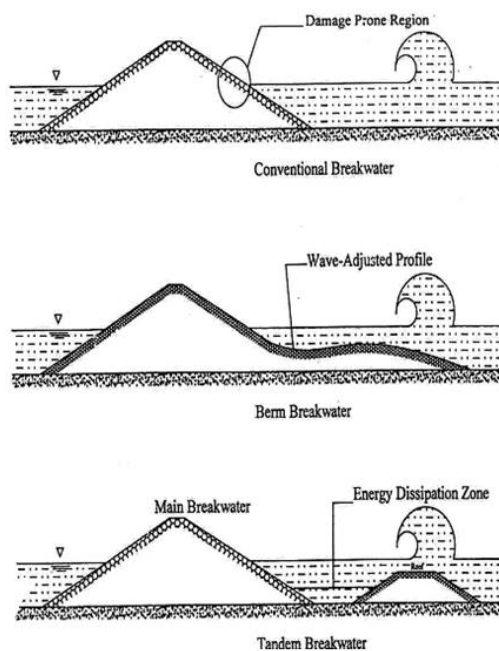


Fig. 2.1 The evolution of tandem breakwater

The tandem breakwater may not always provide the least cost alternative, as section costs are strongly related to material costs and water depths. However, the tandem breakwater has offered significantly reduced design risk since high return period events such as large storm waves are reduced to a more manageable level, reducing the chance of catastrophic

failure of the main breakwater in storm events outside the design envelope. The proper formulation of the problem is necessary before carrying out any research work. For this purpose, an extensive literature review is carried out on submerged reef and rubble mound breakwater of tandem breakwater. Literatures on theoretical determination of the transmission coefficient over an outer submerged reef and damage level of inner conventional rubble mound breakwater have been discussed.

In order to understand the behavior of tandem breakwater due to wave action a detailed study on submerged reef and rubble mound breakwater is necessary. It is important to get safe and optimal structure. However, it is noticed that theoretical determination of the transmission coefficient over an outer submerged reef and damage level of inner conventional rubble mound breakwater with all its coastal boundary and depth variation is extremely difficult. This is because of complexity and non-linearity associated with the wave structure interaction.

Considering the complexity and significance of accuracy in estimating wave transmission and damage level of tandem breakwater, coastal engineers over the period of time have mainly focused on developing more reliable and accurate methods for estimating wave transmission and damage level of tandem breakwater. In the following sections, various techniques employed by researchers in estimating the transmission coefficient over an outer submerged reef and damage level of inner conventional rubble mound breakwater have been discussed. Literatures on applications of mathematical and physical modeling are presented in the first section. In the subsequent sections recent reviews of soft computing technique applications in modeling wave transmission over submerged reef and damage level of the conventional rubble mound breakwater of tandem breakwater are presented.

2.2 STUDIES ON REVIEW OF BREAKWATER

Breakwaters are generally constructed to protect the port and harbour facilities from the dynamic forces due to the ocean waves. Breakwaters have been built throughout the centuries, but their design procedure is still under investigation in the search of optimum structure. In this section the detailed literature study has been carried out with the interest of new findings and innovations about the recent developments in structures such as rubble mound breakwaters, submerged reefs and protected breakwater system. The

performance of rubble mound breakwaters, reef structures and protected structures are clearly enumerated.

Many researchers have carried out experimental and numerical studies on breakwaters in the past and some of them are discussed below:

2.2.1 Rubble Mound Breakwater

Hudson (1959) conducted laboratory investigations to determine the criteria for the design and construction of rubble mound breakwaters. A general stability equation was derived which was used to guide the experimental and test data. A new breakwater stability formula was obtained after unknown function in the stability equation was determined for the selected breakwaters and test wave conditions by using the test data results. Also wave run-up studies were carried out. According to Hudson, the weight of the individual armor unit is given by

$$W = \frac{\gamma_r H^3}{K_D \Delta^3 \cot \alpha} \quad (2.1)$$

Where, γ_r is the specific weight of armor units; H is the design wave height; Δ is the relative mass density of armor and K_D is the stability coefficient. In deriving the stability formula Hudson neglected the friction between the armor units. It was also assumed that the dynamic effect of the waves was to lift and roll the armor units from their initial positions on the breakwater slope.

A mathematical model was developed by Kobayashi and Jacobs (1985) to predict the flow characteristics in the down rush of regular waves and movement of armor units on the slope of a coastal structure. Stability analysis of armor units was performed, including the drag, lift and inertial forces acting on an armor unit which vary along the slope. Then the comparison was made with the large scale test data based on their earlier study. Their model did not consider the effects of permeability, bottom friction and water depth, but, the model was able to predict the observed zero-damage stability number satisfactorily.

A mixed numerical model was developed by Hannoura and McCorquodale (1985) to simulate wave motion over rubble-mound structures. Their model was applied to check the dynamic stability of the seaward slope under severe wave attack of the port sines rubble mound breakwater. The predicted internal water surface values were compared with a physical model measurement which was found to be reasonable. But, the model showed a lower factor of safety than the traditional analysis. It has provided additional

terms to take into account the effect of added mass which improved the detection of internal wave breaking and the entrainment of air near the interface.

Van der Meer (1988) established new stability formulae for rubble mound breakwaters under random wave attack with comprehensive model investigations at Delft Hydraulics, Netherlands. The experiments were conducted to include a variety of structures with differing core and under layer permeability for a wide range of wave conditions. Considering the type of wave breaking two formulae were derived, one for plunging waves and other for surging waves. These equations are now popularly known as the Van der Meer formulae. All the test results showed a clear difference between plunging and surging waves. The minimum stability of a structure was during the transition of waves from surging to plunging waves. Using the curve-fitting technique, Van der Meer (1988, 1988a) specified two stability formulae, as follows.

For plunging waves:

$$\frac{H_s}{\Delta D_{n50}} = 6.2P^{0.18} \left(\frac{S}{\sqrt{N}} \right)^{0.2} \xi_m^{-0.5} \quad (2.2)$$

For surging waves:

$$\frac{H_s}{\Delta D_{n50}} = 1.0P^{-0.13} \left(\frac{S}{\sqrt{N}} \right)^{0.2} (\cot \alpha)^{0.5} \xi_m^P \quad (2.3)$$

where, Δ is the relative mass density of armor, S is the damage level, H_s is the significant wave height at the toe of the structure in meters, α is the angle of the breakwater slope with horizontal, P is the permeability coefficient, N is the number of waves, ξ_m is the surf similarity parameter using average wave period T_m , D_{n50} is the nominal diameter of the armor unit in meters.

Another equation to calculate the critical ξ_m during the transition from plunging to surging waves was given as,

$$\xi_m = \left(6.2P^{0.31} \sqrt{\tan \alpha} \right)^{1/(P+0.5)} \quad (2.4)$$

Depending on slope angle and permeability the transition lays between $\xi_m = 2.5$ to 4. For $\cot \alpha$ greater than or equal to 4.0 the transition from plunging to surging does not exist and for these slope angle Equations (2.3) must be used.

2.2.1.1 Stability of rubble mound breakwater

The commonly used criterion for breakwater stability was given by the following expression.

$$N_s = \frac{H}{\Delta \times D_{n50}} \quad (2.5)$$

Where,

N_s = Hudson's stability number,

H = wave height parameter,

$\Delta = (\rho_r - \rho_w)/\rho_w$ = relative submerged weight, ρ_r and ρ_w are the mass densities of the armour units and water respectively,

D_{n50} = nominal diameter of the stone.

For, Static stability $N_s = 1 - 4$

Dynamic stability $N_s = 6 - 20$

The wave height parameter that commonly used in this formula was the significant wave height, $H_{1/3}$ or H_{mo} (H_{mo} is the estimate of significant wave height deduced from spectral information). The value of N_s is usually established by testing the breakwater until its damage reaches equilibrium. To attain this equilibrium, the time series of the sea state may have to be recycled many times. The number of times it is recycled is an important parameter to be taken into an account.

Factors affecting the stability of non-overtopping breakwater: A number of researchers have concluded from their studies that the armour stability is a function of water depth, wave period, wave characteristics and unit weight of armour, structure slope, porosity and storm duration. Each of them investigated the structure stability with respect to different parameters (Hudson, 1959; Ahrens, 1970; Brunn and Gunbak, 1976; Johnson et al., 1978; Ahrens, 1984; Timco et al., 1984; Van der Meer and Pilarczyk, 1984; Gadre et al., 1985; Van der Meer, 1988 and Hegde and Samaga, 1996). After reviewing the literature on the breakwaters, it is observed that a large number of parameters affect the stability and hence the design of breakwaters. The various factors affecting the stability of breakwaters can be classified under three groups as given below.

- a) Environmental Variables.
- b) Structural Variables.
- c) Armour unit parameters.

2.2.1.2 Damage of rubble mound breakwater

An exact definition of 'damage' is essential for quantitative analysis of stability of rubble mound structures. The traditional method of quantifying damage is physical counting of

displaced units caused by wave action. In this process the question raised is that whether the stone dislocated from upper area, rolled and settled in a new position from where units get removed during early stages of damage should be counted or not. The above mentioned phenomenon affects the final profile of the damaged breakwater. The damage parameter was defined by Hudson as the percentage of armour units displaced from the cover layer. The removal of up to 1% of the total number of armour units in the cover layer is considered as no damage (Hudson, 1959). The damage to the breakwater usually occurs in the area between SWL+H and SWL-H for both normal and oblique wave attack (Kreeke, 1969). Kreeke defined the damage percentage as the number of displaced stones divided by the number of stones in the attacked area (SWL+H and SWL-H) times hundred. In computing the total number of stones in the attacked area, a double layer armour stone was used.

Van der Meer used the following relation to measure the damage:

$$\text{Damage level, } S = \frac{A_e}{D_{n50}^2} \quad (2.6)$$

Where, A_e is the area of erosion and D_{n50} is the nominal diameter of the stones.

The limits of damage (S) observed by Van der Meer (1988) is given as follows in Table 2.1.

Table 2.1 Limits of damage level (S)

Cot α	Start of Damage	Failure (Filter layer visible)
1.5	2	8
2.0 - 3.0	2	8 - 12
4.0 - 5.0	2	17

A physical description of the damage S is given as the number of squares with side D_{n50} that fitted into the erosion area. Another description is that the number of cubic stones with a side of D_{n50} eroded within a width of one D_{n50} . The actual number of stones eroded within this width one D_{n50} could be more or less than S, depending on the porosity, the grading of armour units and the shape of stones. But generally, the actual number of stones eroded within a width of one D_{n50} is equal to 0.7 to 1.0 times the damage (S) (Pilarczyk and Zeidler, 1996).

Burcharth and Hughes (2000) defined zero damage wave height as the wave height corresponding to 0-5% damage. The percentage of damage is based on the volume of

armour units displaced from the active breakwater zone for a specific wave height. This zone may extend from the middle of the breakwater crest down the seaward face to a depth equal to one zero-damage wave height, below the still water level.

2.2.1.3 Failure of Breakwater

Failure of a structure implies that the structure ceases to perform its designed function. Being flexible structure, rubble mound breakwaters normally do not fail catastrophically. On the other hand, failure is gradual and it shows visible signs of distress prior to failure. With the increasing use of specially shaped artificial armour units which depend on interlocking for stability, the above concept may need a modification. Most of these units are slender and have outstanding legs to ensure interlocking. Large interlocking units, under wave attack or during construction, may develop cracks due to movements as the structural strength of the units may be unable to withstand the stresses which result in breakage of the units, principally at the roots of the legs. This causes the units to lose their interlocking ability. These broken pieces, being lighter than the required stable armour weight are easily displaced by wave action, also these broken units crash against neighbouring armour units, causing further breakage. This leads to a rapid unravelling of the armour layer, exposing the under layer and the core to direct wave action. These layers not being designed to resist the direct action of the waves get degraded very fast, causing a catastrophic failure of the structure.

In 1978, breakwater of Port Sine's in Portugal which was a massive rubble mound structure built with 42Tons Dolos in deep waters, failed badly due to cyclonic waves which led to the loss of interlocking between the armour units. Of course, this was not only the reason for the failure of this breakwater. Rather a conclusion drawn from these experiences of failure indicates that, such artificial armour units have reached the limit of their capability. They are no longer able to sustain their own weights (Hettiarachchi et al., 1991). The other breakwaters which were damaged due to extreme waves in excess to design waves were at Kahului, Hawaii, 1958, Gansbaai Cape Town, South Africa, 1970 and 1977, Torshavn 1972, Hirt Shab Harborn, 1973, Crescent city California, US 1974, Nawi Liurili Hawaii, 1976, Rosslyn Bay Queensland, 1976, Comeau, Qubec, Canada, 1976, Humbolt Jetty California, 1976, Azzawiya Libya, 1979, El Djedid Port of Arzew, 1980, Tipoli Libya, 1982 and Mogadishu Somaliya, 1982. Most of these structures had artificial concrete armour units. Most of these structures were badly damaged due high

wave loads, poor interlocking and insufficient structural strength of the units and geotechnical instability, while, other breakwaters failed due to loss of toe support and morphological changes (Edge and Magoon, 1979; Zwamborn, 1979). These failures gave birth to safer breakwaters like berm breakwater, submerged breakwater and reef breakwater.

2.2.2 Submerged Reef

Reef is a kind of offshore structure with its crest at or below the SWL. Reef is a homogeneous pile of stones, with individual stone weight sufficient to resist the wave attack. It breaks the incoming waves and dissipates the wave energy due to turbulence and offer low transmission coefficient. These are used basically to protect a beach or to reduce the beach erosion. These types of structures are constructed where only partial attenuation of the waves on the lee side of the structure is required or where the overtopping is allowed.

Low crested and submerged structures (LCS) such as detached breakwaters and artificial reefs are becoming very common coastal protection measures (used alone or in combination with artificial sand nourishment). Apart from dumping of rubble all along the affected coastal zone, there are other means of offering protection to the coast. Submerged breakwater is often a potentially an economical solution in a few cases, where, complete protection from waves is neither necessary nor desirable.

Seelig (1979) as quoted by Ahrens (1987) conducted a series of model tests to determine the wave transmission and reflection characteristics of low crested breakwaters. From these tests it was concluded that the component of transmission due to wave overtopping was very strongly dependent on the relative free board (F/H_i).

Since, reef structures do not have core, it cannot fail catastrophically. Hence, a logical strategy is to allow them to adjust and deform to some equilibrium condition. Because of high porosity, reef structures are more stable than the rubble mound breakwaters and at the same time it would dissipate wave energy efficiently. It is also believed that their simplicity would be a significant factor in keeping down the construction cost and suggested that a reef breakwater would be an optimum structure type for many situations

(Fulford, 1985). The performance of reef breakwater as shoreline stabilization measure and response of the shoreline at Chesapeake Bay, USA, against conventional methods like groynes, seawalls and revetment is discussed by Fulford (1985).

Gadre et al. (1989) experimented with light and economic submerged breakwaters constructed with sand filled bags and chained concrete blocks as an armour with less than 200 kg of weight which can easily be constructed. In 1989, a submerged breakwater at 80 m seaward was designed to protect a damaged breakwater head of the west breakwater at Veraval port in Gujarat, India. This submerged structure broke the storm waves, protecting the damaged breakwater which was repaired later.

The best morphological effects, pronounced as accretion of sediment between the submerged breakwaters and shoreline, have been reached for the slope of the seaward wall ranging from 1V: 2H to 1V: 3H. Better dissipation of waves, lower reflection, and easier transport of water and sediment over the structure is also noticeable for such breakwaters (Pilarczyk and Zeidler, 1996).

The Submerged reef breakwater is a structure that is optimized to the highest degree. For this structure, the critical conditions of stability have at low water level and it became more stable at increased depth of submergence. This is due to sheltering effect provided by the overlying water cushioning of the impact forces and attenuating the drag forces of the waves (Smith et al., 1996).

Franco (2001) writes about perching artificial beach contained by L-shaped rock groins and submerged barrier for enhancing recreation and urban social life was built along the waterfront of Civitavecchia, Rome. An interesting addition to this scheme was the novel design of artificial reef for surfing of rocky foreshore slope of 1:33.

Reef breakwater is a mound of uniform sized armour units whose weight are sufficient to resist the wave attack and without core and secondary layer. It is a low crested structure. Nizam and Yuwono (1996) gave the stability criteria for submerged reef. Armono and Hall (2003) experimentally investigated the wave transmission at submerged breakwater made of hollow hemispherical shaped artificial reef and found on an average about 60% of the incoming wave energy was reduced.

With increasing erosion rates and limited resources, alternative methods of shore protection are needed to protect the upland property and provide recreational and environmental habitat at a lower cost than conventional techniques. One such alternative method that has been tried in recent years is submerged prefabricated modular breakwater or artificial reef unit. The purpose of this type of structure is to attenuate waves and provide shoreline stabilization. Historically, artificial reefs have predominantly been used to create habitat, thereby attracting marine life. Waste materials such as ships, automobiles, tires, concrete debris often have been used to construct artificial reefs (Harris, 2003).

2.2.2.1 Stability of submerged reef

Ahrens (1984) worked on the reef breakwater model of slope 1:1.5, constructed with armour of 17gms to 71gms in water depths of 0.25m to 0.3m with irregular waves of heights varying from 0.01m to 0.18m of period 1.45sec to 3.6sec. The area of cross section (A) of the breakwater varied between 0.117m² to 0.19m². About 3500 to 4000 waves were passed to get the equilibrium profile of the structure. It was found that the reef was damaged more for waves of longer period than shorter period. The damage was defined by

$$D^l = A_d / (W_{50} / \gamma_r)^{2/3} \quad (2.6)$$

where, A_d is the damaged area of the reef and W₅₀ and γ_r are the mean weight and specific weight of the armour respectively.

It is found that for the spectral stability number (N_s^{*}) less than or equal to 6, there was little or no stone movement and for the number greater than or equal to 8, there was noticeable stone movement and the damage to the structure. For a given depth, the maximum stable height increased with wave period T and K_t is a function of crest width, depth of submergence and wave steepness. Further, the maximum wave energy reflected was about 18% for long waves for crest at SWL and it was about 8% for short waves. The wave reflection reduced as depth of crest submergence F/H increased (Ahrens, 1984).

Ahrens (1987) as stated by Pilarczyk and Zeidler (1996) included the local wave steepness in a modified spectral stability number (N_s^{*}).

$$N_s^* = N_s S_p^{-1/3} = \left[\frac{H_s}{\Delta D_{n50}} \right] (S_p^{-1/3}) \quad (2.7)$$

where, S_p = local wave steepness, it is calculated using the local wave length from Airy theory. The design curve based on the Equation (2.4) is given (Pilarczyk and Zeidler, 1996). The weight of the armour unit is calculated from the formula:

$$M = \rho_r \times D_{n50}^3 \quad (2.8)$$

where, ρ_r = mass density of armour units

D_{n50} = nominal diameter of armour units.

Ahrens (1989) further analysed the stability of reef structures and calculated its response with respect to the variable called average cotangent of reef as

$$C = A/h_c^2 \quad (2.9)$$

where,

A is the cross section of the reef; h_c is the crest height at equilibrium after damage.

It was found that for N_s^* less than 7, there was little or no adjustment of reef armour to the wave action. Then the stability coefficient was defined similarly to Hudson's as

$$K_D^* = N_s^*/\log C \quad (2.10)$$

where, C can also be calculated as

$$C = \text{Exp} (0.0945N_s^*) \quad (2.11)$$

It was concluded that reefs with the greater bulk B_n resist the degradation better than small reefs and are stable if there are low profile, where, bulk number is calculated as

$$B_n = A/D_{n50} \quad (2.12)$$

Gadre et al. (1992) tested a reef structure as a protection measure for the buried submarine pipelines. The reef was constructed with rocks of weight 0.5 Ton to 4 Ton placed randomly at a slope of 1: 3 in a water depth of 6 m, 8 m, 10 m subjected to maximum wave height limited to breaking wave height in a particular depth, of period 10 sec. The test was conducted for regular and irregular waves. The following stability number was arrived.

$$N_s^* = \frac{\gamma_r H^3}{(W_{50} \Delta^3)} \quad (2.13)$$

The design graph of $(N_s^*)^3$ vs. F/d was also given. The wave heights, causing initiation of damage to the armour of submerged reef were different for regular and irregular waves and $H_{reg}/H_{rand} = 1.12$.

Cornett et al. (1993) after conducting experimental investigation conclude that there may be an optimum location for submerged reef of relative height $h/d > 0.6$ which protects the inner main breakwater.

Nizam and Yuwono (1996) conducted experiments on efficiency of artificial reefs as alternative beach protection. Physical model studies were conducted on 0.2m to 0.45m high, 1:2 sloped model of the reef breakwater with its crest width varying from 0.15m to 0.4m constructed with the armour of mean diameter of 0.01m to 0.03m. The model was constructed at a depth of 0.2m to 0.7m and subjected it to regular waves of height 0.0191m to 0.2m with periods varying from 0.89sec to 2.68sec. K_t obtained was of the order between 0.1 and 1.0 and the following stability coefficient (K'_D) was derived to calculate the weight of reef armour.

$$K'_D = \frac{\gamma_r H^3}{(W_{50} \Delta^3)} \quad (2.14)$$

The authors studied the damage of the reef crest in detail and have provided a graph of stability number K'_D vs relative distance B/X' (i.e., Crest width parameter) on either side of the center line of the crest. It was concluded that a significant economy can be achieved by zoning the crest width into several parts and reducing armour weights farther away from the position of wave breaking.

Shirlal et al. (2008) derived the design equation for the stability of the submerged reef as

$$\left[\frac{h_c}{h} \right] \left[\frac{D_{n50}}{gT^2} \right] 10^{-3} = 8.9303e^{-0.284N_s^*} \quad (2.15)$$

Where,

h_c/h is the dimensionless damage, gT^2/D_{n50} is the dimensionless wave period and N_s^* is the spectral stability number.

It was found that an optimum armour weight of the submerged reef breakwater is 30gms for a 0.25m height reef structure of slope 1V:2H which was tested to a depth of 0.3m and waves of 0.1m to 0.16m of period 1.5sec to 2.5sec.

Manu et al. (2011) carried out a physical model study of the stability of tandem Breakwater with Concrete Cube Armour. They concluded that for a submerged reef of crest width 0.4m placed at a seaward distance of 2.5m, coefficient of transmission (K_t) varies between 0.39 and 0.74 and completely protects the main breakwater.

2.2.2.2 Crest width of submerged structure

The effectiveness of the submerged breakwater in wave damping is lower than that of the emerging breakwaters having same geometry and layout. To achieve comparable results, the wave transmission by a submerged breakwater should be decreased by enlarging the crest width or by reducing the spacing of submerged breakwater. According to many authors, relative crest width is the important factor in determining the effectiveness of the submerged breakwater.

Johnson et al. (1951), from their experimental investigation found the relationship for crest width based on the steepness. For good wave damping,

In the case of low wave steepness, $B/L_0 = 0.1$

$$\frac{B}{L_0} = \frac{1}{4} \sqrt{1 - h_s/d}, \frac{3}{4} \sqrt{1 - h_s/d} \quad (2.16)$$

In the case of steeper waves, $B/L_0 = 0.1$ to 0.24

Where, h_s = submerged breakwater height; d = depth of water; L_0 = deep-water wave length and B = crest width. The wave damping could be improved with an increase in crest width beyond the values given by the above equation.

Dattatri et al. (1978) concluded, based on the experimental investigation that, the important parameters that influence the performance are the crest width and the depth of crest submergence. The relation to calculate an optimum crest width was derived as $B/L = 0.2$ to 0.3 .

According to CEM (2001), crest width can be calculated by using a simple relationship, which is defined by the construction method or functional requirements.

$$B_{\min} = (3 \text{ to } 4) D_{n50} \quad (2.17)$$

2.2.2.3 Wave transmission over submerged reef

In recent years, the conceptual design of coastal defence structures has involved more than just the consideration of physical factors. Certain non-physical factors such as the environmental and aesthetic value of the nearshore landscape have also become important aspects to consider (Makris and Memos, 2007). This has played a part in the development of low-crested and submerged structures that offer the benefit of low visual impact (Tomasicchio and D'Alessandro, 2013).

A commonly used measure of the performance of such structures is the transmission coefficient. This coefficient provides the anticipated decrease in wave height due to the presence of the structure under consideration. The primary parameter that impacts the transmission coefficient is the freeboard of the structure, i.e. the distance between the water level and the crest level of the structure (Makris and Memos, 2007). A mathematical description of the transmission coefficient is given as (Van der Meer and Daemen, 1994):

$$K_t = \frac{H_t}{H_i} \quad (2.18)$$

where,

K_t = transmission coefficient

H_t = transmitted wave

H_i = incident wave

Several parameters effect the value of the transmission coefficient, including the crest width of the breakwater (B), the freeboard (R_c), the water depth (h), the height of the structure (h_c), the front slope of the structure (m), the nominal rock diameter of the armour slope (D_{n50}), the incident significant wave height at the toe of the structure (H_i), the local wavelength (L), the peak period (T_p), the Iribarren number, and the wave steepness (Makris and Memos, 2007). Fig. 2.2 gives a graphical representation of these parameters.

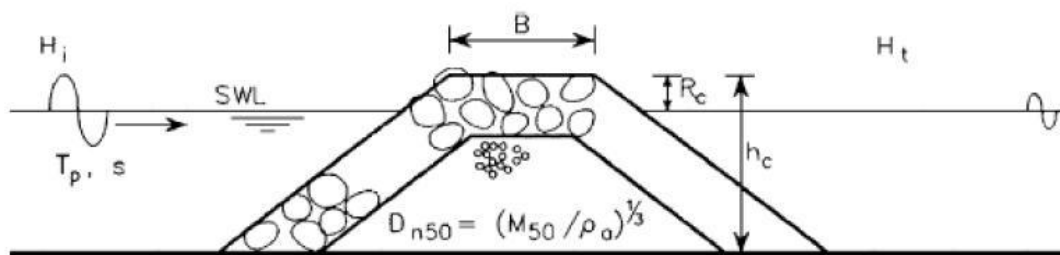


Fig. 2.2 Wave transmission coefficient (Van der Meer et al., 2005)

Extensive research has been done on the topic of transmission coefficients by various authors, including Seelig (1980), Van der Meer et al. (2005), and Shirlal et al. (2007). Several of the above mentioned authors have proposed empirical formulae for the wave transmission coefficient based on regression analysis of physical model data.

Advantages of submerged reef are demanding to utilize them in combination with Conventional rubble mound breakwater: The reef interferes with the incoming wave field so as to create partial obstruction

1. First of all, submerged breakwater can sustain habitants and helps to protect and sustain the marine environment.
2. Reflects some of the wave energy
3. Offer friction and resistance to wave motion
4. Induce wave breaking and causing turbulence
5. Resulting in wave energy dissipation and energy loss
6. Transmit smaller waves with reduced energy
7. Submerged breakwaters have a relatively mild but steady effect in retaining shore side sediment and have a milder effect on the surrounding coast. Therefore submerged breakwaters have recently replaced emerging breakwaters in many places of the world.
8. Water exchange behind submerged breakwaters is better than that for the emerging ones. Thus, stagnant water can be avoided.
9. Submerged breakwaters may be foreseen as long continuous structures (thus avoiding gaps and drawbacks connected with them).
10. Sometimes, submerged breakwaters can dissipate wave energy more efficiently than emerging ones due to the fact that in emerging breakwaters longshore transport can be interrupted by the growing salient or even a tombolo.
11. Do not spoil the aesthetic aspect of the beach.
12. The advantages include preservation of environment and relatively low capital investments.

Last but not least, one should not neglect any disadvantages of submerged breakwaters.

1. It may become fatal obstacles for fishing boats or small pleasure boats
2. The effect of a submerged breakwater on a coast with a wide tidal range is not obvious because the hydraulic function of the submerged breakwater depends on the water depth at the crown, especially at tidal coasts.
3. The reef may be difficult to inspect since it is underwater.
4. It may be difficult and expensive to build the reef because it is both offshore and submerged. Construction requires a floating plant and thus may be expensive.

2.2.3 Protected Breakwater System

Designing breakwaters are primarily based on selection of design wave height which is $H_{1/10}$. In fact, one cannot rule out the possibility of a cyclone creating a huge wave which

may cause severe damage to the structure or initiate gradual morphological changes, changes in site conditions triggering the damage of the breakwater. However, the better the available data, there is always some doubt and considerable uncertainty about wave conditions during storm attack (Owen and Briggs, 1986). Hence, there is always this element of risk inbuilt in the design of breakwaters. So what is the solution? One way out could be the protection to breakwaters which can mitigate damage of storm waves to some extent. Though this concept was evolved in 1953 by Danel, it was realised only in the 1980's (Gadre et al., 1985).

Groeneveld et al. (1984) recognized the construction of a submerged barrier in front of a breakwater or providing a submerged berm attached to the seaward face of the breakwater as rehabilitation measures for damaged breakwaters as submerged barriers break high waves and transmits the attenuated waves. K_t was always found to be greater than 0.4. However, according to Goda (1996) the submerged structures are usually designed with a $K_t = 0.6$.

Based on limited study Gadre et al. (1985) designed a submerged bund in front the revetment for reclamation of land between outer harbour and fisheries harbour north of the Bharathi dock of Madras Port, Chennai, India. The normal conventional type of reclamation bund in a water depth of 8m would require armour stones of 15Ton or tetrapod of 6.5Ton on the slope of 1:2 to withstand waves of 5m height. Considering the non-availability of stones over 2Ton to 3Ton in the vicinity of the port, it was suggested to construct a submerged bund, pump sand and then provide upper pitched revetment. This resulted in a low cost construction in comparison with conventional types of bund. A model study was conducted on a 1:30 scaled submerged breakwater of slope 1:1.5, crest width B/d of 0.625 and height h/d of 0.5 at a seaward distance X/d of 14.2 was used as a protection to reclamation bund such that the submergence F/H was 0.6 to 0.65, and wave steepness H/gT^2 of 0.0051 where, X , B , h and d are the spacing between two structures, crest width of the reef, reef height of the submerged breakwater and depth of water respectively. It was tested for regular as well as for irregular waves. The structure broke 5m design wave and transmitted a 4m wave ($K_t=0.8$) and these waves further got attenuated by the friction offered by the reclamation fill between the structures and only a wave of height of 3.5m impinged on the inner revetment. Hence, it now required armour of weight of 2Ton to 3Ton at a slope of 1:3 and stones of 0.5Ton to 1.5Ton at a slope of

1:2.5 at higher level, where it was constructed as a berm type structure. The submerged bund of 4m high was constructed in a depth of 7m to 3m with a crest width of 5m with armour of 0.5Ton to 1.5Ton at a slope of 1:1.5. There was no damage of submerged bund. The breakwater head was damaged due to extreme waves crossing 9m in height. Several rehabilitation measures were tried. Ultimately, it was decided to construct a submerged breakwater at 80m seaward of the damaged structure which was selected as a solution. A submerged breakwater, of crest width B/d of 1.06 and height h/d of 0.5 at a seaward distance X/d of 8.88, with a crest submergence F/H of 0.22, was used as a rehabilitation structure for a damaged breakwater head at the Veraval Port in Gujarat, India, to secure it from storm waves (Gadre et al., 1989).

Cornett et al. (1993) conducted a limited set of small scale physical model tests on the tandem breakwater system. A breakwater of medium armour diameter of 0.042m on a uniform slope of 1:1.75 was constructed at a water depth of 0.55 m. Reef breakwater built with slope 1:1.5, a crest width of 0.1m (i.e. B/d of 0.18) and heights of 0.17m, 0.25m and 0.33m (i.e. h/d of 0.31 to 0.60) at a seaward distance of 2.11m from the breakwater (i.e. X/d of 3.83). The model was tested with about 320 to 440 regular and irregular waves of heights 0.12m and 0.2m of periods 1.5sec to 3sec. It was observed that at $F/H_i=2.5$, K_t approached 1.0 and then it remained unaffected for $F/H_i>2.5$. It was found that, the reflection coefficient K_r increased with reef submergence F/H_i .

Cornett et al. (1993) concluded that,

1. For a reef of $h/d < 0.6$, no significant wave attenuation occurred.
2. For reef of $h/d=0.6$ and $X/L=2$, the incident wave is reduced by 15% at the toe of breakwater, wave loading on breakwater armour is reduced by 15% while its damage is reduced by 50%.
3. For reef of $h/d>0.6$, largest wave heights are significantly reduced.
4. Wave period influences wave transmission at the reef and also performance of tandem breakwater.
5. Depending upon the geometry of tandem structures, an optimal spacing between the structures may exist.

Even a modest reduction in wave heights and load levels can have a dramatic effect on the performance of breakwater armour. In conditions near the threshold of armour stone motion, such a reduction in loading can make the difference between extensive damage

and no damage. Higher and broader reefs are likely to cause more pronounced wave transformation, greater reduction in extreme loading events and even more dramatic attenuation of damage. Such attenuation would allow the more economic design of the breakwater (Cornett et al., 1993). Further, it was observed that considerably more research and testing of reef breakwaters and tandem breakwaters concept are required to develop a complete understanding of the transformation to transmitted waves, loading events and implications for the performance of diverse tandem breakwater systems.

Neelamani et al. (2002) experimentally investigated the hydraulic performance of an impermeable plain seawall, of varying inclination θ from 30° to 90° , defenced by a detached breakwater as shown in Fig. 2.3. It was concluded that, for a breakwater of width (B/d) of 0.25 to 0.40 and height (h/d) of 0.75 to 1.2, constructed a seaward distance (X/d) of 6.63 to 10.6 from the seawall, wave pressures on the seawall are reduced by 45%, wave run-up and run-down on the seawall are reduced by 10% to 40% and 10% to 70% respectively and reflections are reduced by about 10% for the breakwater submergence of $0.33 < F/H < 4.0$ and wave steepness of $0.004 < H/gT^2 < 0.115$.

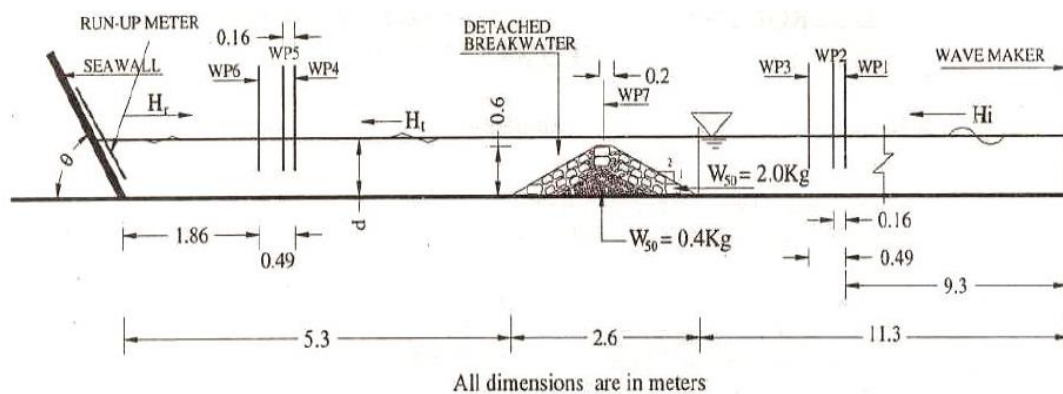


Fig. 2.3 Submerged defenced reef

Neelamani (2004) studied the effect of the presence of an offshore breakwater on wave pressures on vertical seawalls by performing a series of physical model tests. A seawall model of 1.96m length, 1.2m high and 0.87m wide was constructed and a designed rubble mound breakwater was placed seaward of seawall. Water depth of 0.3m and breakwater crest width (B) of 0.4m was kept constant throughout the experiment, but varied its height from 0.2m to 0.4m. The distance between the seawall and the leeward side toe of the breakwater (pool length L_p) were selected as 0.5m and 1m. The incident wave steepness (H_i/L), where 'L' was a wave length and H_i was the incident wave height and relative wave heights (H_i/d) of regular monochromatic waves were varied from 0.003-0.06 and

0.15-0.51 respectively. Five different relative heights (h/d), where 'h' was the height of the breakwater were used during the study. It was noticed that as the relative height (h/d) of the breakwater increased from 0.66 to 1.33, the pressure ratio decreased from 2.26 to 1.15.

Munireddy and Neelamani (2006) in continuation of the above study varied the crest widths (B) by 0.4m and 1.2m and water depths from 0.5m to 0.7m with an increment of 0.05m. Finally, it was concluded that the wave interaction with the low crested offshore breakwater is significantly different with varying water depth. The wave force reduction was significant when the crest level of the breakwater was very close to the still water level. It was also noticed that, when the crest level of the breakwater was at still water level, there were about 52% and 62% reduction in the wave force for crest widths (B) = 0.4m and 1.2m respectively. It was shown that shorter period waves dissipate more energy than the long period waves.

Tsai et al. (2010) carried out the physical model study to investigate the wave transmission between a submerged permeable breakwater and seawall along with a variation of the wave profile, the piling up of water and wave run-up. A 0.6m wide submerged permeable breakwater was built using 120gm dolos armour units at a seaward distance of 2m from the seawall of 1:2 slope. The porosity of the submerged permeable breakwater was 0.63. There were 12 capacitance type wave gauges used to measure the surface elevation transformation from deep water to seawall. Four different wave periods of 1.3, 1.5, 1.7 and 1.9secs with different wave heights ranging from 0.11m to 0.18m were used in the experiments, where the steepness of incident waves in deep water varied from 0.019 to 0.068. The water depth at the center of submerged permeable breakwater of 0.26m was kept constant and three different free boards (0, 0.065m and 0.13m) were considered during the study. The tests were conducted in 2D wave flume with regular waves. The spatial transformation of free surface displacements and their corresponding variation of harmonic amplitudes were obtained. Based on the results obtained from the physical model tests, it was noticed that the piling up of water in the lee of breakwater due to the wave transmission decreases as the free board of the breakwater increases. The results showed that the larger transmitted wave through the submerged permeable breakwater induces the larger wave run-up on the seawall. Finally, the authors opined that

the installation of the submerged permeable breakwater is capable of reducing the wave run-up on the seawall efficiently.

2.2.4 Tandem Breakwater System

The concept of the conventional rubble mound breakwater and submerged reef operating together as a single unit is called the tandem breakwater.

In the actual field conditions, the submerged reef interferes with the incoming wave field so as to (Turker, 2014)

- (1) Create a partial obstruction
- (2) Change the water particle velocity and motion
- (3) Reflects some of the wave energy
- (4) Offer friction and resistance to wave motion
- (5) Wave of various configuration
- (6) Induce wave breaking and causing turbulence
- (7) Resulting in wave energy dissipation and energy loss
- (8) Transmit smaller waves with reduced energy.

This results in smaller waves passing in the space between the two structures losing some more energy and finally impinging on the main breakwater. In this way the submerged reef offers protection to the inner conventional rubble mound breakwater from extreme waves. Therefore, the breakwater can be economically designed with lighter armour units. Many researchers through their studies have proved that armor stability is a function of wave height, wave period, wave groupiness, wave breaking, water depth, structure slope, armor unit weight, armor gradation, storm duration and porosity. Each one of them investigated structure stability with respect to different parameters (Johnson et al., 1978; Carver and Davidson, 1982; Poonawala et al., 2001; Shirlal and Rao, 2008; Manu et al., 2011).

The tandem breakwater may not always provide the least cost alternative, as section costs are strongly related to material costs and water depths. However, the tandem breakwater has offered significantly reduced design risk since high return period events such as large storm waves are reduced to a more manageable level, reducing the chance of catastrophic failure of the main breakwater in storm events outside the design envelope (Cork and Clare, 1992).

Based on limited study, it was found that a reef structure of crest width B/d of 1.53 and of height h/d of 0.86, constructed at a seaward distance X/d of 9.0, attenuated the waves considerably and protected the breakwater.

Many investigators opine that the lowest values for which no scale effects are present can be set at Reynolds number (R_e) greater than 6.0×10^3 - 4.0×10^4 (Hughes, 1993). Owen and Briggs (1986) recommended R_e range between 3.0×10^3 and 3.0×10^4 , scale effects would be insignificant.

A physical model should be designed correctly to get reliable results. In the present study, the similitude is achieved by dimensional analysis while keeping the non-dimensional parameters in the same range for both model and prototype. The best model is the prototype. But the limitations of the lab resources, etc., most of the times, do not permit testing of a prototype. The choice of a scale, for the model test, is often limited by constraints put by experimental facilities available. Within this constraint, an optimum scale should be selected (Chakrabarti, 1996).

Cox and Clark (1992) designed submerged breakwater in tandem with conventional breakwater to give least total cost for the breakwater, for a marina on Lake Michigan, USA and saved about \$1 million. The submerged reef breakwater broke waves, dissipated energy and attenuated waves, thereby reducing the intensity of wave loads on the main breakwater, which was then designed with lighter armour units, hence proved economical.

Cornett et al. (1993) after conducting experimental investigation concluded that a submerged reef of relative height (h/d) greater than 0.6 protects the inner main breakwater and there may be an optimum location for reef of a given geometry of tandem breakwater. Shirlal et al. (2007) proved from the physical model studies that the submerged reef located seaward of the main breakwater dissipates the wave energy and completely protects the structure from damage for the test conditions and can save about 21% to 27% in the construction cost compared to a single conventional breakwater.

Park et al. (2007) experimentally proved that the submerged structure in front of the rubble mound breakwater is effective in dissipating the wave energy and reducing the wave run-up on the structure.

2.3 REVIEW OF APPLICATIONS OF SOFT COMPUTING TECHNIQUES IN COASTAL ENGINEERING

Several researchers have adopted soft computing techniques to solve complex associated with coastal/ocean engineering problems and some of them are discussed below:

2.3.1 Artificial Neural Network

The neural network technique was applied to predict the stability of rubble mound breakwater (Mase et al., 1995). They considered several parameters such as stability number, the permeability of the breakwater, damage level, and surf similarity parameter, number of attacking waves, spectral shape parameters and dimensionless water depth. The developed model predicted the damage level satisfactorily.

Mase and Kitano (1999) applied neural network techniques to predict the impact of wave force which would act on the upright section of a composite breakwater. Four non-dimensional parameters were fed as input *viz.* h/L , H/h , d/h , and B_m/h where, h denotes the total water depth, H represents the wave height, L is the wavelength, B_m is the horizontal distance from the shoulder of the mound to the caisson and d is the water depth above the mound. The parameters of the model were determined through self-learning and the results were accurate.

Deo and Kumar (2000) estimated the weekly mean significant wave heights using neural network, and model based statistical and numerical methods, from their monthly mean observations. The network was trained using error back propagation, conjugate gradient and cascade correlation algorithms. The training of the model using cascade correlation took minimum training time with better correlation coefficient between observations and network output.

A model to estimate the significant wave heights and average wave period from the generating wind speed was developed by Deo et al. (2001) using 3-layered feed forward neural network. The network was trained with different algorithms and used three sets of data. The trained network provided satisfactory results in deep water, in open wider areas and also when the sampling and prediction interval were large, such as a week. It was revealed that a proper choice of training patterns was found to be crucial in achieving adequate training.

The feed forward backpropagation neural network technique was applied for accurate prediction of tides (Mandal et al., 2001). Their neural network model predicted the time series of hourly tides using a quick learning process called quick prop. The correlation coefficient between predicted tides and measured tides was found to be 0.998. It showed a good agreement between neural network prediction and measured data set. Large data required by the traditional method for prediction tidal level can be avoided by adopting neural network with little dataset (Lee and Jeng, 2002).

Deo and Jagdale (2003) developed neural network models for prediction of breaking waves. The network was trained by using the existing deterministic relations with a random component. Fresh laboratory observations were used for validating the model. The results showed that the prediction of breaking height and water depth of the model was more accurate than the available traditional empirical formulae.

An ANN model to improve short term wave forecasts was developed by Makarynskyy (2004). The model was trained and validated using hourly observations of significant wave heights and zero-up-crossing wave periods from two offshore sites. Two approaches were adopted for the forecasting. One approach corrected the predictions using the initial simulations of the wave parameters with lead times from 1h to 24h and the other approach was used for merging the measurements and initial forecast. Results showed satisfactory predictions at both locations.

The ANN approach was used for estimating the wave parameters from cyclone generated wind fields (Mandal and Rao, 2005). Estimation of H_s and periods was carried out using back propagation neural network with three updated algorithms, namely R_{prop} , Quick prop and super SAB. The predicted values using neural networks matched well with those estimated using Young's model and a high correlation coefficient of 0.99 was obtained.

The ANN technique was used to predict the significant wave height (H_s) and zero crossing wave periods (T_z) by Makarynskyy et al. (2005). This tool achieved a higher accuracy of simulating the H_s and forecasting T_z by using ANN.

A neural network was developed in order to estimate the wave surface density over a wide range of wave frequencies from average wave parameters of H_s , T_z , spectral width and peakedness parameters (Naithani and Deo, 2005). The neural network predicted values were compared with the measured ones and found that the predictions were

acceptable than those yielded by Pierson Markowitz (PM), JONSWAP and Scott's spectra.

Yagci et al. (2005) used a neural network technique to predict the damage ratio of the breakwater. According to them, the accurate estimation of damage levels of the breakwater was a vital issue in the design of the breakwater. The network was constructed by considering input parameters like wave steepness (H/L), significant wave period (T_s) and slope angle (α). The fuzzy logic system has been used for mapping the inputs and output. The fuzzy model estimations of damage ratios were close to the predicted values by neural network methods. The employment of Artificial intelligence (AI) methods enable the consideration of wave period; wave steepness, breakwater slope and wave height in estimating damage ratio. This application is useful especially when there is less number of laboratory data set. The experimental data set was plotted effectively using AI technique in order to generate more number of data set.

The ANN was applied to design rubble mound breakwaters (Kim and Park, 2005). Neural network technique yielded more accurate results compared to the conventional empirical model and also the accuracy of the results was influenced by neural network structure. They showed that the solutions of Monte Carlo simulation technique could be improved by incorporating the trained neural network model into it.

The recurrent neural network with updated algorithms was used to forecast ocean waves (Mandal and Prabakaran, 2006). The recurrent neural network of 3, 6 and 12 hourly wave forecasting yielded the correlation coefficient (CC) of 0.95, 0.90 and 0.87 respectively. According to them, the wave forecasting using recurrent neural network yielded better results compared to previous neural network applications.

The marine structures in Taiwan suffer from typhoon attack every year. The earlier theoretical models were not properly predicting the typhoon waves. According to Mandal et al. (2007) used a neural network technique to predict the stability number and damage levels of the rubble mound breakwater. It was seen that a good correlation was obtained between network predicted stability numbers and estimated ones with less computational time as compared to Mase et al. (1995) and Kim and Park (2005).

Gent et al. (2007) developed a neural network model to estimate wave-overtopping discharges for a wide range of coastal structures. The presented results show that Neural

Networks can successfully be used to model the relationship between the input parameters involved in wave overtopping and the mean overtopping discharge at coastal structures.

Mandal et al. (2008) applied NN technique in predicting the stability number and compared it with the estimated stability number by Hudson and Van der Meer. The neural network was modeled with parameters, which affects the stability, namely Permeability of breakwater, number of attacking waves, significant wave height, mean wave period, damage level, slope angle, berm width and reduced armor weight ratio. It was found that the network predicted lesser armor units when compared to empirical formulae which could make the design more economical and safe. The coefficient of correlation between the estimated stability number by empirical formulae and predicted stability number of neural networks were close to one.

Zamani et al. (2008) developed ANN and Instance-Based Learning (IBL) models to forecast significant wave heights for several hours ahead using buoy measurements. Experiments showed that the ANN's yielded slightly better agreement with the measured data than IBL. According to them, ANN's could also predict extreme wave conditions better than the other existing methods.

Gaur and Deo (2008) applied genetic programming (GP) to forecast ocean waves on real-time. It was analyzed that the wave riders buoy which was measurements at two locations in the Gulf of Mexico. The forecasts of significant wave height were made over lead times of 3, 6, 12 and 24h. A sample size belongs to a period of 15 years and a testing period of 5 years was used. The forecast made by the approach of GP could be regarded as a promising tool for future applications to ocean predictions.

Londhe (2008) presented ANN and GP for estimation of missing wave heights at a particular location on a real time basis using wave height at other locations. Both approaches performed well in terms of accuracy of estimation, whereas GP model worked better in case of extreme events.

ANN and regression method was used by Gunaydin (2008) to predict the mean monthly significant wave height from meteorological data. Seven different ANN models were compared each comprising of various combinations of input. The inputs were monthly mean wind speeds, air temperature ratios and sea level pressures collected on an hourly

basis. Out of seven ANN models that the model with all the input parameters outperformed other models.

Liang et al. (2008) developed three Back-Propagation Neural Networks (BPNN) models viz. Difference Neural Network Model (DNN) for the supplementing of tidal record; Minus-Mean-Value Neural Network (MMVNN) for corresponding prediction between the tidal gauge station and Weather-Data Based Neural Network model (WDNN) for the prediction of set up and set down. It was found that the above models performed well in the prediction of tidal level or supplement of tidal record including strong meteorological effects.

Balas et al. (2010) artificial intelligence models were developed for the stability analysis of rubble mound breakwaters. Although, ANN models (without Principal Component Analysis (PCA)) were not adequate in capturing the non-linear characteristics of the complex hydraulic system, using PCA in the process of choosing the appropriate training data and the number of PC's enhanced the NN prediction capabilities (HNN case). Therefore, a better agreement between the predicted stability numbers of hybrid artificial neural networks and measurements was obtained when compared to the stability equations of Van der Meer, and ANN trained by the data sets that were not pre-processed. As a result, the hybrid neural network has the advantage of robustness as an alternative for the stability assessment of coastal structures.

Seasonal beach profile evolution was predicted by Hashemi et al. (2010) using ANN at several locations along the Tremadoc Bay, eastern Irish Sea. The beach profile data collected at 19 stations for a period of 7 years were studied using ANN. Principal Component Analysis and correlation analysis were used to develop a proper input data set. The local wave climate, wind data, geometric properties of the beach, and the corresponding beach level changes were fed to a feed forward back propagation ANN. The field data and the model results were compared and found that model was best with an MSE of 0.0007.

Iglesias et al. (2010) developed an ANN model to predict the draft required to provide floating boom in open waters. The dataset was obtained from laboratory investigations on seven model booms subjected to various waves and current combinations. The obtained dataset was divided into two random sets, one for training and another for testing. The

model was further improved to find efficient network architecture using 640 neural networks. The model was trained and then generalized them to other cases for validation.

Zanuttigh et al. (2013) developed an ANN model to predict the reflection coefficient for different coastal and harbour structures. The 600 data sets was used for training and testing of the model. The data sets included the smooth rock armour units, slopes, berm breakwaters, vertical walls, low crested structures and oblique wave attacks. The 13 input parameters were used to represent the various aspects of the reflection process. The algorithm and input elements are selected based on the sensitivity analysis. The network model developed was compared with the limited set of data selected from the literature and it was found that the model could accurately predict the measured reflection coefficients better than the empirical formulae with RMSE=0.037 and $R^2=0.96$.

Hagras (2013) used ANN with different topologies were evaluated to predict hydrodynamic coefficients, wave transmission coefficient (K_t) and wave reflection coefficient (K_r) of the permeable paneled breakwater. Two neural network models were constructed to predict. Back propagation algorithm was used to train a multi-layer feed-forward network (LM algorithm) and coefficients are evaluated using the Mean squared Error (MSE). The results of the developed ANN models proved that this technique was reliable. A good match between the measured and predicted values was observed with correlation values varying in the range (0.9508-0.9805) for the training set and (0.9159-0.9877) for the testing set.

Kim et al. (2014) suggested an ANN-based damage estimation procedure for a breakwater. ANN is used to predict the shallow wave height by using o shore wave height and tidal level at near shore. The predicted shallow wave height was used to estimate breakwater damage. By using ANN in the estimation of expected breakwater damage, total analysis time was drastically reduced, while maintaining the allowable error level in the damage estimation.

2.3.2 Adaptive Neuro-Fuzzy Inference System

The Adaptive Neuro-Fuzzy Inference System (ANFIS) and Coastal Engineering Manual (CEM) methods were used to predict the ocean wave parameters (Kazeminezhad et al., 2005). According to them, the results indicated that the ANFIS outperforms Coastal Engineering Manual (CEM) method in terms of prediction capability. The CEM method

overestimated the significant wave height (H_s) and underestimated the peak spectral period, while ANFIS resulted in predictions that are more accurate.

For forecasting of wave parameters considering the wind speed and its direction, and the lagged wave characteristics, Takagi-Sugeno rule based fuzzy inference system was used by Sylaios et al. (2009). The initial and final antecedent fuzzy membership functions were identified using Subtractive clustering method. The developed model was verified by predicting the wind and wave data set recorded in years 2000 to 2006 (12,274 data points) in the Aegean Sea between Greece and Turkey collected by an oceanographic buoy. For the training period, the model showed perfect fit and further was verified using the 2006 data (1,044 data points). Significant wave height and zero up-crossing periods for a lead time of three hours were predicted well by the model.

Patil et al. (2011) used ANFIS model for predicting wave transmission coefficient of horizontally interlaced multilayer moored floating pipe breakwater (HIMFPB). It showed that the ANFIS model outperformed the ANN model for predicting wave transmission coefficient.

The reliability based risk analysis for rubble mound breakwaters was carried out by Koc and Balas (2013) using fuzzy Monte Carlo simulation approach. The results show that the theory of fuzzy random variables is generally applicable and can be used in combination with arbitrary computational models for the numerical simulation of structural reliability of coastal structures. Fuzzy random variables may have a good potential to calculate the reliability of coastal structures and may serve as a reference for future studies in coastal engineering literature.

2.3.3 Support Vector Machines

Support Vector Machine (SVM) was used by Mahjoobi and Mosabbebi (2009) for the prediction of significant wave height. The data were collected from deep water locations in Lake Michigan. Current and previous six hours wind speed data was used as input variables and significant wave height (H_s) as output parameter. The SVM results were compared with the results of a Multi-Layer Perceptron (MLP), ANN, and radial basis function (RBF) models. It was found that SVM could be used successfully for the prediction of H_s . The error statistics of the SVM model marginally outperforms ANN with less computational time.

Malekmohamadi et al. (2011) compared the efficiency of soft computing techniques (SVM, ANN, BN and ANFIS) in wave height prediction. Wind speed was taken as the input and wave height as output. Statistical measures used were bias, scatter index, RMSE, MAE and CC. The results of the work showed that ANN could not consider the uncertainty of input-output variables, whereas, BN and SVM were capable of handling the uncertainties of model inputs. Also, BN was applicable even when the exact value of one of the input variable is not available. But the unreliability in the results produced by BN made SVM, ANFIS and ANN the better techniques.

Kim et al. (2011) predicted the stability number of armor blocks of breakwaters using Support Vector Regression. The proposed method proved to be an effective tool for designers of rubble mound breakwaters to support their decision process and to improve design efficiency.

Kalanaki and Soltani (2013) performed performance assessment among hybrid algorithms in tuning SVR parameters to predict pipe failure rates. They employed various hybrid models for various works related to the entire study. A hybrid Multi-Objective algorithm based on GA is used for predicting ground water levels. Results obtained from EPANET are used as inputs for the SVM. The effective parameters are taken into three models and compared with the SVR-GA, SVR-CACO, SVR-PSO, ANN and ANFIS. Results obtained from the study are compared with results from earlier studies on ANN-GA model. From the results obtained ANN-GA model and SVR-PSO model performed well, but took a long time, whereas ANFIS model utilized small time but lacked accuracy comparatively. Values of RMSE and R^2 made SVR based models better in prediction compared to ANFIS and ANN.

Mlybari et al. (2014) used SVM for the prediction of daily tidal levels along Jeddah coast, Saudi Arabia and compared the results with back propagation neural network output. GA is used to select the proper parameters so as to enhance efficiency to the SVM model. Previous day tidal observations are taken as the inputs. Results showed that percentage error was lesser for SVM model compared to back propagation neural network, proving SVM as an alternative tool to neural network in forecasting of tidal levels.

Duan et al. (2016) developed a hybrid Empirical Mode Decomposition (EMD) Support Vector Regression (SVR) for prediction of significant wave height. Measured wave time

series are first decomposed into several stationary components called intrinsic mode functions, whose components are forecasted by SVR individually and then combined to obtain the expected wave prediction. Performance of EMD-SVR model is compared with the SVR, AR and EMD-AR models. Further comparison is done between EMD-SVR and WD-SVR models. Results obtained highlighted the applicability of EMD-SVR in forecasting non-linear and non-stationary wave heights, as most of the peaks and troughs correctly captured and the general tendencies satisfactorily reproduced. Also, higher accuracy in prediction of EMD-SVR compared to WD-SVR makes it the best tool.

2.3.4 Hybrid Artificial Intelligence Models

Conventional models are found to be weak in dealing with nonlinear and complexity of data sets resulting due to the variation in the needs for coastal protection because of climatic changes and anthropogenic influences and seasonal changes which impacts on the performance of coastal protective structures. Various hybrid models tested have yielded good results (Patil et al., 2012 and Harish et al., 2015). Recently, Particle swarm intelligence has become a popular optimizing tool due to its ability to overcome the local minima and give the globally generalized error and its accuracy.

ANN and SVM are commonly used by many researchers to evaluate or predict wave parameters like wave height, wave period, wave direction, tidal levels and its timings, sea levels, water temperature, wind speeds, etc. Damages of coastal structures, stability of breakwaters, storm surges and wave transmission have also been predicted using ANN and SVM. For calibration and verification of the both the models, many researchers used in-situ data, experimental data, and data generated by numerical or mathematical analysis. Comparing to the traditional methods, the performance of the ANN and SVM were improved in terms of computational effort and time needed for training and testing. It is also reported that ANN model can learn with much less data set and SVM gives a unique solution. Sometimes a single network may not always fit the entire domain of the training sample and in such cases different networks are developed over a different sub-domain of the training sample size.

Many researchers have highlighted that hybrid models like ANN with fuzzy, and SVM with genetic algorithm, PSO can be adopted when the performance of the ANN and SVM models is poor in mapping input-output relation. Apart from ANN and SVM, other new

techniques like Particle Swarm Optimization or combinations of these can be used to solve problems in coastal engineering. Some of the recent literatures on development of hybrid PSO-ANN and PSO-SVM models are included below.

The determination of hyper-parameters including kernel parameters and the regularization is important to the performance of SVM. PSO is a method for finding a solution of stochastic global optimizer based on swarm intelligence. Using the interaction of particles, PSO searches the solution space intelligently and finds out the best one. Pan et al. (2010) built a model to forecast the hydrogen producing reactor temperature using global optimization of PSO and SVM local accurate searching. It was found that the developed model be feasible and effective. Comparative studies, by the authors, with other existing methods showed that the developed model was highly accurate and effective.

Perceptron were trained using particle swarm optimization model by Chau (2006). The model was used for prediction of water levels in the ShingMun river of Hong Kong. Different lead times calculated on the basis of the time history or upstream gauging stations were adopted at the specific station. It was observed that PSO can be an alternative technique to ANN.

Ahmadi et al. (2011) estimated gas-oil MMP using a model based on a feed-forward ANN optimized by Stochastic Particle Swarm Optimization (SPSO). Initial weights of the neural network were decided using SPSO. The performance of the SPSO-ANN model was compared with the field data and was found to be an effective model.

Tripathy et al. (2011) applied ANN and PSO model for weather prediction based on time series data. The parameters considered to be rainfall, maximum and minimum temperature, humidity, etc. It was tried that ANN and PSO tools for the prediction of future weather condition. They developed different training and testing to obtain the accurate result. Their experimental results showed that the proposed model was useful for weather forecasting.

Xi et al. (2012) applied PSO-Neural Network model in the prediction of groundwater level in Handan city based on the available old data and their influence factors. The random characteristics of ground heads in Handan city were analyzed by using PSO-NN. Their results indicated that the method was reliable and reasonable.

Nikelshpur et al. (2013) used particle swarm optimization to pre-train artificial neural networks for selecting initial weights for feed-forward back-propagation neural networks and showed that the average network training, validation, testing performance was improved significantly.

Hadi et al. (2016) studied, a new hybrid artificial neural network (ANN) models are developed for predicting K_t of π -type floating breakwaters (FB). Actually, a new algorithm that combines particle swarm optimization (PSO) and Levenberg-Marquardt (LM) is used for learning ANN models. These models are developed by the use of experimental data sets obtained from the K_t of π -type FBs using a wave basin of the University of a Coruna, Spain. It was found that model can be successfully applied for the prediction of the K_t . Also, results of proposed model showed that the efficiency of above model is improved compared to already introduce formulas. After assuring the acceptability of the prediction results, this model as one of an efficient tool was used for extending the experimental data and selection of the optimal design of π -type FBs in terms of the geometric characteristics.

Harish et al. (2015), applied hybrid PSO-SVM to predict the damage level of the non-reshaped berm breakwater. The results of research states that the PSO-SVM method gave higher accuracy compared to other soft computing models and can be used as an efficient tool.

2.3.5 Summary of Literature

From the economic point of view the breakwater represents a significant portion of capital investment of the port. These structures are prone to damage due to extreme wave loads during cyclones, storms, etc. Hence, shielding breakwaters from damage under such situations could be one of the solutions. One of the things engineers can do, is to design a protective structure in the front, which will withstand, resist and manage such destructive extreme events and at the same time, mitigate large damage of the inner main breakwater.

It is clear from the literature that the traditional protective structure to breakwater is the submerged reef as it breaks the steeper waves. These reef structures are used worldwide and possess certain advantages over the emerging structures in terms of cost and stability. The submerged reefs are used not only for the beach and harbour protection, but also for rehabilitation of damaged breakwater.

For decades, the breakwaters have been designed by conducting experiments on its stability through physical model studies (Hall and Kao, 1991; Van der Meer, 1992). Several researchers have carried out experimental, analytical and numerical studies on breakwaters in the past, but failed to give a simple mathematical model to predict the wave transmission over a submerged reef by considering all the boundary conditions. To understand the stability of tandem breakwater, a proper study of wave transmission over a submerged reef is essential.

The design of breakwater is site specific and physical model study in a laboratory is a must. However, under similar site conditions, where a new tandem breakwater has to be designed, the results of these soft computing techniques can be very well used. From literature, it is evident that experimental studies are expensive, laborious and lengthy in the procedure to conduct and are inconvenient for immediate needs. Subsequently, for minimizing cost, time and complexity involved in conducting the experiments, soft computing tools like Artificial Neural Network (ANN), Support Vector Machine (SVM) and their hybridization with various optimization techniques are being applied to solve wide variety of coastal engineering problems, when sufficient quantity of data is available.

Artificial neural networks and Support Vector Machines are effective and successful in solving various coastal engineering problems. ANN is trained using a set of data and once the model learns from the training data, predictions are better (Mase et al., 1995; Yagci et al., 2005; Kim et al., 2005). Support Vector Machines (SVM) has been used for the prediction of stability number of armor blocks of breakwaters (Balas, 2010) and also used to predict significant wave heights (Kim et al., 2010). Some of the hybrid techniques were used for the fundamental design of conventional rubble mound breakwaters and the results are found to be better compared to traditional designs (Van der Meer, 1988). The hybrid Genetic Algorithm based Support Vector Machine (GA-SVM) models are implemented for predicting wave transmission coefficient of horizontally interlaced multilayer moored floating pipe breakwater (Patil et al., 2012).

The soft computing models have also been used successfully for predicting damage levels, damage ratios of rubble mound breakwaters and different coastal engineering problems (Kennedy and Eberhart, 1995; Mehmet et al., 2011; Castro et al., 2011; Harish et al., 2012; Jian-Chuan et al., 2015; Hadi et al., 2016).

Further, Harish et al. (2015), applied hybrid PSO-SVM to predict the damage level of the non-reshaped berm breakwater. The results of his research states that the PSO-SVM method gave higher accuracy compared to other soft computing models. But, it is observed from literature that there are hardly any applications of ANN, SVM, ANFIS, PSO-ANN and PSO-SVM models to study the stability of tandem breakwaters. Hence, the objective of the present study is to investigate the applicability of soft computing and hybrid modelling approach for predicting the transmitted wave height (H_t/H_{tmax}) over a submerged reef and damage level conventional rubble mound breakwater of the tandem breakwater based on experimental data obtained by Rao and Shirlal in 2004.

2.4 PROBLEM FORMULATION

The literature review carried on theoretical and experimental analysis on breakwater revealed that, researchers have carried out a number of studies by considering conventional and submerged breakwaters individually and considering some common assumptions in hydrodynamics to derive mathematical models for wave transmission and damage. But, the mathematical models show very poor agreement with experimental or in-situ data (Allsop and Herbert, 1991). Waves in nature are random and hence, very difficult to model it in the lab. Also, the physical model studies are expensive and laborious. Further, literature on application of soft computing techniques in coastal engineering reveals that soft computing techniques have been successfully used to solve complex problems associated with coastal engineering. However, it is observed that there are hardly any applications of soft computing techniques in predicting wave transmission and damage of tandem breakwater. In view of the above aspects, a detailed study is taken up with developing soft computing techniques for the prediction of wave transmission over a submerged reef and damage level of the conventional rubble mound breakwater of tandem breakwater. These techniques are data driven and site specific, which will not replace the physical modelling. When the experimental data is available soft computing models developed using these data under similar site conditions, where a new tandem breakwater has to be designed, then soft computing techniques can be used effectively.

2.5 RESEARCH OBJECTIVE

The objectives of the present investigation involve the development of soft computing models to predict the wave transmission over a submerged reef and damage of the conventional rubble mound breakwater of tandem breakwater which are presented below

- To study the effects of various parameters on wave transmission over submerged reef and damage level of the conventional rubble mound breakwater of tandem breakwater through the development of Artificial Intelligence (AI) models.
- To investigate the ability of soft computing techniques such as Artificial Neural Networks (ANN), Support Vector Machines (SVM) to address various problems associated with tandem breakwater.
- To integrate and develop hybrid techniques of different combinations Adaptive Neuro-Fuzzy Inference System (ANFIS), Particle Swarm Optimization (PSO) based ANN and PSO based SVM to enhance accuracy and reliability of soft computing techniques.
- To analyze and recommend the most reliable soft computing model to predict the wave transmission and damage level of tandem breakwater.

CHAPTER 3

EXPERIMENTAL MODEL SETUP AND DATA USED

3.1. GENERAL

Breakwaters are massive structures absolutely necessary for building port and harbour and its structural stability and economy in construction are the need of the hour. This calls for an innovative design of the structure. But the stark reality is that, however safe the breakwater designs are, there are internal as well as external uncertainties which may become the prime reason for extensive damage to the structure. This may have catastrophic consequences for the port. Hence, it is decided that some kind of protection to the breakwaters could ward off significant damage or reduce its magnitude. Breakwaters may be protected by providing a submerged berm attached to the seaward side of the breakwater or providing a detached underwater/submerged breakwater depending upon the geometry of structure, type of damage, causes of failure, availability of construction material and equipment, financial constraints, future requirements for port expansion and other construction works (Groeneveld et al., 1984).

After going through the number of literature, it is observed that some kind of protection could ward off any danger to the stability of the breakwater. In this context, it is decided that a submerged reef could be an effective structure to protect the breakwater which reflects, dissipates energy and attenuate waves significantly, thereby reducing the intensity of wave action on the main conventional breakwater. Such a combined structure where the reef and the conventional breakwater acting together in resisting the wave attack is called tandem breakwater. Most of the literature indicates that the presence of submerged reef influences greatly the wave attenuation characteristics of the breakwater. The experimental data on wave transmission over a submerged reef and damage level of conventional rubble mound breakwater of tandem breakwater are collected from Rao and Shirlal (2004). The study was conducted in a two dimensional wave flume of the Marine

Structures laboratory, Applied Mechanics and Hydraulics Department, National Institute of Technology Karnataka, Surathkal, India. In the hydraulic model investigation, field conditions existing off Mangalore coast in Karnataka state of India were considered. The Laboratory conditions were decided through hydraulic modeling. The waves break over the reef, losing a major portion of energy and then lose some more energy while propagating in the zone between the structures as shown in Fig. 3.1(a). This phenomenon is difficult to express mathematically and one has to depend upon experimental investigations. The results of such investigations are more useful when expressed in the form of dimensionless relations. To arrive at such non-dimensional relationships between different variables, dimensional analysis was carried out using Buckingham- π theorem. The non-dimensional parameters influencing the phenomenon were obtained through dimensional analysis and are given in the Equation (3.1) and (3.2).

$$(K_t) = H_t / H_i = f [H_i / gT^2, X/d, H / \Delta D_{n50}, B/d, B/L_o, h/d, F/H_i, d/gT^2] \quad (3.1)$$

$$(S) = f [H_i / gT^2, X/d, H / \Delta D_{n50}, B/d, B/L_o, h/d, F/H_i, d/gT^2] \quad (3.2)$$

Rao and Shirlal (2004) conducted the non-dimensional parameters influencing the wave transmission (H_t / H_{tmax}) and damage level (S) of main breakwater are relative wave steepness (H_i / gT^2), the relative spacing (X/d), stability number ($H_i / \Delta D_{n50}$), relative crest widths (B/d), (B/L_o), relative crest height (h/d), relative submergence (F/H_i), relative water depth (d/gT^2).

The collected experimental data from the physical model study are used for developing computational intelligence models to predict the wave transmission over a submerged reef and damage level of main conventional rubble mound breakwater of tandem breakwater. Experimental data are collected and categorized and organized systematically. These data are divided into two sets, about 70% of the data for training and remaining data for testing models. While separating the data sets for training and testing care is taken to include all (full range) the range of data points.

In this chapter details of the experiments are explained along with the methodology adopted for the present study. Also, details about Artificial Neural Network, Support Vector Machines, and Hybrid models Adaptive Neuro-Fuzzy Inference System, PSO-ANN and PSO-SVM are described in chapter 4.

3.2 EXPERIMENTAL SET-UP

3.2.1 Details of wave flume

Rao and Shiral in 2004 tested the physical model in a two dimensional wave flume of Marine Structures laboratory, Department of Applied Mechanics and Hydraulics, National Institute of Technology Karnataka, Surathkal, India for regular waves. The wave flume is 50m long, 0.71m wide and 1.1m deep. It has a 41.5 m long, smooth concrete bed. About 15m length of the flume is provided with glass panels on one side. It has a 6.3m long, 1.5m wide and 1.4m deep chambers at one end where the bottom hinged flap generates the wave. The flap is controlled by an induction motor of 11Kw power at 1450rpm. This motor is regulated by an inverter drive (0-50Hz) rotating in a speed range of 0-155rpm. By changing the frequency through inverter one can generate the desired wave period. Regular waves of 0.08 m to 0.24 m heights and of periods 0.8sec to 4.0sec in a maximum water depth of 0.5m can be generated by this facility. Fig. 3.1(b) gives a schematic diagram of wave flume and Plate 3.1 shows the view of the experimental setup used.

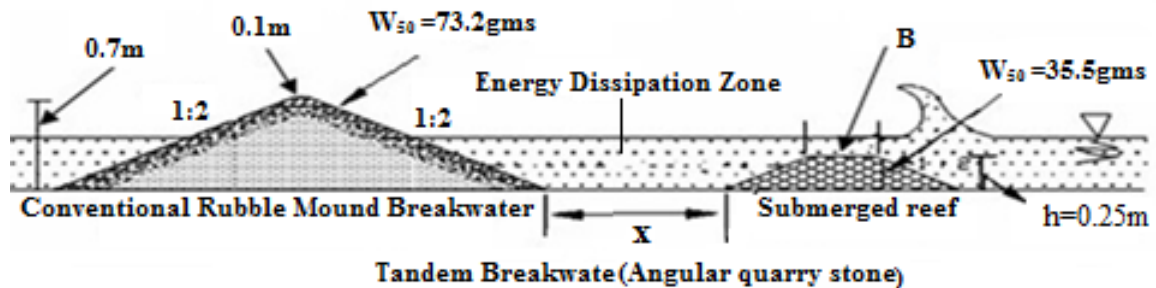


Fig. 3.1(a) Cross section of tandem breakwater

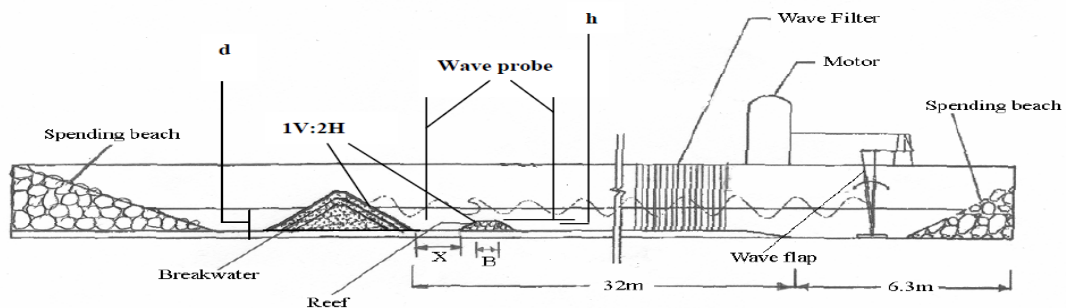


Fig. 3.1(b) Schematic diagram of regular wave flume setup with tandem breakwater



Plate 3.1 View of the experimental setup (Rao and Shirlal, 2004)

The capacitance type wave probes along with amplification units were used for data acquisition. Four such probes were used during the experimental work, three for acquiring incident and reflected wave heights (H_i and H_r) and one for transmitted wave heights (H_t). The spacing between probes was adjusted to one third of the wavelength to ensure accuracy as suggested by Isaacson (1991). The signals from wave probes are recorded by the computer through the data acquisition system. Then these signals were processed for separating the incident and reflected components using software based on the Isaacson's method. The data was collected using wave probes and data acquisition system, as shown in Plate 3.2. The damage level was measured using profiler system; the surface profiler system consists of a wooden frame with nine sounding probes at 0.075m centers to center. This was mounted on the railings on the side walls of the flume and can be moved along to take the profile of the breakwater model used in the experimental study (refer Plate 3.3).



Plate 3.2 View of wave flume with wave probes



Plate 3.3 View of wave flume with profiler

3.2.1.1 Experimental Procedure

The Wave flume was filled with water to the required depth (0.30m, 0.35m or 0.40m). The wave probes were calibrated at the beginning of the work. For a given wave period, waves of different heights were generated by changing the eccentricity of the crank which controls the movement of the wave flap. Thus, the flume was run for different combinations of wave periods and wave heights. Before starting the experiments, the flume was calibrated without breakwater structure for 0.4m, 0.45m and 0.5m water depths to find the incident wave heights for different combinations of frequency and eccentricity. The combinations producing the secondary waves in the flume were not considered in the experiments. The signals from the wave probe were recorded for transmitted wave height. Incident and transmitted wave heights were also cross-checked by measuring them manually. The waves were generated in bursts of five waves to avoid wave distortion due to reflection and re-reflection in the flume. The wave height on the seaside and the leeside of the breakwater were recorded for each burst. Six such trials were conducted and the average of the six values was recorded. Similarly, the peak values of the mooring forces were recorded, for both seaside and leeside mooring lines.

3.2.2 Data Collection and Interpretation

The data are collected from the experiments conducted by Rao and Shirlal (2004). The interpretation of the data is explained below.

Totally five phases of experiments (set no. I, II, III, IV and V), were conducted. In the first phase, this conventional breakwater model is tested. A 1:30 scale model of a breakwater, of trapezoidal cross section with a uniform slope of 1V:2H is constructed on the flat bed of the flume. The primary armour weight (W_{50}) for a design wave of 0.1m is determined using Hudson's formula to be 73.2gm (i.e. nominal diameter (D_{n50}) of 0.0298m). The actual weights of the armour stone used were varied from 55gm to 91gm with a mean value of 73.2gm. The model characteristics and the standard deviation and coefficient of variation of armour stone weight are given in Table 3.1. Plate 3.4 shows the cross section of conventional breakwater. The test section was subjected to normal wave attack of 3000 regular waves of height ranging from 0.1m to 0.16m of periods varied from 1.5sec to 2.5sec in a depth of water (d) of 0.3m, 0.35m and 0.4m. The Table 3.2 lists the test wave conditions (wave characteristics). The mean weight of the stones in the secondary layer was taken as 73.2gm. The model crest width was 0.1m and height of 0.70m. The core was designed with rock flour of size 300microns. The armour units were painted with different colours and placed in bands of heights of 0.2m to 0.3m to track their movement during damage.

Table 3.1 Model characteristics conventional breakwater

Variable	Expression	Value
Slope	α	1V: 2H
Armour type	--	Angular quarry stone
Armour weight	W_{50}	73.2gm
Standard deviation is	Σ	0.13
Coefficient of variation	C_v	0.046
Mass Density	P	2.8 gm/cc
Stability coefficient	K_D	3.5
Relative mass density of armour unit	Δ	1.6gm/cc
Layer coefficient	K_{Δ}	1.15
Nominal size of secondary armour unit	--	0.0298 m
Size of core material	--	300 microns
Crest width	--	0.1 m
Crest height	--	0.7 m
Thickness of primary armour layer	--	0.070 m
Thickness of secondary armour layer	--	0.032 m
Porosity of primary armour	p_1	43%

Porosity of secondary armour	p ₂	39%
Porosity of core	p ₃	36%



Plate 3.4 View of conventional rubble mound breakwater

The various sea state and structural parameters were considered by Rao and Shirlal (2004) for the experimental study is given in Table 3.2. They also performed dimensional analysis and arrived at the non-dimensional parameters, which influence the wave transmission over a submerged reef and damage level of conventional rubble mound breakwater of tandem breakwater as tabulated in Table 3.3.

Table 3.2 Wave characteristics

Variable	Expression	Values
Wave height	H _i	0.10, 0.12, 0.14 and 0.16 m
Wave period	T	1.5, 2.0 and 2.5 sec
Water depth	d	0.30, 0.35 and 0.40 m
Storm duration	N	3000 waves
Angle of wave attack	-	90 ⁰
Wave type	-	Regular
Depth parameter	d/gT ²	0.004 - 0.013, 0.005 - 0.015, 0.006 - 0.018
Steepness parameter	H _i /gT ²	0.00145 - 0.00785

In the second phase, a 1:30 scale model of trapezoidal submerged reef of slope 1V:2H, height (h) of 0.25m and crest width (B) of 0.1m was constructed, with natural armour of varying weight, on the flume bed at 28m away from the generator flap. Five such reef models were designed with natural armour weights considering various design criteria

(Ahrens, 1984, 1989; Gadre et al., 1992; Nizam and Yuwono, 1996 and Pilarczyk and Zeidler, 1996). The test section was subjected to normal wave attack of 3000 regular waves of height ranged from 0.1m to 0.16m, wave periods varied from 1.5sec to 2.5sec in a depth of water (d) of 0.3m as the reef stability was critical at the lowest water level (Smith et al., 1996). The damage to the structure was recorded in the form of reduction in crest height (h_c). From the test model an optimum design for stable submerged reef was derived. Plate 3.5 shows the cross section of the actual submerged reef with conventional rubble mound breakwater model constructed on the flume bed. The reef characteristics are tabulated in Table 3.3.

Table 3.3 Non-dimensional input parameters and their range used in the experiment

Sl. No.	Non-dimensional parameters	Notation	Range
1	Slope	α	1V: 2H
2	Reef Armour type	--	Angular quarry stone
3	Nominal diameter for reef	D_{50}	0.0221m
4	Reef Armour weight	W_{50}	15.4gm, 20.3gm, 25.5gm, 30.2gm, 35.3gm
5	Standard deviation	σ	2.61gm, 2.45gm, 3.42gm, 3.28gm, 4.56gm
6	Coefficient of variation	CV	0.17, 0.12, 0.13, 0.11, 0.13
7	Crest height of reef	h	0.25m
8	Crest width of reef	B	0.10, 0.20, 0.30 and 0.40m
9	Porosity of reef	--	43%
10	Reef spacing	X	At 1.0m, 2.5m and 4.0m seaward of main breakwater
11	Deep water wave steepness parameter	H_i/gT^2	1.46×10^{-3} to 7.85×10^{-3}
12	Depth parameter	d/gT^2	0.004 to 0.018
13	Relative Reef crest width	B/d	0.25 to 1.33
14	Relative Reef crest width	B/ L_o	0.01 to 0.114
15	Relative Reef submergence	F/ H_i	-0.312 to -1.5
16	Relative Reef crest height	h/d	0.625 to 0.833
17	Relative Reef spacing	X/d	2.5 to 13.33
18	Stability number	$H_i/\Delta D_{n50}$	2 to 3



Plate 3.5 View of submerged reef

In the third phase, the submerged reef of same geometry was constructed with armour of optimum weight and subjected to waves of heights (H_i) of 0.1m to 0.16m of period (T) of 1.5sec to 2.5sec in the depth of water (d) varying from 0.3m to 0.4m. The incident waves were recorded at 1m seaward of the reef. The transmitted wave heights (H_t) on the leeside were recorded for a distance of every metre up to 8m and required reef spacing was derived depending upon the maximum wave height attenuation achieved.

In the fourth phase, a stable trapezoidal submerged reef having a slope of 1V:2H with a crest width (B) of 0.1m and height (h) of 0.25m was constructed, with homogeneous pile of stones of optimum weight at varying seaward distances (X) from the conventional (main) breakwater within the required spacing derived (Fig. 3.1(b)). Plate 3.6 shows the top view of the protected breakwater with a conventional breakwater and seaward submerged reef. Plate 3.7 exhibits the top view of the protected breakwater. The submerged reef was constructed with a height (h) of 0.25m and varying crest width (B) from 0.1m to 0.4m (i.e. B/d of 0.25 to 1.33), using a homogeneous pile of natural stones of 30gms (i.e. D_{n50} of 0.0221m) optimum weight (Shirlal et al., 2003). The reef was located at varying seaward distance (X) of 1.0, 2.5 and 4.0m (i.e. X/d of 2.5 to 13.33) from the main breakwater as shown in Fig. 3.1(b). Then the model was tested for stability of breakwater under the same wave characteristics. After analysing the results, an optimum configuration for the tandem breakwater was derived and then models were tested.

Once the location of the reef was selected, the tests were repeated, in the fifth phase, with a reef of different crest widths (B) of 0.1m, 0.2m, 0.3m and 0.4m to arrive at the crest

width that protects the main breakwater. The model characteristics together with their possible range of application and wave characteristics are listed in Table 3.3.



Plate 3.6 View of protected breakwater



Plate 3.7 Top view of protected breakwater

3.2.3 Normalization of data and consistency check

Before dividing the data points into training and testing, the data points are normalized. Normalization of the training data set is required before loading it to the network for its supervised learning so that it satisfies the internal activation function range which lies between 0 to 1. Normalization is also necessary if there is a wide difference between the ranges of input and output data values. The normalization process increases the learning speed of the network and it avoids the possibility of saturation of the network earlier.

Normalization of each variable is done using the equation below, to make them in the range (Min value = 0, Max value = 1) using Equation (3.3).

$$X_{\text{norm}} = \frac{X - X_{\text{min}}}{X_{\text{max}} - X_{\text{min}}} \quad (3.3)$$

Where,

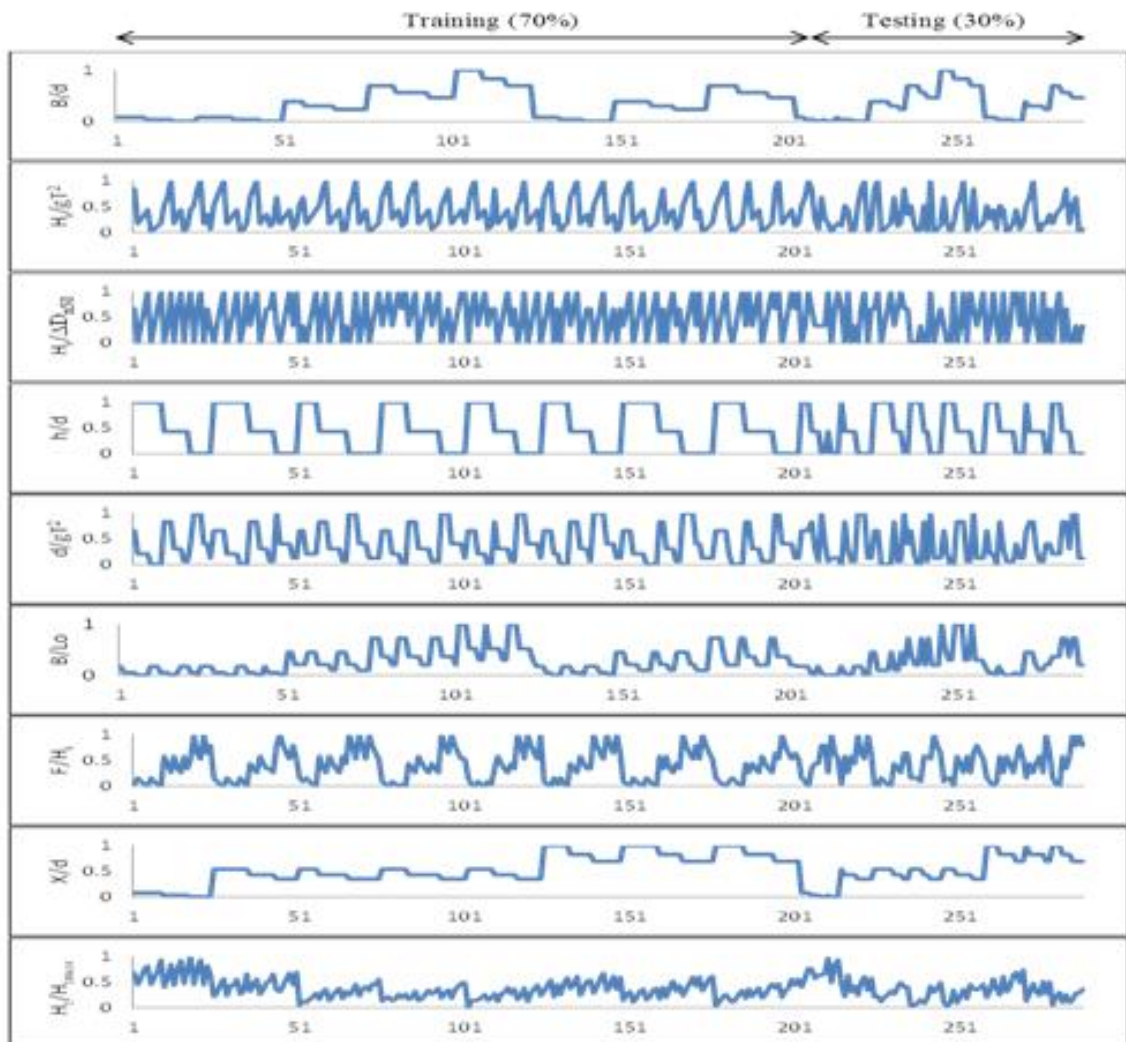
X_{norm} :The data points normalized between 0 to 1

X :Each data point

X_{max} : Maximum among all the data points

X_{min} : Minimum among all the data points

The consistency of the normalized data is checked using the time series plots as shown in the Fig. 3.2(a) for wave transmission and Fig. 3.2(b) for damage level.



Data set number (Number = 288) →

Fig. 3.2(a) Consistency of H_i/gT^2 , X/d , $H/\Delta D_{n50}$, B/d , B/L_0 , h/d , F/H_i , d/gT^2 and H_t/H_{tmax}

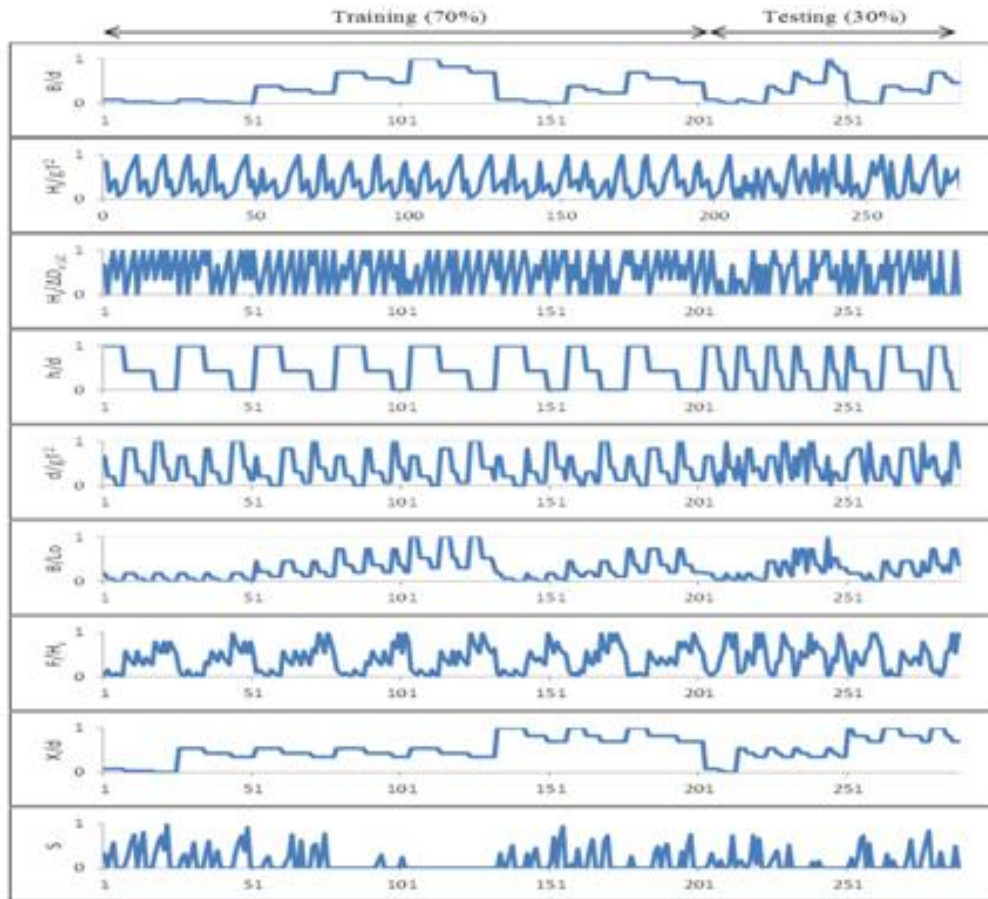


Fig. 3.2(b) Consistency of H_i/gT^2 , X/d , $H/\Delta D_{n50}$, B/d , B/L_0 , h/d , F/H_i , d/gT^2 and S

3.3 SUMMARY

This chapter discusses in detail the physical model study on Tandem breakwater carried out by Rao and Shirlal in 2004. It also discusses the wave flume features, experimental setup, experimental procedure and wave-specific and structure-specific parameters of outer submerged reef and inner conventional rubble mound breakwater. Non-dimensional input parameters are relative wave steepness (H_i/gT^2), the relative spacing (X/d), stability number ($H/\Delta D_{n50}$), relative crest widths (B/d), (B/L_0), relative crest height (h/d), relative submergence (F/H_i), relative water depth (d/gT^2), which influence the output parameters namely wave transmission (H_t/H_{tmax}) and damage level (S) of tandem breakwater are presented. Moreover, chapter also discusses how the data is collected, categorized, compiled and organized on wave transmission over the submerged reef and damage level of the main breakwater in a systematic way, which is considered for developing the soft computing models.

RESEARCH METHODOLOGY AND MODEL DEVELOPMENT**4.1 GENERAL**

As this study is based on developing AI and hybrid AI models for predicting wave transmission (H_t/H_{tmax}) and damage level (S) of a tandem breakwater, the basics of various modeling paradigms such as artificial neural network, adaptive neuro-fuzzy inference system, support vector machines and particle swarm optimization are discussed in this chapter.

4.2 ARTIFICIAL NEURAL NETWORK (ANN)

Artificial Neural network is a group of interconnected artificial neurons that can be used as a computational model for information processing. These are nonlinear statistical data modeling tools, used to develop a relationship between input and output. Mathematically, an ANN can be treated as universal approximations having ability to learn from examples without the need of explicit physics.

Neural Networks are computational models naturally performing a parallel processing of information. Essentially, an ANN can be defined as a pool of simple processing units (neurons) which communicate among themselves by means of sending analogue signals. These signals travel through weighted connections between neurons. Each of these neurons accumulates the inputs it receives, producing an output according to an internal activation function. This output can serve as an input for other neurons, or can be a part of the network output. There is a set of important issues involved in the ANN design process. As a first step, the architecture of the network has to be decided. Initially, two major options are usually considered: feed forward networks and recurrent networks.

4.2.1 Feed-forward backpropagation network (FFBP)

In the present research work, feed forward back-propagation neural network is used. The feed forward back-propagation architecture is developed in the early 1970s. Its greatest strength is in non-linear solutions to ill-defined problems. The

typical back-propagation network has an input layer, an output layer, and at least one hidden layer. There is no theoretical limit on the number of hidden layers but typically, there is just one or two. Each layer is fully connected to the succeeding layer, as shown in Fig. 4.1.

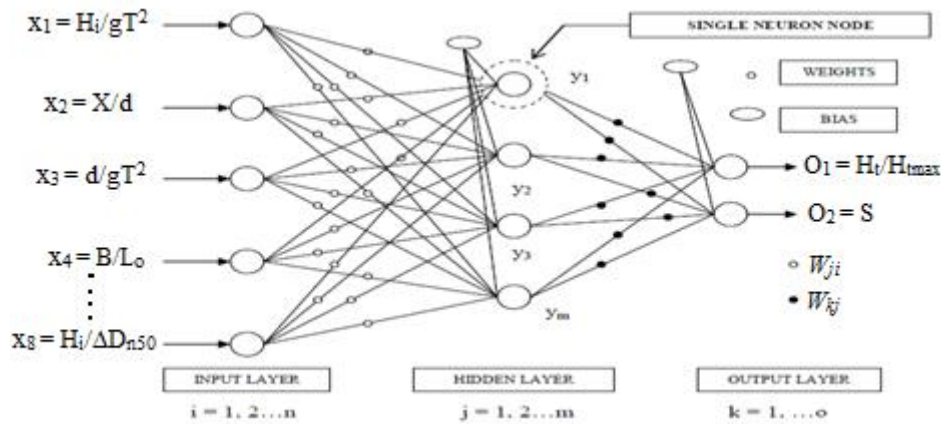


Fig. 4.1 Feed forward backpropagation neural network used in study

According to Kosko (2003), learning of feed forward backpropagation neural network is based on some variant of the Delta Rule, which begins with the calculated difference between the actual outputs and the desired outputs. The complex part of this learning mechanism is for the system to determine which input contributed the most to an incorrect output and how is that element changed to correct the error. An inactive node would not contribute to the error and would have no need to change its weights. To solve this problem, training inputs are applied to the input layer of the network, and desired outputs are compared at the output layer. During the learning process, a forward sweep is made through the network, and the output of each element is computed layer by layer. The difference between the output of the final layer and the desired output is back propagated to the previous layer(s), usually modified by the derivative of the transfer function, and the connection weights are normally adjusted using the Delta Rule. This process proceeds for the previous layer(s) until the input layer is reached. There are many variations of the learning rules for back-propagation network. A Different error functions, transfer functions, and even modifying method of the derivative of the transfer function can be used. A linear and non-linear transfer function is applied between input nodes and hidden nodes. In the present research work, 'purelin' and 'Tansig' are used as the linear and nonlinear transfer function respectively.

4.2.2 Training a neural network

In recent years, the research interest in Artificial Neural Network (ANN) has increased and many efforts have been made on applications of neural networks to various coastal engineering problems. ANN in coastal engineering is commonly used by the researchers to predict ocean wave parameters such as wave height, wave period, impact wave force etc. (Deo et al., 2001; Deo and Jagdale, 2003; Gunaydin, 2008; Londhe and Deo, 2003). Apart from this, it has provided promising results in prediction of tidal levels (Chang and Lin, 2006), damages to coastal structures (Mandal et al., 2007), depth of eroded caves in a seawall (Lee et al., 2009), storm surges (Tseng et al., 2007). The most significant features of neural networks are the extreme flexibility due to learning ability and the capability of non-linear function approximations. This fact leads us to expect neural networks to be an excellent tool for solving the governing characteristics of the tandem breakwater while overcoming complexity and non-linearity associated with wave-structure interaction of tandem breakwater. The process of training ANN models involves optimization of various parameters and is similar to calibration of a breakwater model. Generally, ANN models do not have any prior knowledge about the problem. The data enters the network through the input layer. The nodes in the input layer are not computational nodes and simply broadcast the data over weighted connections to the hidden nodes (Patil et al., 2012). The ANN are trained with a set of known input and output pairs called the training set.

In the training process, the weights are optimized to get a specific response from ANN. The network weights are initialized based on some previous experience or with a set of random values. These initial values of weights are then corrected during a training (learning) process. The weights in the hidden and output layer neurons are calculated using Equations (4.1) and (4.2) respectively,

$$w(N + 1) = w(N) - \eta \delta \phi \quad (4.1)$$

$$w(N + 1) = w(N) + \eta x \sum_{q=1}^r \delta_q \quad (4.2)$$

Where, w is training weight, N is the number of iterations, x is input value, η is learning weight and ϕ is the output. δ is defined as $2\varepsilon_q \partial\phi / \partial I$, where I is the sum of the weighted inputs, q is a neuron index of the output layer, and ε_q is error signal. The above training method is the standard backpropagation training method. The architecture of a typical FFBP network used in this study is also shown in Fig. 4.1. In the training

process, predicted results are compared to target, then the errors occurred are back propagated to obtain the appropriate weight adjustments necessary in minimizing the errors. The neural network model stops iteration for training, when the error becomes smaller than the target error. This error signal is propagated back and the weights are adjusted to reduce the difference between desired and computed outputs. The process of adjusting weights is continued until the required level of accuracy is obtained between target values and computed outputs. After learning, the weights are frozen. Then a data set that the ANN has not used before is presented to validate its performance. Depending on the outcome, the ANN has to be either retrained or can be implemented for its designated use.

4.2.3 Levenberg-Marquardt (LM) method

A number of training algorithms are developed for error back propagation learning. In the present research work, Levenberg-Marquardt method is used to train the feed forward back-propagation neural network. The Levenberg-Marquardt method is a second-order method (Hagan and Menhaj, 1994; Masters, 1995). Rather than finding the error minimum directly, it aims to locate the zero of the error gradient. LM is a combination of steepest descent and Gaussian-Newton method. LM algorithm has the fast convergence among other algorithms and it is able to obtain lowest mean square error in many cases. Referring to the recommendations given by many researchers, all the ANN models in this study used only one hidden layer. Different ANN architectures for modeling wave transmission and damage level are tested by varying the number of neurons in the hidden layer. A trial and error procedure was adopted to find the optimum number neurons in the hidden layer.

In the present study, three-layered feed forward backpropagation with Levenberg-Marquardt updated algorithm is used to predict the wave transmission and damage level of tandem breakwater.

4.2.4 Feed forward backpropagation neural network for wave transmission and damage level prediction of tandem breakwater

In order to allow the network to learn both non-linear and linear relationships between input nodes and output nodes, multiple-layer neural networks are often used. In the present work, the three layers feed forward backpropagation neural network is used to

represent the input nodes as first layer, hidden nodes as second layer and output nodes as the third layer.

The back-propagation is a supervised learning technique used for training the neural network. The back propagation needs to know the correct output for any input parameters. The number of input nodes depends upon the complexity of the problem and the parameters, which influence the output parameters.

The main objective of back propagation neural network technique is to train the model such that the resultant outputs are nearer to the desired values. Therefore, the error between network output and desired value is minimized.

Mathematically, the feed forward artificial neural network is expressed as:

$$Z_k(x) = \sum_{j=1}^m W_{kj} \times T_r(y) + b_{ko} \quad (4.3)$$

$$y = \sum_{i=1}^n W_{ji} \times x_i + b_{ji} \quad (4.4)$$

Where, x is input value from 1 to n , W_{ji} - are the weights between input layer and hidden layer nodes and W_{kj} are the weights between hidden layer and output layer nodes. b_{ji} and b_{ko} are bias values of hidden and output layer respectively. m is the number of hidden layer nodes and $T_r(y)$ is transfer function. This transfer function allows a non-linear conversion of summed inputs.

A non-linear transfer function is applied between input nodes and hidden nodes. In the present research work, *Tansig* is used as the transfer function, which is expressed as:

$$T_r(y) = \left[\frac{2}{1 + \exp(-2 \times y)} - 1 \right] \quad (4.5)$$

Where, y is the summation of input values with weights and biases. The transfer function improves the network generalization capabilities and speeds up the convergence of the learning process. The bias values for both hidden layer (b_{ji}) and output layer (b_{ko}) get adjusted at each time of iterations. The weights between hidden and output layers are calculated using updated Levenberg-Marquardt algorithm.

In the present research work, the linear transfer function *purelin* is applied between hidden layer and output layer, and it is expressed as:

$$purelin(n) = n \quad (4.6)$$

The overall objective of training algorithm is to reduce the global error, E , defined as:

$$E = \frac{1}{p} \sum_{p=1}^p \left[\sum_{k=1}^k (d_{kp} - o_{kp})^2 \right] \quad (4.7)$$

Where, p is the total number of training patterns, d_{kp} is the desired value of the k^{th} output and the p^{th} pattern, o_{kp} is the actual value of the k output and p pattern.

Here, Levenberg-Marquardt (LM) updated algorithm (Wilamoski et al., 2001) is used to train the network. The codes are written in MATLAB 13 platform. The correlation coefficient is calculated to know the how best the network predicted values are matched with the measured values. The straight line is drawn at an angle of 45° between the two axes to fit the data points. A high correlation is obtained when all the points lie exactly on this straight line.

4.3 ADAPTIVE NEURO-FUZZY INFERENCE SYSTEM (ANFIS)

ANFIS was first introduced by Jang (1993). Fuzzy logic has a great advantage of representing knowledge very precisely giving good explanation and reasoning in an understandable manner. ANN is fault tolerant and it has a great capability of learning on its own. But, the representation of knowledge stored is in the form of connection between the neurons which is difficult to understand. Hence, if both the techniques are combined, a huge advantage of self-learning and an understanding knowledge representation is possible. Further, ANN requires crisp data and preparation of such data is tedious and time consuming. This can be avoided by developing an interface that directly inputs the environmental fuzzy data which can be done by using fuzzy logic. This combination is the neuro-fuzzy approach, popularly called as Adaptive Neuro-Fuzzy Inference System (ANFIS) has been developed.

4.3.1 Architecture of ANFIS

ANFIS is a combination of least-squares and back propagation gradient decent methods, used for training Takagi-Sugeno type fuzzy inference system, which is used in an effective search for the optimal parameters for obtaining single output by feeding multi inputs. It can provide a starting point for constructing a set of fuzzy ‘if-then’ rules, with appropriate membership functions to generate the fixed input-output pairs. ANFIS is a simple structure with effective learning algorithm and high speed (Vairappan et al., 2009). ANFIS training can use alternative algorithms to reduce the error of the training. The advantage of a hybrid approach is that it converges much faster, since it reduces the

search space dimensions of the back propagation method used in neural networks. Using the experimental data, ANFIS models are developed using different membership functions. The results obtained will be compared with experimental data for validation.

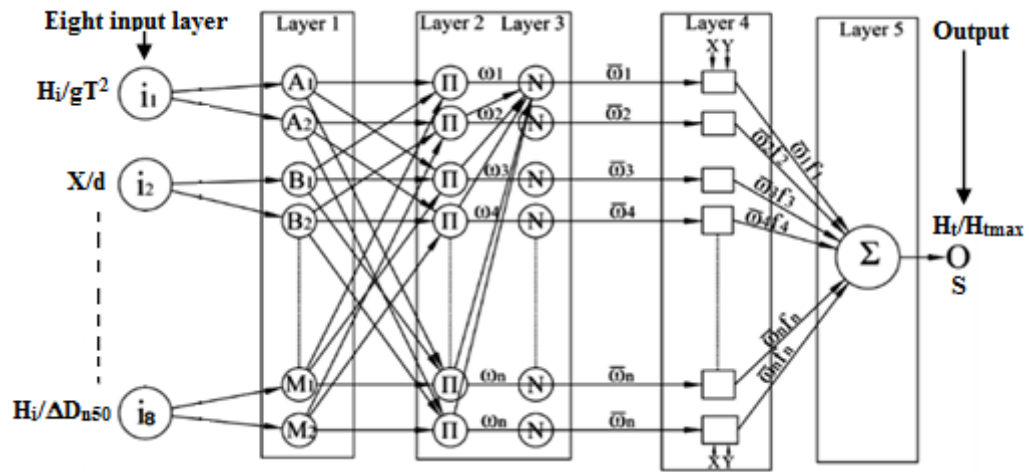


Fig. 4.2 ANFIS structure used in the study

A general and simple architecture of ANFIS with eight input variables namely H_i/gT^2 , X/d , $H_i/\Delta D_{n50}$, B/d , B/L_o , h/d , F/H_i , d/gT^2 and the output variable is $O = (H_t/H_{tmax})$ and $S = A_e/D_{n50}^2$ (refer Fig. 4.2). A conventional ANFIS model consists of five layers and each layer is explained below in brief by Jang et al. (1997)

Layer 1

Every node in this layer is an adaptive node with a node function

$$O_{1,i} = \mu A_i(x), \quad \text{for } i=1,2 \quad (4.8)$$

$$O_{1,i} = \mu B_{i-2}(x), \quad \text{for } i=3,4 \quad (4.9)$$

x (or y) is the input node and A_i (or B_{i-2}) is a linguistic variable associated with the membership function of a fuzzy set A_1, A_2, B_1, B_2 . Typical membership function:

$$\mu A(x) = \frac{1}{1 + \left[\frac{c_i}{a_i} \right]^{2b_i}} \quad (4.10)$$

Where a_i, b_i and c_i is the parameter set. The parameters are called as premise parameters.

Layer 2

Each node in this layer is a fixed node, indicated by π Norm. The output is the product of all the incoming signals.

$$O_{2,i} = w_i = \mu A_i(x) \cdot \mu B_i(y), \quad i=1,2 \quad (4.11)$$

Output signal w_i represents the fire strength of a rule.

Layer 3

Each node in this layer is a fixed node N Norm. The i^{th} node calculates the ratio of the firing strength to the sum of the firing strength.

$$O_{3,i} = \bar{w}_i = \frac{w_i}{w_1 + w_2}, \quad i=1,2 \quad (4.12)$$

Output signal \bar{w}_i is called normalized firing strengths.

Layer 4

Each node in this layer is an adaptive node, indicated by square node with a node function:

$$O_{4,i} = w_i f_i = w_i (p_i x + q_i y + r_i) \quad (4.13)$$

Where, w_i is the normalized firing strength from layer 3. $\{p_i, q_i, r_i\}$ is the parameter set which is called as consequent parameters.

Layer 5

Each node in this layer is a fixed node, indicated by circle which computes the overall output as the summation of all incoming signals:

$$\text{Overall output, } S = O_{5,1} = \sum_i \bar{w}_i f_i = \frac{\sum_i w_i f_i}{w_i} \quad (4.14)$$

The different membership functions assigned for input parameters are: Gauss membership function:

$$f(x, \sigma, c) = e^{-\frac{(x-c)^2}{2\sigma^2}} \quad (4.15)$$

where, x is input parameters, c and σ are mean and variance respectively. Triangular membership function

$$f(x, a, b, c) = \max\left(\min\left(\frac{x-a}{b-a}, \frac{c-x}{c-b}\right), 0\right) \quad (4.16)$$

where, x is an input parameter, a and c locate the feet of the triangle and b locate the peak.

Generalized bell-shaped membership function is given by:

$$f(x, a, b, c) = \frac{1}{1 + \left|\frac{x-c}{a}\right|^{2b}} \quad (4.17)$$

where, x is an input parameter, c locates the centre of the curve.

Thus, an adaptive network is functionally equivalent to a Sugeno-type fuzzy inference system. In this study, a hybrid approach combining least square error and backpropagation methodology is adopted to develop all the ANFIS models. The performance of 2, 3 and 4 membership functions (MF) with triangular, trapezoidal, Gaussian, and generalized bell-shapes are evaluated to determine the most efficient model.

4.4 SUPPORT VECTOR MACHINE REGRESSION (SVMR)

SVM is the recently developed learning techniques that have gained enormous popularity in the field of classification, pattern recognition and regression. SVM works on structural risk minimization principle that has a greater generalization ability and is superior to the empirical risk minimization principle as adopted in conventional neural network models. Han et al. (2007) applied SVM for flood forecasting, Msiza et al. (2008) used ANN and SVR for water demand prediction, Rajasekaran et al. (2008) developed a support vector machine regression (SVMR) model for forecasting storm surges. They compared these results with numerical methods and ANN, which indicated that storm surges and surge deviations are efficiently, predicted using SVMR.

Mahjoobi and Mosabbebi (2009) presented that the SVMR creates a more reliable model with better generalization error, in comparison to ANN, they also reveal that SVMR do not over-fit, while ANN may face such problem and need to deal with it. However, it is observed that there are less number of applications of SVMR in predicting wave transmission and damage level of tandem breakwater. This fact leads us to use SVMR models in this work.

4.4.1 Theoretical background of SVMR

Support Vector Machine is a unique state-of-the-art classification and regression technique based on the framework of Vapnik's statistical learning theory. Cortes and Vapnik (1995) designed SVM to solve complex regression problems. The SVMR technique has been effectively used to perform multivariate function estimation, nonlinear regression problems, etc. due to its competence to escape from local minima, improved generalization capability and sparse representation of the solution (Vapnik, 1999). SVMR is based on structural risk minimization principle wherein it addresses the problem of overfitting by balancing the model's complexity. Nonlinear problems are tackled by transforming them into linear ones in multi-dimensional feature space using Kernel functions. The structure of SVMR is represented in Fig. 4.3. With the innovation of Vapnik's ϵ -insensitivity loss function, the SVMR is more capable of solving nonlinear regression problems (Smola and Scholkopf, 2004). In order to achieve a good generalization performance, it is essential to find certain optimal hyperparameters of SVMR model. The hyper-parameters that need to be tuned are the SVM parameter (C) that controls the generalization performance of SVMR, secondly, the kernel parameter

specific to the type of kernel adopted and finally the radius of the e-insensitive zone which determines the number of support vectors (Kecman, 2001). A brief description and derivation of support vector regression can be referred from various literature such as Cristianini and Shawe-Taylor (2000); Gunn (1998); Cortes and Vapnik (1995).

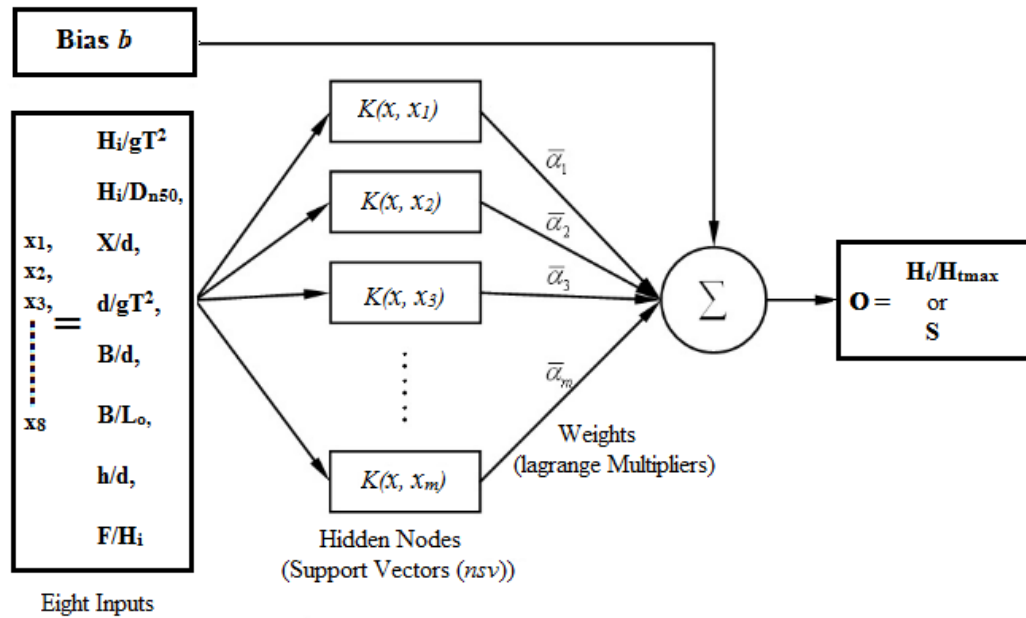
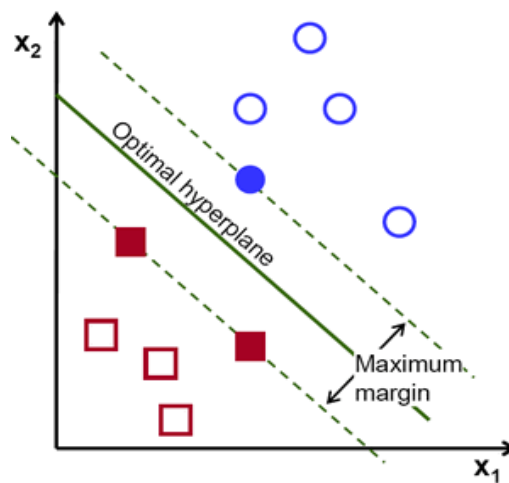


Fig. 4.3 Network- architecture of SVM

4.4.2 Support Vector Machine (SVM) Model Development

The methodology followed in developing the SVM models with different kernel functions and selecting the best kernel configured SVM model to predict the wave transmission and damage level is discussed below



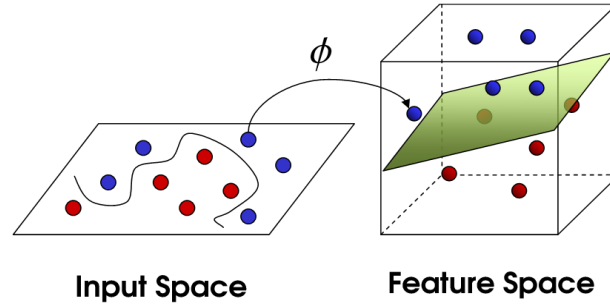


Fig. 4.4 The loss margin setting corresponds to one-dimensional linear SVM to D dimensional nonlinear SVM

In a theoretical background, a simple description of the Support Vector Machine algorithm is provided as follows. Given a training set be $\{(x_i, y_i), i = 1, \dots, n\}$, where x_i and y_i are i^{th} input training pattern & i^{th} target output and has 'n' data sets for training. For nonlinear case SVM has the form as shown below

$$f(x, \alpha) = (w \cdot \phi(x)) + b \quad (4.18)$$

Where, 'w' is the weight vector and 'b' is the bias. $\phi(x)$ is a mapping function to a higher dimensional feature space from input features. The regression problem will be as similar as minimizing the regularized risk function (Lee et al., 2007) is shown below.

$$R(f) = \frac{1}{n} \sum_{i=1}^n L(y_i, f(x_i, w)) \quad (4.19)$$

Where,

$$L(y_i, f(x_i, w)) = \begin{cases} \varepsilon, & \text{if } |y_i - f(x_i, w)| \leq \varepsilon \\ |y_i - f(x_i, w)| - \varepsilon, & \text{otherwise} \end{cases} \quad (4.20)$$

Smaller weight parameters are required to increase the smoothness of target function and to enhance its generalization capability. Target function $(y_i, f(x_i, w))$ is found out with maximum error in ε -SV regression problem (Smola and Scholkopf, 2004). To accomplish this, Vapnik introduced ε -insensitive loss function. According to this concept, $|y_i - f(x_i, w)|$ should not be more than ε . This can be explained with the help of Fig. 4.4. The above figure represents the soft margin loss of a linear SVMR model. The firm line in the figure is the predicted values and circular points are the measured or target values within the ε -insensitive tube, represented by dashed lines. These circular points have less than ε deviation from actual target function $(y_i, f(x_i, w))$ or predicted values. However, the box points are lying outside the ε -insensitive tube. Three box points are shown as examples. One point has ξ_i deviation from the upper bound and another point has ξ_i^* , the

deviation from the lower bound. Therefore, these points should be penalized to maintain the ε precision with convex optimization of the prediction model.

Where, ε is an insensitive loss function, on substitution in Equation (4.19), optimization equation will be minimized,

$$\frac{1}{2}w \cdot w + C \cdot \left(\sum_{i=1}^n \xi_i^* + \sum_{i=1}^n \xi_i \right) \quad (4.21)$$

Where,

$$\text{subject to } \begin{cases} y_i - w \cdot x_i - b \leq \varepsilon + \xi_i^* \\ w \cdot x_i + b - y_i \leq \varepsilon + \xi_i, \quad i = 1, \dots, n \\ \xi_i, \xi_i^* \geq 0 \end{cases}$$

Where, the constant $C > 0$ means the penalty degree of the sample with error exceeds epsilon, ξ_i, ξ_i^* are slack variables. By using this optimization a dual problem can be attained by maximizing the function,

Maximize,

$$\sum_{i=1}^n y_i (\alpha_i^* - \alpha_i) - \varepsilon \sum_{i=1}^n (\alpha_i^* - \alpha_i) - \frac{1}{2} \sum_{i,j=1}^n (\alpha_i^* - \alpha_i) (\alpha_i^* - \alpha_j) \{ \varphi(x_i) \cdot \varphi(x_j) \} \quad (4.22)$$

Where

$$\text{Subject to } \begin{cases} \sum_{i=1}^n (\alpha_i^* - \alpha_i) = 0 \\ 0 \leq \alpha_i^*, \alpha_i \leq C \end{cases}$$

Where α_i^* and α_i are Lagrange multiplier and $(\varphi(x_i) \cdot \varphi(x_j) = K(x_i, x_j))$ is kernel function.

The key idea is to construct the Lagrange function from the primal objective function and corresponding constraints by introducing the dual set of variables. By using the above maximization function the non-linear regression function is obtained as,

$$f(x, \alpha^*, \alpha) = \sum_{i=1}^n (\alpha_i^* - \alpha_i) K(x_i, x) + b \quad (4.23)$$

Where,

$$w \cdot \varphi(x) = \sum_{SVs} (\alpha_i^* - \alpha_i) K(x_i, x) \quad (4.24)$$

$$b = -\frac{1}{2} \sum_{SVs} (\alpha_i^* - \alpha_i) [K(x_r, x_i) + K(x_s, x_i)] \quad (4.25)$$

Where, x_r and x_s are support vectors (SVs) number of support vectors, $0 \leq \alpha_i^*, \alpha_i \leq C$. There are various kernels like linear, polynomial, radial basis function, sigmoid kernel, etc. Here polynomial kernel with second degree (Quadratic Kernel) form of the same is presented below

$$K(x_i, x_j) = ((\gamma * x * y) + c)^d \quad (4.26)$$

Where, ‘ γ ’ is a kernel function parameter, c is the coefficient of the polynomial. When $c = 0$ polynomial is homogenous and ‘ d ’ is the degree of the polynomial. The role of the kernel function simplifies the learning process by changing the representation of the data in the input space to a linear representation in a higher-dimensional space called a feature space. A suitable choice of kernel allows the data to become separable in the feature space despite being non-separable in the original input space. This allows us to obtain a non-linear algorithm from algorithms previously restricted in handling linearly separable datasets. The function that satisfies Mercer’s condition (Vapnik, 1995) can be used as the kernel function.

In the present work, the different kernel functions and inputs are experimented as shown in Table 4.1 and Table 4.2. The linear kernel function is used for linear SVMR model, whereas the polynomial, radial basis function (RBF) kernels are used for non-linear SVMR models. According to Karatzoglou and Meyer (2006), Gaussian radial basis function kernel is the general purpose kernel used when there is no prior knowledge about the data. The linear kernel is useful, when dealing with large sparse data vectors, as usually the case in text categorization. The polynomial kernel is popular in image processing. Selection of two kernel parameters (d, γ) and support vector machine parameters (C, ε) of a SVM model is significant in accuracy of the forecasting, where, the parameter d represents the degree of polynomial kernel functions, whereas, γ is the width of RBF kernel functions.

Table 4.1 Data used for training and testing the SVMR models with input parameters

Model	Input Parameters	Number of data points for training	Number of data points for testing
SVMR(linear)	$H_i/gT^2, X/d, H/\Delta D_{n50}, B/d, B/L_o, h/d, F/H_i, d/gT^2$	201	87
SVMR(polynomial)			
SVMR(RBF)			
SVMR(sigmoid)			

Table 4.2 Different kernel functions

Kernels	Functions
linear	$K(x_i, x_j) = ((x_i, x_j) + 1)^d$
polynomial	$K(x_i, x_j) = (\gamma * x * y + c)^d$
RBF	$K(x_i, x_j) = \exp\left(-\frac{\ x_i - x_j\ }{2\gamma^2}\right)$

The generalization performance of SVMR depends on a good setting of C , ε and kernel parameters d and γ . Parameter C determines the trade-off between the model complexity (flatness) and the degree to which deviations larger than ε tube (Smola, 1996; Gunn, 1998). If C is too large (infinity), then the objective is to minimize the empirical risk only, without regard to the model complexity (Cherkassky and Ma, 2004). In the present study, the quadratic loss function is used. The main idea of using this loss function is to ignore the errors, which are situated within the certain distance of the true value. Parameter ε controls the width of the ε -insensitive zone, which is used to fit the training data. The number of support vectors (nsv) used to construct a regression function depends on ε and the big ε , the fewer support vectors are selected and results in data compression (Kecman, 2001). The performance of SVMR depends on the good setting of SVM and kernel parameters. As there are no general rules to determine the free parameters, the optimum values are set by two-stage grid search method. Initially a coarse search (i.e. for $C=100, 500, 1000$; $\varepsilon=1, 2$; d and $\gamma = 1, 2, 3$) is performed to identify the near optimal values, and then a fine search (i.e. for $C=10, 20, 30$; $\varepsilon=0.001, 0.01, 0.1, 1$; d and $\gamma=0.001, 0.01, 0.1, 1$) is done to identify the optimal values.

Choice of kernel functions and hyper-parameters are some critical issues needed to be addressed before the application of SVM. Radial basis function (RBF) a more compactly supported kernel function is able to reduce the computational complexity of the training process and provides a good performance. Hence, the RBF kernel function is employed in this study. Different techniques for tuning of the hyper-parameters related to the regularization constant are available in the literature. In this study the regularization parameter gamma (γ) and kernel function tuning parameter ($1/2\gamma^2$) are obtained by K -fold technique based on leave-one-out cross validation (Bethani et al., 2016). The RBF Kernel function shown in Equation (4.26), says that the distance between two support

vectors is computed and used as the input to a Gaussian with one tuning parameter $T=1/2\gamma^2$. The RBF does not take into account the potential bandwidth differences between dimensions in the input data which may cause tension and norm (very small values) between support vectors may result in the loss of information. It can be extended to include another tuning parameter for each dimension in the input space referred as multi Gaussian Kernel function. In this study the non-dimensional input parameter are used instead of improved tuning parameters so that model prediction is accurate and efficient (Bethani et al., 2016).

4.5 PARTICLE SWARM OPTIMIZATION (PSO)

Swarm Intelligence (SI) is artificial intelligence based on the collective behaviour of decentralized, self-organized systems.

Origins

PSO is an optimization technique, which is based on the population. It is a stochastic optimization technique motivated by social behaviour, such as bird flocking and fish schooling. PSO was first proposed by Kennedy and Eberhart in 1995. The behavior of PSO is very simple and is displayed in three steps as shown in the Fig. 4.5 (Reynolds, 1987), in step 1: the flocks are separated by avoiding crowding local flock mates, next in step 2: the local flock mates will move towards heading average by forming an alignment and finally in step 3: the local flock mates will lastly move towards the average position by the process known as cohesion. The PSO application is to optimize the particle swarms. PSO gathers the social experience and combine it with the self-experience.

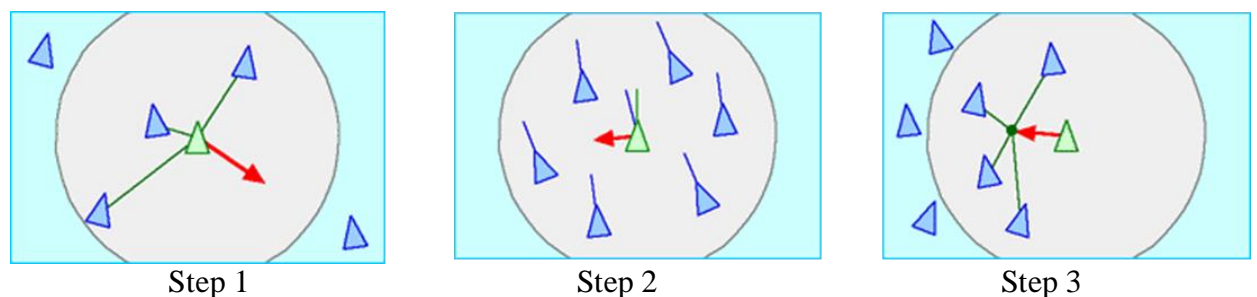


Fig. 4.5 Separation, alignment and cohesion stage of PSO process respectively, (Reynolds, 1987)

Concept

The concept of PSO is such that, it uses a number of agents (particles) that constitute a swarm, moving around in the search space looking for the best solution. Each particle in the search space adjusts its “flying” according to its own flying experience as well as the flying experience of other particles. Firstly, collects flying particles (swarm) by changing solutions and then it search the area and finds possible solutions. After finding possible solution, the process moves towards a promising area to get the global optimum. In which, each particle keeps track: such as its best solution, personal best, pbest and the best value of any particle, global best, gbest. Each particle adjusts its travelling speed dynamically corresponding to the flying experiences of itself and its colleagues. Once particles adjust their travel speed and then modify its position according to its current position, its current velocity, the distance between its current position and pbest and the distance between its current position and gbest.

4.5.1 PSO Algorithm and Rules

The parameters and rules used for developing the hybrid algorithms in the present study are explained below

A : Population of agents, p_i : Position of agent a_i in the solution space, f : Objective function, v_i : Velocity of agent's a_i , $V(a_i)$: Neighborhood of agent a_i (fixed). The neighborhood concept in PSO is not the same as the one used in other meta-heuristics search like GA, since in PSO each particle's neighborhood never changes (is fixed). The general particle update rule is defined as, $p = p + v$ and $v = v + c_1 * rand * (pBest - p) + c_2 * rand * (gBest - p)$

where, p : particle's position, v : path direction, c_1 : weight of local information, c_2 : weight of global information, $pBest$: best position of the particle, $gBest$: best position of the swarm, $rand$: random variable.

The importance of algorithm parameters can be explained by the selection of the number of particles usually between 10 and 50, where, c_1 implies the importance of personal best value and c_2 implies the importance of neighbourhood best value. Usually, $c_1 + c_2 = 4$ (empirically chosen value). If the velocity is too low we can say that algorithm is too slow and if velocity is too high, the algorithm is too unstable.

4.5.2 Proposed hybrid PSO-ANN and PSO-SVM models

Hybrid models are proposed to enhance the convergence speed of ANN model and model accuracy and to ensure the global optimal response. An avoid overfitting or under fitting caused due to improper selection of SVM model with suitable kernel parameters. PSO is used to select suitable governing parameters of ANN and SVM. PSO is an optimization technique, which has the number of advantages over the other optimization techniques such as insensitive to scaling of design variables, implementation of technique is very simple and has a capacity to easily parallelize the concurrent processing by using very few algorithm parameters with derivative free and very efficient global search algorithm. In the present study, ANN tool box is interfaced with particle swarm optimization to optimize the hidden neurons of the proposed PSO-ANN model. Similarly, PSO tool box is interfaced with SVM and kernel parameters simultaneously for better generalization of proposed PSO-SVM model.

4.5.3 Training PSO-ANN and PSO-SVM

ANN hybrid models are developed by using various numbers of hidden layers, hidden nodes and SVM model with various kernel parameters. To study the performance of each ANN network and SVM model, ANN and SVM hybrid models are developed to predict both the wave transmission and damage level of tandem breakwater. The experimental data set is then divided a priori (Swingler, 1996) into two subsets, namely training (70%) and testing (30%) data sets, respectively, since there are no mathematical rules to determine the required sizes of these data subsets (Basheer et al., 2000). The training set is used in learning phase while the testing set is used to check the generalization capabilities of the first model. The range of parameters used in the training and testing phases of neural networks and SVM models is given in Table 4.3.

In the training stage of PSO-ANN for predicting the wave transmitted and damage level the 'trainlm' parameter is replaced by 'trainps' so that the number of hidden layers and hidden nodes are optimized by PSO and error is measured using the fitness parameters as RMSE (Ghasemi et al., 2017); Roy et al., 2013). The statistical parameters are calculated for ANN hybrid for varying numbers of hidden neurons and the network with best prediction is considered as optimum.

Table 4.3 The range of parameters in the data set used for the training and testing phases of artificial intelligence models.

Design Parameters	B/d	H _i /gT ²	X/d	F/H _i	H _i /ΔD _{n50}	B/L ₀	h/d	d/gT ²	H _t /H _{t max}	S
Maximum	1.33	0.72	13.3	15	3.51	0.11	8.33	1.81	1	14
Minimum	0.25	0.16	2.5	3.13	2.19	0.01	6.25	0.49	0.279	0
Mean	0.62	0.38	8.3	7.9	2.9	0.04	7.2	1.01	0.55	1.97
Standard Deviation	0.32	0.17	3.06	3.58	0.493	0.03	0.85	0.44	0.140	3.35
Coefficient of variation	0.83	1.21	0.04	0.06	0.061	17.6	0.02	0.43	0.469	0.86

4.5.3.1 The steps followed in PSO-ANN model development

Step 1: Select the ANN network architecture with different hidden layers and hidden neuron to optimize using PSO.

Step 2: Initialize random positions and velocities to each selected data point. In this study, 201 particles (data points) are selected for learning different networks by PSO.

Step 3: After initialization, the objective of the technique is to update the each particle with new particle velocity as given by the equation

$$Vel_{j+1}^i = W_j Vel_j^i + C_1 rand_1 (pbest_j - pos_j^i) + C_2 rand_2 (gbest_j - pos_j^i) \quad (4.27)$$

Step 4: Once the velocity is updated, the particle position should also be updated successively as given by equation

$$pos_{j+1}^i = pos_{j+1}^i + Vel_{j+1}^i \quad (4.28)$$

In the equations above, the details are given below

pos_j^i is the current position of the particle i corresponding to the representing iteration count j , Vel_j^i is the search velocity of the i^{th} particle for j^{th} iteration count, C_1 and C_2 the cognitive and social scaling parameters, $rand_1$ and $rand_2$ are the random numbers in the interval $[0, 1]$ applied to the i^{th} particle, w_j is the particle inertia, $pbest_j$ is the best position found by the i^{th} particle (personal best), and $gbest_j$ is the global best position found among all the particles in the swarm. The number of companions will affect the convergence speed of the algorithm. The cognitive component represents learning achieved from an individual particle search come across. In contrast, the social scaling parameter represents the cooperation among the companions learning from search experience.

Step 5: Lastly, calculate the fitness value.

$$W_j = w_{Max} - [(w_{Max} - w_{min}) \times iter] / \max_{iter} \quad (4.29)$$

Where, w_{Max} = initial weight, w_{min} = final weight,

\max_{iter} = maximum iteration number, $iter$ = current iteration number.

The particle inertia controls the balance of global and local search abilities, where a larger inertia weight (w) helps for global search while a small inertia weight helps for a local search. By decreasing the inertia weight linearly from the larger value to a smaller value through the course of the PSO run gives the best PSO performance comparisons with fixed inertia weight settings. Particle i flutters towards a new position using Equation (4.27) and Equation (4.28), which allow all particles in the swarm to update their $pbest_j$ and $gbest_j$, (refer Fig. 4.6).

Step 6: Repeat step 2 to 4 until the targets are met.

Step 7: Once the target is reached, performance of the model predictions is evaluated using Model performance indicators such as Equations (4.30) (4.31) (4.32) and (4.33).

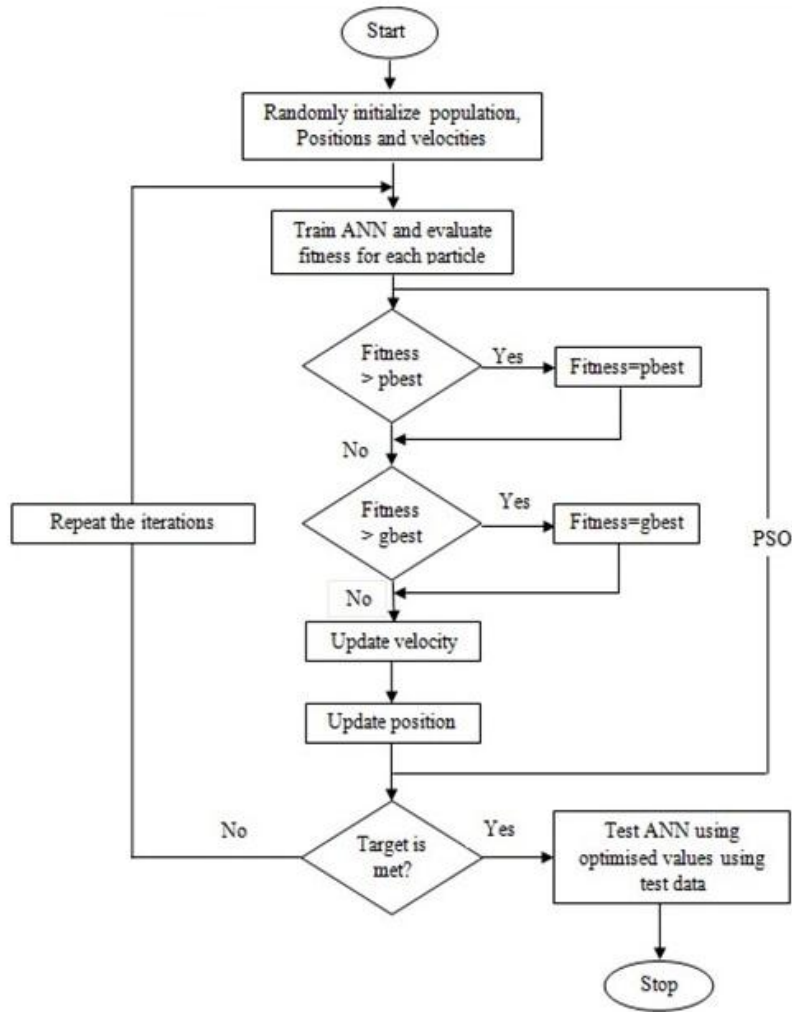


Fig. 4.6 Flowchart of PSO-ANN used in the study

4.5.3.2 The steps followed in PSO-SVM model development

The effectiveness of the result obtained depends upon the proper selection of SVM parameters (C, ϵ) and kernel parameters (γ, d), which can be obtained using particle swarm optimization. Initially, random range of values is provided for the parameters within the range given by software documentation. From the range given the parameter values corresponding to which the best fitness is achieved, is found by particle searching. If the value selected at random from the range provided does not satisfy the fitness function, then the loop continues with the next available value in the input range.

The PSO idea comprises of, at every single time step, varying the speed of (quicken) every particle toward its $pbest_j$ (best found particles) and $lbest$ (best found locations) (Kennedy and Eberhart, 1995). Increasing speed is weighted by an irregular term, with isolated arbitrary numbers being produced for $pbest$ and $lbest$ areas and particle swarm

model can be utilized as an optimizer. The optimization technique is performed as given below:

Step 1: Define upper and lower bound values of SVM and kernel parameters. The values are selected based on limits given by the software.

Step 2: Within the range provided, random values are selected, for which SVM trains and evaluates the objective function (RMSE).

Step 3: Fitness values of each particle in the swarm are calculated, followed by evaluation of optimum position and velocity of the particles.

Step 4: Using Equations (4.27) and (4.28), the position and velocity of each particle is updated from its previous value.

Step 5: Steps 2-4 are repeated until the termination criteria is met, i.e. the minimum value of RMSE.

The flow chart of the proposed PSO-SVM model is shown in Fig. 4.7

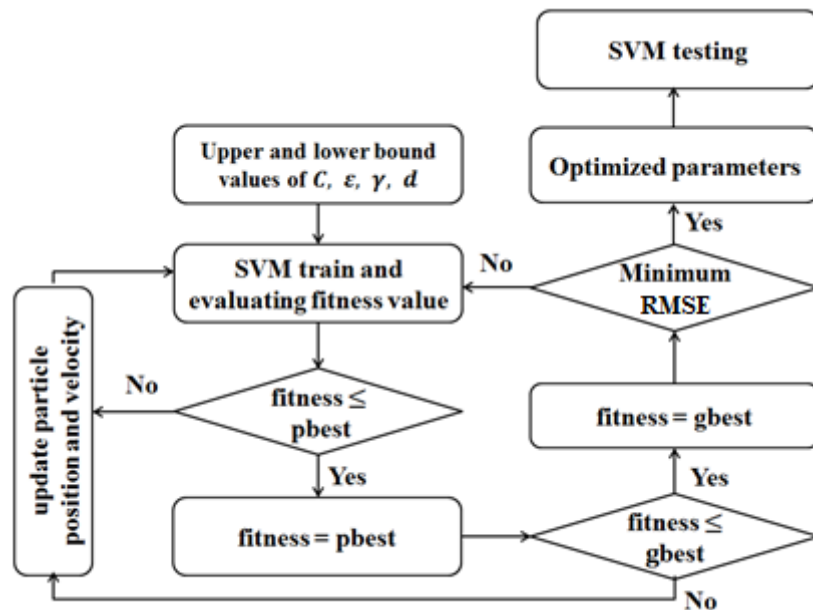


Fig. 4.7 Flowchart of PSO-SVM used in the study

4.6 MODEL PERFORMANCE CRITERIA

For the current study various statistical parameters like Root Mean Square Error (RMSE), Nash-Sutcliffe Efficiency (NSE), Correlation Coefficient (CC) and Scatter Index (SI) were used to check the accuracy of predicted values with measured data sets. The model will be considered good when RMSE, SI are minimum while NSE and CC are maximum.

4.6.1 Root mean square error (RMSE)

RMSE is frequently used to evaluate the performance of the models by measuring the differences between values (sample and population values) predicted by a model or an estimator and the values actually observed. The RMSE represents the sample standard deviation of the differences between predicted values and observed values. These individual differences are called residuals when the calculations are performed over the data sample that was used for estimation, and are called prediction errors when computed out-of-sample. The RMSE serves to aggregate the magnitudes of the errors in predictions for various times into a single measure of predictive power. RMSE is a good measure of accuracy, but only to compare forecasting errors of different models for a particular variable and not between variables, as it is scale-dependent.

$$\text{RMSE} = \sqrt{\frac{1}{N} \sum_{i=0}^N (P_{pi} - O_{pi})^2} \quad (4.30)$$

Where, O_{pi} = observed/actual values, P_{pi} = computed values and N = total number of data points. The lowest RMSE results in the best model.

4.6.2 Nash-Sutcliffe Efficiency (NSE)

In order to test the robustness of the developed model it is also necessary to test the model using some other performance evaluation indicators like Nash–Sutcliffe model efficiency coefficient (NSE). The Nash-Sutcliffe efficiency (NSE) is a normalized statistic that determines the relative magnitude of the residual variance (noise) compared to the measured data variance (information). The Nash–Sutcliffe coefficient was used to access efficiency of the models. NSE for a model can range from -1 to 1. An efficiency of 1 (NSE = 1) corresponds to a perfect match between estimate and observations. An efficiency of 0 (NSE = 0) indicates that the model predictions are as accurate as the mean of the observed data, whereas an efficiency less than zero ($E < 0$) occurs when the observed mean is a better predictor than the model or in other words, when the residual variance (described by the numerator in the expression below), is larger than the data variance (described by the denominator). Essentially, the closer the model efficiency is to

1, the more accurate the model.

$$NSE = 1 - \frac{\sum_{i=1}^N (P_{pi} - O_{pi})^2}{\sum_{i=1}^N (O_{pi} - \overline{O_{pi}})^2} \quad (4.31)$$

Where, $\overline{O_{pi}}$ is the mean of actual data.

4.6.3 Correlation Coefficient (CC)

A correlation coefficient (CC) is a number that quantifies some type of correlation and dependence, meaning statistical relationships between two or more random variables or observed data values. The CC ranges from 0 to 1. Range 1 shows that the equation is a linear which describes the relationship between x and y perfectly, with all data points lying on a line for which y increases as x increases. A value of 0 implies that there is no linear correlation between the variables.

$$CC = \frac{\sum_{i=1}^N (P_{pi} - \overline{P_{pi}})(O_{pi} - \overline{O_{pi}})}{\sqrt{\sum_{i=1}^N (P_{pi} - \overline{P_{pi}})^2} \sqrt{\sum_{i=1}^N (O_{pi} - \overline{O_{pi}})^2}} \quad (4.32)$$

4.6.4 Scatter Index (SI)

In statistics, dispersion (also called variability, scatter, or spread) denotes how stretched or squeezed a distribution (theoretical or that underlying a statistical sample) is. Common examples of measures of statistical dispersion are the variance, standard deviation and interquartile range. Dispersion is contrasted with location or central tendency, and together they are the most used properties of distributions.

$$SI = \frac{\sqrt{\frac{1}{N} \sum_{i=1}^N (P_{pi} - O_{pi})^2}}{\overline{O_{pi}}} \quad (4.33)$$

Scatter plots are also used to evaluate the accuracies of the models while, box plots are used to analyse the spread of the data points estimated by the models.

PERFORMANCE OF ANN AND SVM MODELS

5.1 GENERAL

In this chapter, performance of the ANN and SVM models for predicting the wave transmitted over submerged reef and damage level of the conventional rubble mound breakwater of tandem breakwater are analyzed and discussed. An effort is made to identify efficient and reliable soft computing tool for predicting wave transmission and damage level using statistical measures. The results of the same are discussed first, followed by comparison to find the best model.

In the present study, the data set is collected from the physical model study on tandem breakwater carried out in a two dimensional wave flume of the Marine Structures laboratory NITK, Surathkal, India (Rao and Shirlal, 2004). They conducted experiments to study the stability of the tandem breakwater by taking stone as armour unit. The wave parameters considered for their study are to represent the Mangalore coast. The prototype conditions corresponding to model study are waves of height ranging from 3 m to 4.8m and period varying from 8s to 12s. The depth of water in front of the structure also varied from 9 m to 13.5m. The dimensional analysis is carried out on the parameters considered using Buckingham's- π theorem and the important dimensionless parameters influencing the phenomenon obtained are used in the present chapter to study the performance of ANN, and SVM techniques. Methodologies of these techniques are briefly discussed in the Chapter 4. Further, the collected data are normalized and randomly divided into two sets, one for training consisting of 70% data and remaining 30% for testing. While dividing data set a care is taken to include all the range of data points in both training and testing.

Soft computing techniques such as ANN and SVM approach have been used to predict the wave transmission through the submerged reef and the damage level of conventional rubble mound breakwater. The capability of approach is checked by using statistical measures such as Correlation Coefficient (CC), Root Mean Square Error (RMSE) Nash-Sutcliff Efficiency (NSE) and Scatter Index (SI), which are defined in the chapter 4.

5.1.1 Performance of Artificial Neural Network (ANN) Model for predicting transmitted wave height (H_t/H_{tmax})

In the present study, eight input parameters, namely Incident wave steepness (H_i/gT^2), Relative reef spacing (X/d), Hudson's stability number ($H_i/\Delta D_{n50}$), Relative reef crest width (B/d), (B/L_o), Relative reef submergence (F/H_i), Relative reef crest height (h/d), Relative depth (d/gT^2) and the output parameters wave transmission (H_t/H_{tmax}) and Damage level (S) are considered. The training and testing are carried out using LM algorithm, MSE performance function, 'tansig' as activation function for hidden layer and 'purelin' for the output layer. The hidden layer is kept as one, but the number of neurons is varied from 1 to 5 and the best model is chosen. The network is prepared well using the training data set containing 201 data samples (70%) and then using the weights and biases obtained, the network is then used for predicting the desired output with the testing data set of 87 data samples (30%). The results obtained are tabulated below:

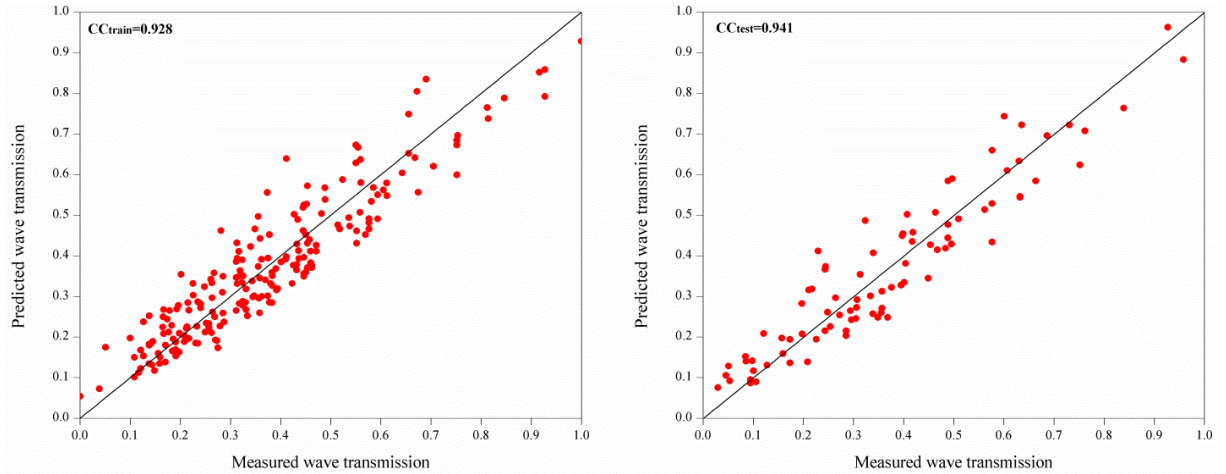
Table 5.1 Statistical parameter for ANN models for predicting H_t/H_{tmax}

Models	Networks	RMSE		CC		SI		NSE	
		Train	Test	Train	Test	Train	Test	Train	Test
ANN1	8-1-1	0.07	0.07	0.928	0.941	0.188	0.193	0.862	0.886
ANN2	8-2-1	0.038	0.043	0.979	0.979	0.102	0.118	0.959	0.957
ANN3	8-3-1	0.029	0.031	0.988	0.990	0.078	0.086	0.976	0.978
ANN4	8-4-1	0.025	0.031	0.991	0.989	0.067	0.086	0.982	0.977
ANN5	8-5-1	0.023	0.031	0.992	0.989	0.062	0.085	0.985	0.978

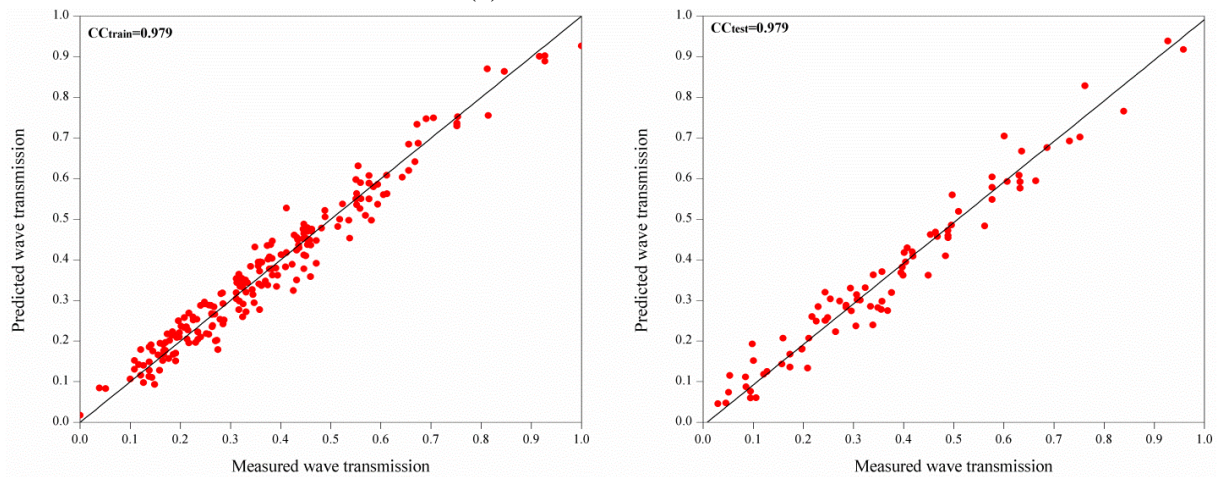
From Table 5.1, it is observed that the ANN1 model gives a lower prediction as it can be seen from all 5 statistical parameters. With the increase in hidden neurons, the performance of the model goes on increasing in terms of all the statistical parameters. But there is not much observed difference between the results of RMSE, CC, SI, and NSE for the models with hidden neurons from 3 to 5. The models show a small increase in training efficiency and almost constant testing efficiency beyond 3rd hidden neuron.

It is also observed that ANN3 model is giving a very good result with CC for testing as 0.99 and for training as 0.988. Also the RMSE value and SI value are close to zero for testing and NSE value shows a similar trend as CC. Hence, from all the observations, it can be concluded that a neural network model with 3 hidden neurons is the best model which shows a higher testing efficiency among all the other models. In general, ANN

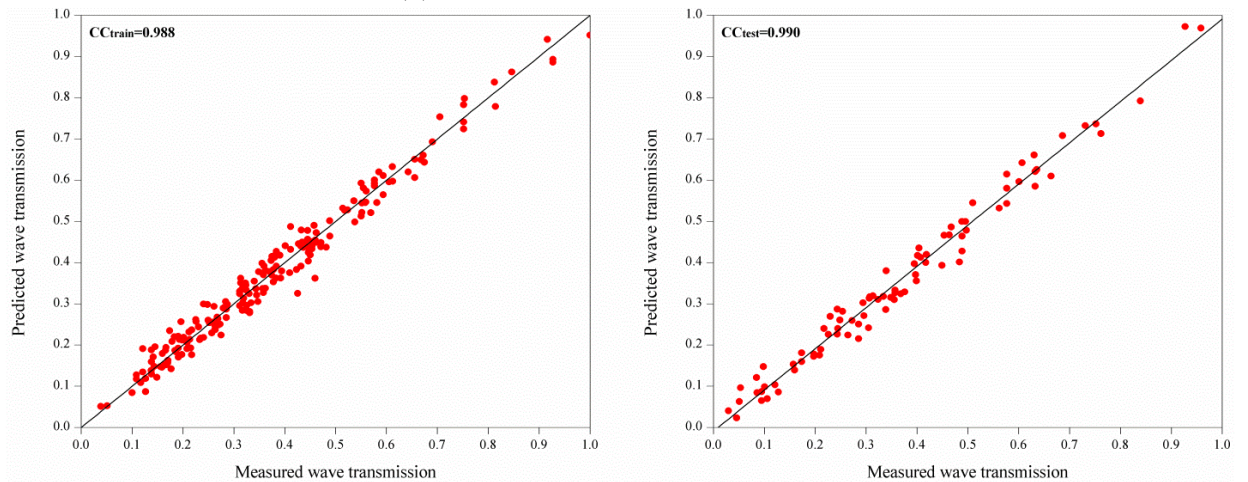
models are giving CC value more than 0.90. The models with increase in hidden neurons from 3 to 5 are found to be saturated resulting with a small increase in statistical parameter values. Fig. 5.1 gives the scatter plots for all the ANN networks with all the hidden neurons.



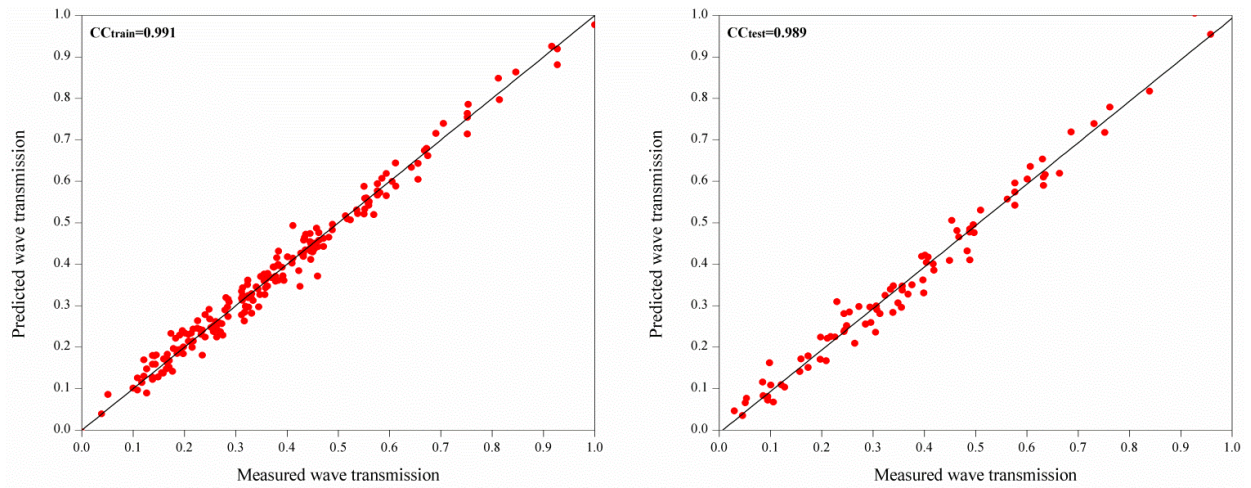
(a) Train and test of ANN1



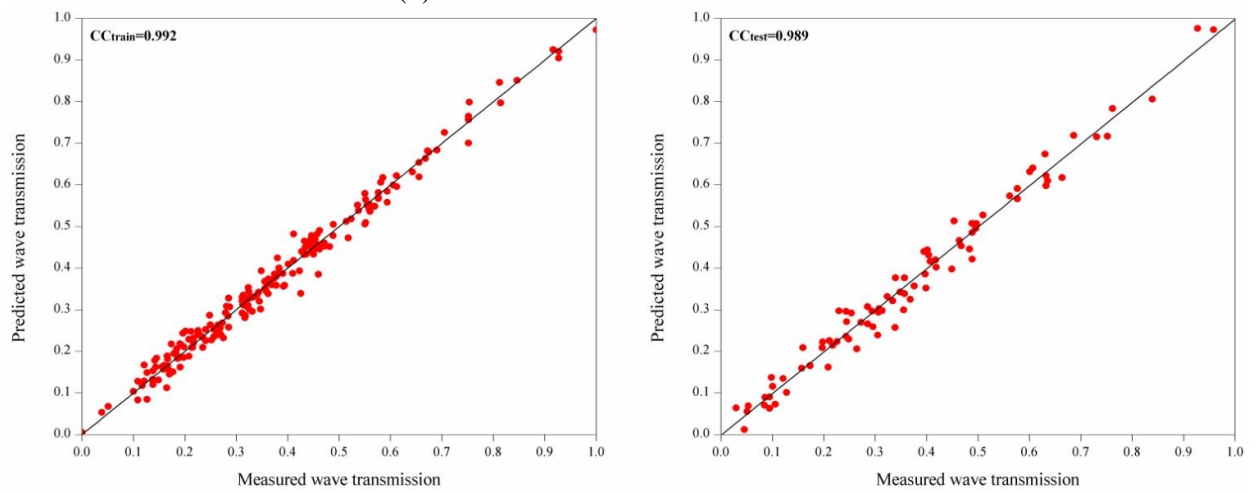
(b) Train and test of ANN2



(c) Train and test of ANN3



(d) Train and test of ANN4



(e) Train and test of ANN5

Fig. 5.1 Scatter plots for ANN1 to ANN5 model for H_t/H_{tmax}

From Fig. 5.1(a) to (e), it is observed that the predicted points are in a good correlation with observed data points in case of ANN3 model (Fig. 5.1(c)) with 3 hidden neurons compared to other ANN models with 1, 2, 4 and 5 hidden neurons as shown in Fig. 5.1(a), (b), (d) and (e). The scatter plots of ANN1 model with $CC=0.941$ value shows poor correlation compared to other ANN networks due to the wide scatter in the predicted points as shown in Fig. 5.1(a). For the models with hidden neurons from 3 to 5, show a small increase in training efficiency and almost constant testing efficiency. Hence, from the above discussion, ANN3 model is considered as the best network configuration to predict wave transmission (H_t/H_{tmax}) over the submerged reef of tandem breakwater. Fig. 5.2 represents the Box-Whiskers plot for ANN1 to ANN5 networks. In box plot, the spread of the predicted wave transmission with reference to the observed data are depicted. In the lower quartile predicted values of the ANN3 and ANN4 shows the better

prediction with reference to observed data points compared to ANN1, ANN2 and ANN5. Hence, ANN3 model performance is considered as best model based on results of scatter plots and box plots statistics. Comparison plot of best model ANN3 with observed data is illustrated in Fig. 5.3. It is found from the above figure that predicted values of wave transmission are closely matching with the observed values. Therefore, from the above discussion ANN3 model is considered as the best model for wave transmission prediction.

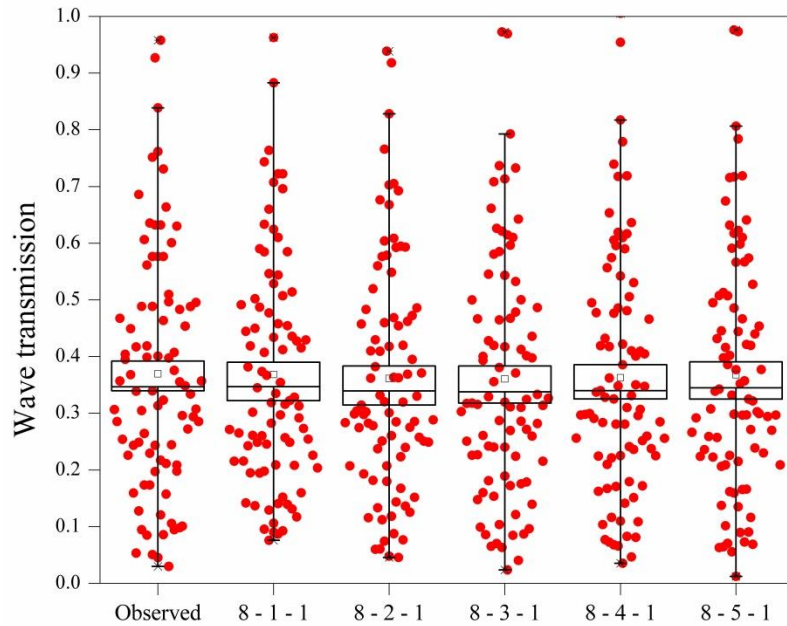


Fig. 5.2 Box-Whisker plots for ANN1-ANN5 and observed model for H_t/H_{tmax}

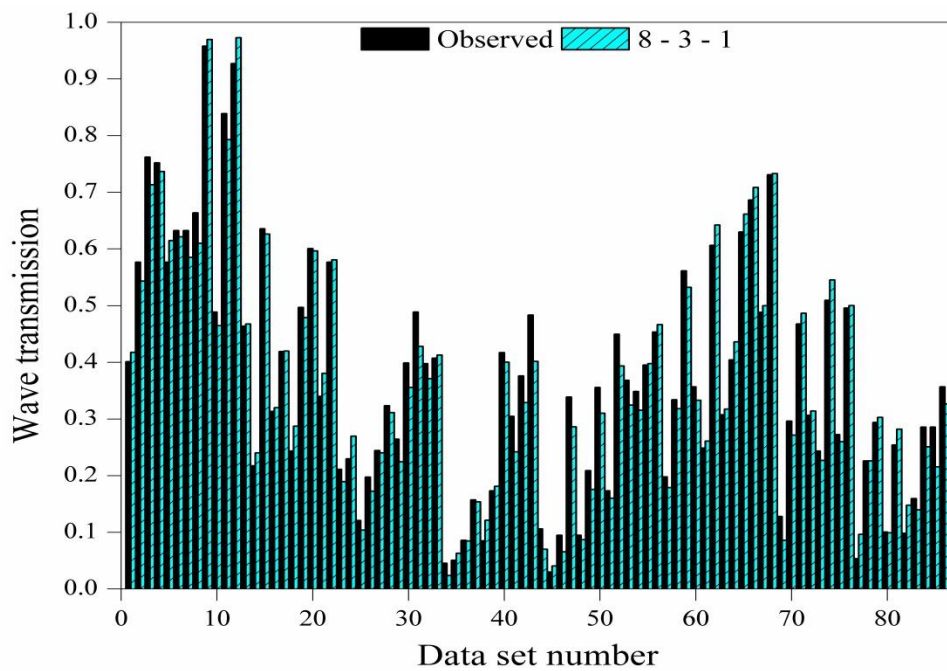


Fig. 5.3 Comparison of H_t/H_{tmax} predicted by ANN3 with observed values

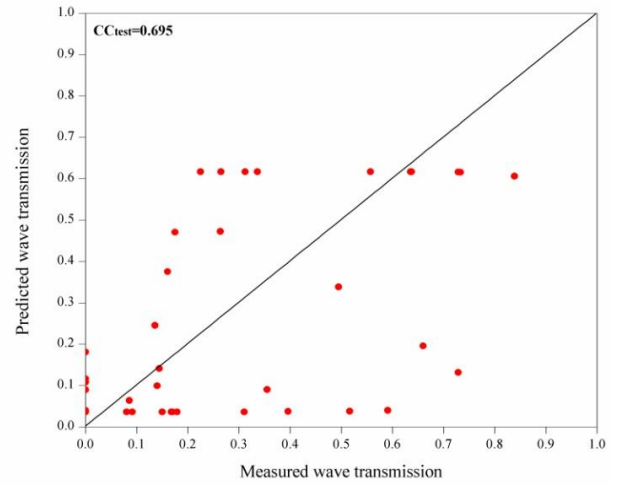
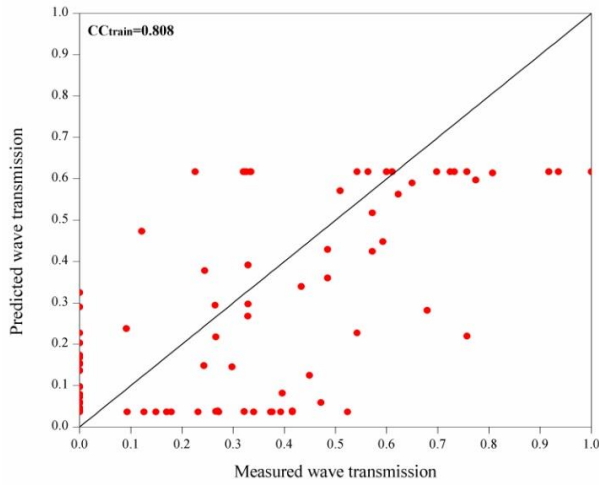
5.1.2 Performance of ANN model in the prediction of damage level (S)

To predict damage level (S), training and testing are carried out using LM algorithm, MSE performance function, ‘tansig’ as activation function for hidden layer and ‘purelin’ for the output layer. The hidden layer is kept as one, but the number of neurons is varied from 1 to 5 and the best model is chosen. The network is trained using the training data set containing 201 data samples (70%) and the trained network tested with the data set of 87 samples (30%). The results obtained are listed in Table 5.2.

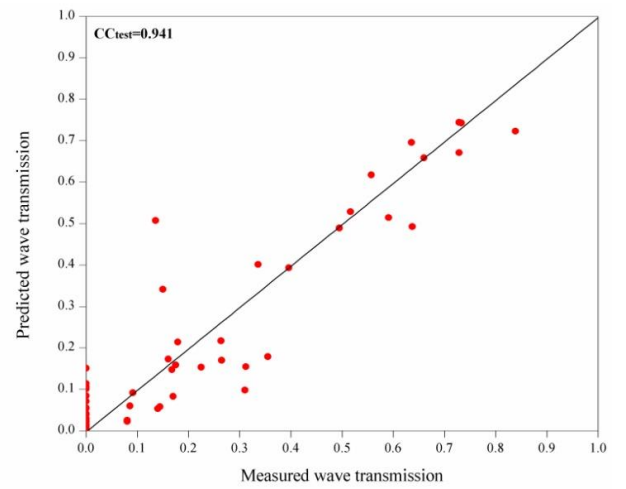
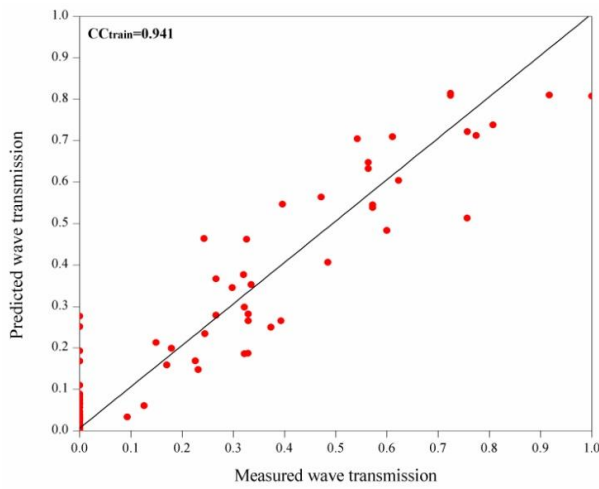
Table 5.2 Statistical results for ANN models for predicting damage level (S)

Models	No. of hidden neurons	RMSE		CC		SI		NSE	
		Train	Test	Train	Test	Train	Test	Train	Test
ANN1	8-1-1	0.144	0.163	0.808	0.695	1.00	1.264	0.653	0.451
ANN2	8-2-1	0.083	0.075	0.941	0.941	0.576	0.581	0.885	0.884
ANN3	8-3-1	0.069	0.072	0.959	0.947	0.481	0.555	0.920	0.894
ANN4	8-4-1	0.066	0.082	0.963	0.932	0.455	0.640	0.928	0.859
ANN5	8-5-1	0.055	0.064	0.974	0.956	0.382	0.515	0.949	0.909

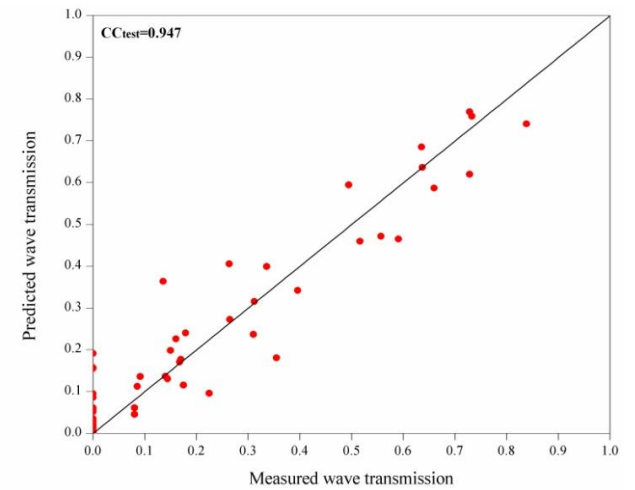
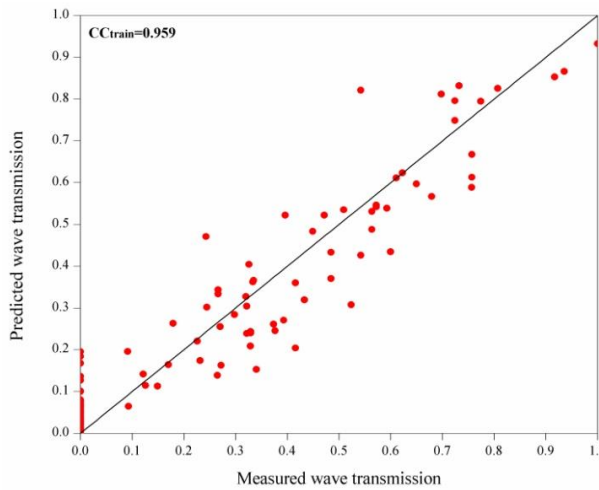
From Table 5.2, it can be seen that ANN1 model gives a very poor results which can be seen from all the 5 statistical parameters. The network efficiency improves with increase in hidden neuron size from 1 to 5. Increase in neurons beyond 3, the efficiency of the model remains constant. The ANN5 model gives best performance compared to other ANN models based on the values of different statistical measures. The CC value of best model ANN5 is 0.956 for testing ensuring good correlation between observed and predicted damage levels. The scatter observed during damage level predictions with value of SI=0.515 is more compared to scatter observed during wave transmission prediction. This is due to the presence of more number of zero damage levels and same can be confirmed from the scatter plots between experimental and predicted values in the Fig. 5.4.



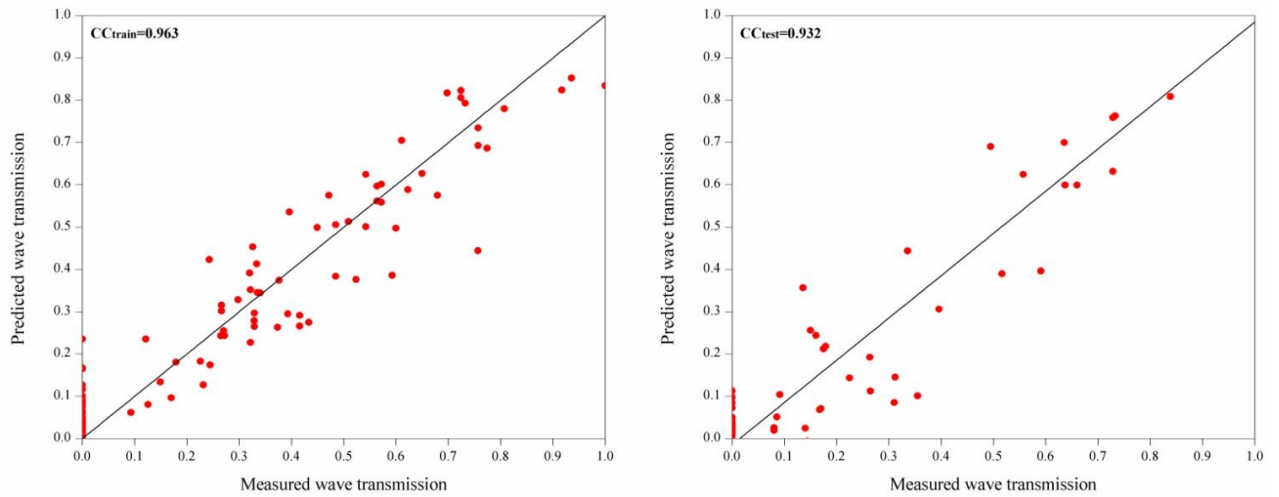
(a) Train and test of ANN1



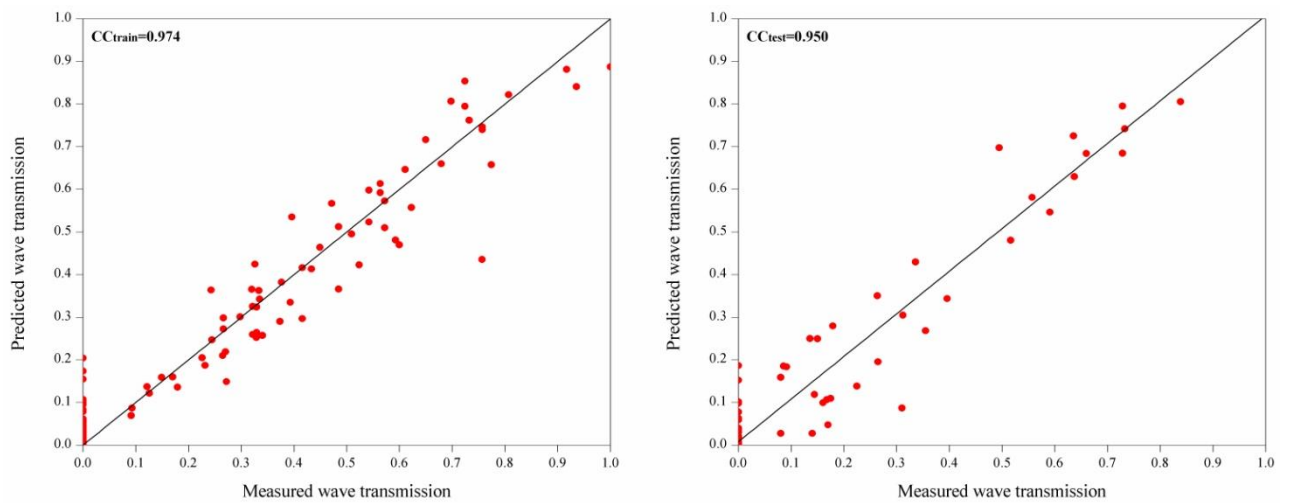
(b) Train and test of ANN2



(c) Train and test of ANN3



(d) Train and test of ANN4



(e) Train and test of ANN5

Fig. 5.4 Shows scatter plots of ANN1 to ANN5 models for damage level

Box-Whisker plot in the Fig. 5.5 shows the spread of the predicted damage levels at the lower quartile to the upper quartile prediction in reference to observed by ANN models with various numbers of hidden neurons. The lower quartile values predicted by ANN2 and ANN5 models match with observed values. Predicted damage level values by ANN5 model are in close and good agreement with observed damage level values as shown in Fig. 5.6. Therefore, it is confirmed that ANN5 is best model to predict damage level of conventional rubble mound breakwater of tandem breakwater.

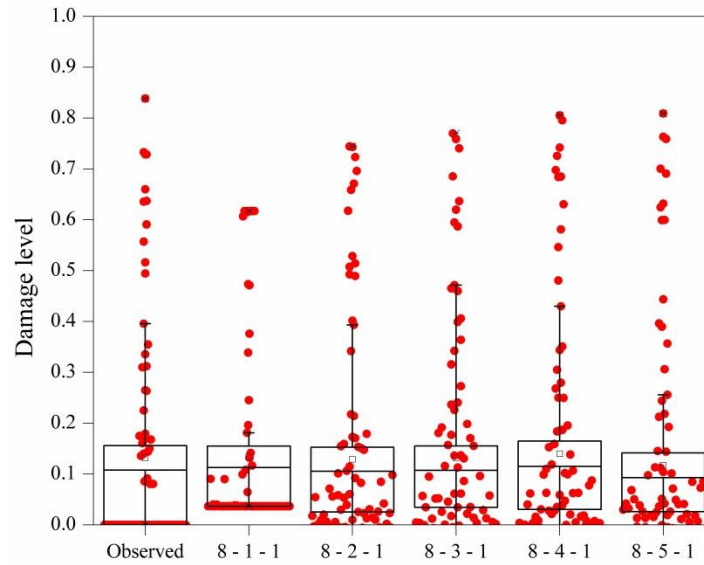


Fig. 5.5 Box-Whisker plot for ANN1-ANN5 and observed model for S

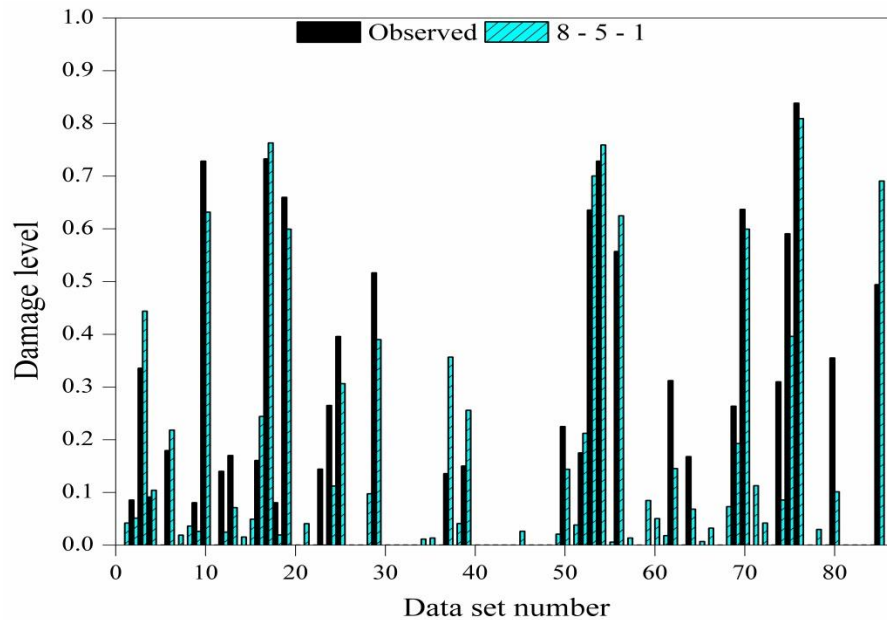


Fig. 5.6 Comparison of damage level predicted by ANN5 model with observed values

Further, LM algorithm is used for network analysis of wave transmission and damage level prediction with varying hidden nodes from 1 to 5 for 100 epochs. Here, the CC of predicted values increase with an increase in the number of hidden nodes upto 5 and the error between the observed and predicted output is found to be decreasing.

Mirchandani and Cao (1989) and Huang and Huang (1991) have suggested that the number of hidden layers may be equal to less than the number of input parameters to increase the learning efficiency. Considering the above said criteria and observing Fig. 5.3 and Fig. 5.6 in the present case, it is noticed that, 3 and 5 numbers of hidden neurons gives least error with RMSE = 0.031, SI = 0.086 and efficiency of NSE = 0.978 for

testing data sets is achieved with 3 hidden neurons and 100 epochs for wave transmission. Similarly, for damage level prediction it is observed that a high $CC = 0.956$, lower $RMSE = 0.064$, $SI = 0.515$ and high efficiency $NSE = 0.909$ for testing sets are achieved with 5 hidden neurons and 100 epochs. Therefore, based on the above discussion, ANN3 model for H_t/H_{tmax} and ANN5 model for S prediction are considered as reliable models among other ANN models.

5.1.3 Summary of ANN Model results

According to the experimental investigation carried out by Rao and Shirlal (2004), eight parameters H_i/gT^2 , X/d , $H_i/\Delta D_{n50}$, B/d , B/L_o , F/H_i , h/d , d/gT^2 are influencing the H_t/H_{tmax} and S . ANN models are developed by varying hidden neuron number from 1 to 5. The ANN models are compared using the statistical measures such as RMSE, CC, SI and NSE to select the best network. Although the results of this study are not exactly the substitute to the experimental method it can be a feasible method for predicting the transmitted wave heights over the submerged reef and the damage level of the conventional rubble mound breakwater of tandem breakwater.

5.2 PERFORMANCE OF SUPPORT VECTOR MACHINE (SVM) MODEL

5.2.1 The performance of the SVM model for predicting the wave transmission (H_t/H_{tmax})

The proper selection of kernel parameters for SVM decides the performance of the models. In developing SVM models, initially parameters are randomly searched by coarse search (i.e. for $C=100, 200, 300 \dots 2000$; $\varepsilon = 0.5, 1 \dots 2$; $\gamma = 1, 2, \dots 6$ and $d = 1, 2, \dots 6$) to identify the near optimal values, and then a fine search (i.e. for $C=1, 10, 20, 30 \dots 2000$; $\varepsilon = 0.000001, \dots 2$; $\gamma = 0.01, 0.02, \dots 6$ and $d = 1, 2, \dots 6$) to identify the final optimal values using K -fold cross validation optimization technique. In case of RBF kernel, the optimal width (γ) obtained by the manual search is found to be 3. The optimal value of d (degree) in the case of polynomial kernel function obtained by the manual search is 3. The number of support vectors for the prediction of the wave transmission over submerged reef and damage level of the conventional rubble mound breakwater of a tandem breakwater is same for all the kernel functions. K -fold Cross validation, two grid

and leave-one-out-error search is used for finding the optimal values of C, γ and ϵ as listed in Table 5.3.

Table 5.3 Optimal parameters for SVM models for predicting H_t/H_{tmax}

Kernel Type	Linear	Polynomial	RBF	Sigmoid
C	1380	263	294	186
ϵ	0.0012	0.00009	0.0001	0.00248
γ	-	-	3	4
d	-	3	-	-
nsv	80	80	80	80

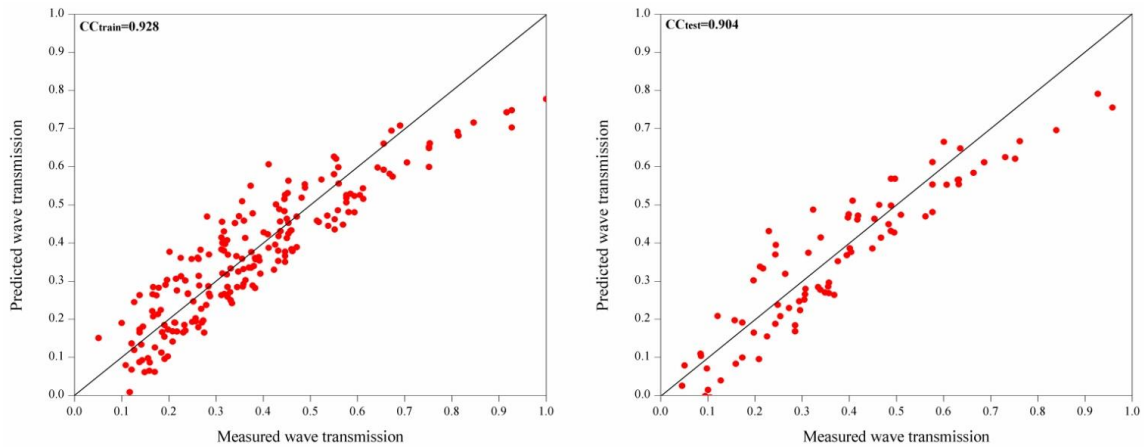
To study the effectiveness of the approach in predicting the values of H_t/H_{tmax} are evaluated using statistical measures and results are presented in Table 5.4 and also illustrated in the form of scatter plots and Box-Whiskers plot.

Table 5.4 Statistical measure for H_t/H_{tmax} of SVM model with different kernel functions

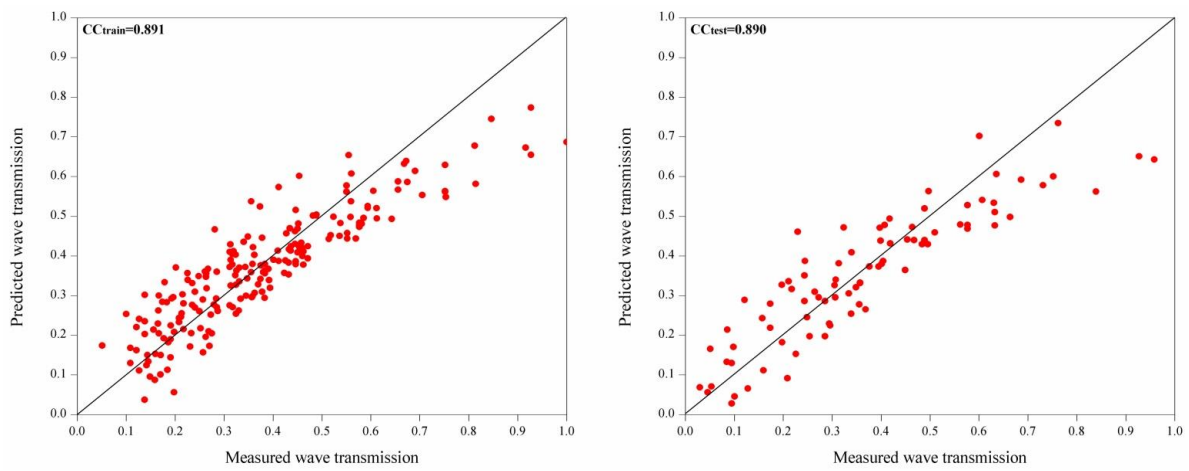
Statistical measures	Linear		Polynomial								RBF		Sigmoid	
			Quadratic		Cubic		Quartic		Quintic					
	Train	Test	Train	Test	Train	Test	Train	Test	Train	Test	Train	Test	Train	Test
RMSE	0.082	0.081	0.098	0.087	0.068	0.059	0.075	0.061	0.079	0.064	0.056	0.055	0.084	0.083
NSE	0.847	0.813	0.785	0.775	0.900	0.895	0.893	0.872	0.886	0.857	0.929	0.911	0.841	0.798
CC	0.928	0.904	0.891	0.890	0.952	0.949	0.948	0.940	0.947	0.938	0.977	0.965	0.928	0.905
SI	0.221	0.218	0.266	0.234	0.184	0.160	0.202	0.165	0.214	0.171	0.151	0.150	0.227	0.225

In case of the RBF and sigmoid kernels, the width (γ) obtained by manual search are found to be 3 and 4 respectively. The optimal values of d (degree) in case of polynomial kernel function obtained by manual search are 3. The SVM model with RBF kernel function outperformed other kernel functions with high CC=0.965 and NSE= 0.911 and lowest RMSE=0.055 and SI=0.150 for testing when compared to other kernel functions. The scatter plots of observed and predicted wave transmission for different models are shown in Fig. 5.7. Scatter plot shows the linear correlation between the observed and predicted H_t/H_{tmax} where least square method is used to find best fit line. The Box-Whisker plots in the Fig. 5.8, depicts the spread of the predicted points with the observed by different SVM models. The predicted wave transmission values in the upper and lower quartile of the box plot statistics shows that, RBF kernel function performed better compared to other kernel functions with SVM model. The performance of best SVM model is compared with observed values to validate the model as shown in Fig. 5.9. The

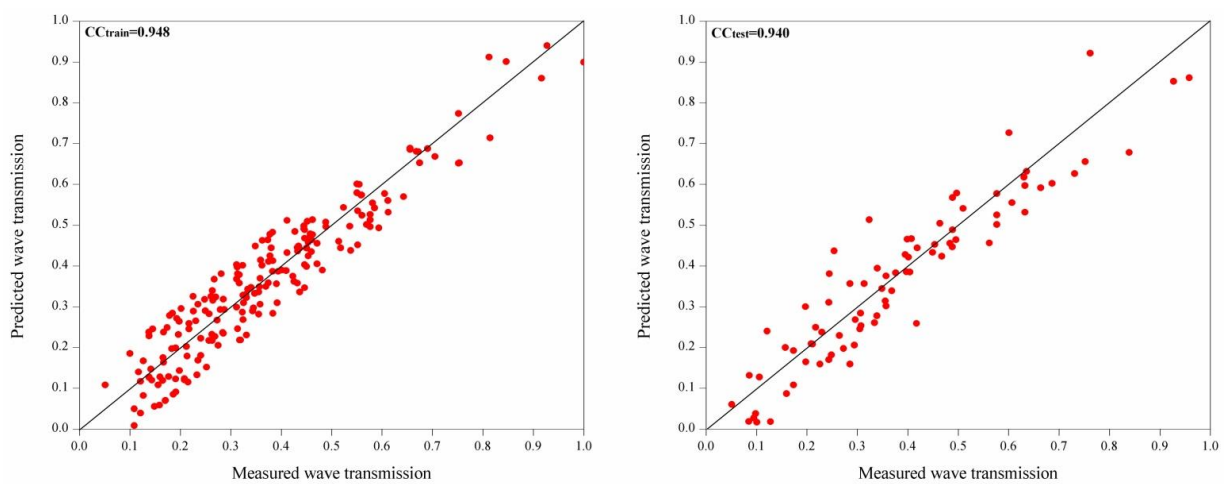
wave transmission predicted by SVM with RBF kernel function is in good agreement with observed values and same is witnessed in the comparison graph.



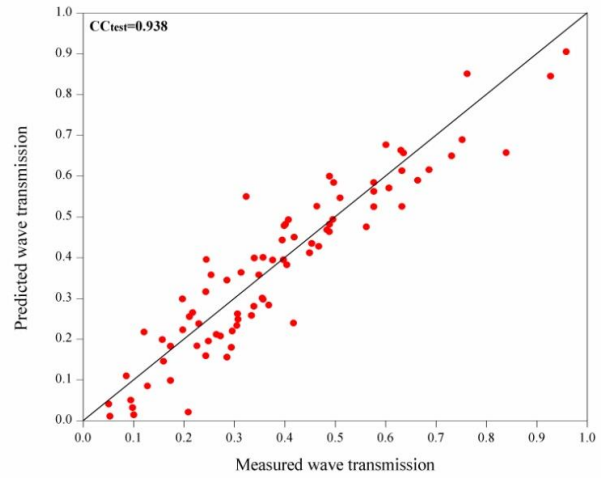
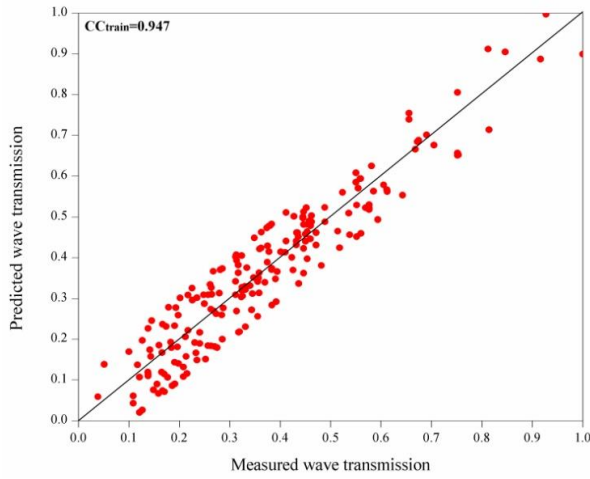
(a) Linear kernel function



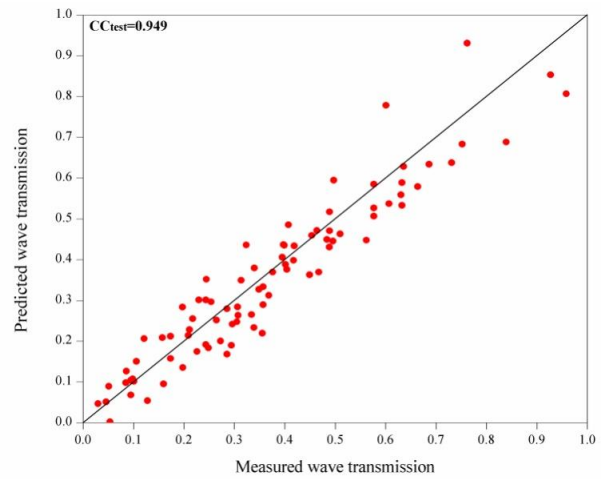
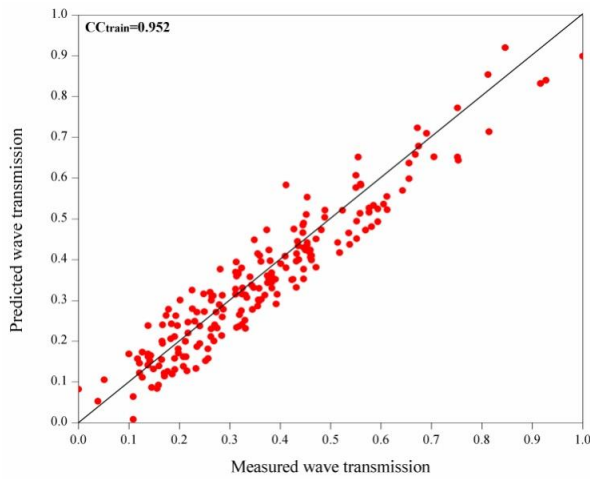
(b) Quadratic kernel function



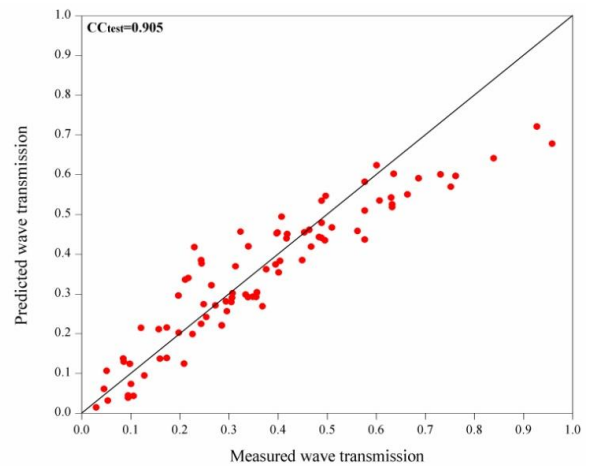
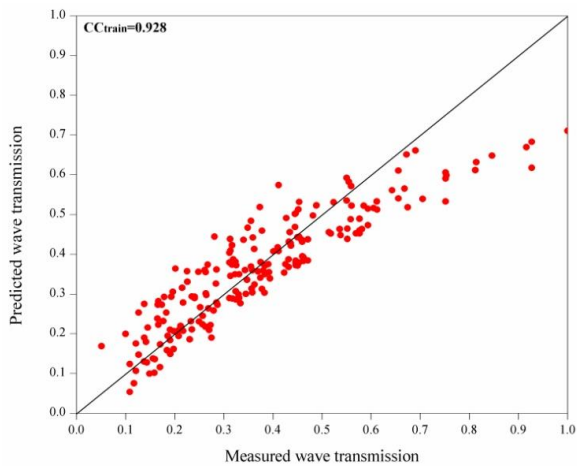
(c) Quartic kernel function



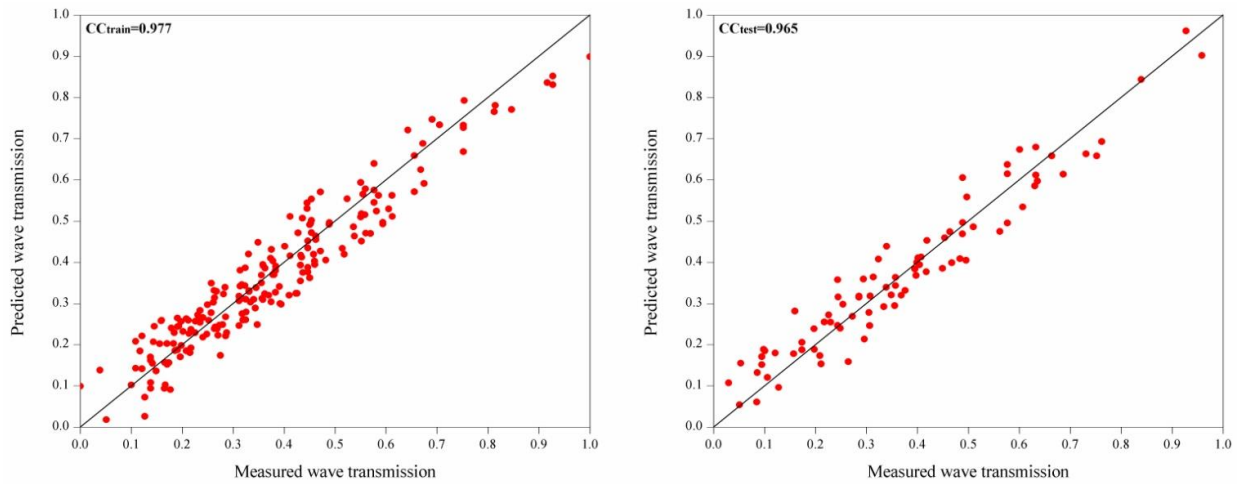
(d) Quintic kernel function



(e) Cubic kernel function



(f) Sigmoid kernel function



(g) RBF kernel function

Fig. 5.7 Scatter plots of predicted and observed H_t/H_{tmax} by SVM for different kernel functions

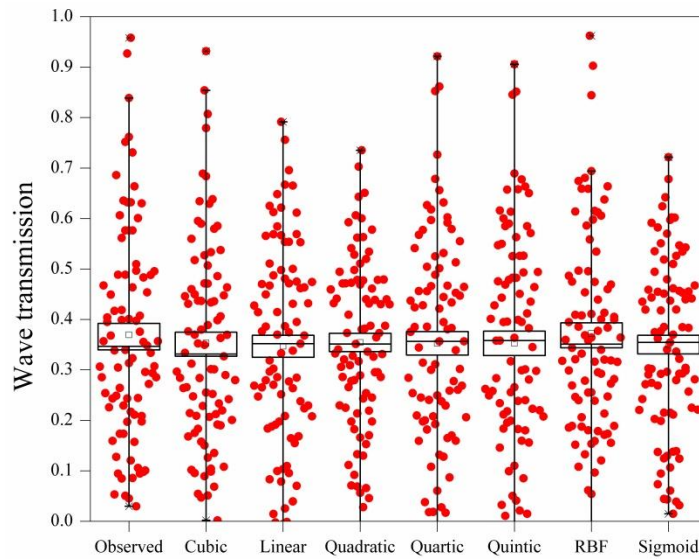


Fig. 5.8 Box-Whisker plots of predicted and observed wave transmission by SVM

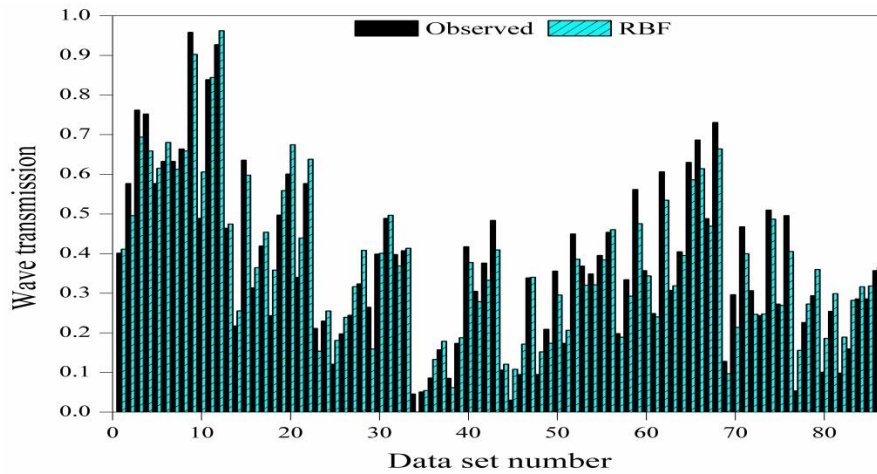


Fig. 5.9 Comparison of wave transmission predicted by SVM with observed values

5.2.2 The performance of the SVM model in predicting the damage level (S)

The performance of SVM depends on the good setting of kernel parameters. In developing SVM models, initially parameters are randomly selected by coarse search (i.e. for $C=100, 200, 300\dots2000$; $\varepsilon = 0.5, 1\dots2$; $\gamma = 1, 2, \dots, 6$ and $d = 1, 2, \dots, 6$) to identify the near optimal values, and then a fine search (i.e. for $C=1, 10, 20, 30\dots2000$; $\varepsilon = 0.000001, \dots, 2$; $\gamma = 0.01, 0.02, \dots, 6$ and $d = 1, 2, \dots, 6$) is made to identify the final optimal values. In the case of RBF kernel, the optimal width γ obtained by the manual search is found to be 3. The number of support vectors for the prediction of the damage level of the main breakwater is same for all the kernel functions. K-fold cross validation search is used for finding the optimal values of C, γ, ε and d . The optimal parameters obtained by SVM (C, ε) model with proper kernel parameter (γ, d) are listed in Table 5.5.

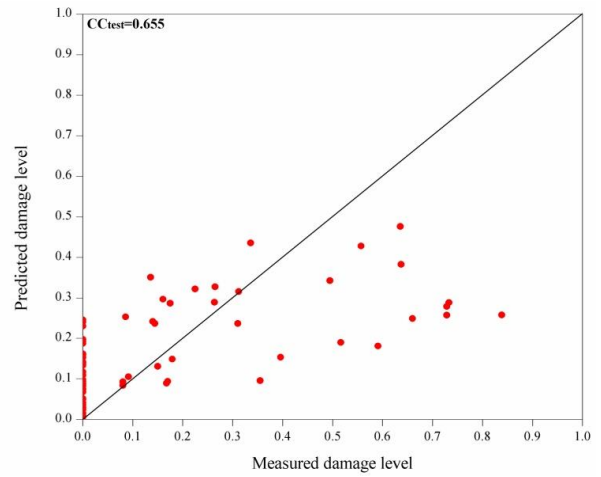
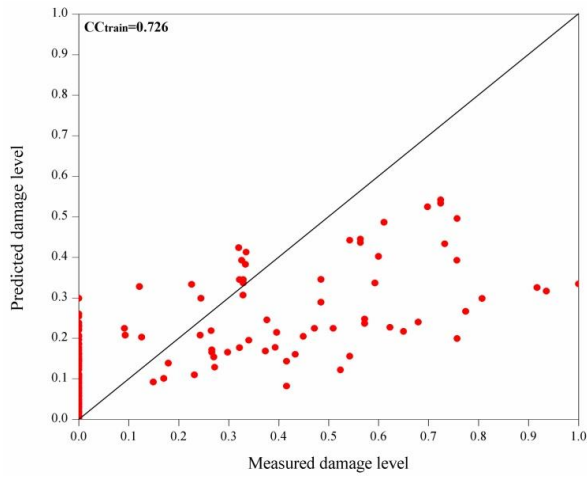
Table 5.5 Optimal parameters for SVM models for S

Kernel Type	Linear	Polynomial	RBF	Sigmoid
C	2418	364	328	258
ε	0.00169	0.00075	0.00007	0.00396
γ	-	-	3	4
d	-	3	-	-
nsv	82	82	82	82

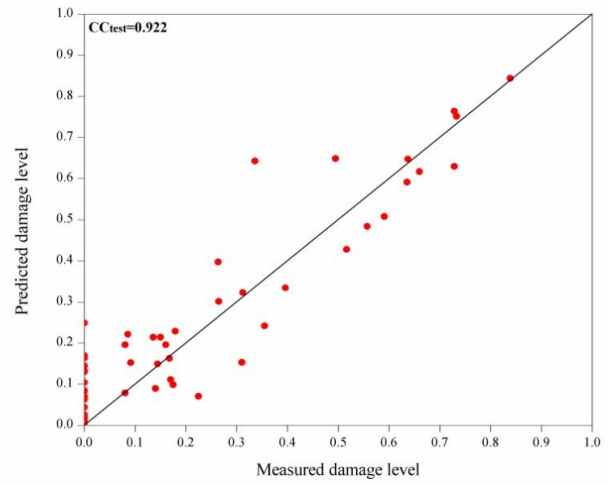
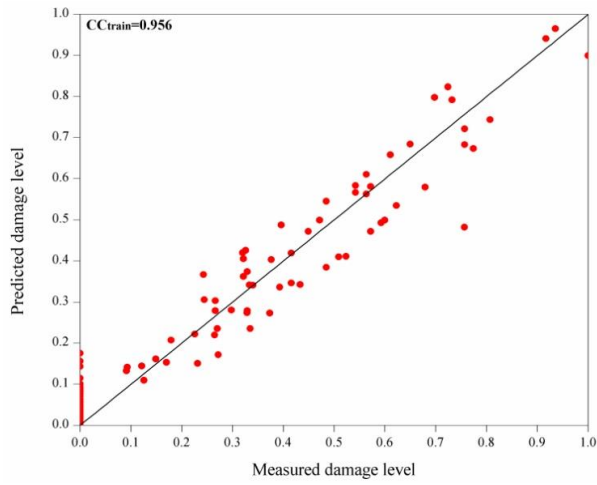
Table 5.6 Statistical measures of SVM models for S prediction with different kernel functions

Statistical Measures	Linear		Polynomial								RBF		Sigmoid	
			Quadratic		Cubic		Quartic		Quintic					
	Train	Test	Train	Test	Train	Test	Train	Test	Train	Test	Train	Test	Train	Test
RMSE	0.175	0.170	0.094	0.091	0.102	0.073	0.106	0.071	0.122	0.072	0.091	0.076	0.194	0.180
NSE	0.488	0.412	0.854	0.832	0.912	0.787	0.914	0.771	0.911	0.697	0.903	0.834	0.376	0.342
CC	0.726	0.655	0.926	0.918	0.956	0.922	0.956	0.905	0.956	0.877	0.953	0.935	0.691	0.624
SI	1.293	1.215	0.690	0.648	0.776	0.504	0.806	0.496	0.927	0.504	0.690	0.529	1.367	1.341

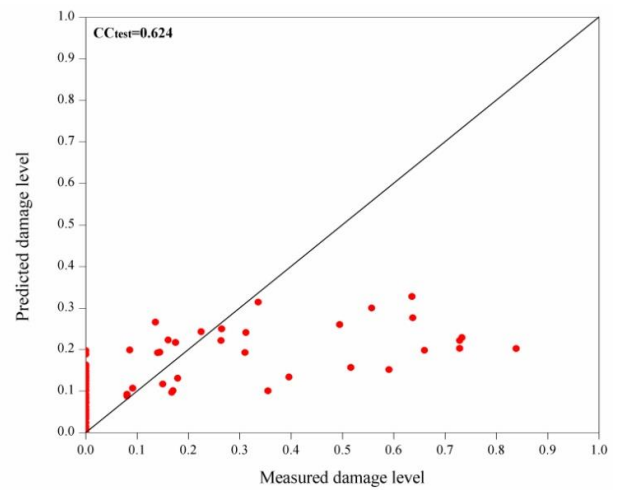
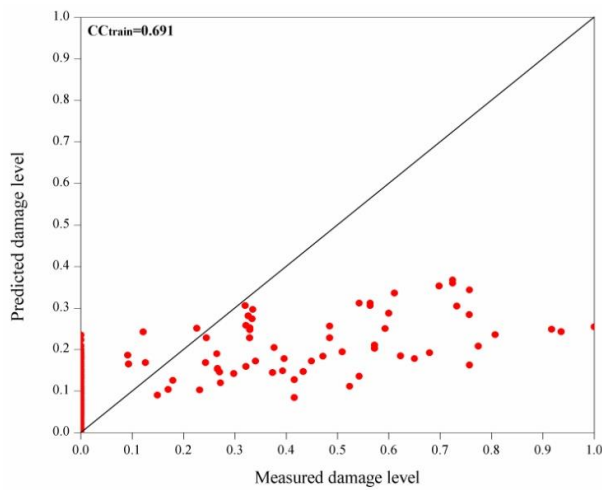
Statistical measures CC, RMSE, SI and NSE are computed for damage levels predicted by SVM models with different kernels are listed in Table 5.6. The CC values obtained by SVM models with different kernels functions for the training and testing data sets during damage level prediction is depicted in the form of scatter plots as shown in the Fig. 5.10. The SVM model with RBF kernel function shows better performance in predicting damage level with $C=0.935$, $RMSE=0.076$, $SI=0.529$ and $NSE=0.834$ for testing data set.



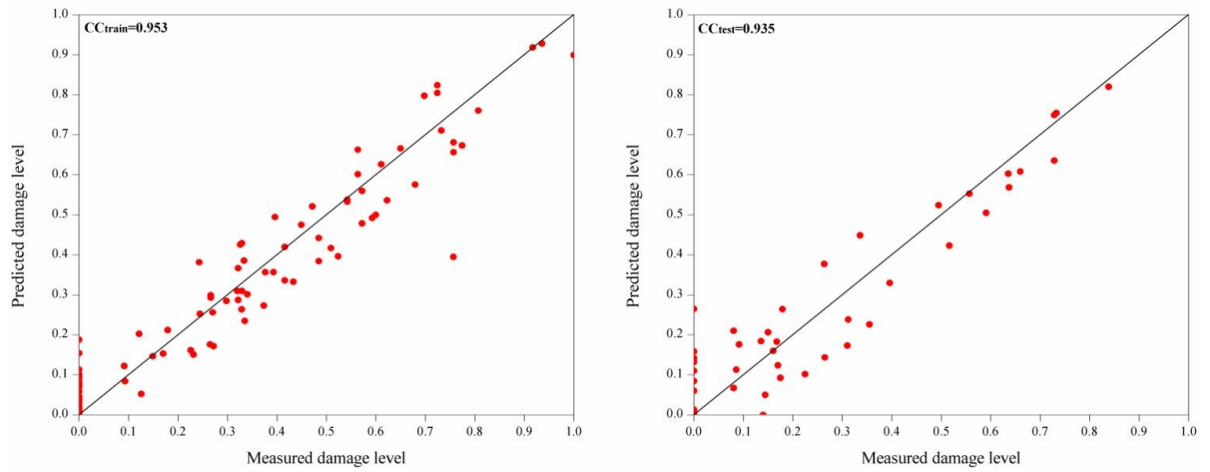
(a) Linear Kernel function



(b) Polynomial Kernel function



(c) Sigmoid Kernel function



(d) RBF Kernel function

Fig. 5.10 Scatter plots of S for SVM model for damage level with different kernel function

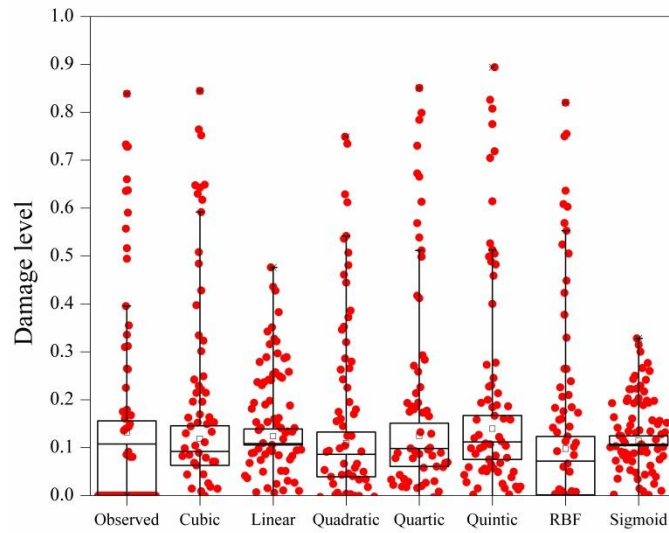


Fig. 5.11 Box-Whisker plots of SVM model for damage level with different kernel function

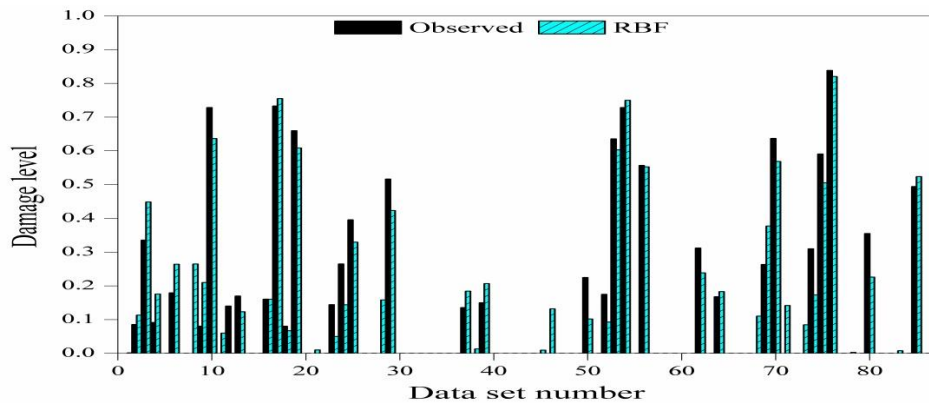


Fig. 5.12 Comparison of damage level predicted by SVM (RBF) with observed values

Fig. 5.11 illustrates the box plot statistics for evaluating the performance of the SVM model with different kernels in predicting damage level. This can be confirmed by observing the spread of the data points predicted with observed data points. In which the RBF kernel of the SVM model shows the similar trend of spread of predicted values in the upper and lower quartile of the box and upper and lower whiskers of the plot with respect to the observed damage level. This proves that, SVM with RBF kernel function predicts damage level better than other kernel functions. The best model SVM with RBF kernel is validated and comparison of predicted and observed damage level is shown in Fig. 5.12. It is also observed from the above figure that the damage levels predicted by SVM model with RBF kernel function are in good agreement with observed values. The zero values in the graph indicate the zero damage level observed while conducting the experiments in a wave flume.

5.2.3 Summary of SVM model results

The predictive capacity of the SVM enhanced due to the presence of kernel functions and support vectors which help to reduce the error by increasing the margin against the scattered points and reduce the slack variables and in turn reduce the error. The weights and biases also help to correlate the high dimensional space with the input parameters which makes the SVM model with RBF kernel function a suitable tool for predicting wave transmission over submerged reef and damage level of the conventional rubble mound breakwater of tandem breakwater. The SVM model showed the comparable and reliable results with respect to ANN model. Among all the kernel functions RBF kernel function gives best results in both cases of H_t/H_{tmax} and S prediction models. The SVM model with RBF kernel function gives the best performance compared to other kernel functions with low RMSE=0.055, SI= 0.150 and high CC=0.965, NSE=0.912 for testing data set to predict H_t/H_{tmax} . SVM with RBF kernel function with high CC=0.935, low RMSE=0.077, SI=0.529 and high efficiency NSE=0.833 for testing to predict damage levels. The wave transmission and damage level predictions by SVM model with RBF kernel function are in good agreement with observed values.

Therefore, SVM model with RBF kernel function can also be used as an alternate method for predicting the wave transmission over a submerged reef and damage level of conventional rubble mound breakwater of tandem breakwater.

Results obtained from both the best models are tabulated in Table 5.7. Statistical measures of both the models gave satisfactory results. The ANN model with (8-3-1) network with three hidden neurons for wave transmission and (8-5-1) network with five hidden neurons for damage level outperformed the SVM model with RBF kernel function in term all the statistical measures in the present discussion. Hence, ANN model can be used as efficient tool for predicting wave transmission and damage level of tandem breakwater.

Table 5.7 Comparison of ANN and SVM statistical measures

Model		Train Data				Test Data			
		CC	RMSE	SI	NSE	CC	RMSE	SI	NSE
Wave transmission	ANN (8-3-1)	0.988	0.029	0.078	0.976	0.990	0.031	0.086	0.978
	SVM (RBF)	0.977	0.0559	0.150	0.929	0.965	0.055	0.150	0.911
Damage level	ANN (8-5-1)	0.974	0.055	0.382	0.949	0.956	0.064	0.515	0.909
	SVM (RBF)	0.935	0.0557	0.1505	0.903	0.935	0.055	0.151	0.833

PERFORMANCE OF ANFIS, PSO-ANN AND PSO-SVM MODELS

6.1 GENERAL

By observing the results discussed in chapter 5, the capacity of the ANN and SVM models can be further cross checked or improve the efficiency of the model by hybridizing the model with other optimization techniques such as Fuzzy and PSO. From the literature, it is also observed that hybrid models give better results than the single models (Patil et al., 2012; Harish et al., 2014) in most of the cases. To improve the results, hybridizing technique such as ANN with Fuzzy Inference System and PSO and SVM with PSO are implemented and analysis is carried out. The obtained results are discussed in this chapter.

6.2 PERFORMANCE OF ADAPTIVE-NEURO FUZZY INFERENCE SYSTEM (ANFIS) MODEL

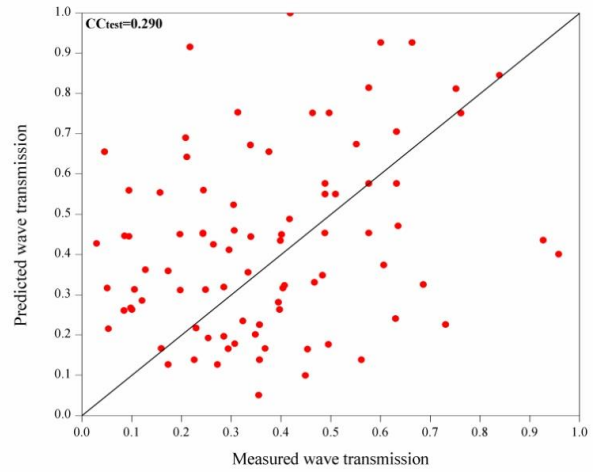
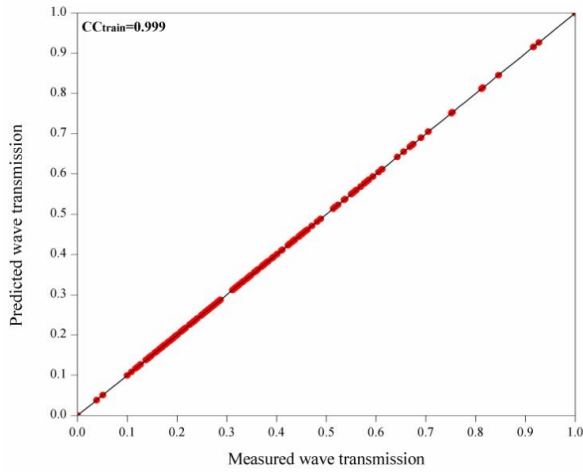
The ANFIS model with eight input parameters and one output parameter is built with different membership functions, fuzzy rules and epoch numbers. The various membership functions considered are Triangular-shaped built-in membership function (TRIMF), Trapezoidal-shaped built-in membership function (TRAPMF), Generalized bell-shaped built-in membership function (GBELLMF), and Gaussian curve built-in membership function (GAUSSMF). An ANFIS model with built-in 2 membership functions for each variable, and 100 epoch numbers are selected and trained using the Levenberg-Marquardt algorithm with tangent sigmoid and linear transfer functions in the hidden and output layers, respectively. In the present chapter ANFIS models are developed for the prediction of wave transmission over submerged reef and damage level of main conventional rubble mound breakwater of tandem breakwater. The performances of these models are evaluated based on statistical measures, namely RMSE, CC, SI and NSE. The CC between desired output and network predicted outputs are calculated by using Equation (4.30). The RMSE, SI and NSE between target output and network predicted output is determined by using Equations (4.31), (4.32), and (4.33) respectively. Each model is developed and results are discussed in the following section.

6.2.1 Simulation results of ANFIS Model for predicting wave transmission (H_t/H_{tmax})

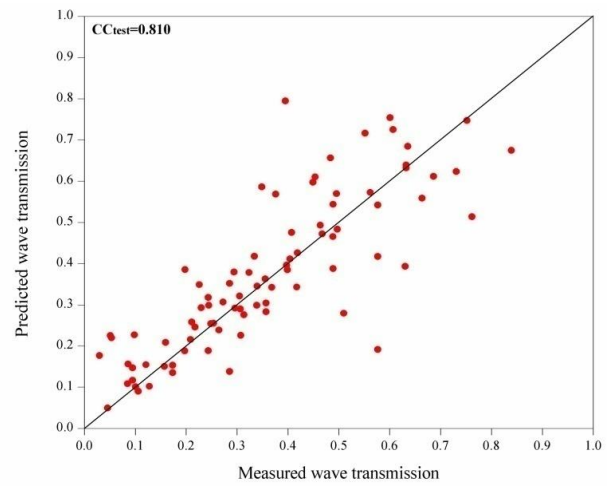
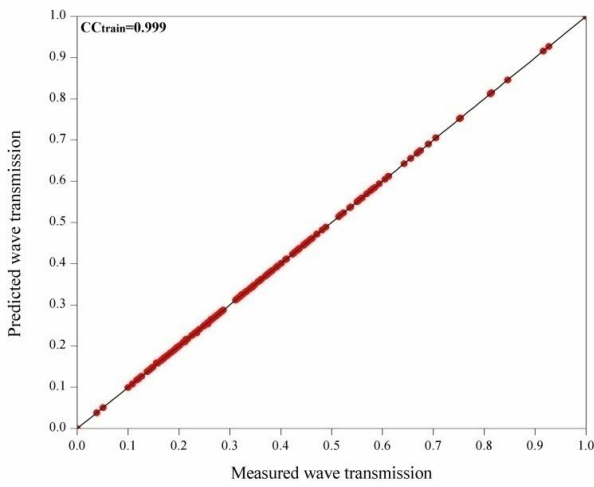
Fuzzy models are developed to predict the wave transmission over submerged reef of tandem breakwater. The proper selection of ANFIS and its membership functions and their number decides the performance of these models. The different membership functions with their performances in the form of scatter plots are shown in Fig. 6.1 and the values of statistical measures are tabulated in Table 6.1. In the present study, with 8 input parameters and 1 output, using Sugeno first order with (2^8) 256 fuzzy rules and 2 generalized ‘Triangular (trimf)’, ‘Trapezoidal (trapmf)’, ‘Gbell (gbellmf)’ and ‘Gaussian (Gaussmf)’ membership functions and 100 epochs the model is trained. Among all the membership functions, the ANFIS model with Gaussian membership function performs better than the other membership functions. It is believed that Gaussian membership function has the capacity to handle higher degree of error tolerance compared to other membership functions. The statistical measures obtained for ANFIS model with Gaussian membership function are RMSE= 0.0754, CC= 0.935. It is also observed that, there is good correlation between the observed and predicted wave transmission in this model with less scatter, SI= 0.0023. Good efficiency, NSE = 0.869 is obtained for testing. The ANFIS model, with a combination of gradient descent algorithm and least squares algorithm, is used in an effective search for the optimal parameters to yield good results. Based on this hybrid approach, correlations of training and testing are increased as presented in Fig. 6.1.

Table 6.1 Statistical measure of ANFIS models for predicting wave transmission

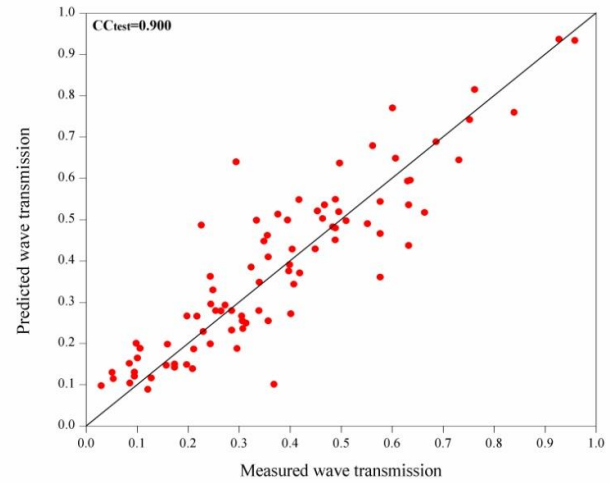
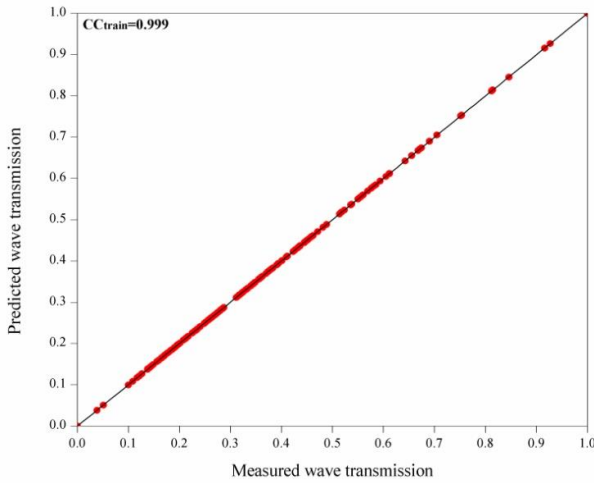
Statistical measures	Membership Functions							
	Triangular		Trapezoidal		Gbell		Gaussian	
	Train	Test	Train	Test	Train	Test	Train	Test
RMSE	0.0003	0.263	0.0004	0.136	0.00021	0.0935	0.0002	0.0754
NSE	0.999	0.588	0.999	0.576	0.999	0.799	0.999	0.869
CC	0.999	0.290	0.999	0.810	0.999	0.900	0.999	0.935
SI	0.0001	0.0081	0.0002	0.004	0.0007	0.0029	0.0006	0.0023



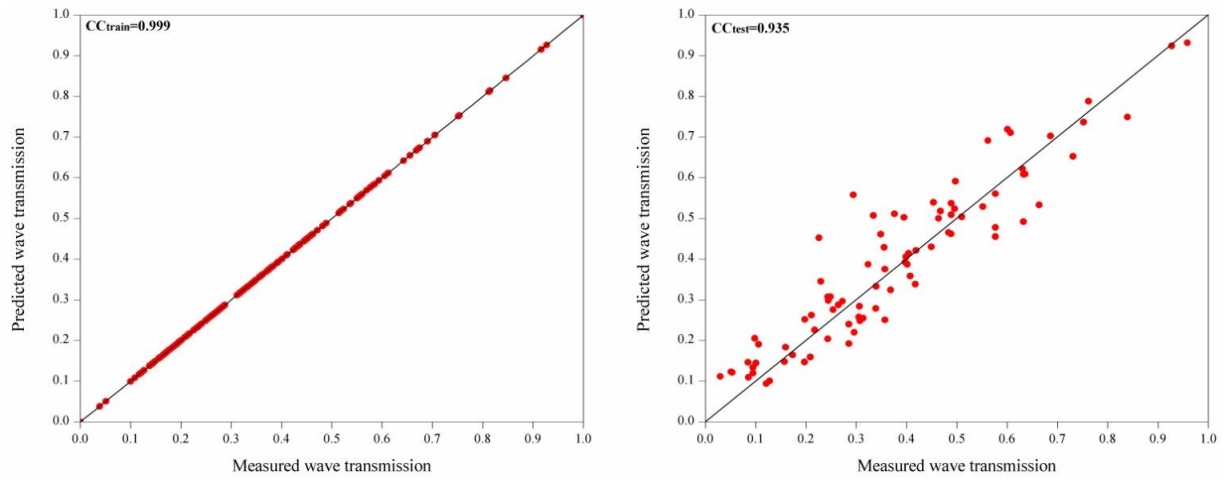
(a) Triangular membership function



(b) Trapezoidal membership function



(c) Gbell membership function



(d) Gaussian Membership function

Fig. 6.1 Scatter plots of predicted and observed H_t/H_{tmax} by ANFIS for different membership functions

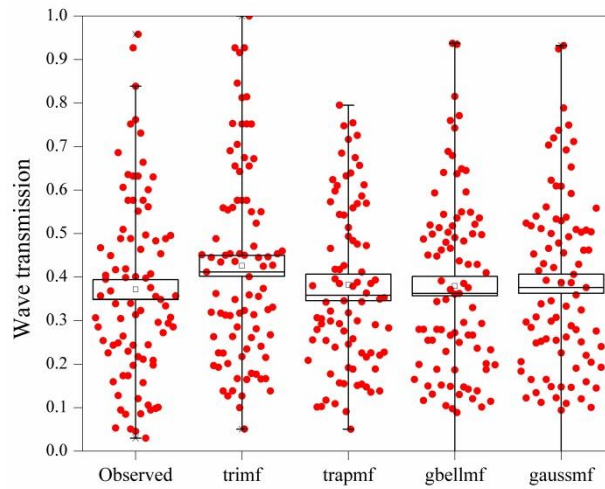


Fig. 6.2 Box-Whiskers plots of H_t/H_{tmax} for ANFIS model with different membership functions

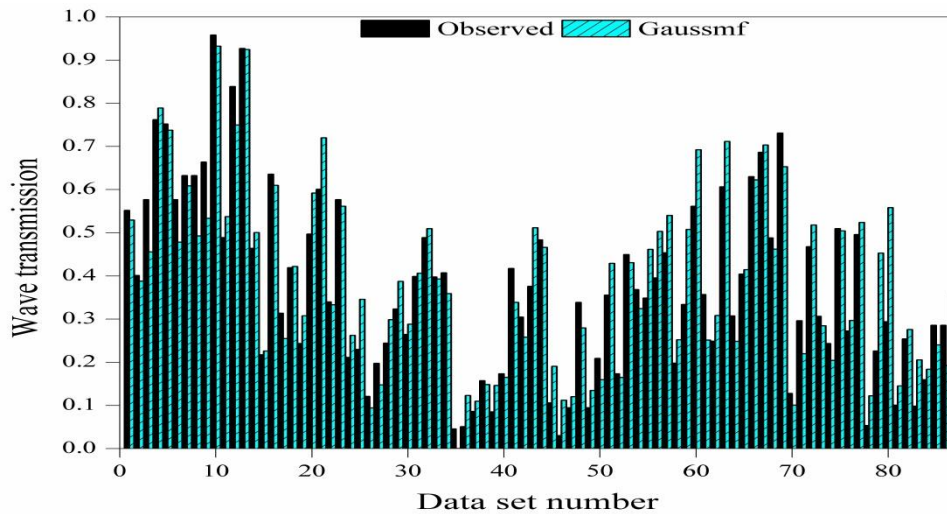


Fig. 6.3 Comparison of H_t/H_{tmax} predicted by ANFIS model with observed values

The box plot statistics are also used to check the variability of the predicted wave transmission by ANFIS model with different membership functions as shown in Fig. 6.2. Distribution of the predicted H_t/H_{tmax} values by Gaussmf is close to the observed one in the upper quartile and lower quartile of the box. The performance of the best model out of all the ANFIS models with various membership functions is assessed by plotting the predicted data with observed data points. Therefore, H_t/H_{tmax} predicting efficiency by ANFIS model with Gaussian membership function is compared with observed data for its validation as shown in Fig. 6.3. From the above figure, it is observed that the predicted results are in good agreement with the observed values and is concluded as a reliable model to predict H_t/H_{tmax} .

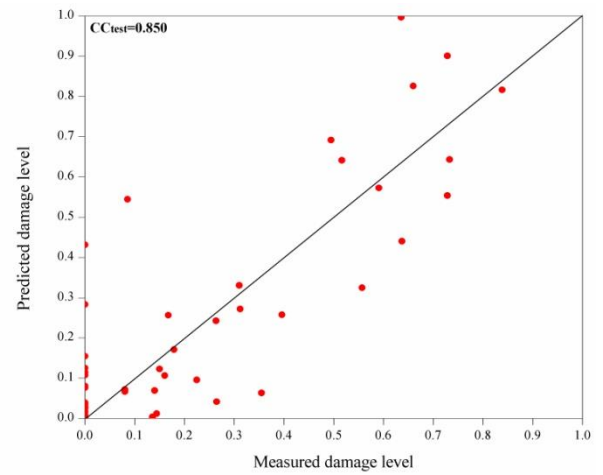
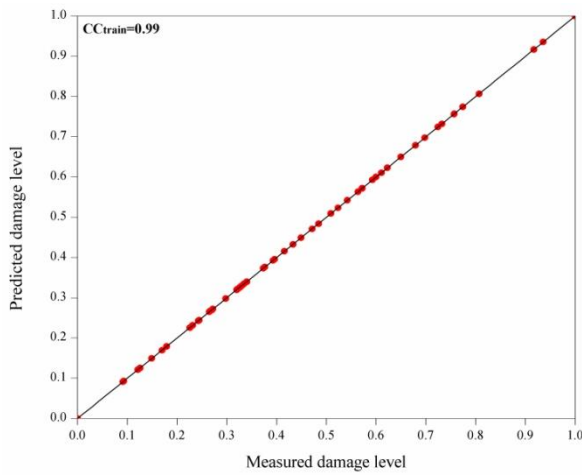
6.2.2 Simulation results of ANFIS Model in predicting the damage level (S)

The performance of different membership functions in terms of statistical measures is presented in the Table 6.2. In the present study, Sugeno first order method is used to trained the model by generating (2^8) 256 fuzzy rules with 2 generalized ‘Triangular (trimf)’, ‘Trapezoidal (trapmf)’, ‘Gbell (gbellmf)’ and ‘Gaussian (Gaussmf)’ membership functions for 100 epochs. To predict damage level, ANFIS model with Gaussmf is chosen as the best ANFIS model based on the model performance indicators, as RMSE = 0.123, CC = 0.875, SI = 0.011, NSE = 0.710 for testing. The ANFIS model is used, with a combination of gradient descent and least squares algorithm for an effective search of the optimal parameters to yield good results. Based on this hybrid approach of feed forward-back propagation neural network (FFBP) and decent gradient-least square principal fuzzy inference system (FIS) correlations of training and testing are increased.

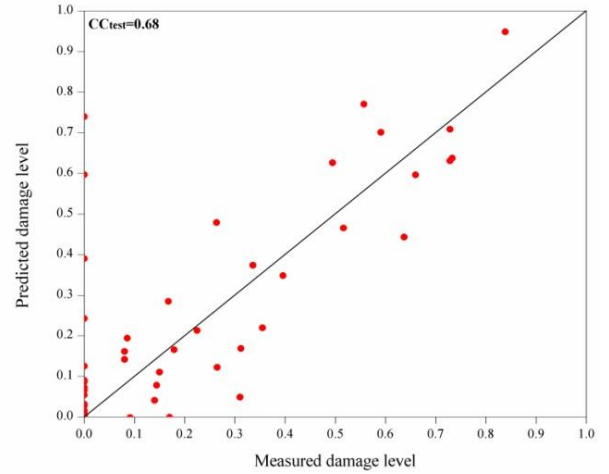
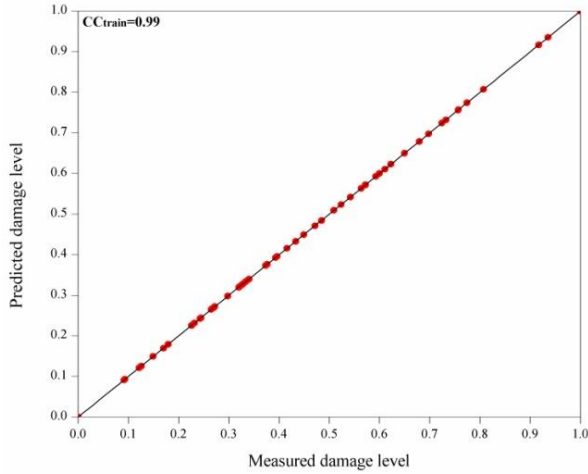
The scatter plots of predicted and observed damage level for ANFIS model with different membership functions are shown in Fig. 6.4. Among all the membership functions, Gaussian membership function is observed to be the best membership function. ANFIS model with Gaussmf outperformed other models with CC=0.875 providing better correlation with measured values and RMSE = 0.123.

Table 6.2 Statistical measure of ANFIS models for prediction of damage level

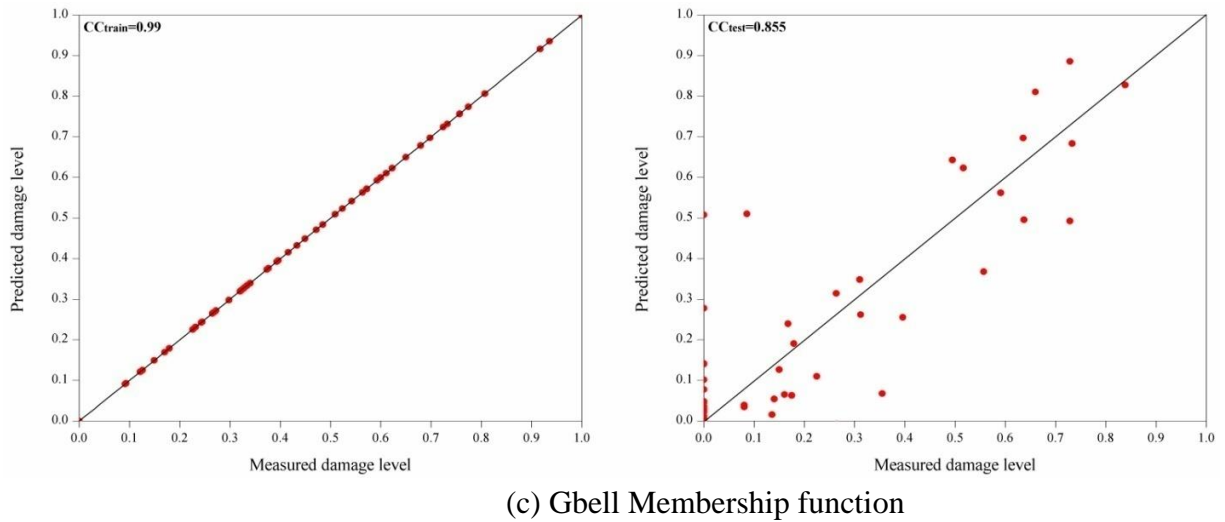
Statistical	Membership functions							
	Triangular		Trapezoidal		Gbell		Gaussian	
	Train	Test	Train	Test	Train	Test	Train	Test
RMSE	0.0001	0.132	0.0096	0.21	0.0002	0.129	0.002	0.123
NSE	0.99	0.64	0.99	0.575	0.99	0.682	0.99	0.710
CC	0.99	0.850	0.99	0.68	0.99	0.855	0.99	0.875
SI	0.0001	0.012	0.0009	0.018	0.00013	0.011	0.0012	0.011



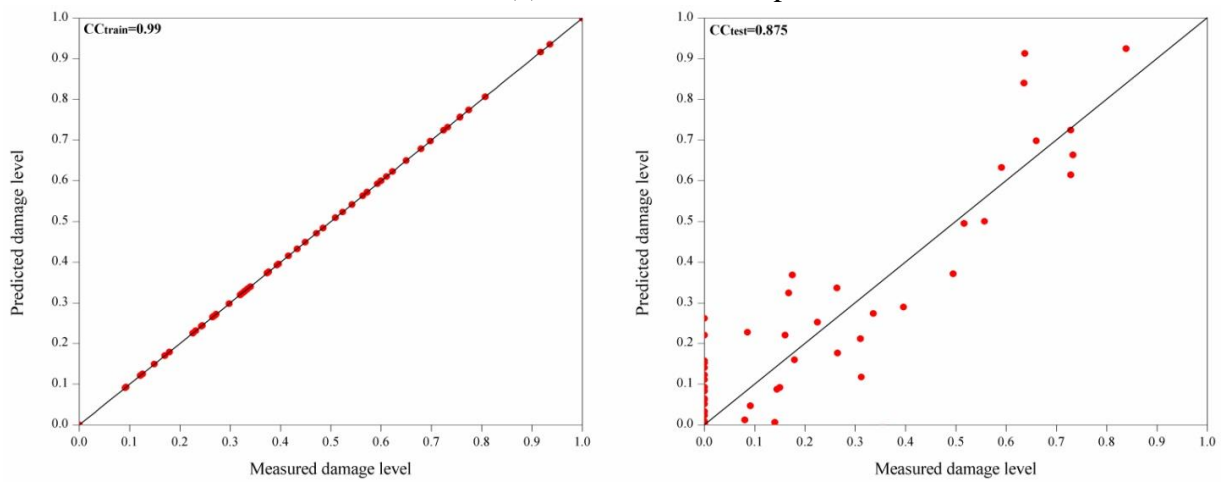
(a) Triangular Membership function



(b) Trapezoidal Membership function



(c) Gbell Membership function



(d) Gaussian Membership function

Fig. 6.4 Scatter plots of predicted and observed S for ANFIS model with different membership functions

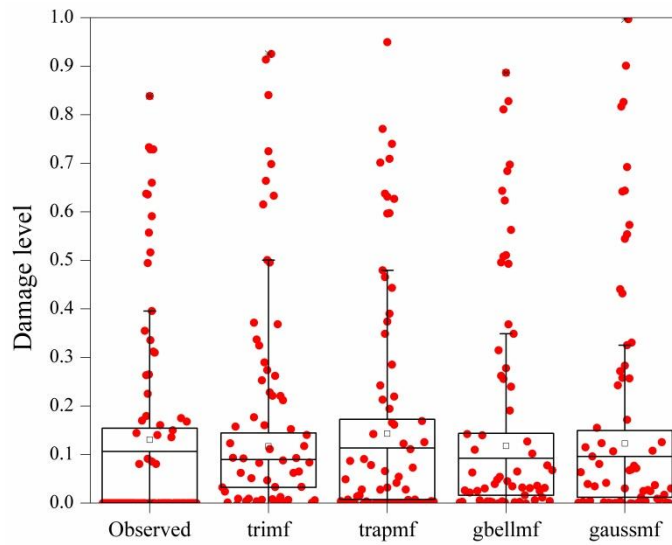


Fig. 6.5 Box-Whisker plots of S for ANFIS model with different membership functions

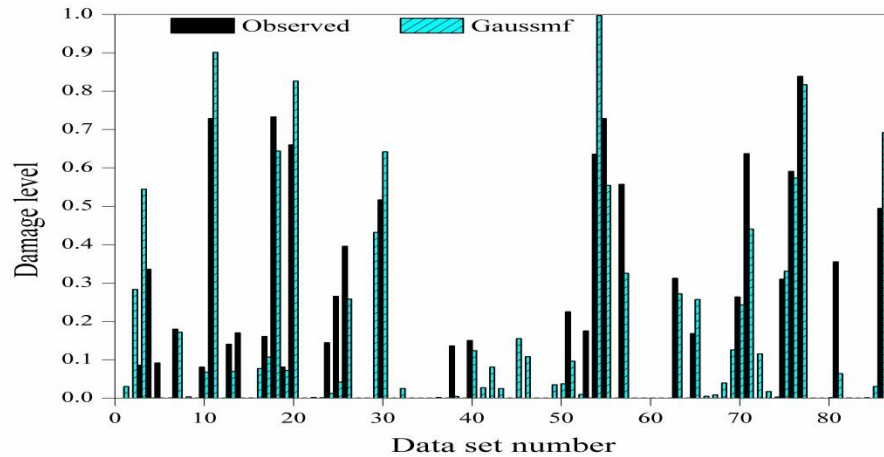


Fig. 6.6 Comparison of damage level prediction by SVM (RBF) with observed values

In terms of box plot statistics, the spread of data at lower and upper quartile of the box are predicted well in comparison with the observed. From Fig. 6.5, it is noticed that, Gbell and Gaussmf predictions match well with observed damage level among other membership functions where many outliers are found. Both box plot and scatter plots illustrations agree that, ANFIS model with Gaussmf is the best model. The efficiency of the best model is validated by presenting the findings in the form of comparison plot and is shown in Fig. 6.6. Out of all, the Gaussmf showed better results in predicting both the H_t/H_{tmax} and damage level. The predicted results of damage level by ANFIS model are scattered more compared to wave transmission, which is due to presence of more number of zero damage levels in the observed data set.

6.2.3 Summary of ANFIS model results

The performance of the ANFIS model in predicting H_t/H_{tmax} and damage level seems to be highly affected by hybridization of FIS with NN. The efficiency of the ANFIS model depends on the type and number of membership functions associated with each input data. The Gaussmf trains the model well before predicting the outputs in the testing phase. Even though results are not exactly matching the observed ones, but can be concluded as tool is efficient and reliable from the obtained results. Therefore, ANFIS can be used to predict the wave transmission and damage level with good correlation.

6.3 PERFORMANCE OF PSO-ANN MODEL FOR PREDICTING WAVE TRANSMISSION (H_t/H_{tmax}) AND DAMAGE LEVEL (S)

Regression analysis is conducted to predict both H_t/H_{tmax} and S by using PSO-ANN and

results are evaluated using different statistical measures such as RMSE, NSE, SI, CC, and box-whiskers plots. Based on the statistical parameters, accuracy of the model is tested. The predicted values are compared with the observed values by plotting the performance variation graph. The prediction will be considered as good when RMSE and SI is minimum ('0') while NSE and CC are maximum ('1').

In case of ANN hybrid model prediction, PSO function is called in place of an LM function by using PSORT and NN in the MATLAB software. The statistical parameters are calculated for various ANN hybrid models with varying size of the hidden neurons and the network with best predictions are considered as optimum. Table 6.3, shows the results of different statistical measures obtained by various ANN hybrid models for predicting transmitted wave heights (H_t/H_{tmax}) and damage level (S).

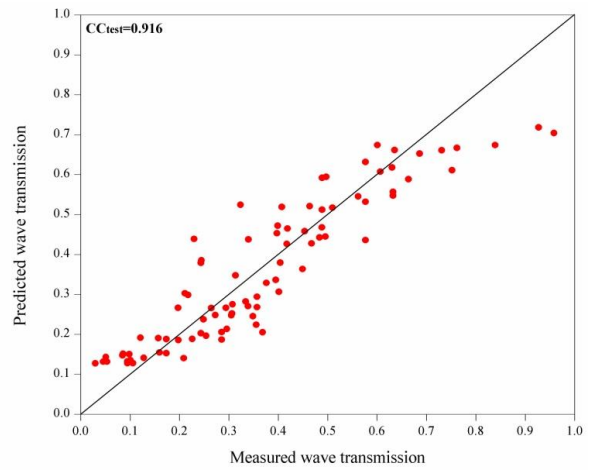
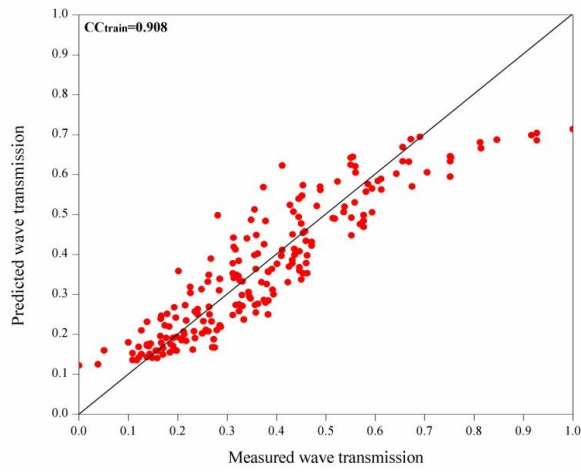
Table 6.3 Statistical parameters of PSO-ANN model predictions for H_t/H_{tmax}

Output	Models	Network	RMSE		C		SI		NSE	
			Train	Test	Train	Test	Train	Test	Train	Test
H_t/H_{tmax}	PSO-ANN1	8-1-1	0.079	0.084	0.908	0.916	0.213	0.232	0.821	0.835
	PSO-ANN2	8-2-1	0.080	0.081	0.904	0.921	0.216	0.224	0.817	0.846
	PSO-ANN3	8-3-1	0.065	0.072	0.940	0.941	0.176	0.199	0.879	0.879
	PSO-ANN4	8-4-1	0.081	0.082	0.903	0.918	0.218	0.228	0.814	0.841
	PSO-ANN5	8-5-1	0.077	0.080	0.912	0.925	0.207	0.222	0.832	0.849

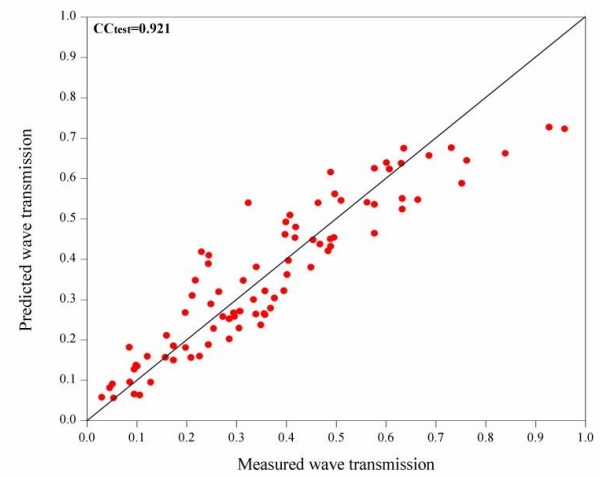
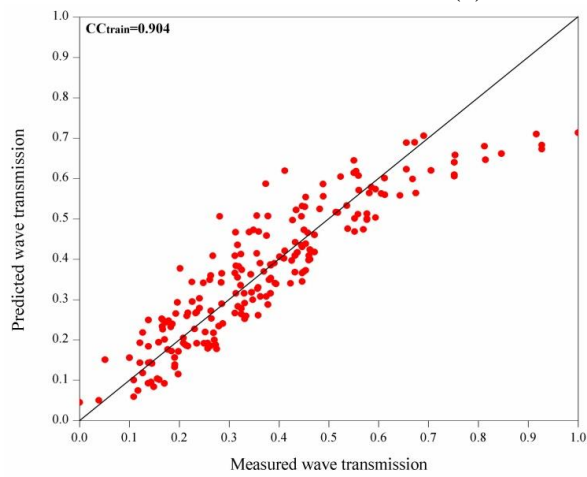
Table 6.4 Statistical parameters of PSO-ANN model predictions for damage level (S)

Output	Models	Network	RMSE		C		SI		NSE	
			Train	Test	Train	Test	Train	Test	Train	Test
S	PSO-ANN1	8-1-1	0.157	0.144	0.772	0.755	1.083	1.119	0.594	0.570
	PSO-ANN2	8-2-1	0.158	0.141	0.767	0.769	1.096	1.093	0.584	0.589
	PSO-ANN3	8-3-1	0.159	0.145	0.763	0.756	1.102	1.125	0.579	0.565
	PSO-ANN4	8-4-1	0.160	0.147	0.761	0.744	1.103	1.142	0.579	0.552
	PSO-ANN5	8-5-1	0.165	0.141	0.740	0.769	1.143	1.094	0.548	0.589

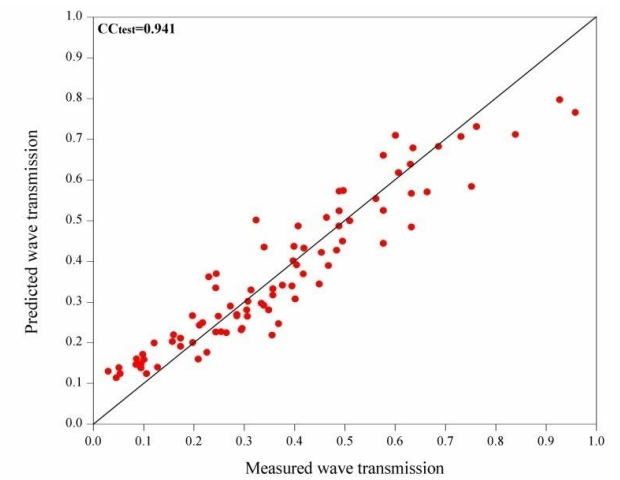
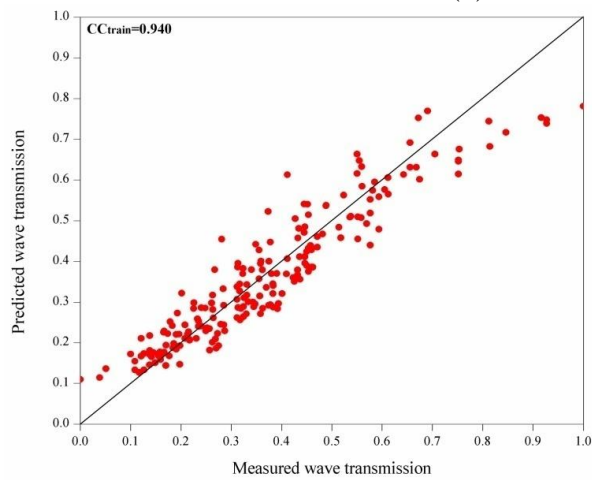
From Table 6.3, it can be seen that PSO-ANN3 model predicts the transmitted wave height better with CC = 0.941, RMSE = 0.072, SI = 0.199 and NSE = 0.879 for testing data. In case of damage level prediction PSO-ANN2 performs better with CC = 0.769, RMSE = 0.141, SI = 1.093 and NSE = 0.589 for testing data points as listed Table 6.4. It is observed that, damage levels obtained by PSO-ANN2 are poor compared wave transmission results by PSO-ANN3. This is due to the presence of more number of zero's in the data of damage levels. This represents that there is zero damage during physical model testing. Therefore, simulation results are displayed in the graphical form as a scatter plots between predicted and observed values of H_t/H_{tmax} in the Fig. 6.7.



(a) PSO-ANN model with 8-1-1



(b) PSO-ANN model with 8-2-1



(c) PSO-ANN model with 8-3-1

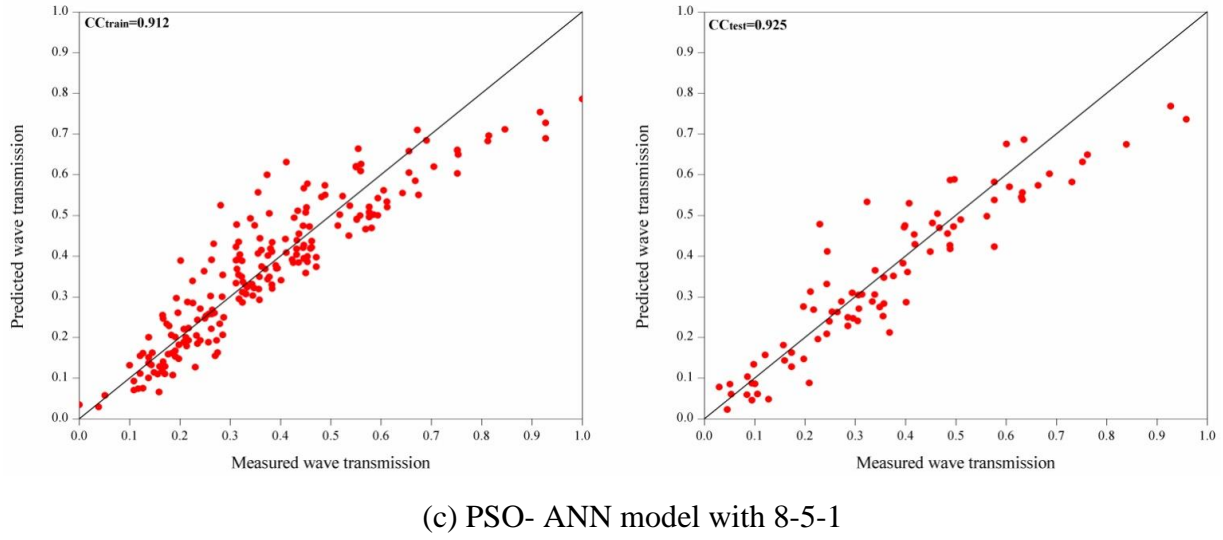
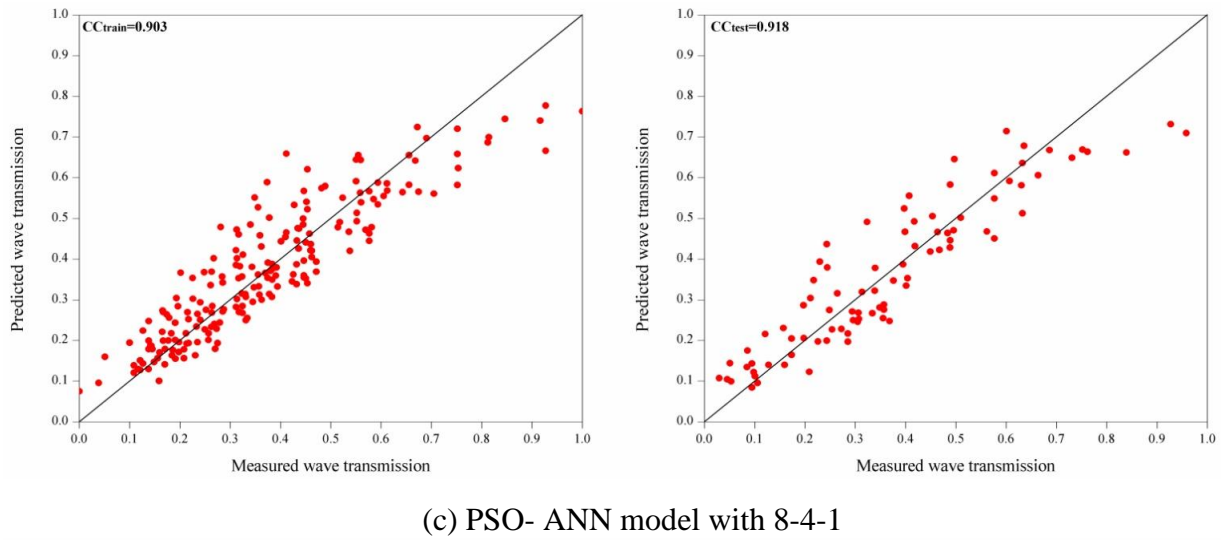


Fig. 6.7 Scatter plots of H_t/H_{tmax} by PSO-ANN model

It is observed that the scatter is less in Fig. 6.7(c) compared to Fig. 6.7(a), (b), (d) and (e). Similarly, in the prediction of damage level in the Fig. 6.10(b) showed good correlation with observed values whereas, Fig. 6.10(a), (c), (d) and (e) showed more scatter and poor correlation compared to Fig. 6.10(b). It can be summarized that, PSO-ANN3 with (8-3-1) network for H_t/H_{tmax} and PSO-ANN2 with (8-2-1) network for damage level gives the best results. These models can be used efficiently to predict the parameters effecting tandem breakwater stability.

The box plots statistics, is also a kind of measuring tool through which the variability of the predicted values with respect to observed data points, is identified to asses best model. In the Fig. 6.8, the ANN hybrid model with 2 and 4 hidden neurons show almost similar distribution of the predicted values of wave transmission of submerged reef with the observed values in both the lower and upper quartiles of the box plot. Similarly, the ANN

hybrid with 2 hidden neurons predicted damage level of the main breakwater successfully and are depicted in the Fig. 6.11.

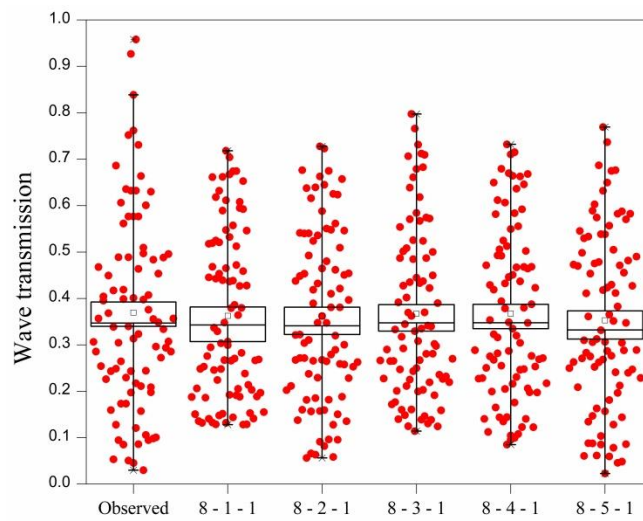


Fig. 6.8 Box-Whisker plots of wave transmission prediction by PSO-ANN with observed values

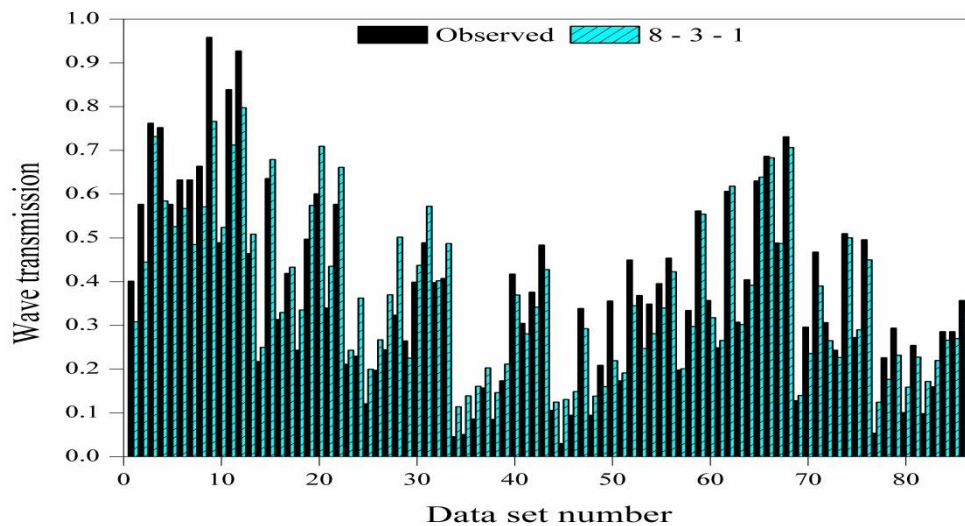
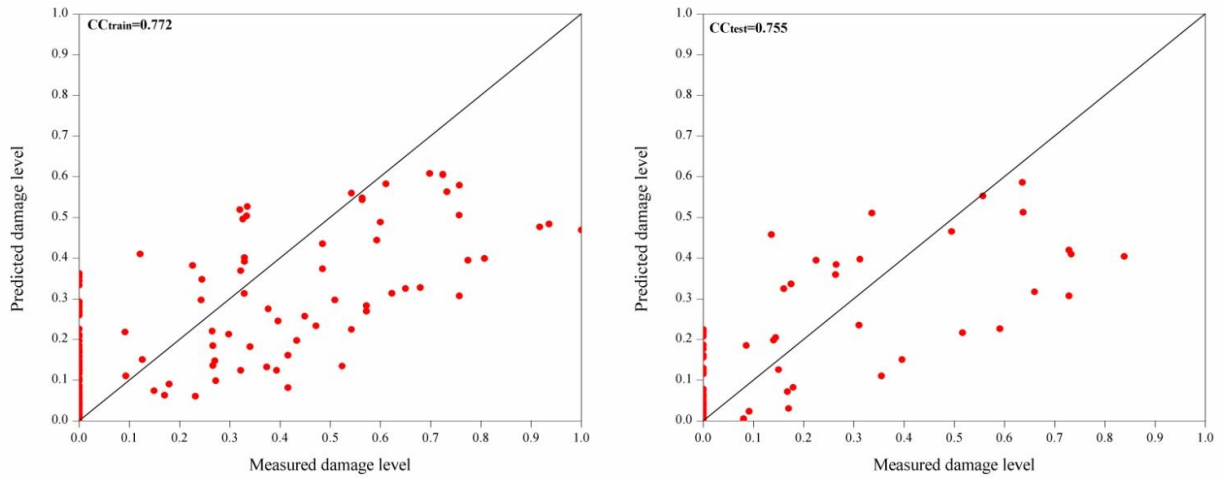


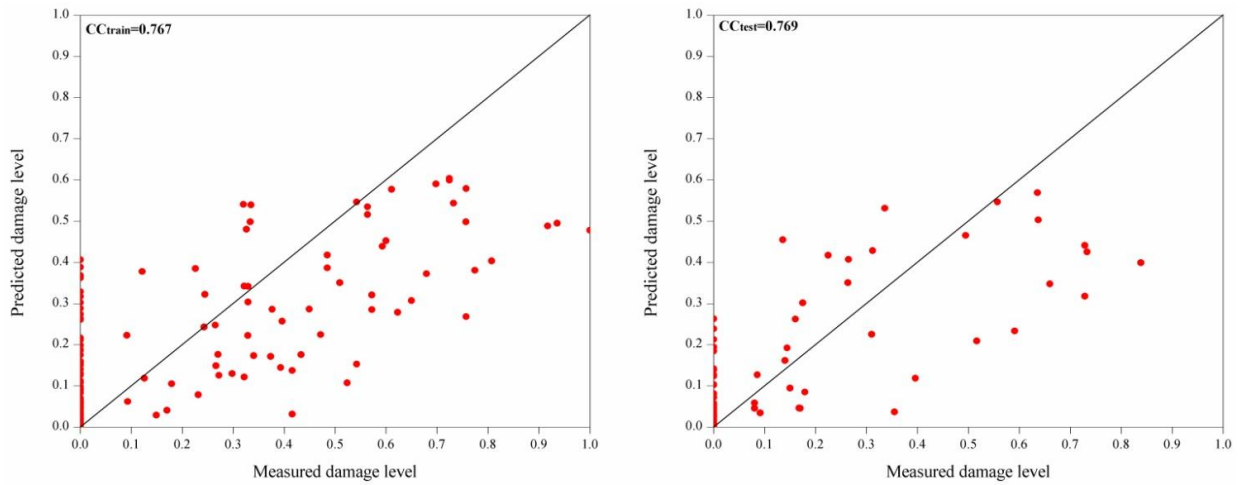
Fig. 6.9 Comparison of wave transmission predicted by PSO-ANN3 with observed values

Fig. 6.9 shows, the validation of PSO-ANN3 model for predicting wave transmission with respect to observed values in the form of comparison graph. Similarly, Fig. 6.12 shows the validation of PSO-ANN2 model performance in predicting damage level with respect to observed values in the form of comparison graph. It is observed that the prediction of PSO-ANN values match well with the observed values of wave transmission and damage level of tandem breakwater. Based on all the statistical measures and different plots, PSO-ANN3 technique can be considered as better model

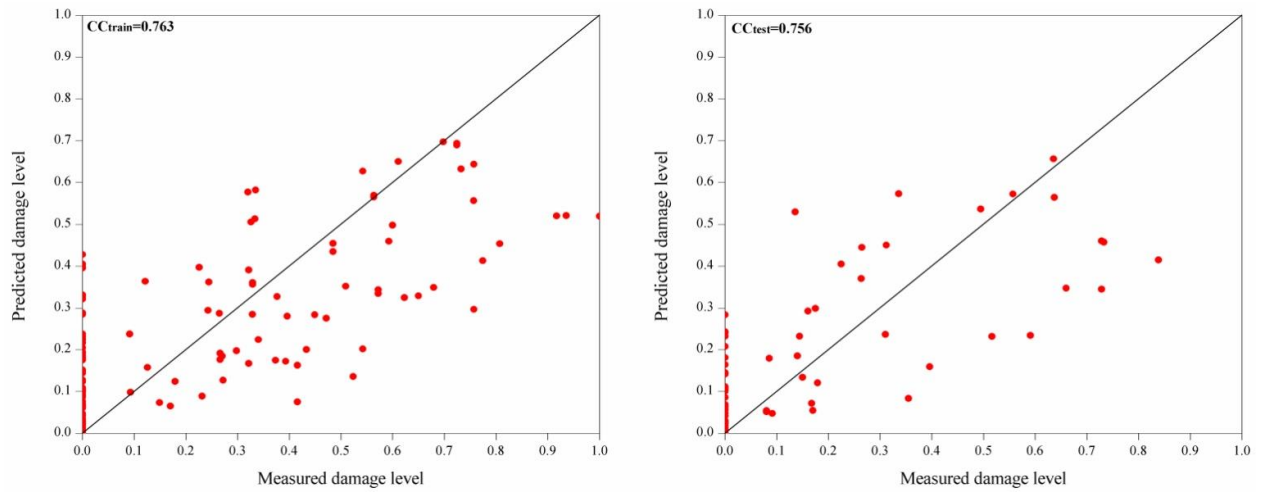
and can be used as an alternate method for prediction of wave transmission successfully for the immediate need or requirement for analysis if the sufficient or a large set of data is available. ANFIS with Gaussmf predicts the damage level better than PSO-ANN2. Hence, ANFIS with Gaussmf can be used as an alternate and reliable tool for damage level prediction.



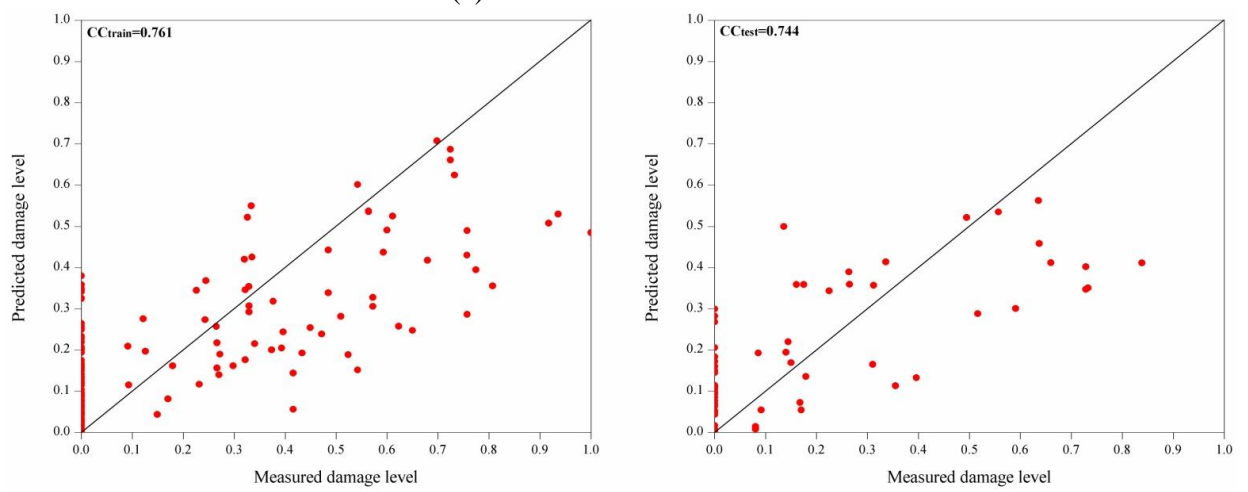
(a) PSO-ANN model with 8-1-1



(b) PSO-ANN model with 8-2-1



(c) PSO-ANN model with 8-3-1



(d) PSO-ANN model with 8-4-1

Fig. 6.10 Scatter plots for S for PSO-ANN hybrid models

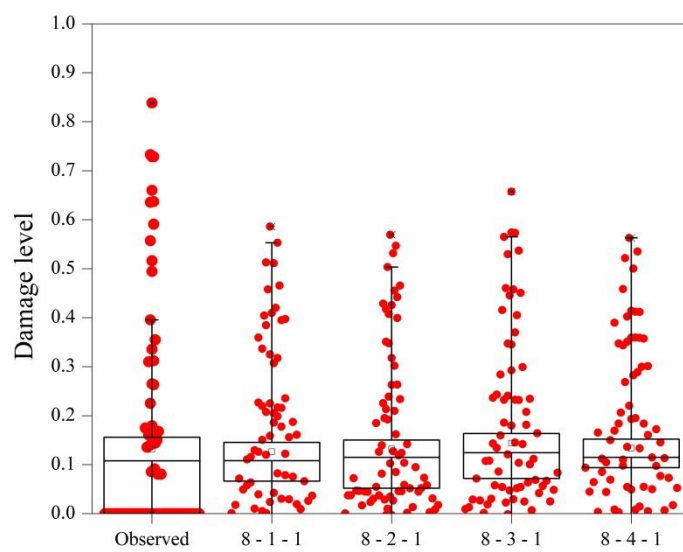


Fig. 6.11 Box-Whisker plots of damage level prediction for different PSO-ANN models

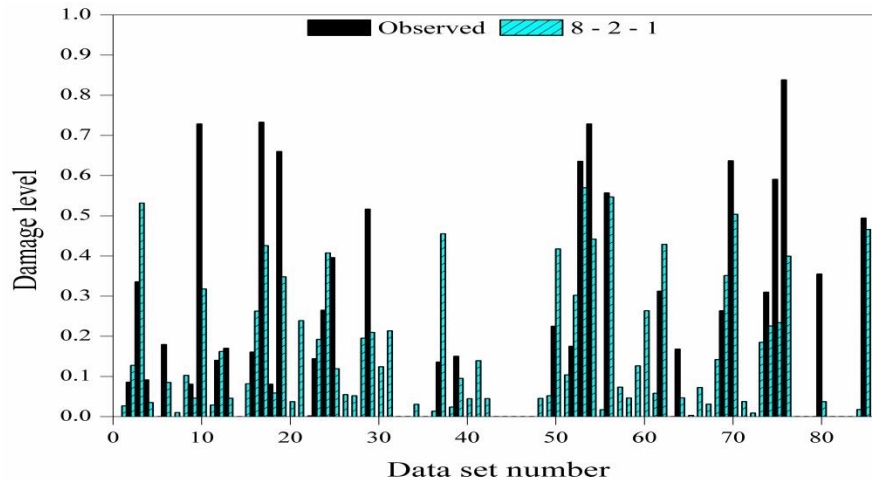


Fig. 6.12 Comparison of damage level predicted by PSO-ANN2 with observed values

6.3.1 Summary of PSO-ANN model results

PSO-ANN with various numbers of hidden neurons is attempted, for selecting the efficient ANN hybrid model using different statistical measures. The results obtained by PSO-ANN3 and PSO-ANN2 models show that, the soft computing techniques can be applied successfully for the prediction of wave transmission over submerged reef and damage level of conventional rubble mound breakwater of tandem breakwater.

6.4 PERFORMANCE OF PSO-SVM MODEL FOR PREDICTION OF WAVE TRANSMISSION AND DAMAGE LEVEL OF TANDEM BREAKWATER

The performance of PSO-SVM model depends on the good setting of SVM parameters such as regularization parameter C and ε with kernel parameters γ and d . Initially the upper and lower bound values of SVM parameters and kernel widths are given as input (i.e. for $C \in [1, 5000]$; $\varepsilon \in [0.000001, 1]$; $\gamma \in [0.01, 5]$ and $d \in [2, 5]$). In the next stage, the marginal difference in range between upper and lower bound values of the SVM parameters are reduced such that both should have in close proximity to the optimal parameter value obtained initially (i.e. for $C \in [(1, 500), (500, 1000), \dots, (4500, 5000)]$; $\varepsilon \in [(0.000001, 0.00001), (0.00001, 0.0001), \dots, (0.1, 1)]$; $\gamma \in [(0.01, 1), (1, 2), \dots, (4, 5)]$ and $d \in [(2, 3), \dots, (4, 5)]$). In associated with such various trials the optimal parameters are obtained and corresponding to that models are developed using linear, polynomial and RBF kernel functions. For each model developed, statistical indicator values such as CC, RMSE, NSE and SI are calculated as evaluation criteria. The kernel function

best suited for the SVM hybrid model is finally determined by evaluating the values of statistical measures obtained as model performance indicators.

The effectiveness and efficiency of the model results obtained during simulation depends upon the proper selection of SVM parameters (C , ε) and kernel parameters (γ , d), which can be obtained using particle swarm optimization. Initially, random range of values is provided for the parameters within the range given by software documentation. From the range given the parameter values corresponding to that the best fitness is achieved, and is found by particle searching. If the value selected at random from the range provided does not satisfy the fitness function, then the loop continues with the next available value in the given input.

6.4.1 Simulation results of PSO-SVM model for predicting wave transmission (H_t/H_{tmax}) over submerged reef and damage level (S) of emerged breakwater of tandem breakwater

The prediction of transmitted wave heights over a submerged reef of the tandem breakwater is conducted by considering the 8 inputs variables H_i/gT^2 , X/d , $H_i/\Delta D_{n50}$, B/d , B/L_o , F/H_i , h/d , d/gT^2 which influence the output H_t/H_{tmax} . The training of the model is carried out for 201 data points (70%) and then testing is done by considering 87 data points (30%), for validation of the model prediction.

Initially, for a particular kernel type, PSO-SVM model is developed and among them the one which shows best data fitting is adopted as the best model for the corresponding kernel function. The model that shows the best data fitting is found out by evaluating the statistical parameters. Figs. 6.13, 6.14 and 6.15 depicts the data fitting curves for PSO-SVM models developed using linear, polynomial and RBF kernel functions, respectively using set of testing data. In each figure, it can be observed that predicted value fits better with actual value for specific values of C , ε , γ and d . From Fig.6.13, the best fitting curve corresponds to the model having $C = 1500$ and $\varepsilon = 0.0885$ which shows the data fitting the predicted values with observed values. Similarly, $C = 183.78$, $\varepsilon = 0.0000538$, $d = 3$ and $C = 18.7$, $\varepsilon = 0.0827$, $\gamma = 2.6$ are parameter values corresponding to the best fitting curves for Figs. 6.14 and 6.15 respectively obtained by proposed SVM algorithm.

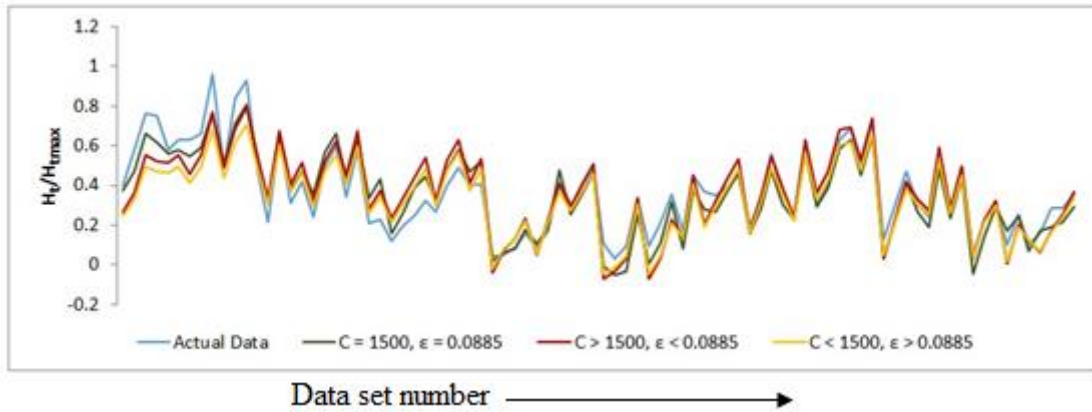


Fig. 6.13 Data fitting of models developed (linear kernel) for prediction of H_t/H_{tmax}

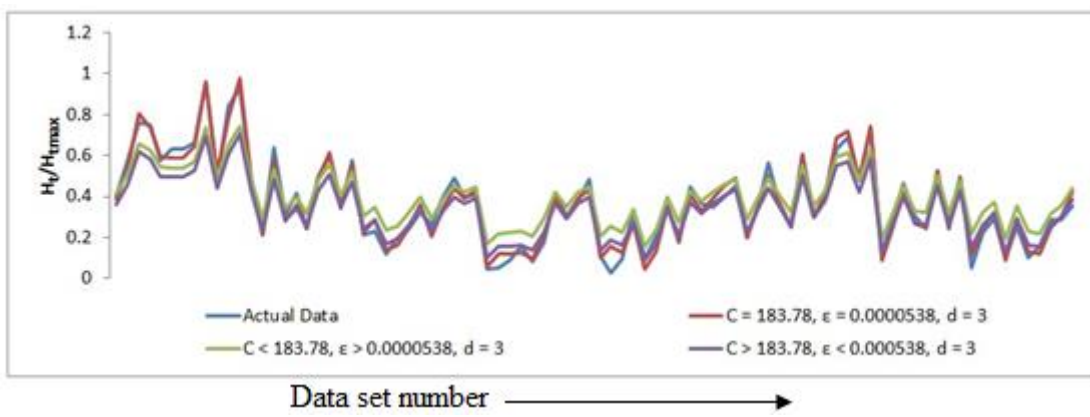


Fig. 6.14 Data fitting of models developed (polynomial) for prediction of H_t/H_{tmax}

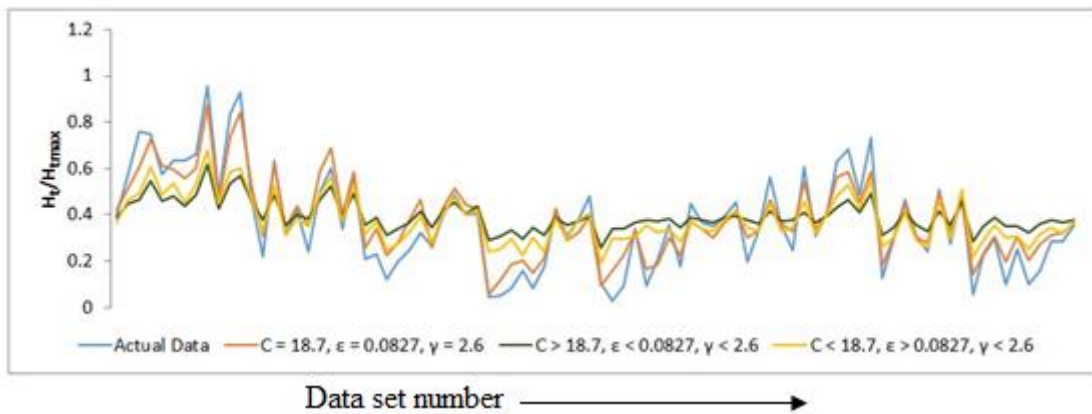


Fig. 6.15 Data fitting of models developed (RBF kernel) for prediction of H_t/H_{tmax}

For the prediction of transmitted wave height, optimal parameters of SVM with linear, polynomial and RBF kernel parameters are obtained using PSO as an optimization searching algorithm. In case of RBF kernel function, the optimal width (γ) is found to be 2.6 and the optimal values of d (degree) in case of polynomial kernel function is 3, as listed in Table 6.5. The optimal parameters obtained are used by the SVM model to predict the transmitted wave height. Thus, the effectiveness, reliability and accuracy of

the model developed are evaluated by calculating the statistical measures as presented in the Table 6.6.

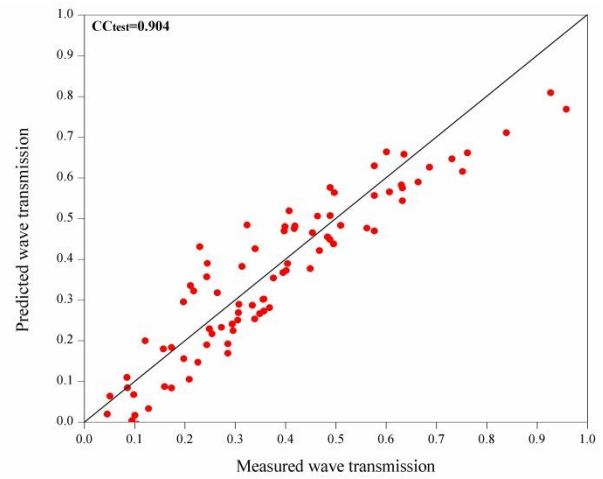
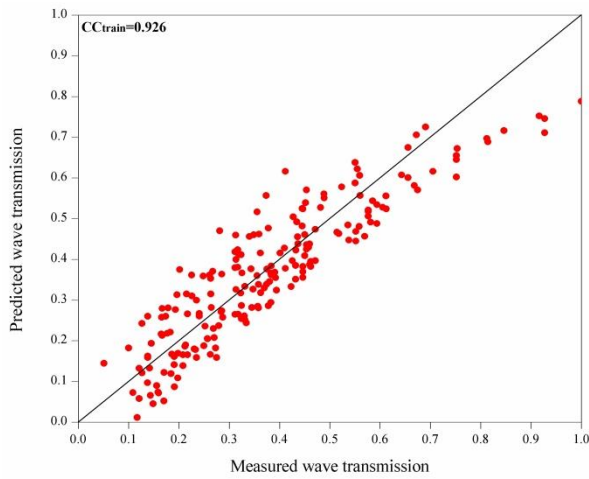
Table 6.5 Optimal parameters for PSO-SVM models for predicting H_t/H_{tmax}

Kernel type	Linear	Polynomial	RBF
C	1500	183.78	18.7
ϵ	0.0885	0.0000538	0.0827
γ	-	-	2.6
d	-	3	-

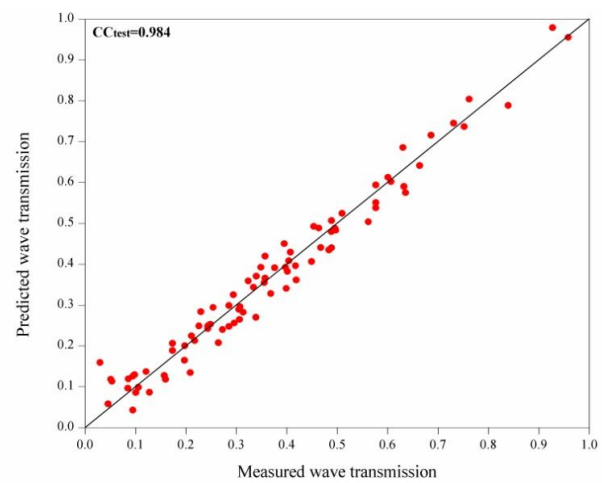
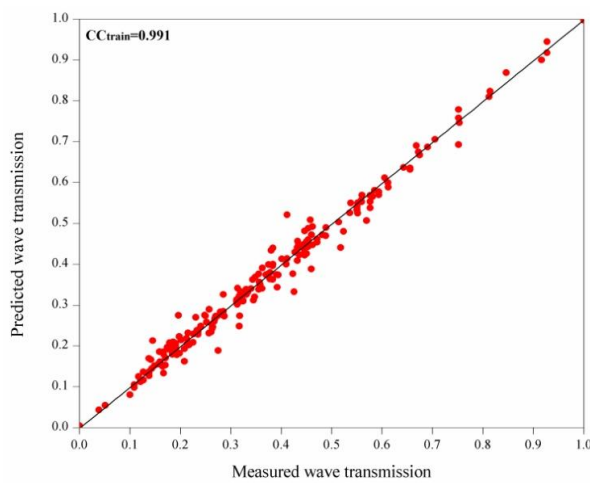
Table 6.6 Statistical parameters for PSO-SVM models for predicting H_t/H_{tmax}

Kernel type	Linear		Polynomial		RBF	
	Train	Test	Train	Test	Train	Test
CC	0.926	0.904	0.991	0.984	0.969	0.960
RMSE	0.077	0.081	0.025	0.037	0.051	0.068
SI	0.217	0.217	0.088	0.102	0.138	0.184
NSE	0.853	0.819	0.982	0.968	0.926	0.894

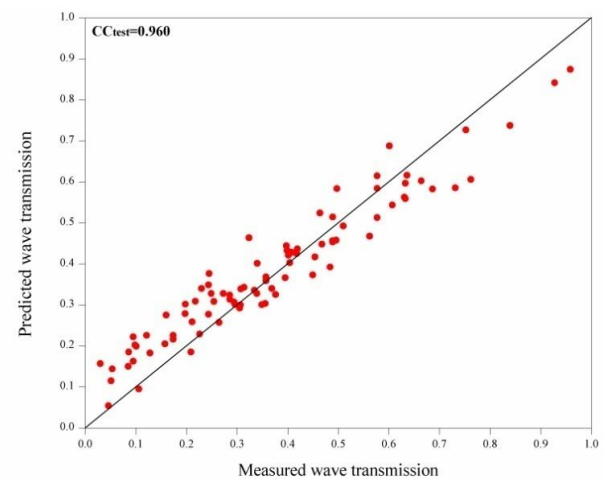
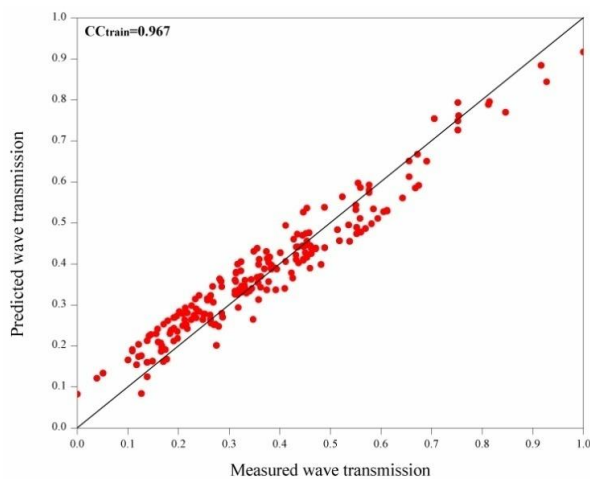
The RMSE=0.037 obtained for testing model for polynomial kernel function is comparatively less than other kernel functions. SI=0.102 value for polynomial kernel function indicates the good correlation and least scattering from actual fitted data. NSE=0.968 for polynomial kernel function indicates the predictive efficiency of PSO-SVM. From all the results obtained, it is observed that PSO-SVM model with polynomial kernel function shows better generalization performance with values of CC=0.984, RMSE=0.037, SI=0.102, NSE=0.968 testing data points, when compared with other kernel functions. The scatter diagram which shows the CC of the models for the training and testing data using various kernels are shown in Fig. 6.16.



a) Linear kernel



b) Polynomial kernel function



(c) RBF kernel function

Fig. 6.16 Scatter plots of PSO-SVM model for H_t/H_{tmax} with observed data

From the scatter plots, it is noticed that, PSO-SVM model using polynomial kernel function gives the best data fitting between predicted and observed data. The box plots

are another type of statistical measures in which the variability of the predicted data is found with reference to observed data and is depicted in the discussion. Fig. 6.17 indicates box plot with the upper and lower quartile values predicted is matching well with the observed wave transmission over submerged reef. SVM model with polynomial kernel, predicted data points are distributed well in the lower quartile of the box plot with reference to the observed values.

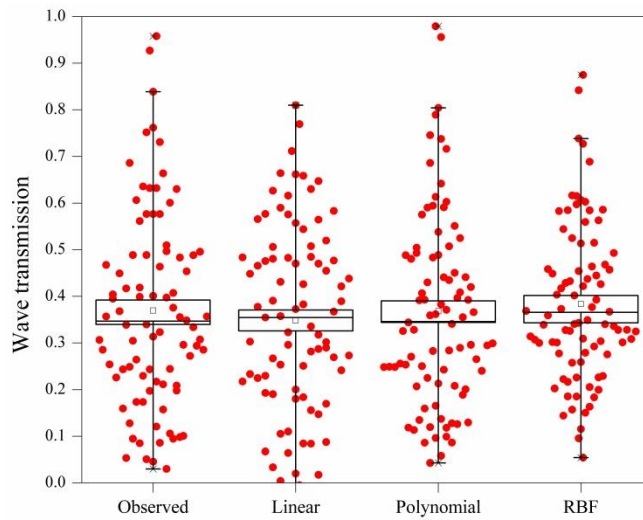


Fig. 6.17 Box-Whiskers plot of H_t/H_{tmax} for PSO-SVM model

The validation of PSO-SVM model using polynomial kernel function for the prediction of wave transmission is shown in Fig. 6.18, using the comparison graph. From the graph, it is clearly noticed that, the predicted data follows similar trend compared to observed data. Even though model developed with RBF kernel function provides results with high correlation, for both training and testing. PSO-SVM model using polynomial kernel function gives 4.36% improved correlation, 48.61% reduced RMSE, SI and maximum NSE value is found to be the best model for prediction of transmitted wave height over submerged reef of a tandem breakwater.

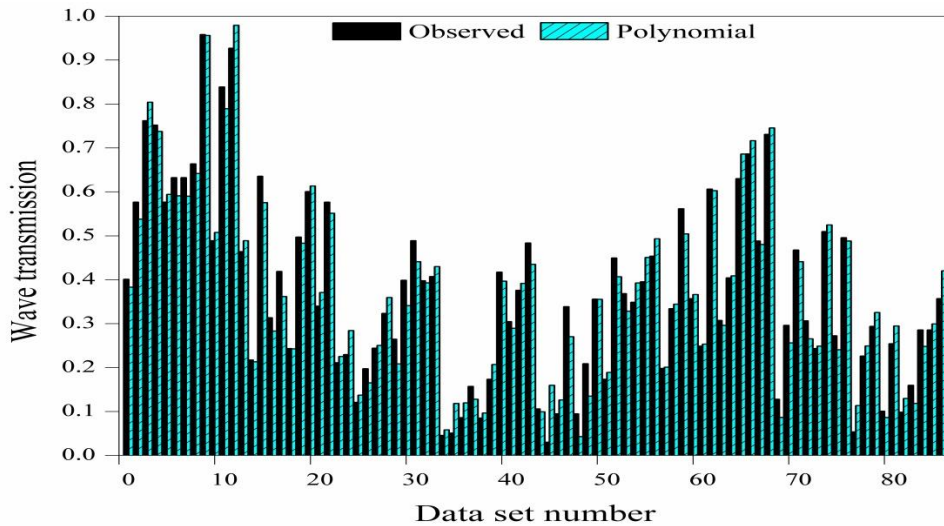


Fig. 6.18 Comparison of PSO-SVM model (polynomial kernel) for H_t/H_{tmax} with observed values

6.4.2 Simulation results of PSO-SVM model for predicting damage level (S) of Conventional rubble mound breakwater of tandem breakwater

The prediction of damage level of the emergent conventional rubble mound breakwater of the tandem breakwater is performed by considering the 8 inputs H_i/gT^2 , X/d , $H_i/\Delta D_{n50}$, B/d , B/L_o , F/H_i , h/d , d/gT^2 influencing the dependent variable damage level (S). The training is carried out using 202 data points (70%) and testing is done for 86 data points (30%). Figs. 6.19, 6.20 and 6.21 depicts the data fitting curves of PSO-SVM models developed for damage level prediction using linear, polynomial and RBF kernel functions, respectively, for testing. In each figure, it is observed that predicted value fits better with actual value for specific values of C , ε , γ and d . From the Fig. 6.19, the best fit curve corresponds to the model having (linear kernel) $C = 1327.67$ and $\varepsilon = 0.0069$. Similarly, $C = 547$, $\varepsilon = 0.0356$, $d = 3$ and $C = 363.83$, $\varepsilon = 0.0000228$, $\gamma = 3.2$ are parameter values corresponding to the best fitting curves for Figs. 6.20 and 6.21 respectively.

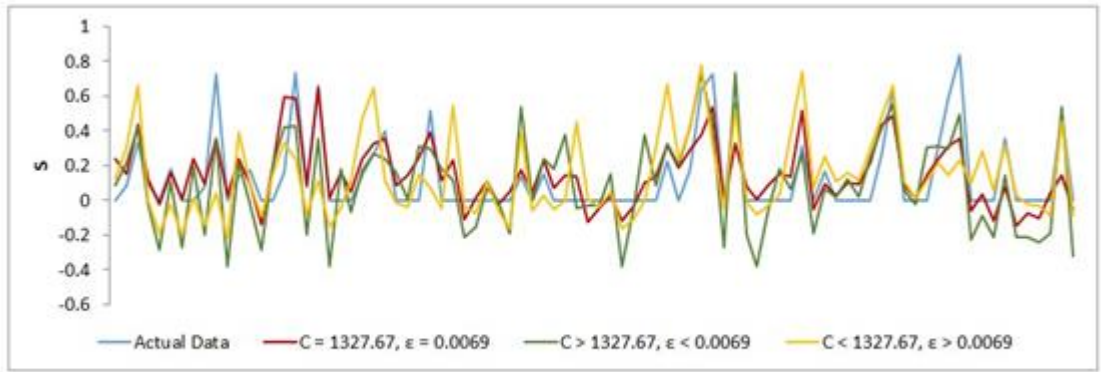


Fig. 6.19 Data fitting of models developed (linear) for prediction of Damage level

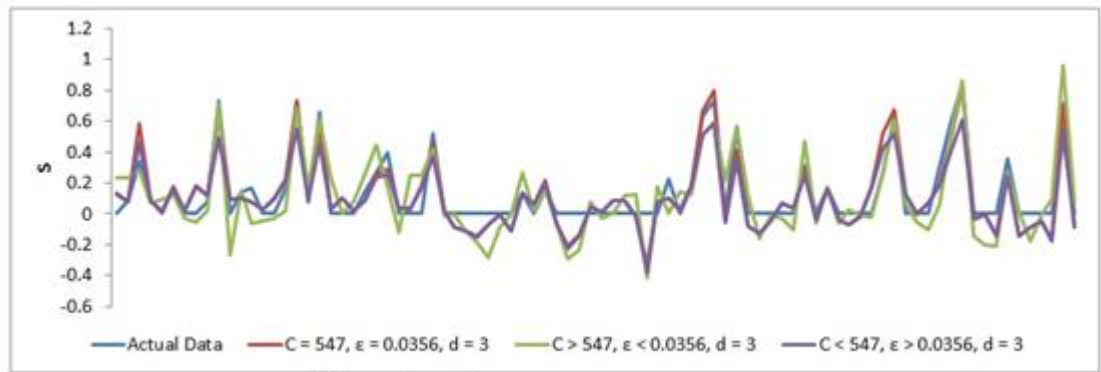


Fig. 6.20 Data fitting of models developed (polynomial) for prediction of damage level

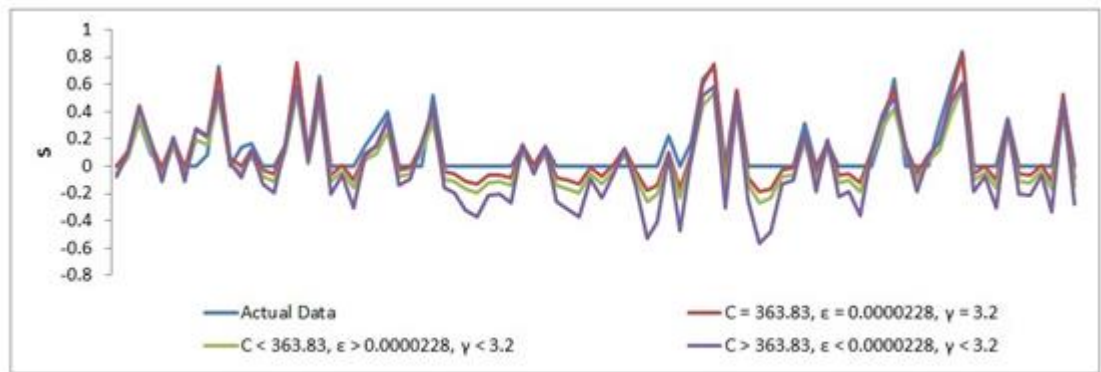


Fig. 6.21 Data fitting of models developed (RBF) for prediction of damage level

Optimal values of SVM and kernel function parameters, obtained using PSO for damage level prediction using linear, polynomial and RBF kernel based models are shown in Table 6.7. The optimal values of the parameters are used by the model in

prediction of damage level of conventional rubble mound breakwater of tandem breakwater. In case of RBF kernel, the optimal width (γ) is found to be 3.2 and the optimal values of d (degree) in case of polynomial kernel function is 3 and effectiveness of the model developed in prediction of damage level is evaluated by calculating the value of statistical parameters.

Table 6.7 Optimal parameters for PSO-SVM models for predicting Damage levels

Kernel type	Linear	Polynomial	RBF
C	1327.6	547	363.83
ϵ	0.0069	0.0356	0.000022
γ	-	-	3.2
d	-	3	-

Model performance indicators of models developed using linear, polynomial and RBF kernels for training and testing are given in Table 6.7. The PSO-SVM model with RBF kernel function gives better correlation of CC = 0.941 for testing compared to all other kernel functions.

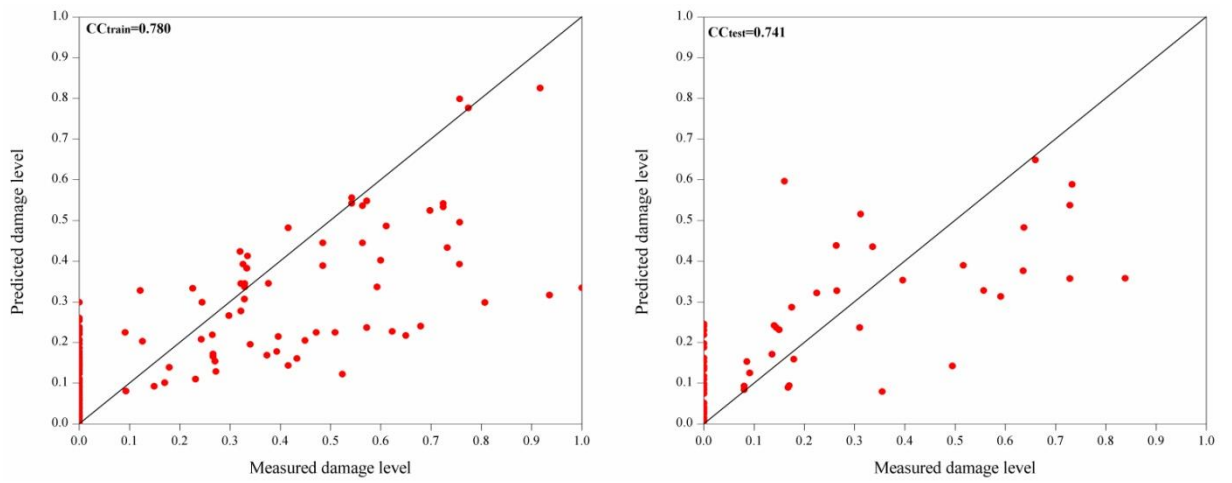
The value of RMSE=0.088 for testing is comparatively lower for developed model using RBF kernel function compared to rest of the kernel functions. This indicates that the predicted data is closer to actual data for RBF kernel function.

Table 6.7 Statistical parameters for PSO-SVM models for predicting Damage levels

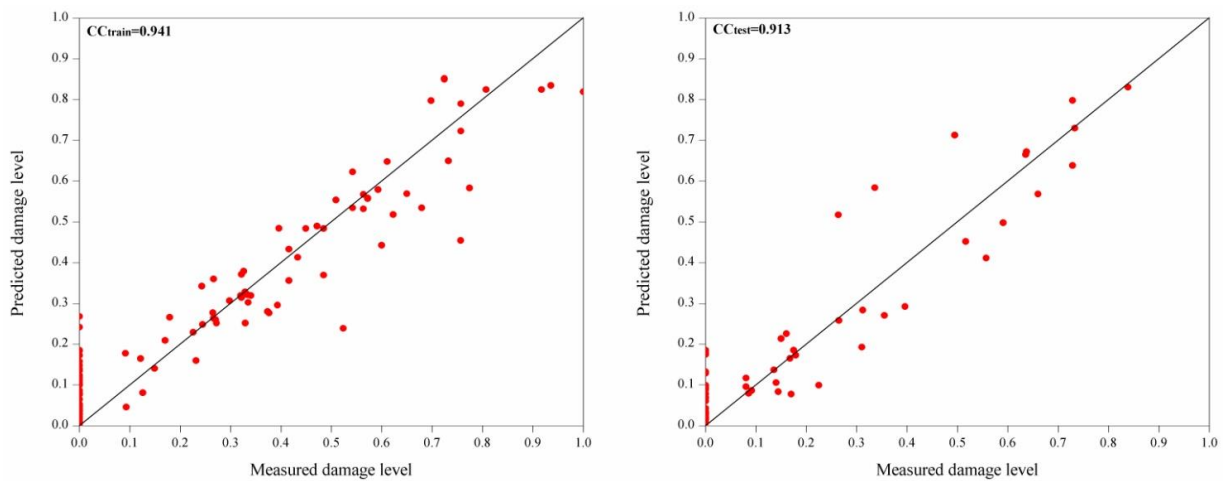
Kernel type	Linear		Polynomial		RBF	
	Train	Test	Train	Test	Train	Test
CC	0.780	0.741	0.941	0.913	0.961	0.941
RMSE	0.154	0.161	0.085	0.099	0.071	0.088
SI	1.067	1.143	0.584	0.756	0.493	0.669
NSE	0.605	0.541	0.882	0.799	0.916	0.843

SI = 0.669 for RBF kernel function indicates the least scattering from actual fitted data compared to 1.143 and 0.756 during testing phase for linear and polynomial kernel functions respectively. NSE value of 0.843 for RBF kernel function compared to 0.541 and 0.799 during testing for linear and polynomial kernels, respectively, indicates the predictive efficiency of model developed using RBF kernel function. Finally, PSO-SVM model with RBF kernel function shows better error generalization performance

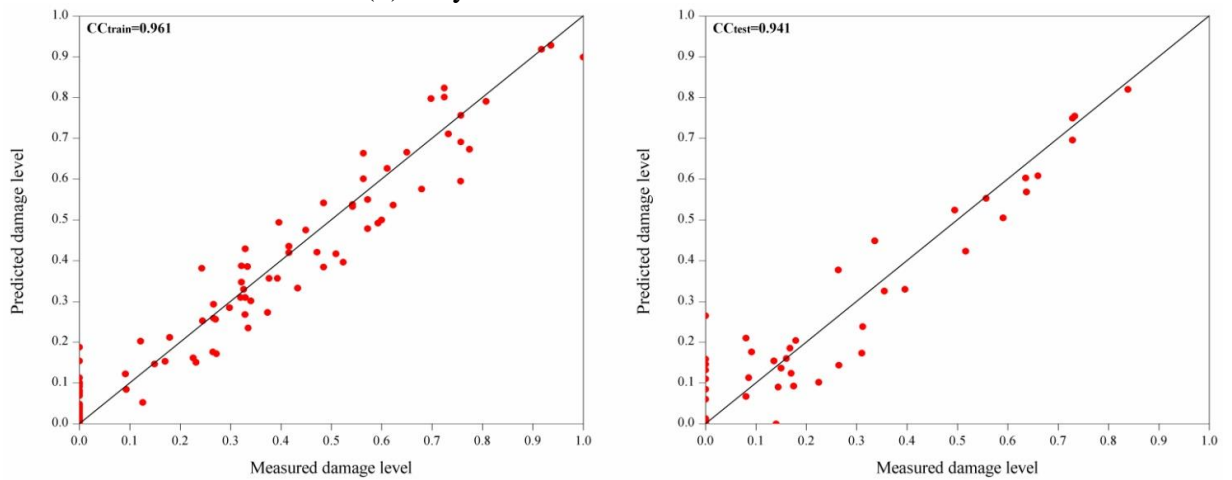
with $CC = 0.941$, $RMSE = 0.088$, $SI = 0.669$ and $NSE = 0.843$ testing, when compared to the rest of the kernel functions. The scatter diagram showing CC of PSO-SVM models for the training and testing data are shown in Fig. 6.22



(a) Linear kernel function



(b) Polynomial kernel function



(c) RBF kernel function

Fig. 6.22 Scatter plots of damage level (S) prediction using SVM model with different kernel functions

From the scatter plots, it is clear that, PSO-SVM model using RBF kernel function gives the best data fitting between predicted data and observed data. The box plot statistics is also used to measure the performance of the PSO-SVM model with different kernel. In terms of box plot assessment of predicted S in respect to observed data points is shown in Fig. 6.23. In the plots spread of predicted values by RBF shows the similar pattern and closely related to the observed values in terms of upper and lower quartile distribution of RBF prediction. Based on the scatter and box plots statistics, PSO-SVM model with polynomial and RBF kernel functions predicts successfully with high accuracy compared to the all other models, can be used as best alternate to predict the wave transmission over submerged reef and damage level of main breakwater of tandem breakwater respectively.

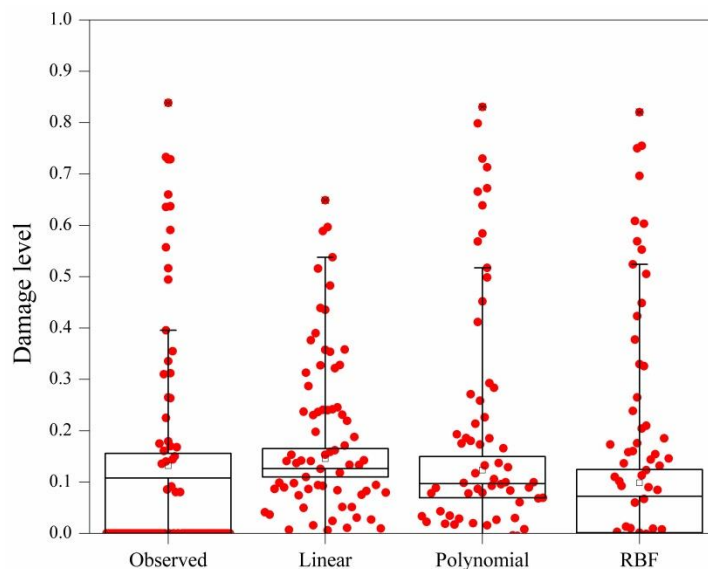


Fig. 6.23 Box-Whiskers plots of damage level (S) for PSO-SVM model

The model developed using linear kernel function gives the least correlation ($CC = 0.741$ for testing) which indicates that the data cannot be separated by a linear hyperplane in a low dimensional space. Fig. 6.24 shows the performance of observed and predicted damage level by PSO-SVM for RBF kernel function. Observing the graph, the PSO-SVM model with RBF kernel function is showing similar pattern compared to actual data with fluctuations are comparatively more around values of $S = 0$. Even though models developed with polynomial kernel function provides results with 83% correlation for both training and testing, the PSO-SVM model using RBF kernel function with 88% correlation, minimum RMSE, SI and maximum NSE value is found to be the best model in prediction of damage level of emergent main breakwater of tandem breakwater.

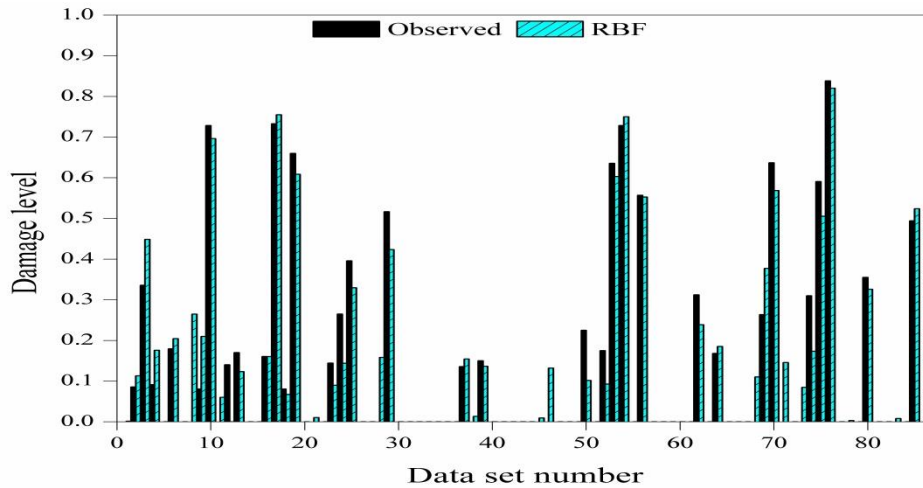


Fig. 6.24 Comparison of damage level predicted by PSO-SVM model (RBF) with observed values

6.4.3 Summary of PSO-SVM model results

Soft computing techniques provide results within a smaller time frame compared to mathematical and physical modeling. The complex nature of mathematical modeling and more expense involved in physical modeling makes soft computing technique a better alternate option for the prediction of transmitted wave height and damage level. As soft computing models are developed based on experimental data, it is essential to have physical model study so as to quantitatively determine the parameters influencing the performance of breakwaters. Therefore, physical model study along with the application of soft computing techniques employed to have effective and faster results. Different soft computing techniques such as ANN, SVM, ANFIS, etc. are successfully used for the prediction of wave parameters as discussed earlier. In this context, effectiveness of model developed for prediction depends on the proper selection of parameters. In this study, an effort is made to check the applicability of PSO-ANN and PSO- SVM model for predicting transmitted wave height and damage level of a tandem and the results are found to be satisfactory and reliable.

6.5 COMPARISON OF PERFORMANCE OF BEST ANN, SVM, ANFIS, PSO-ANN AND PSO-SVM MODELS

The results obtained using individual models have been discussed in previous sections. In this section a comparison of all the selected models have been made to know the best model that could predict wave transmission and damage level of tandem

breakwater accurately. For the given data set, ANN, ANFIS, SVM, PSO-ANN and PSO-SVM models are trained and tested to predict the wave transmission and damage level of tandem breakwater. The ANN (8-3-1), SVM (RBF), ANFIS (Gaussmf), PSO-ANN (8-3-1) and PSO-SVM (polynomial) models performed better among all the soft computing models considered for predicting wave transmission over a submerged reef of tandem breakwater in terms of statistical measures with respect to experimental values are listed in Table 6.9. Similarly, ANN (8-5-1), SVM (RBF), ANFIS (Gaussmf), PSO-ANN (8-2-1) and PSO-SVM (RBF) models performed better among all the soft computing models considered for predicting damage levels of conventional rubble mound breakwater of tandem breakwater in terms of statistical measures with respect to experimental values are listed in the Table 6.10.

Figs. 6.25 and 6.26 illustrate the comparison of wave transmission predicted by ANN with (8-3-1) and SVM with RBF kernel function with respect to experimental values of individual models. Similarly, Figs. 6.27 and 6.28 represent PSO-ANN with (8-3-1) and PSO-SVM with polynomial kernel function with respect to experimental values of hybrid models. ANN with (8-3-1) network outperformed all other soft computing techniques for predicting wave transmission with high CC of 0.989 and high efficiency of 0.978 with least error of 0.031 and small scatter of 0.086. Therefore, ANN with (8-3-1) network can be used as an efficient and reliable soft computing technique for predicting wave transmission over a submerged reef of a tandem breakwater.

Table 6.9 Comparison of Statistical Measures of ANN, SVM, ANFIS, PSO-ANN and PSO-SVM Models for wave transmission (H_t/H_{tmax})

Model	Training Data				Testing Data			
	CC	RMSE	SI	NSE	CC	RMSE	SI	NSE
ANN(8-3-1)	0.988	0.029	0.078	0.976	0.989	0.031	0.086	0.978
SVM (RBF)	0.977	0.055	0.151	0.92	0.965	0.056	0.150	0.911
ANFIS (Gaussmf)	0.99	0.0017	0.006	0.99	0.935	0.075	0.002	0.869
PSO-ANN (8-3-1)	0.940	0.065	0.176	0.88	0.941	0.072	0.199	0.879
PSO-SVM (Polynomial)	0.969	0.051	0.138	0.926	0.960	0.068	0.184	0.894

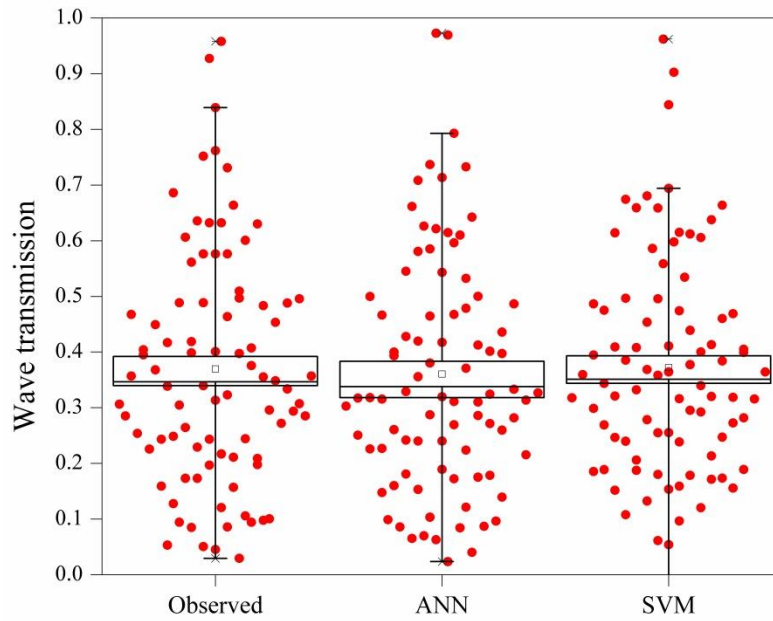


Fig. 6.25 Box-Whisker plot for wave transmission comparison of individual models

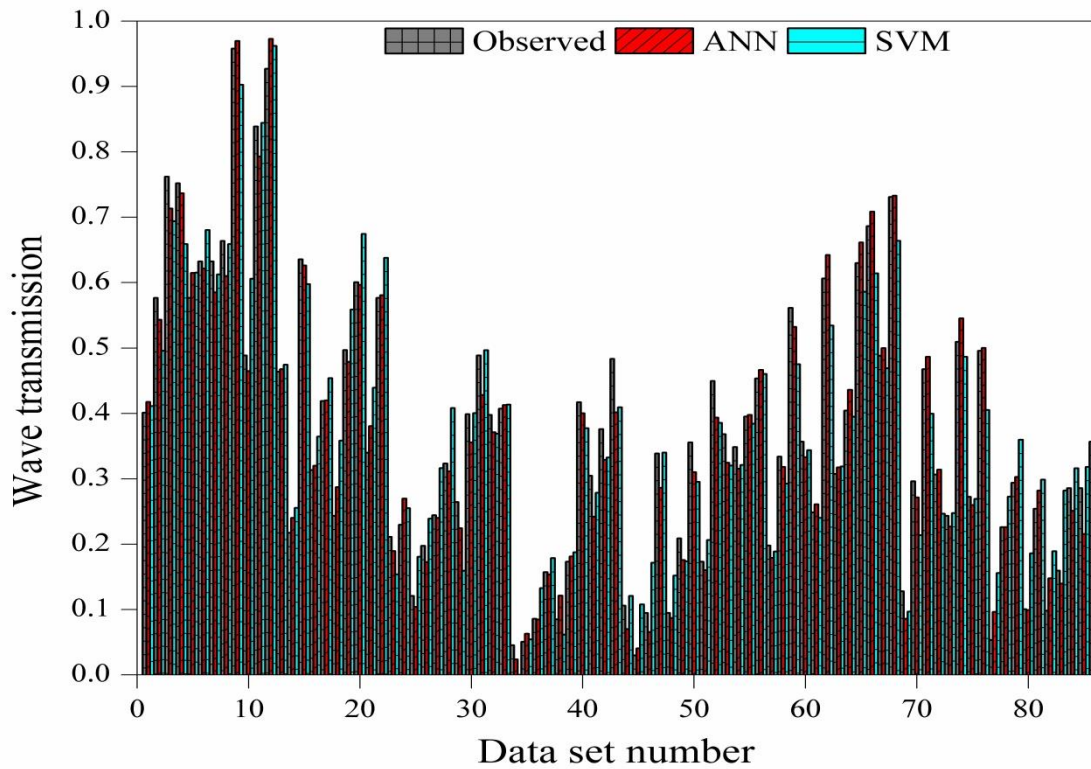


Fig. 6.26 Comparison of ANN (8-3-1) and SVM (RBF) models for wave transmission

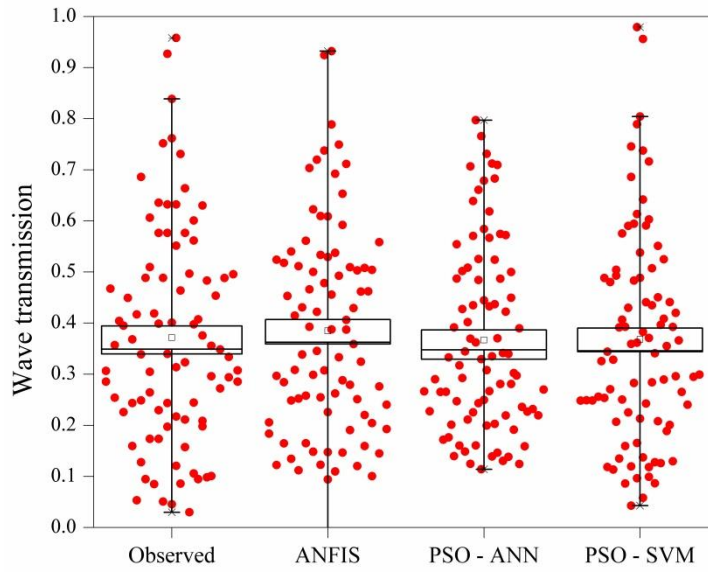


Fig. 6.27 Box-Whisker plot for wave transmission comparison of hybrid models

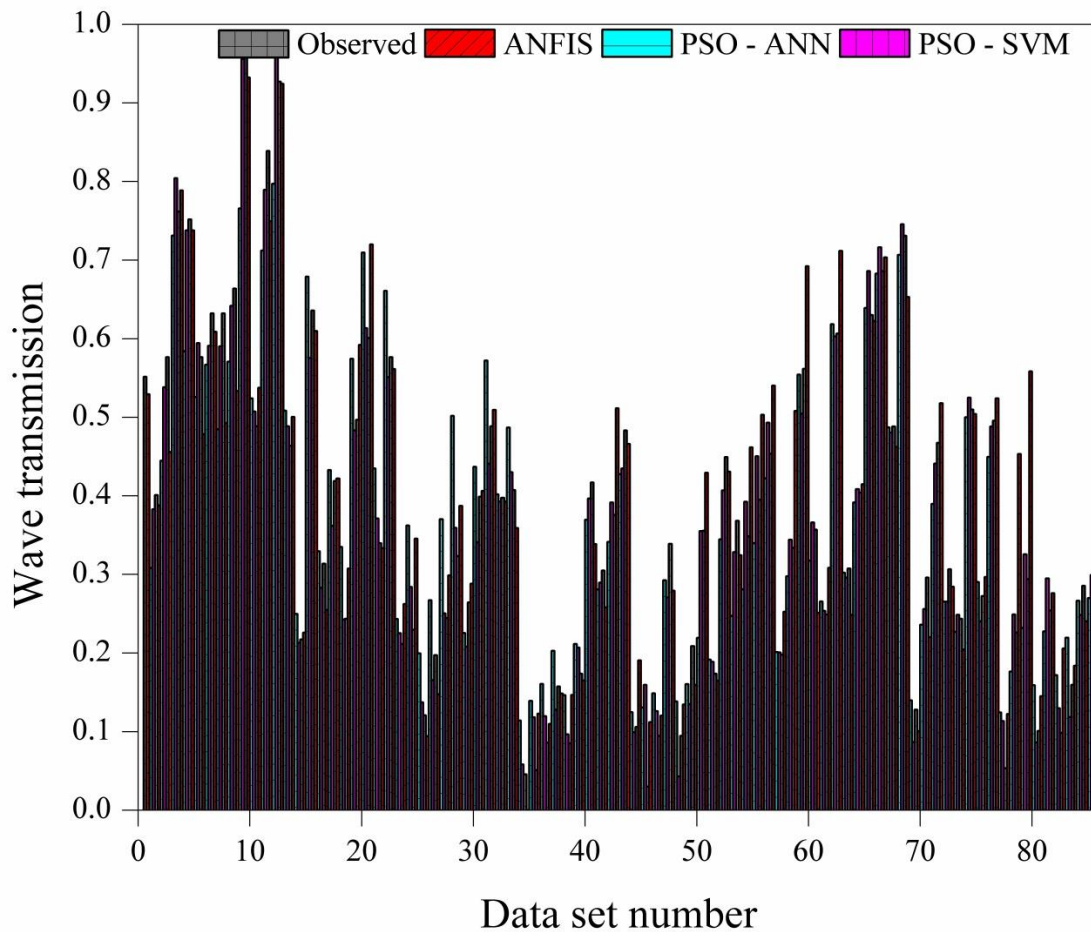


Fig. 6.28 Comparison of ANFIS (Gaussmf), PSO-ANN (8-3-1) and PSO-SVM (Polynomial) models for wave transmission

Table 6.10 Comparison of Statistical Measures of ANN, SVM, ANFIS, PSO-ANN and PSO-SVM Models for damage level (S)

Model	Training Data				Testing Data			
	CC	RMSE	SI	NSE	CC	RMSE	SI	NSE
ANN(8-5-1)	0.974	0.055	0.382	0.949	0.956	0.066	0.515	0.908
SVM (RBF)	0.954	0.0910	0.690	0.903	0.935	0.0765	0.529	0.833
ANFIS (Gaussmf)	0.99	0.0001	0.0012	0.99	0.875	0.123	0.011	0.70
PSO-ANN (8-2-1)	0.767	0.158	1.096	0.584	0.769	0.141	1.093	0.589
PSO-SVM (Polynomial)	0.961	0.071	0.493	0.916	0.941	0.088	0.669	0.843

Similarly, Figs. 6.29 and 6.30 illustrate the comparison of damage levels predicted by ANN with (8-5-1) with respect to experimental values of individual models. Similarly, Figs. 6.31 and 6.32 shows SVM with RBF kernel function, PSO-ANN with (8-2-1) and PSO-SVM with RBF kernel function with respect to experimental values and hybrid models.

ANN with (8-5-1) network outperformed all other soft computing techniques for predicting wave transmission with high CC of 0.956 and high efficiency of 0.908 with least error of 0.066 and small scatter of 0.515. Therefore, ANN with (8-5-1) network can be used as an efficient and reliable soft computing technique for predicting damage level conventional rubble mound breakwater of a tandem breakwater.

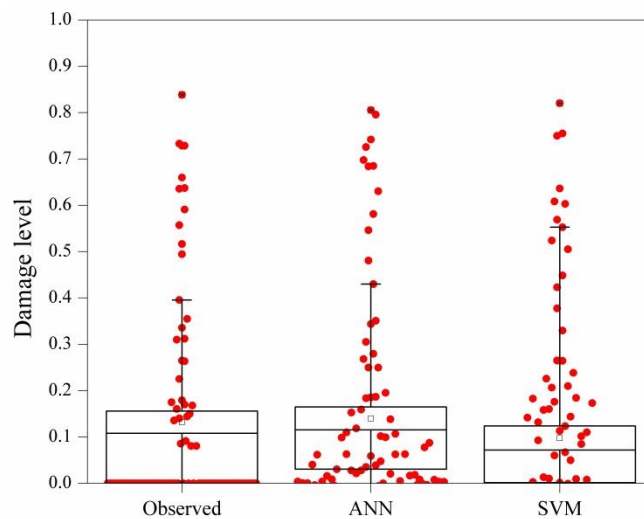


Fig. 6.29 Box-Whisker plot of damage levels comparison for individual models

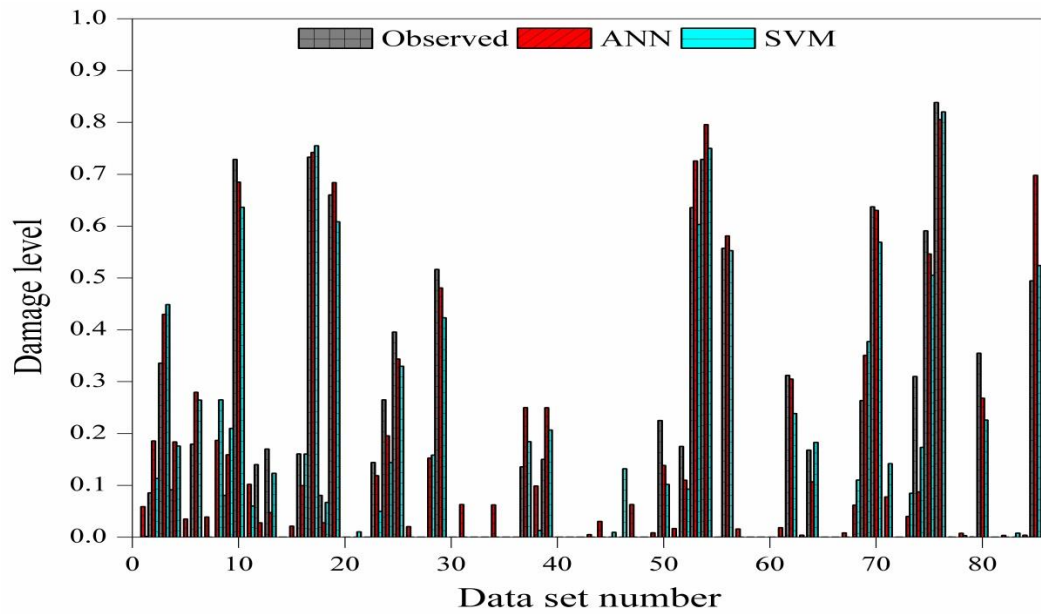


Fig. 6.30 Comparison of ANN (8-5-1) and SVM (RBF) models for damage levels

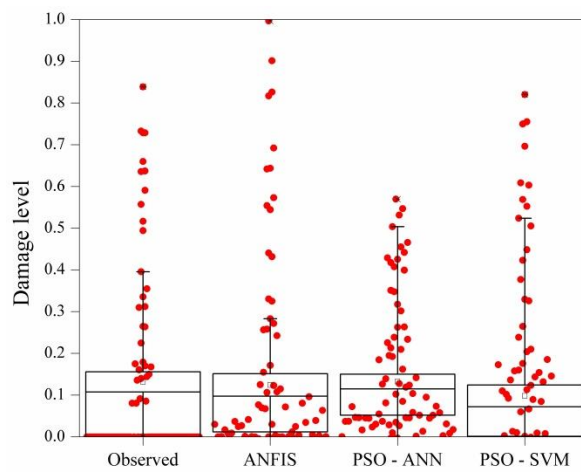


Fig. 6.31 Box-Whisker plot of damage levels comparison of hybrid models

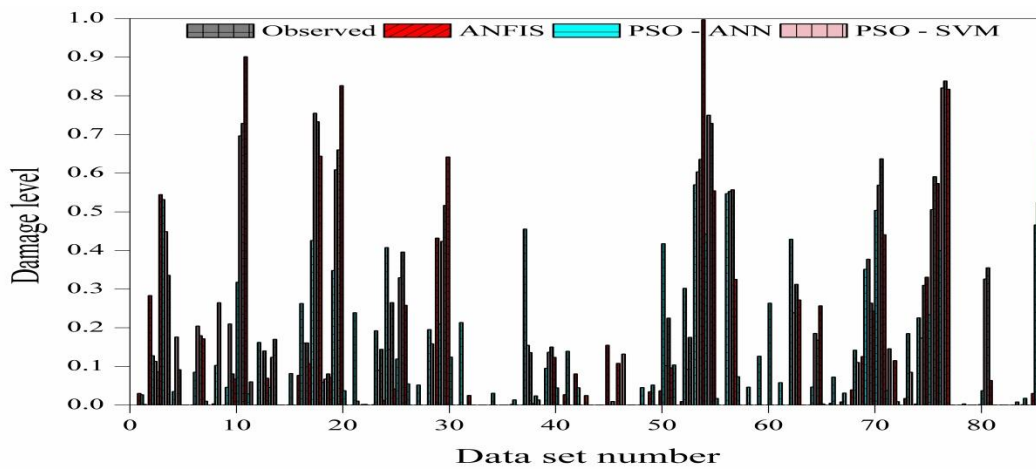


Fig. 6.32 Comparison of ANFIS (Gaussmf), PSO-ANN (8-2-1) and PSO-SVM (RBF) models for damage levels

It is observed that among the individual models ANN (8-3-1) network with high CC of 0.989 and high efficiency NSE of 0.978 and ANN (8-5-1) network with high CC of 0.956 and high efficiency NSE of 0.908 outperformed SVM with RBF in both cases. Similarly, among the hybrid soft computing techniques employed in the present study it is found that the PSO-SVM with polynomial kernel function with high CC of 0.984 and high efficiency NSE of 0.894 outperformed other hybrid techniques ANFIS (Gaussmf) and PSO-ANN with (8-3-1) network with high in case of wave transmission and PSO-SVM with RBF kernel function CC of 0.960 and high efficiency NSE of 0.843 in case of damage level of tandem breakwater. ANN and PSO-SVM models can be used as efficient and reliable techniques for prediction of wave transmission and damage level of tandem breakwater. Among all the individual and hybrid models ANN outperformed with high CC and least RMSE and less scatter and high efficiency for both the cases.

6.5.1 Summary of best model results

It is observed that ANN with 3 hidden layers with 100 epochs are sufficient to get better results from the different models. Firstly, the individual models of the ANN and SVM are tested with eight input parameters. It is observed that ANN with LM algorithm performed better compared to SVM with RBF kernel function.

The individual ANN with LM algorithm and SVM with RBF kernel function are compared to know their respective performance. ANN with LM algorithm showed best performance compared to SVM but a chance for clarification and comparison is available. Hence, in continuation hybrid models are considered for the further study. The different membership functions of the ANFIS and various numbers of hidden nodes of PSO-ANN and also different Kernel functions of PSO-SVM are compared before selecting the best technique. In case of PSO-ANN model, the number of hidden layers and epochs are optimized further before using them in the model. ANN with (8-3-1) and ANN with (8-5-1) shows better results compared to SVM with RBF kernel function. Comparing the different hybrid models, PSO-SVM with polynomial and RBF kernel function performed better than ANFIS (Gaussmf) and PSO-ANN (8-3-1) and PSO-ANN (8-2-1) models. After observing the statistical results of all the individual and hybrid soft computing techniques adopted in the present study ANN with 3 and 5 hidden neurons is found to best model for the prediction of wave transmission and damage levels of tandem breakwater.

PERFORMANCE OF ANFIS, PSO-ANN AND PSO-SVM MODELS**6.1 GENERAL**

By observing the results discussed in chapter 5, the capacity of the ANN and SVM models can be further cross checked or improve the efficiency of the model by hybridizing the model with other optimization techniques such as Fuzzy and PSO. From the literature, it is also observed that hybrid models give better results than the single models (Patil et al., 2012; Harish et al., 2014) in most of the cases. To improve the results, hybridizing technique such as ANN with Fuzzy Inference System and PSO and SVM with PSO are implemented and analysis is carried out. The obtained results are discussed in this chapter.

6.2 PERFORMANCE OF ADAPTIVE-NEURO FUZZY INFERENCE SYSTEM (ANFIS) MODEL

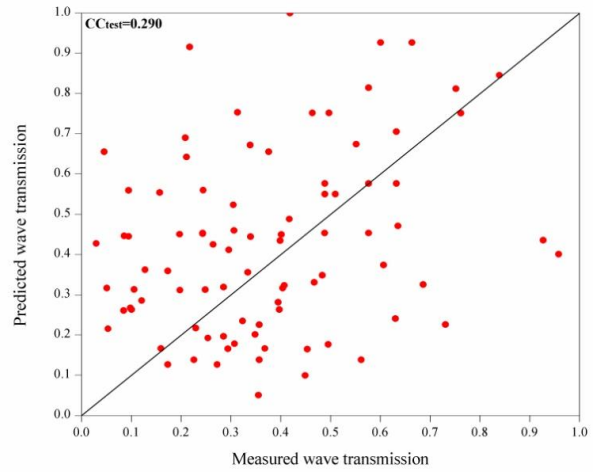
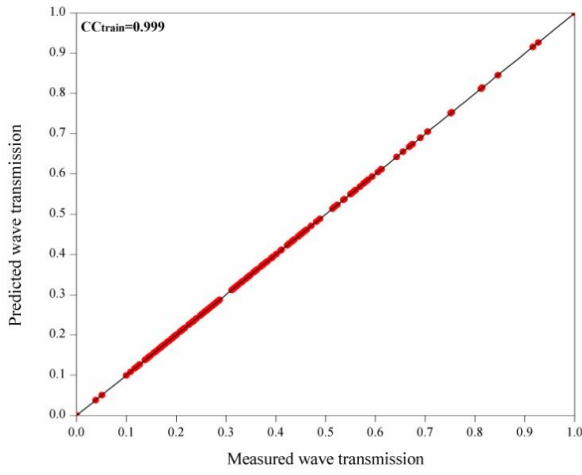
The ANFIS model with eight input parameters and one output parameter is built with different membership functions, fuzzy rules and epoch numbers. The various membership functions considered are Triangular-shaped built-in membership function (TRIMF), Trapezoidal-shaped built-in membership function (TRAPMF), Generalized bell-shaped built-in membership function (GBELLMF), and Gaussian curve built-in membership function (GAUSSMF). An ANFIS model with built-in 2 membership functions for each variable, and 100 epoch numbers are selected and trained using the Levenberg-Marquardt algorithm with tangent sigmoid and linear transfer functions in the hidden and output layers, respectively. In the present chapter ANFIS models are developed for the prediction of wave transmission over submerged reef and damage level of main conventional rubble mound breakwater of tandem breakwater. The performances of these models are evaluated based on statistical measures, namely RMSE, CC, SI and NSE. The CC between desired output and network predicted outputs are calculated by using Equation (4.30). The RMSE, SI and NSE between target output and network predicted output is determined by using Equations (4.31), (4.32), and (4.33) respectively. Each model is developed and results are discussed in the following section.

6.2.1 Simulation results of ANFIS Model for predicting wave transmission (H_t/H_{tmax})

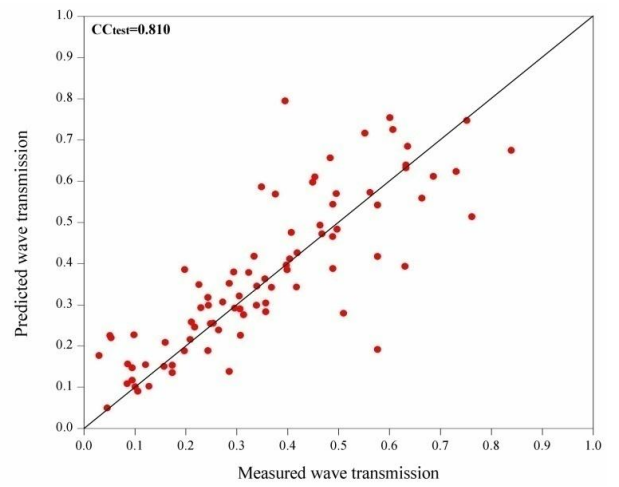
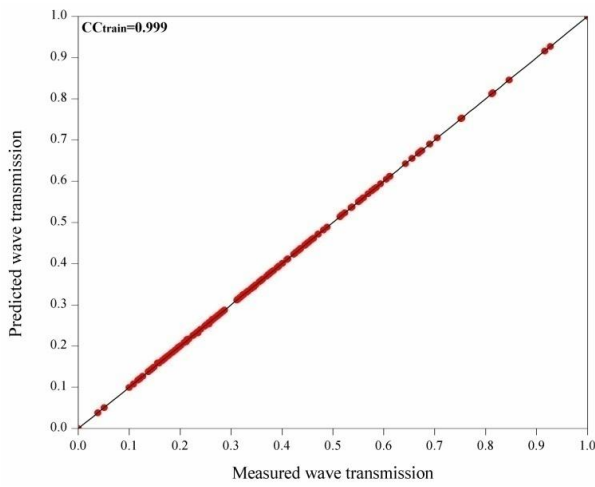
Fuzzy models are developed to predict the wave transmission over submerged reef of tandem breakwater. The proper selection of ANFIS and its membership functions and their number decides the performance of these models. The different membership functions with their performances in the form of scatter plots are shown in Fig. 6.1 and the values of statistical measures are tabulated in Table 6.1. In the present study, with 8 input parameters and 1 output, using Sugeno first order with (2^8) 256 fuzzy rules and 2 generalized ‘Triangular (trimf)’, ‘Trapezoidal (trapmf)’, ‘Gbell (gbellmf)’ and ‘Gaussian (Gaussmf)’ membership functions and 100 epochs the model is trained. Among all the membership functions, the ANFIS model with Gaussian membership function performs better than the other membership functions. It is believed that Gaussian membership function has the capacity to handle higher degree of error tolerance compared to other membership functions. The statistical measures obtained for ANFIS model with Gaussian membership function are RMSE= 0.0754, CC= 0.935. It is also observed that, there is good correlation between the observed and predicted wave transmission in this model with less scatter, SI= 0.0023. Good efficiency, NSE = 0.869 is obtained for testing. The ANFIS model, with a combination of gradient descent algorithm and least squares algorithm, is used in an effective search for the optimal parameters to yield good results. Based on this hybrid approach, correlations of training and testing are increased as presented in Fig. 6.1.

Table 6.1 Statistical measure of ANFIS models for predicting wave transmission

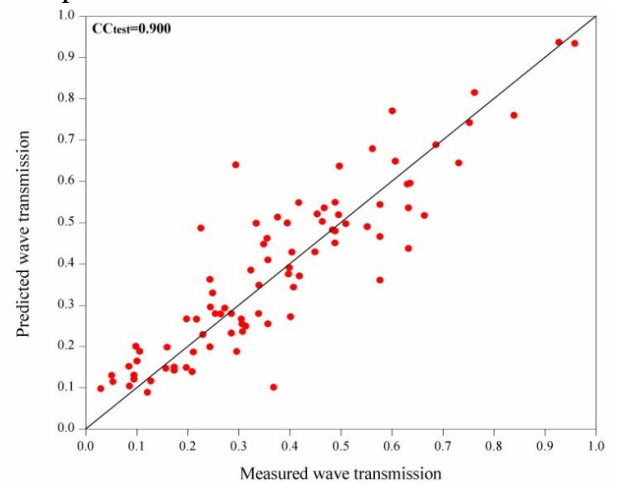
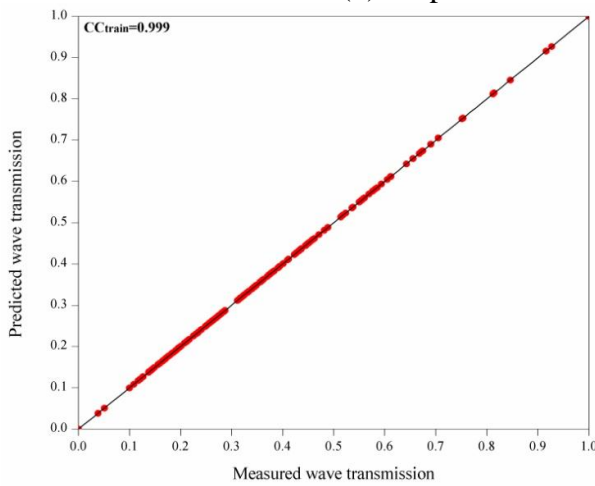
Statistical measures	Membership Functions							
	Triangular		Trapezoidal		Gbell		Gaussian	
	Train	Test	Train	Test	Train	Test	Train	Test
RMSE	0.0003	0.263	0.0004	0.136	0.00021	0.0935	0.0002	0.0754
NSE	0.999	0.588	0.999	0.576	0.999	0.799	0.999	0.869
CC	0.999	0.290	0.999	0.810	0.999	0.900	0.999	0.935
SI	0.0001	0.0081	0.0002	0.004	0.0007	0.0029	0.0006	0.0023



(a) Triangular membership function



(b) Trapezoidal membership function



(c) Gbell membership function

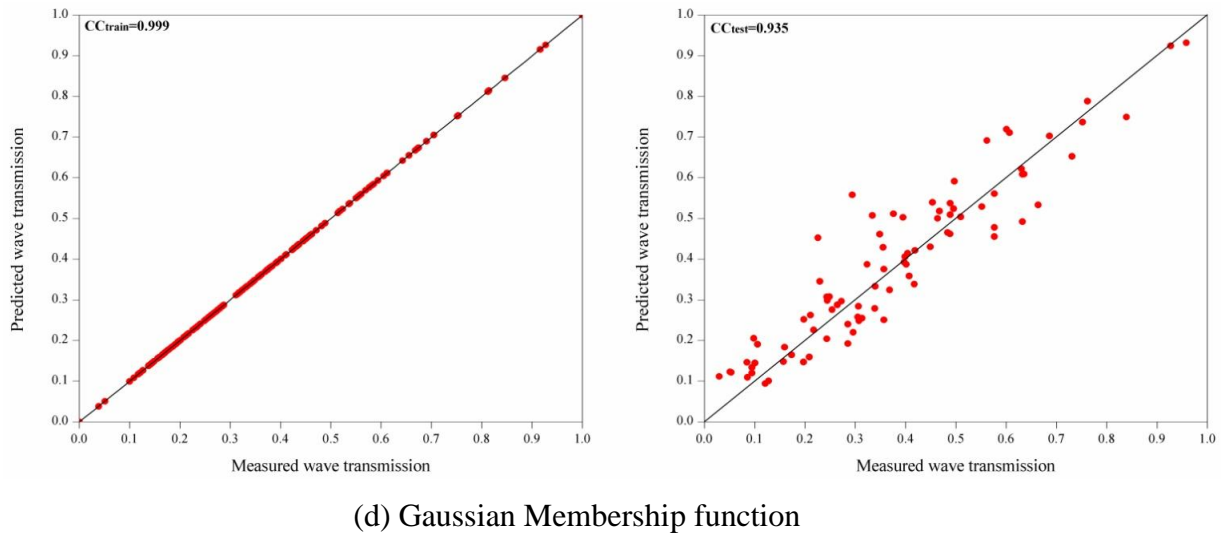


Fig. 6.1 Scatter plots of predicted and observed H_t/H_{tmax} by ANFIS for different membership functions

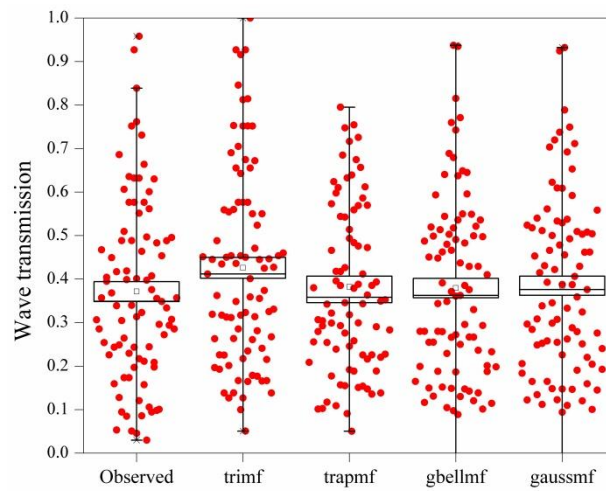


Fig. 6.2 Box-Whiskers plots of H_t/H_{tmax} for ANFIS model with different membership functions

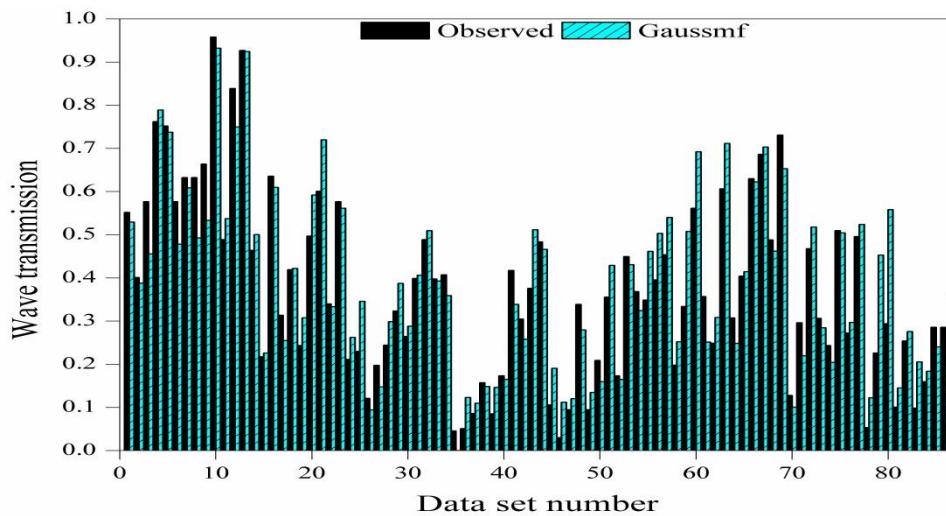


Fig. 6.3 Comparison of H_t/H_{tmax} predicted by ANFIS model with observed values

The box plot statistics are also used to check the variability of the predicted wave transmission by ANFIS model with different membership functions as shown in Fig. 6.2. Distribution of the predicted H_t/H_{tmax} values by Gaussmf is close to the observed one in the upper quartile and lower quartile of the box. The performance of the best model out of all the ANFIS models with various membership functions is assessed by plotting the predicted data with observed data points. Therefore, H_t/H_{tmax} predicting efficiency by ANFIS model with Gaussian membership function is compared with observed data for its validation as shown in Fig. 6.3. From the above figure, it is observed that the predicted results are in good agreement with the observed values and is concluded as a reliable model to predict H_t/H_{tmax} .

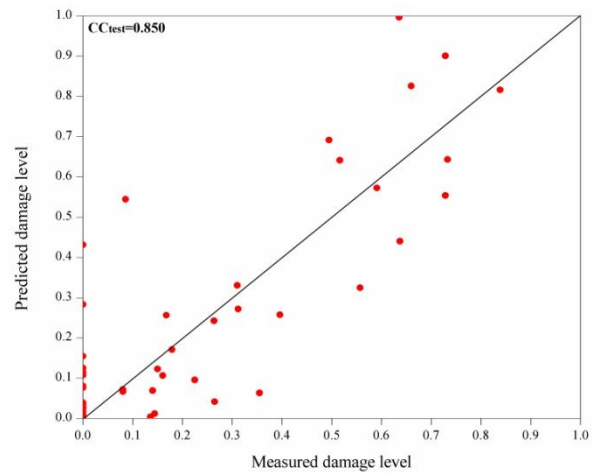
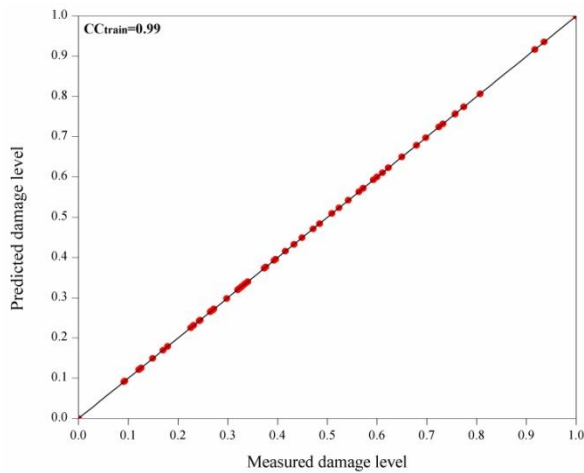
6.2.2 Simulation results of ANFIS Model in predicting the damage level (S)

The performance of different membership functions in terms of statistical measures is presented in the Table 6.2. In the present study, Sugeno first order method is used to trained the model by generating (2^8) 256 fuzzy rules with 2 generalized ‘Triangular (trimf)’, ‘Trapezoidal (trapmf)’, ‘Gbell (gbellmf)’ and ‘Gaussian (Gaussmf)’ membership functions for 100 epochs. To predict damage level, ANFIS model with Gaussmf is chosen as the best ANFIS model based on the model performance indicators, as RMSE = 0.123, CC = 0.875, SI = 0.011, NSE = 0.710 for testing. The ANFIS model is used, with a combination of gradient descent and least squares algorithm for an effective search of the optimal parameters to yield good results. Based on this hybrid approach of feed forward-back propagation neural network (FFBP) and decent gradient-least square principal fuzzy inference system (FIS) correlations of training and testing are increased.

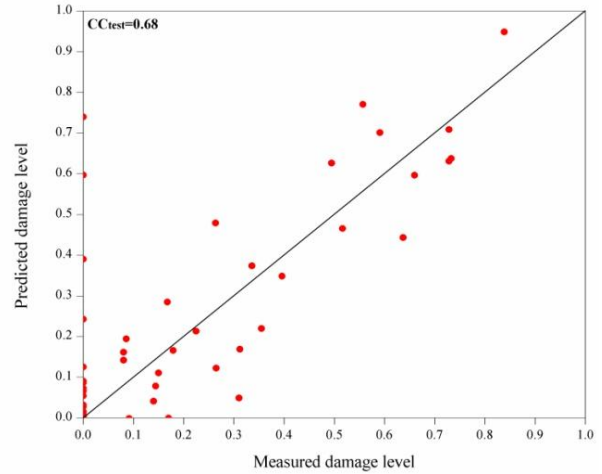
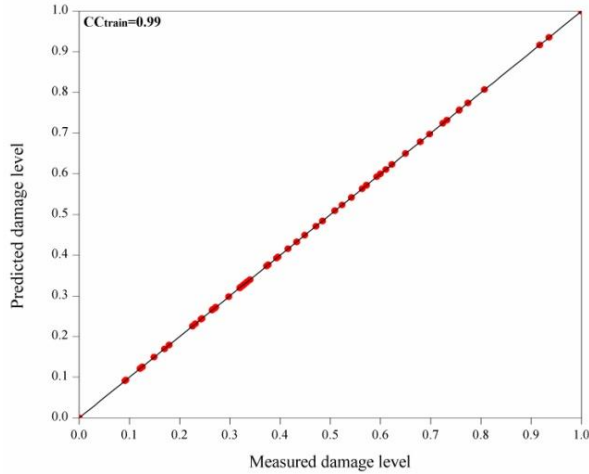
The scatter plots of predicted and observed damage level for ANFIS model with different membership functions are shown in Fig. 6.4. Among all the membership functions, Gaussian membership function is observed to be the best membership function. ANFIS model with Gaussmf outperformed other models with CC=0.875 providing better correlation with measured values and RMSE = 0.123.

Table 6.2 Statistical measure of ANFIS models for prediction of damage level

Statistical	Membership functions							
	Triangular		Trapezoidal		Gbell		Gaussian	
	Train	Test	Train	Test	Train	Test	Train	Test
RMSE	0.0001	0.132	0.0096	0.21	0.0002	0.129	0.002	0.123
NSE	0.99	0.64	0.99	0.575	0.99	0.682	0.99	0.710
CC	0.99	0.850	0.99	0.68	0.99	0.855	0.99	0.875
SI	0.0001	0.012	0.0009	0.018	0.00013	0.011	0.0012	0.011



(a) Triangular Membership function



(b) Trapezoidal Membership function

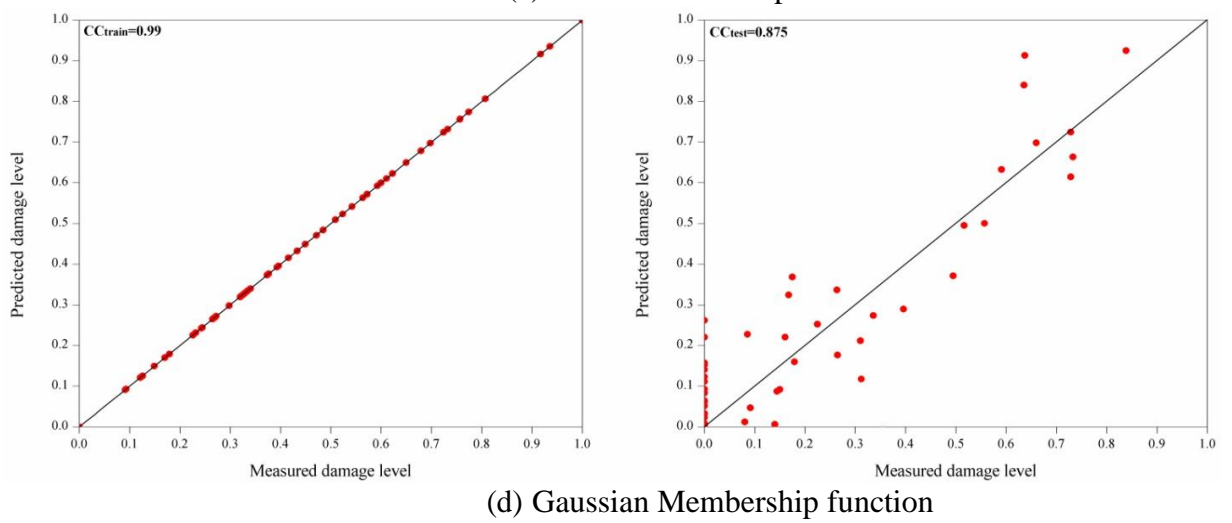
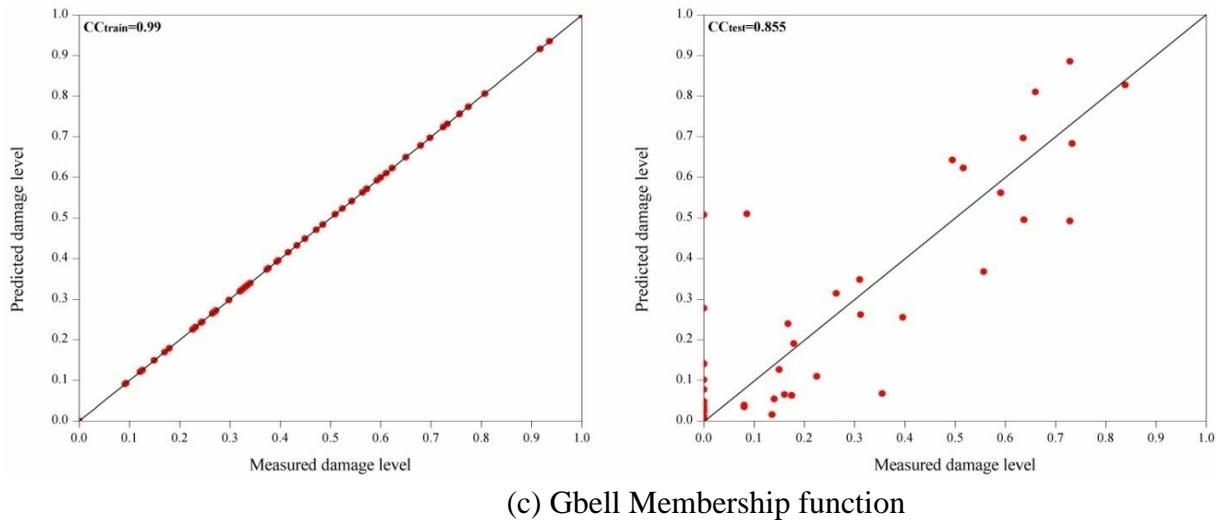


Fig. 6.4 Scatter plots of predicted and observed S for ANFIS model with different membership functions

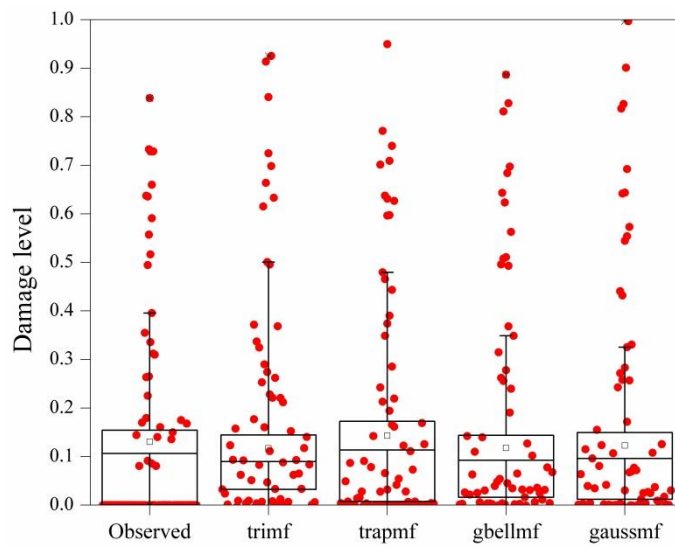


Fig. 6.5 Box-Whisker plots of S for ANFIS model with different membership functions

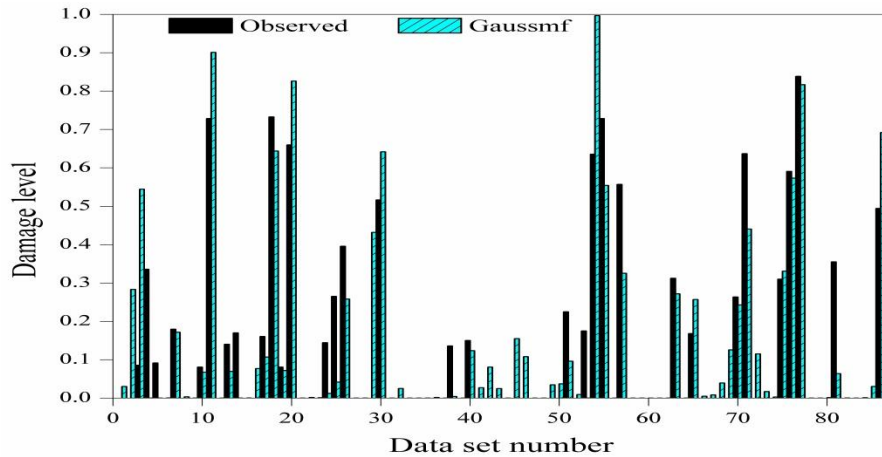


Fig. 6.6 Comparison of damage level prediction by SVM (RBF) with observed values

In terms of box plot statistics, the spread of data at lower and upper quartile of the box are predicted well in comparison with the observed. From Fig. 6.5, it is noticed that, Gbell and Gaussmf predictions match well with observed damage level among other membership functions where many outliers are found. Both box plot and scatter plots illustrations agree that, ANFIS model with Gaussmf is the best model. The efficiency of the best model is validated by presenting the findings in the form of comparison plot and is shown in Fig. 6.6. Out of all, the Gaussmf showed better results in predicting both the H_t/H_{tmax} and damage level. The predicted results of damage level by ANFIS model are scattered more compared to wave transmission, which is due to presence of more number of zero damage levels in the observed data set.

6.2.3 Summary of ANFIS model results

The performance of the ANFIS model in predicting H_t/H_{tmax} and damage level seems to be highly affected by hybridization of FIS with NN. The efficiency of the ANFIS model depends on the type and number of membership functions associated with each input data. The Gaussmf trains the model well before predicting the outputs in the testing phase. Even though results are not exactly matching the observed ones, but can be concluded as tool is efficient and reliable from the obtained results. Therefore, ANFIS can be used to predict the wave transmission and damage level with good correlation.

6.3 PERFORMANCE OF PSO-ANN MODEL FOR PREDICTING WAVE TRANSMISSION (H_t/H_{tmax}) AND DAMAGE LEVEL (S)

Regression analysis is conducted to predict both H_t/H_{tmax} and S by using PSO-ANN and

results are evaluated using different statistical measures such as RMSE, NSE, SI, CC, and box-whiskers plots. Based on the statistical parameters, accuracy of the model is tested. The predicted values are compared with the observed values by plotting the performance variation graph. The prediction will be considered as good when RMSE and SI is minimum ('0') while NSE and CC are maximum ('1').

In case of ANN hybrid model prediction, PSO function is called in place of an LM function by using PSORT and NN in the MATLAB software. The statistical parameters are calculated for various ANN hybrid models with varying size of the hidden neurons and the network with best predictions are considered as optimum. Table 6.3, shows the results of different statistical measures obtained by various ANN hybrid models for predicting transmitted wave heights (H_t/H_{tmax}) and damage level (S).

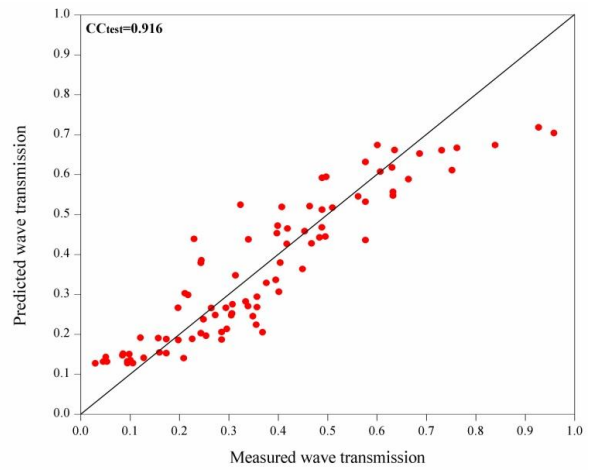
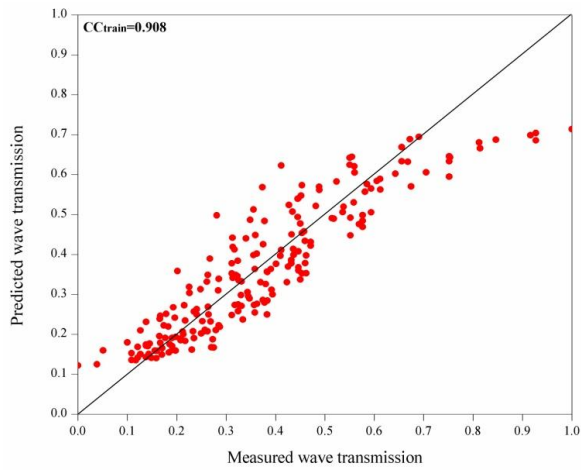
Table 6.3 Statistical parameters of PSO-ANN model predictions for H_t/H_{tmax}

Output	Models	Network	RMSE		C		SI		NSE	
			Train	Test	Train	Test	Train	Test	Train	Test
H_t/H_{tmax}	PSO-ANN1	8-1-1	0.079	0.084	0.908	0.916	0.213	0.232	0.821	0.835
	PSO-ANN2	8-2-1	0.080	0.081	0.904	0.921	0.216	0.224	0.817	0.846
	PSO-ANN3	8-3-1	0.065	0.072	0.940	0.941	0.176	0.199	0.879	0.879
	PSO-ANN4	8-4-1	0.081	0.082	0.903	0.918	0.218	0.228	0.814	0.841
	PSO-ANN5	8-5-1	0.077	0.080	0.912	0.925	0.207	0.222	0.832	0.849

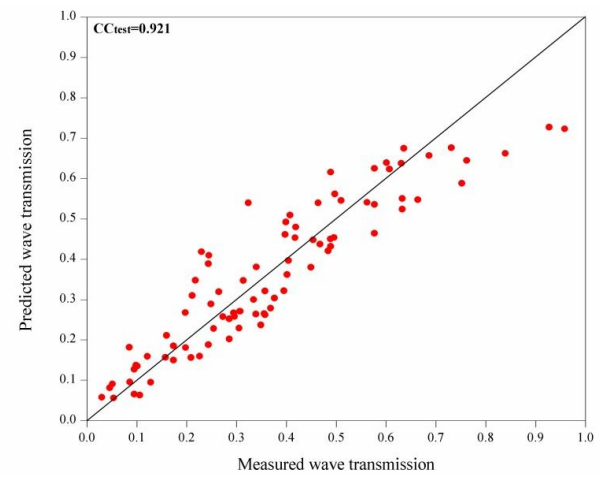
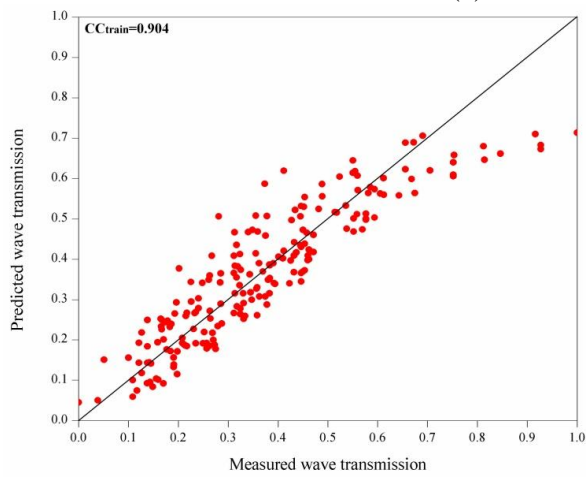
Table 6.4 Statistical parameters of PSO-ANN model predictions for damage level (S)

Output	Models	Network	RMSE		C		SI		NSE	
			Train	Test	Train	Test	Train	Test	Train	Test
S	PSO-ANN1	8-1-1	0.157	0.144	0.772	0.755	1.083	1.119	0.594	0.570
	PSO-ANN2	8-2-1	0.158	0.141	0.767	0.769	1.096	1.093	0.584	0.589
	PSO-ANN3	8-3-1	0.159	0.145	0.763	0.756	1.102	1.125	0.579	0.565
	PSO-ANN4	8-4-1	0.160	0.147	0.761	0.744	1.103	1.142	0.579	0.552
	PSO-ANN5	8-5-1	0.165	0.141	0.740	0.769	1.143	1.094	0.548	0.589

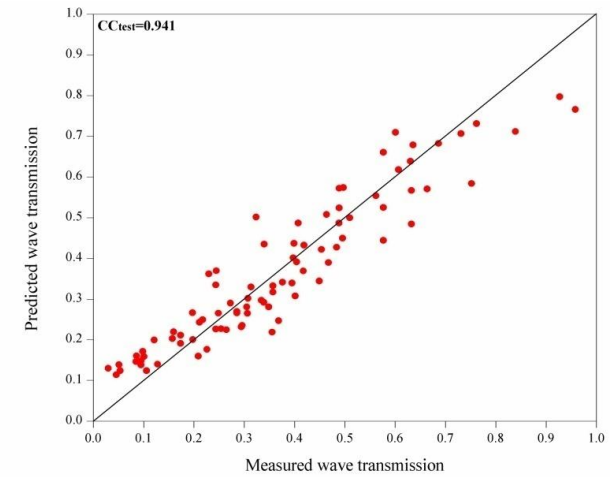
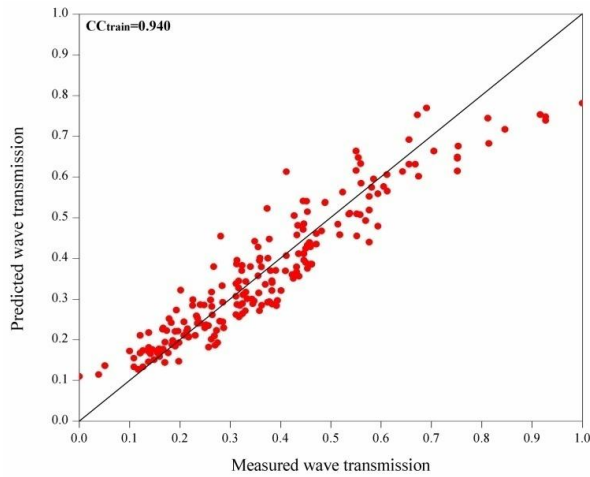
From Table 6.3, it can be seen that PSO-ANN3 model predicts the transmitted wave height better with CC = 0.941, RMSE = 0.072, SI = 0.199 and NSE = 0.879 for testing data. In case of damage level prediction PSO-ANN2 performs better with CC = 0.769, RMSE = 0.141, SI = 1.093 and NSE = 0.589 for testing data points as listed Table 6.4. It is observed that, damage levels obtained by PSO-ANN2 are poor compared wave transmission results by PSO-ANN3. This is due to the presence of more number of zero's in the data of damage levels. This represents that there is zero damage during physical model testing. Therefore, simulation results are displayed in the graphical form as a scatter plots between predicted and observed values of H_t/H_{tmax} in the Fig. 6.7.



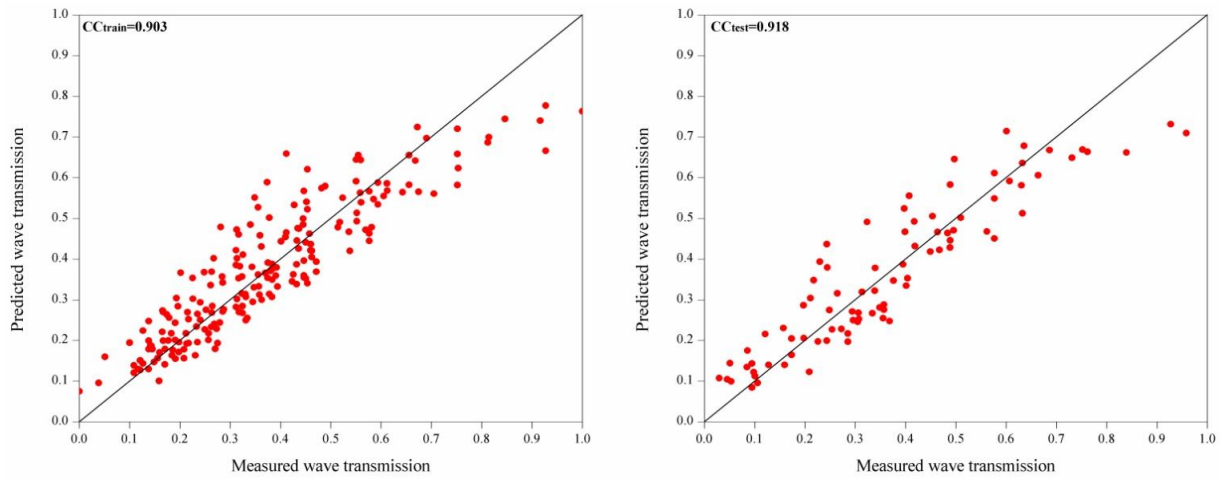
(a) PSO-ANN model with 8-1-1



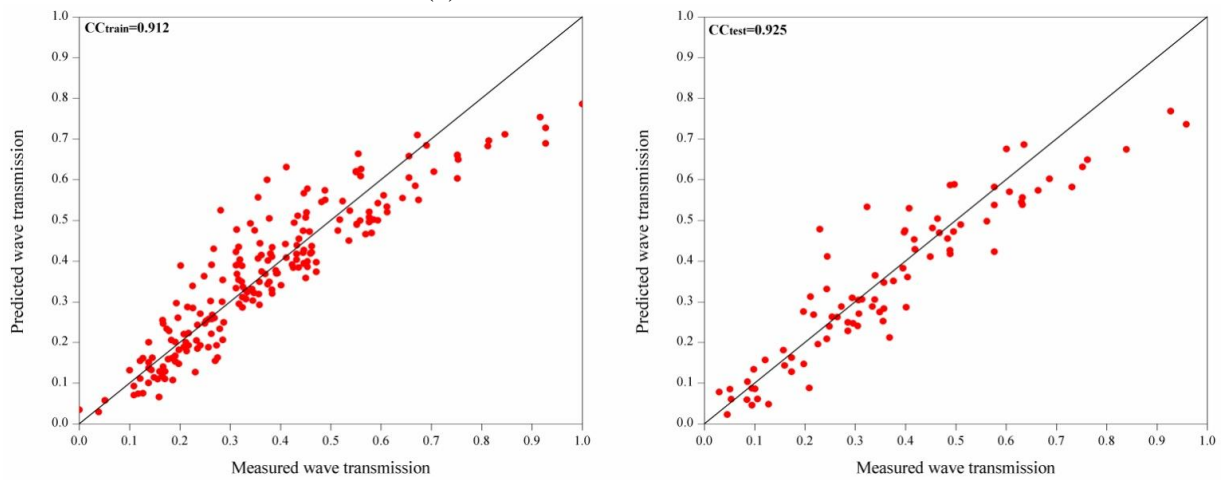
(b) PSO-ANN model with 8-2-1



(c) PSO-ANN model with 8-3-1



(c) PSO- ANN model with 8-4-1



(c) PSO- ANN model with 8-5-1

Fig. 6.7 Scatter plots of H_t/H_{tmax} by PSO-ANN model

It is observed that the scatter is less in Fig. 6.7(c) compared to Fig. 6.7(a), (b), (d) and (e). Similarly, in the prediction of damage level in the Fig. 6.10(b) showed good correlation with observed values whereas, Fig. 6.10(a), (c), (d) and (e) showed more scatter and poor correlation compared to Fig. 6.10(b). It can be summarized that, PSO-ANN3 with (8-3-1) network for H_t/H_{tmax} and PSO-ANN2 with (8-2-1) network for damage level gives the best results. These models can be used efficiently to predict the parameters effecting tandem breakwater stability.

The box plots statistics, is also a kind of measuring tool through which the variability of the predicted values with respect to observed data points, is identified to asses best model. In the Fig. 6.8, the ANN hybrid model with 2 and 4 hidden neurons show almost similar distribution of the predicted values of wave transmission of submerged reef with the observed values in both the lower and upper quartiles of the box plot. Similarly, the ANN

hybrid with 2 hidden neurons predicted damage level of the main breakwater successfully and are depicted in the Fig. 6.11.

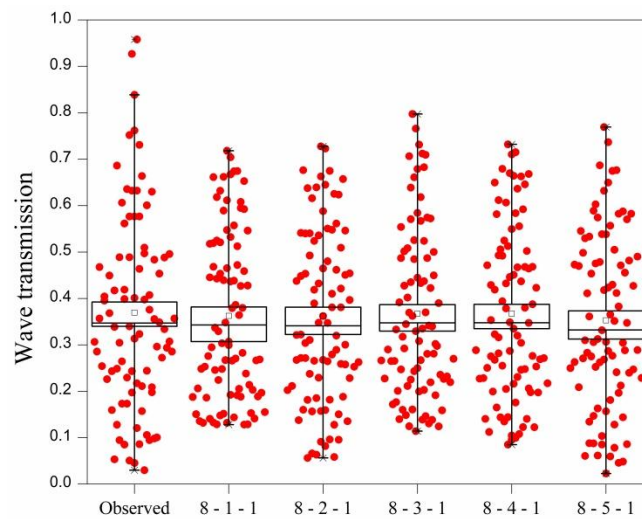


Fig. 6.8 Box-Whisker plots of wave transmission prediction by PSO-ANN with observed values

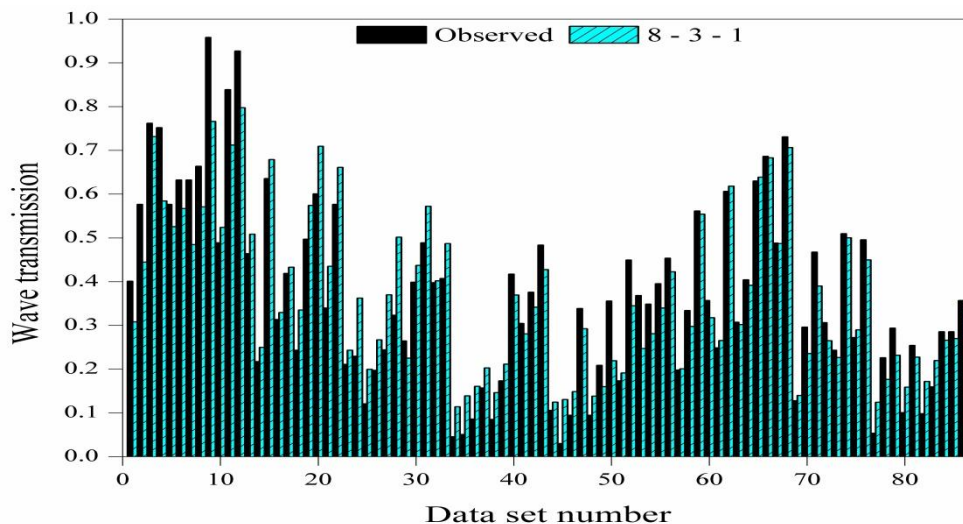
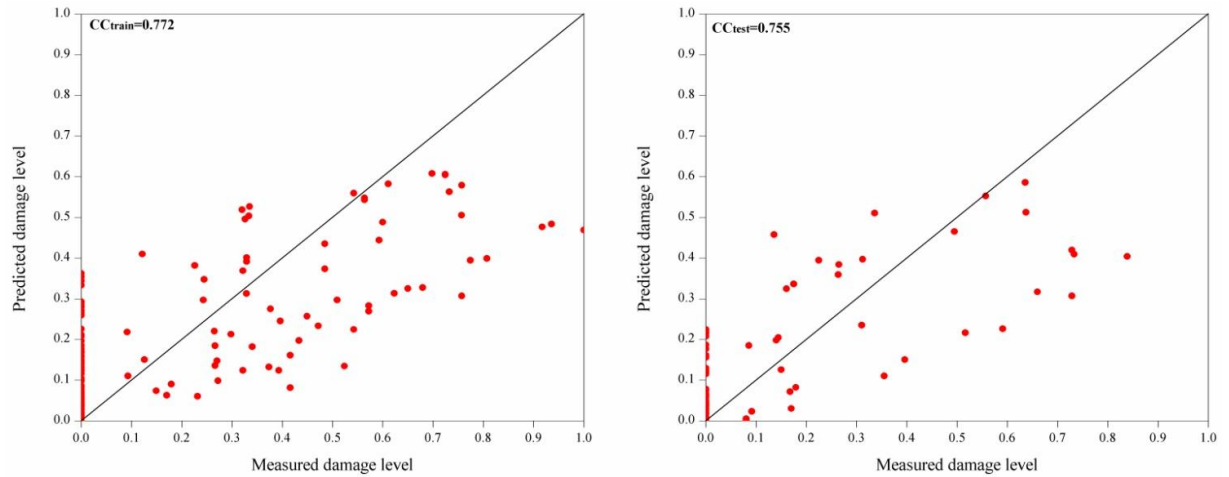


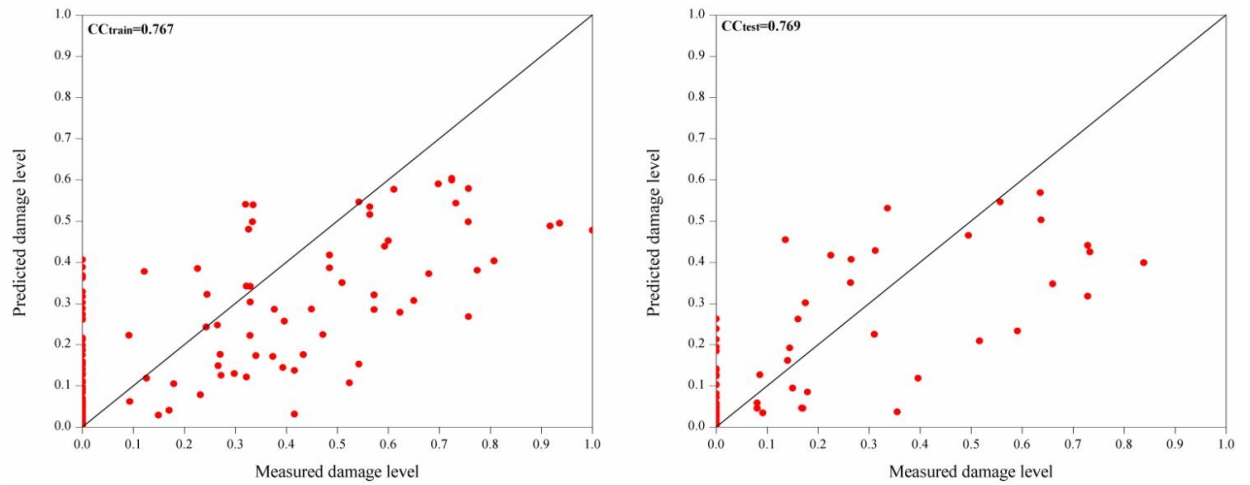
Fig. 6.9 Comparison of wave transmission predicted by PSO-ANN3 with observed values

Fig. 6.9 shows, the validation of PSO-ANN3 model for predicting wave transmission with respect to observed values in the form of comparison graph. Similarly, Fig. 6.12 shows the validation of PSO-ANN2 model performance in predicting damage level with respect to observed values in the form of comparison graph. It is observed that the prediction of PSO-ANN values match well with the observed values of wave transmission and damage level of tandem breakwater. Based on all the statistical measures and different plots, PSO-ANN3 technique can be considered as better model

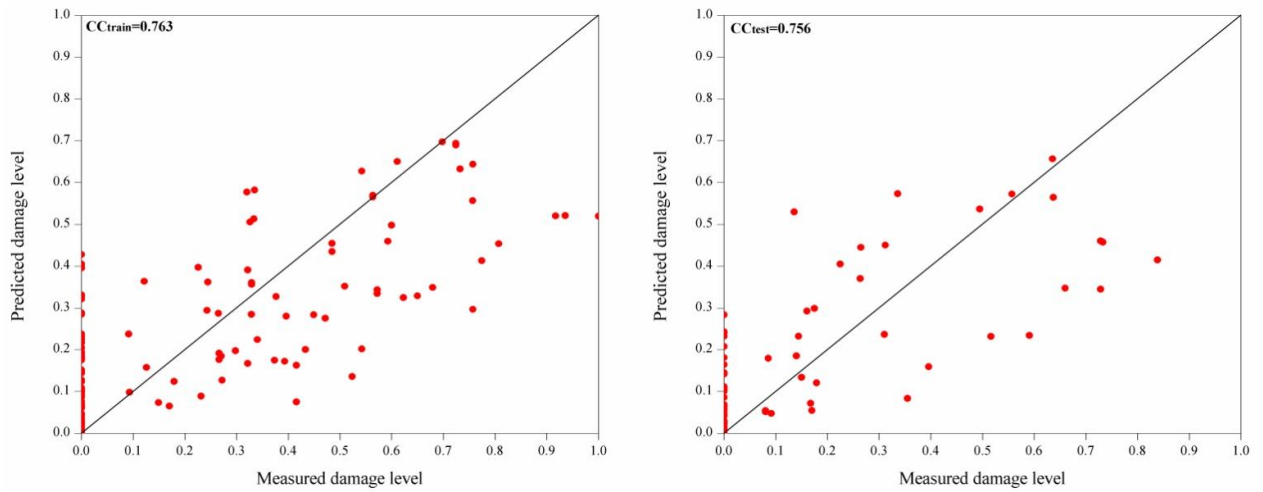
and can be used as an alternate method for prediction of wave transmission successfully for the immediate need or requirement for analysis if the sufficient or a large set of data is available. ANFIS with Gaussmf predicts the damage level better than PSO-ANN2. Hence, ANFIS with Gaussmf can be used as an alternate and reliable tool for damage level prediction.



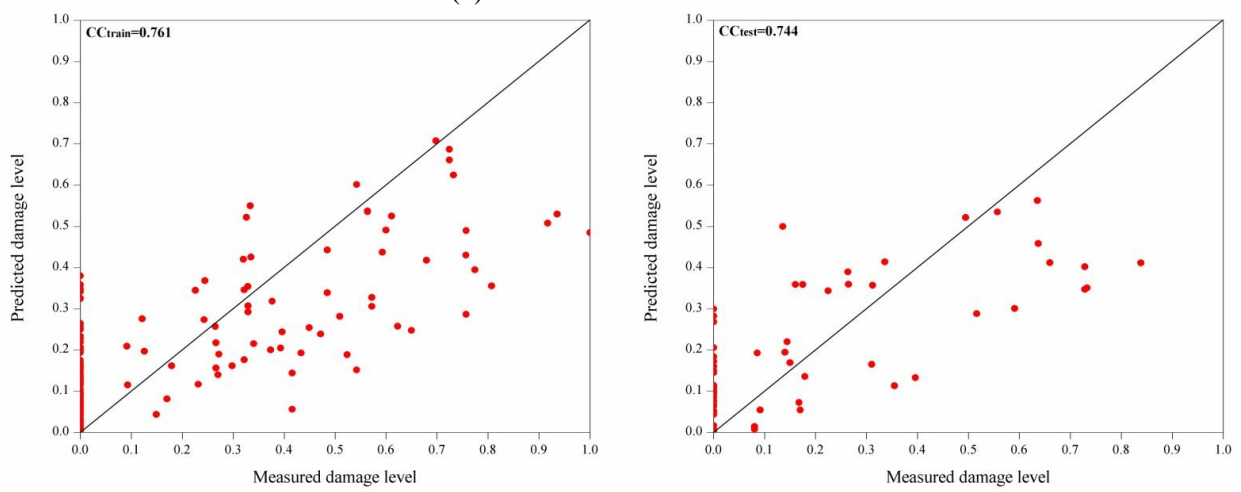
(a) PSO-ANN model with 8-1-1



(b) PSO-ANN model with 8-2-1



(c) PSO-ANN model with 8-3-1



(d) PSO-ANN model with 8-4-1

Fig. 6.10 Scatter plots for S for PSO-ANN hybrid models

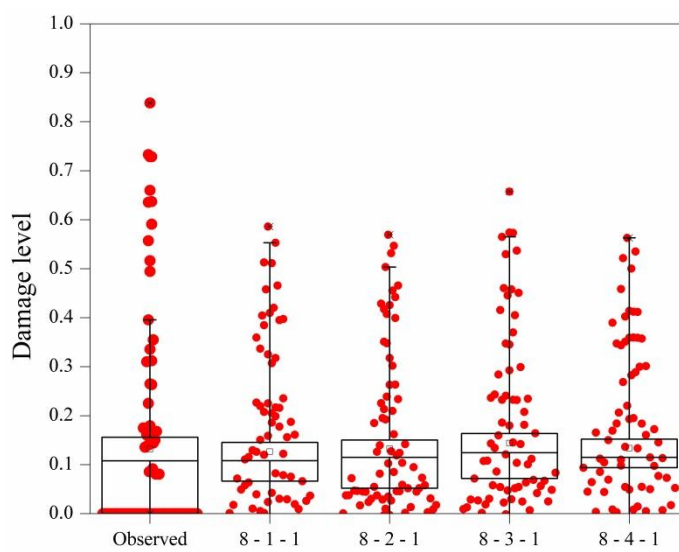


Fig. 6.11 Box-Whisker plots of damage level prediction for different PSO-ANN models

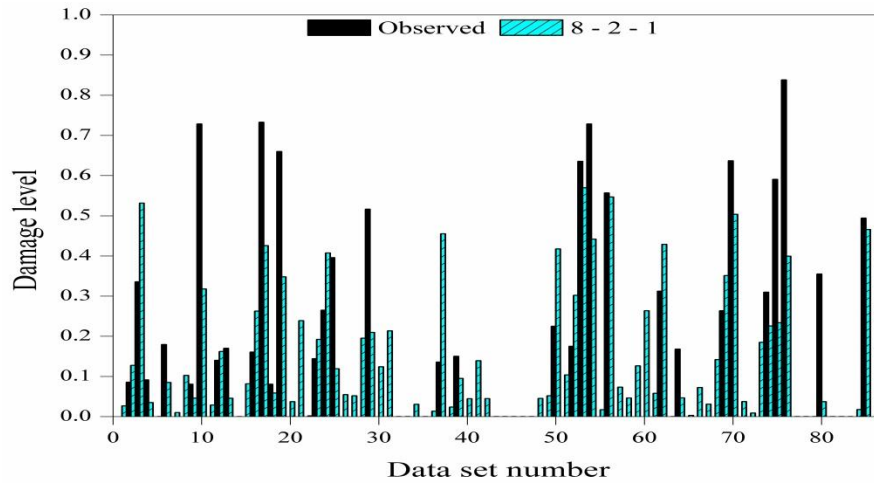


Fig. 6.12 Comparison of damage level predicted by PSO-ANN2 with observed values

6.3.1 Summary of PSO-ANN model results

PSO-ANN with various numbers of hidden neurons is attempted, for selecting the efficient ANN hybrid model using different statistical measures. The results obtained by PSO-ANN3 and PSO-ANN2 models show that, the soft computing techniques can be applied successfully for the prediction of wave transmission over submerged reef and damage level of conventional rubble mound breakwater of tandem breakwater.

6.4 PERFORMANCE OF PSO-SVM MODEL FOR PREDICTION OF WAVE TRANSMISSION AND DAMAGE LEVEL OF TANDEM BREAKWATER

The performance of PSO-SVM model depends on the good setting of SVM parameters such as regularization parameter C and ε with kernel parameters γ and d . Initially the upper and lower bound values of SVM parameters and kernel widths are given as input (i.e. for $C \in [1, 5000]$; $\varepsilon \in [0.000001, 1]$; $\gamma \in [0.01, 5]$ and $d \in [2, 5]$). In the next stage, the marginal difference in range between upper and lower bound values of the SVM parameters are reduced such that both should have in close proximity to the optimal parameter value obtained initially (i.e. for $C \in [(1, 500), (500, 1000), \dots, (4500, 5000)]$; $\varepsilon \in [(0.000001, 0.00001), (0.00001, 0.0001), \dots, (0.1, 1)]$; $\gamma \in [(0.01, 1), (1, 2), \dots, (4, 5)]$ and $d \in [(2, 3), \dots, (4, 5)]$). In associated with such various trials the optimal parameters are obtained and corresponding to that models are developed using linear, polynomial and RBF kernel functions. For each model developed, statistical indicator values such as CC, RMSE, NSE and SI are calculated as evaluation criteria. The kernel function

best suited for the SVM hybrid model is finally determined by evaluating the values of statistical measures obtained as model performance indicators.

The effectiveness and efficiency of the model results obtained during simulation depends upon the proper selection of SVM parameters (C , ϵ) and kernel parameters (γ , d), which can be obtained using particle swarm optimization. Initially, random range of values is provided for the parameters within the range given by software documentation. From the range given the parameter values corresponding to that the best fitness is achieved, and is found by particle searching. If the value selected at random from the range provided does not satisfy the fitness function, then the loop continues with the next available value in the given input.

6.4.1 Simulation results of PSO-SVM model for predicting wave transmission (H_t/H_{tmax}) over submerged reef and damage level (S) of emerged breakwater of tandem breakwater

The prediction of transmitted wave heights over a submerged reef of the tandem breakwater is conducted by considering the 8 inputs variables H_i/gT^2 , X/d , $H_i/\Delta D_{n50}$, B/d , B/L_o , F/H_i , h/d , d/gT^2 which influence the output H_t/H_{tmax} . The training of the model is carried out for 201 data points (70%) and then testing is done by considering 87 data points (30%), for validation of the model prediction.

Initially, for a particular kernel type, PSO-SVM model is developed and among them the one which shows best data fitting is adopted as the best model for the corresponding kernel function. The model that shows the best data fitting is found out by evaluating the statistical parameters. Figs. 6.13, 6.14 and 6.15 depicts the data fitting curves for PSO-SVM models developed using linear, polynomial and RBF kernel functions, respectively using set of testing data. In each figure, it can be observed that predicted value fits better with actual value for specific values of C , ϵ , γ and d . From Fig.6.13, the best fitting curve corresponds to the model having $C = 1500$ and $\epsilon = 0.0885$ which shows the data fitting the predicted values with observed values. Similarly, $C = 183.78$, $\epsilon = 0.0000538$, $d = 3$ and $C = 18.7$, $\epsilon = 0.0827$, $\gamma = 2.6$ are parameter values corresponding to the best fitting curves for Figs. 6.14 and 6.15 respectively obtained by proposed SVM algorithm.

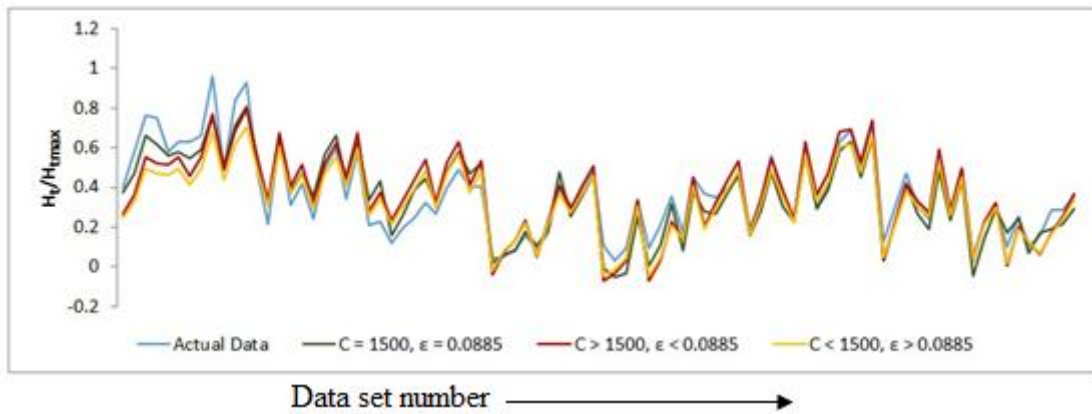


Fig. 6.13 Data fitting of models developed (linear kernel) for prediction of H_t/H_{tmax}

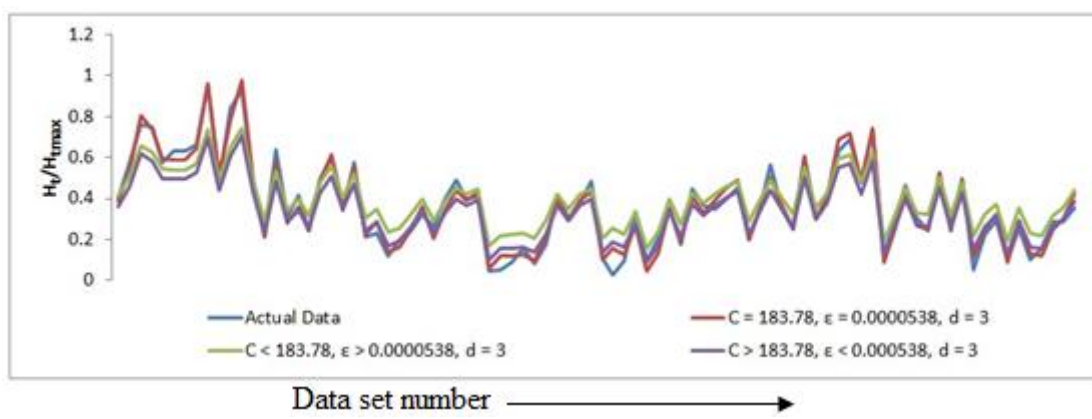


Fig. 6.14 Data fitting of models developed (polynomial) for prediction of H_t/H_{tmax}

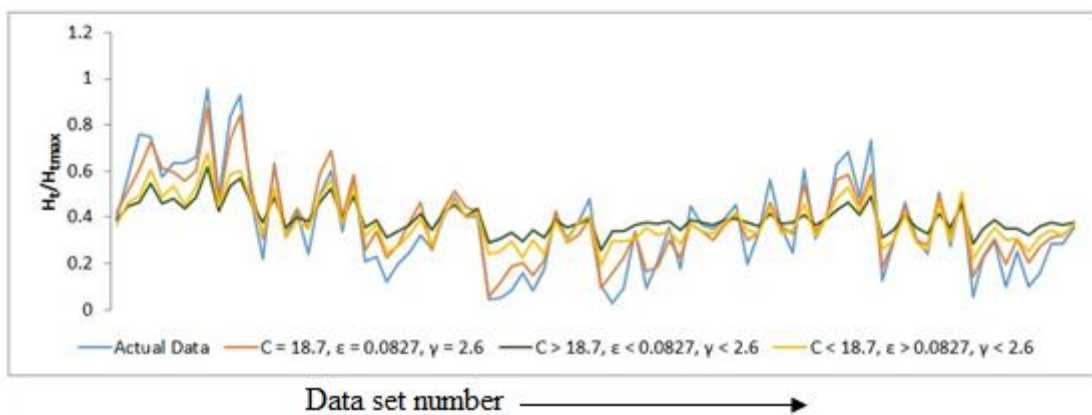


Fig. 6.15 Data fitting of models developed (RBF kernel) for prediction of H_t/H_{tmax}

For the prediction of transmitted wave height, optimal parameters of SVM with linear, polynomial and RBF kernel parameters are obtained using PSO as an optimization searching algorithm. In case of RBF kernel function, the optimal width (γ) is found to be 2.6 and the optimal values of d (degree) in case of polynomial kernel function is 3, as listed in Table 6.5. The optimal parameters obtained are used by the SVM model to predict the transmitted wave height. Thus, the effectiveness, reliability and accuracy of

the model developed are evaluated by calculating the statistical measures as presented in the Table 6.6.

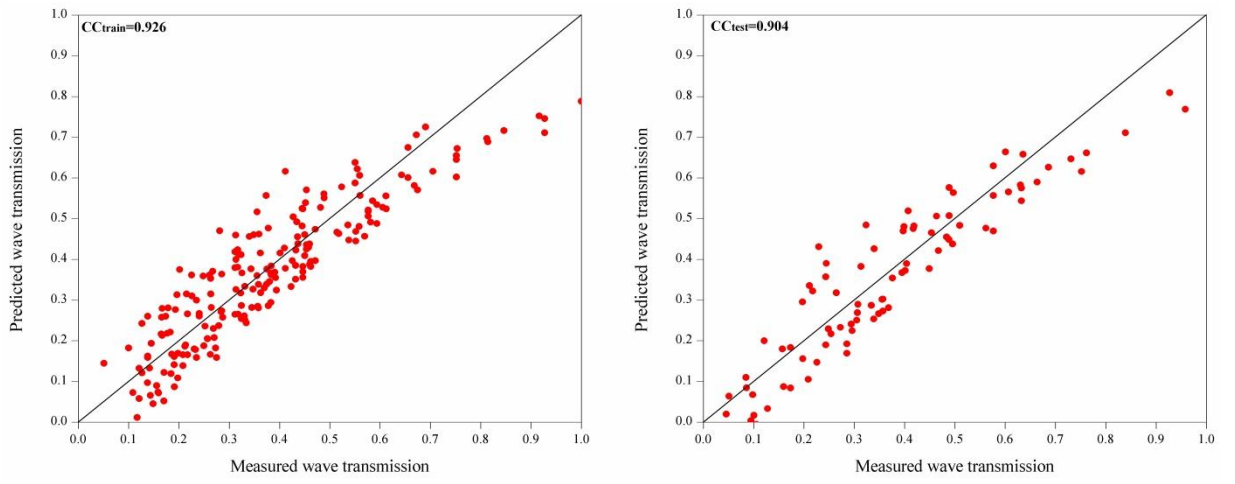
Table 6.5 Optimal parameters for PSO-SVM models for predicting H_t/H_{tmax}

Kernel type	Linear	Polynomial	RBF
C	1500	183.78	18.7
ϵ	0.0885	0.0000538	0.0827
γ	-	-	2.6
d	-	3	-

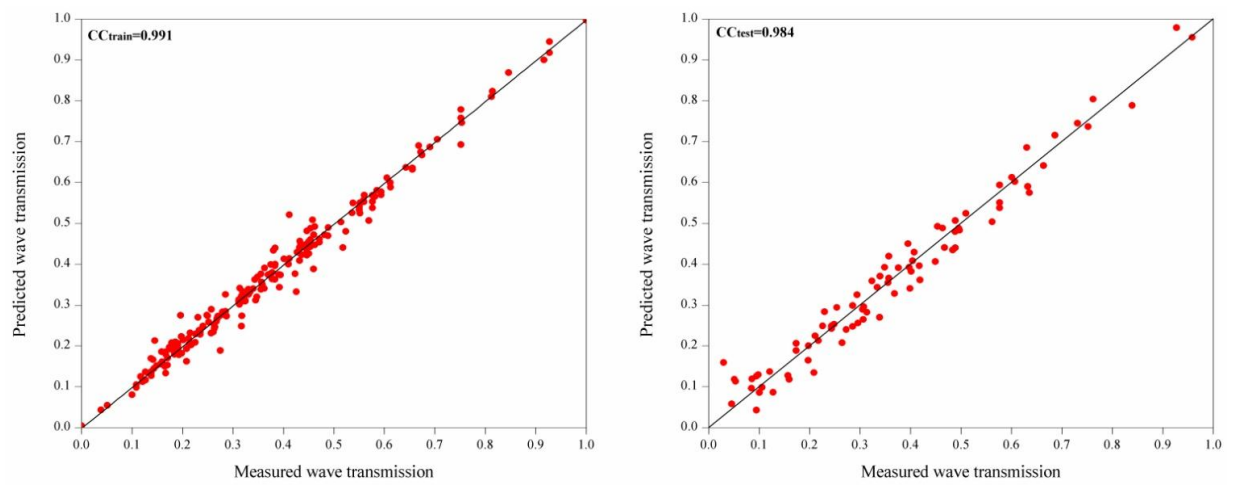
Table 6.6 Statistical parameters for PSO-SVM models for predicting H_t/H_{tmax}

Kernel type	Linear		Polynomial		RBF	
	Train	Test	Train	Test	Train	Test
CC	0.926	0.904	0.991	0.984	0.969	0.960
RMSE	0.077	0.081	0.025	0.037	0.051	0.068
SI	0.217	0.217	0.088	0.102	0.138	0.184
NSE	0.853	0.819	0.982	0.968	0.926	0.894

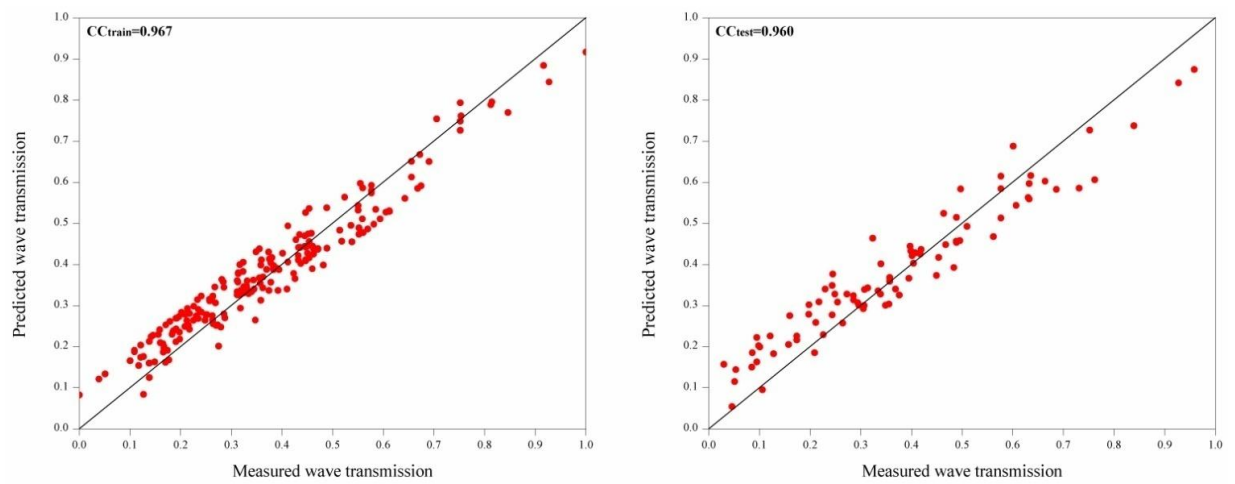
The RMSE=0.037 obtained for testing model for polynomial kernel function is comparatively less than other kernel functions. SI=0.102 value for polynomial kernel function indicates the good correlation and least scattering from actual fitted data. NSE=0.968 for polynomial kernel function indicates the predictive efficiency of PSO-SVM. From all the results obtained, it is observed that PSO-SVM model with polynomial kernel function shows better generalization performance with values of CC=0.984, RMSE=0.037, SI=0.102, NSE=0.968 testing data points, when compared with other kernel functions. The scatter diagram which shows the CC of the models for the training and testing data using various kernels are shown in Fig. 6.16.



a) Linear kernel



b) Polynomial kernel function



(c) RBF kernel function

Fig. 6.16 Scatter plots of PSO-SVM model for H_t/H_{tmax} with observed data

From the scatter plots, it is noticed that, PSO-SVM model using polynomial kernel function gives the best data fitting between predicted and observed data. The box plots

are another type of statistical measures in which the variability of the predicted data is found with reference to observed data and is depicted in the discussion. Fig. 6.17 indicates box plot with the upper and lower quartile values predicted is matching well with the observed wave transmission over submerged reef. SVM model with polynomial kernel, predicted data points are distributed well in the lower quartile of the box plot with reference to the observed values.

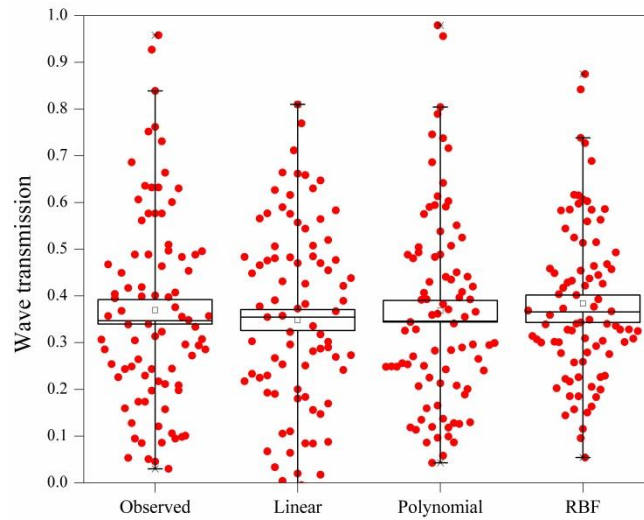


Fig. 6.17 Box-Whiskers plot of H_t/H_{tmax} for PSO-SVM model

The validation of PSO-SVM model using polynomial kernel function for the prediction of wave transmission is shown in Fig. 6.18, using the comparison graph. From the graph, it is clearly noticed that, the predicted data follows similar trend compared to observed data. Even though model developed with RBF kernel function provides results with high correlation, for both training and testing. PSO-SVM model using polynomial kernel function gives 4.36% improved correlation, 48.61% reduced RMSE, SI and maximum NSE value is found to be the best model for prediction of transmitted wave height over submerged reef of a tandem breakwater.

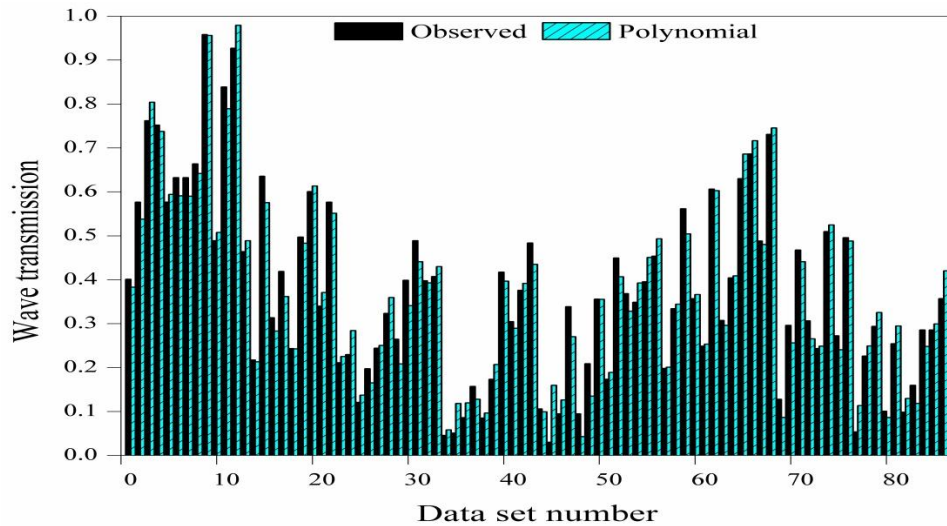


Fig. 6.18 Comparison of PSO-SVM model (polynomial kernel) for H_i/H_{tmax} with observed values

6.4.2 Simulation results of PSO-SVM model for predicting damage level (S) of Conventional rubble mound breakwater of tandem breakwater

The prediction of damage level of the emergent conventional rubble mound breakwater of the tandem breakwater is performed by considering the 8 inputs H_i/gT^2 , X/d , $H_i/\Delta D_{n50}$, B/d , B/L_o , F/H_i , h/d , d/gT^2 influencing the dependent variable damage level (S). The training is carried out using 202 data points (70%) and testing is done for 86 data points (30%). Figs. 6.19, 6.20 and 6.21 depicts the data fitting curves of PSO-SVM models developed for damage level prediction using linear, polynomial and RBF kernel functions, respectively, for testing. In each figure, it is observed that predicted value fits better with actual value for specific values of C , ϵ , γ and d . From the Fig. 6.19, the best fit curve corresponds to the model having (linear kernel) $C = 1327.67$ and $\epsilon = 0.0069$. Similarly, $C = 547$, $\epsilon = 0.0356$, $d = 3$ and $C = 363.83$, $\epsilon = 0.0000228$, $\gamma = 3.2$ are parameter values corresponding to the best fitting curves for Figs. 6.20 and 6.21 respectively.

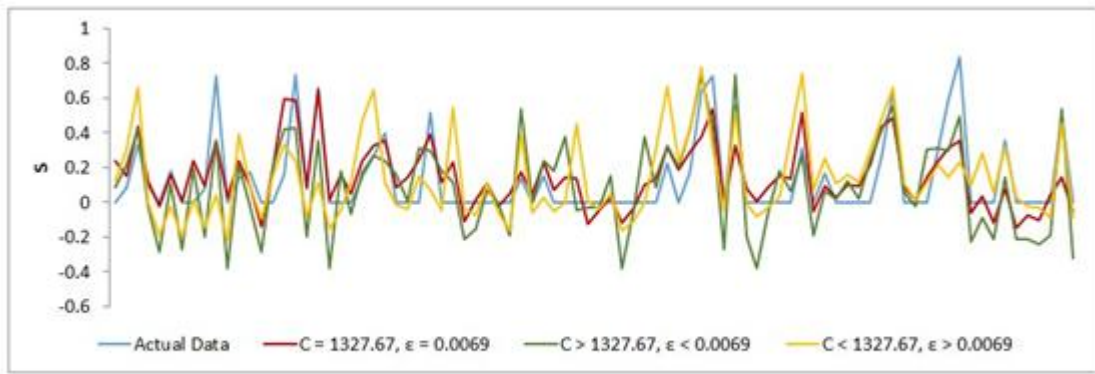


Fig. 6.19 Data fitting of models developed (linear) for prediction of Damage level

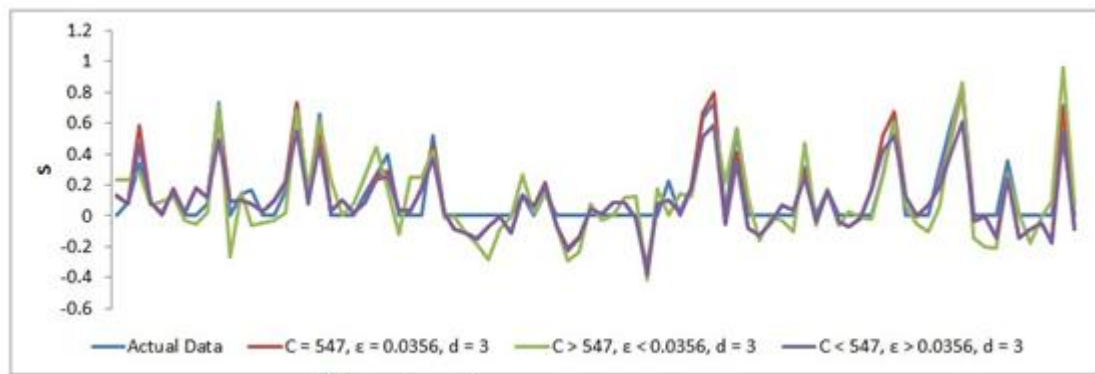


Fig. 6.20 Data fitting of models developed (polynomial) for prediction of damage level

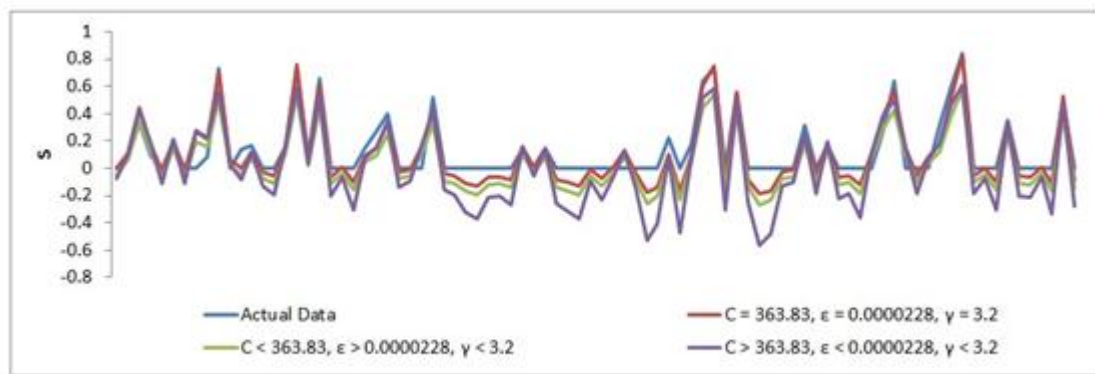


Fig. 6.21 Data fitting of models developed (RBF) for prediction of damage level

Optimal values of SVM and kernel function parameters, obtained using PSO for damage level prediction using linear, polynomial and RBF kernel based models are shown in Table 6.7. The optimal values of the parameters are used by the model in

prediction of damage level of conventional rubble mound breakwater of tandem breakwater. In case of RBF kernel, the optimal width (γ) is found to be 3.2 and the optimal values of d (degree) in case of polynomial kernel function is 3 and effectiveness of the model developed in prediction of damage level is evaluated by calculating the value of statistical parameters.

Table 6.7 Optimal parameters for PSO-SVM models for predicting Damage levels

Kernel type	Linear	Polynomial	RBF
C	1327.6	547	363.83
ϵ	0.0069	0.0356	0.000022
γ	-	-	3.2
d	-	3	-

Model performance indicators of models developed using linear, polynomial and RBF kernels for training and testing are given in Table 6.7. The PSO-SVM model with RBF kernel function gives better correlation of CC = 0.941 for testing compared to all other kernel functions.

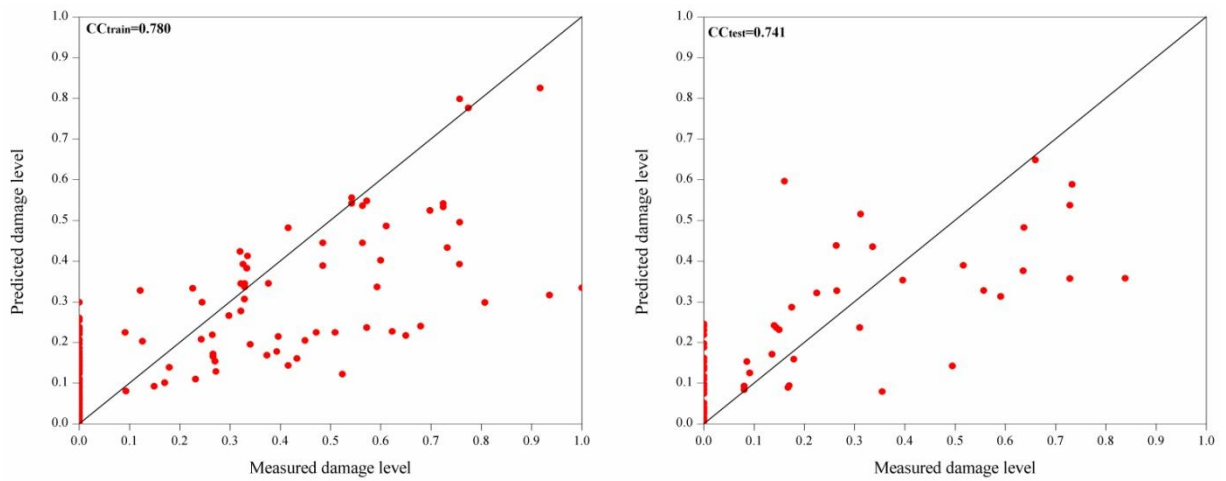
The value of RMSE=0.088 for testing is comparatively lower for developed model using RBF kernel function compared to rest of the kernel functions. This indicates that the predicted data is closer to actual data for RBF kernel function.

Table 6.7 Statistical parameters for PSO-SVM models for predicting Damage levels

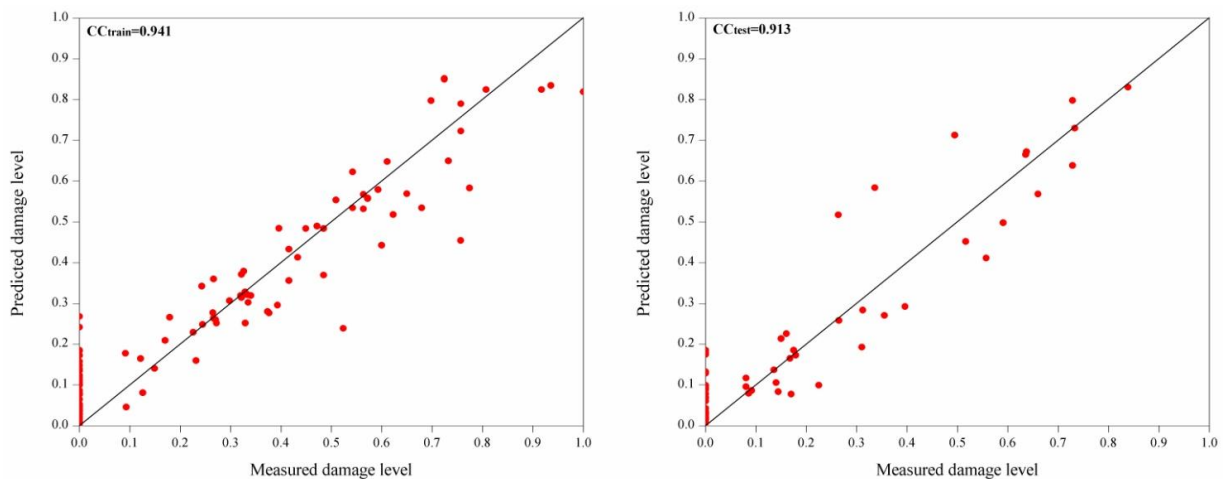
Kernel type	Linear		Polynomial		RBF	
	Train	Test	Train	Test	Train	Test
CC	0.780	0.741	0.941	0.913	0.961	0.941
RMSE	0.154	0.161	0.085	0.099	0.071	0.088
SI	1.067	1.143	0.584	0.756	0.493	0.669
NSE	0.605	0.541	0.882	0.799	0.916	0.843

SI = 0.669 for RBF kernel function indicates the least scattering from actual fitted data compared to 1.143 and 0.756 during testing phase for linear and polynomial kernel functions respectively. NSE value of 0.843 for RBF kernel function compared to 0.541 and 0.799 during testing for linear and polynomial kernels, respectively, indicates the predictive efficiency of model developed using RBF kernel function. Finally, PSO-SVM model with RBF kernel function shows better error generalization performance

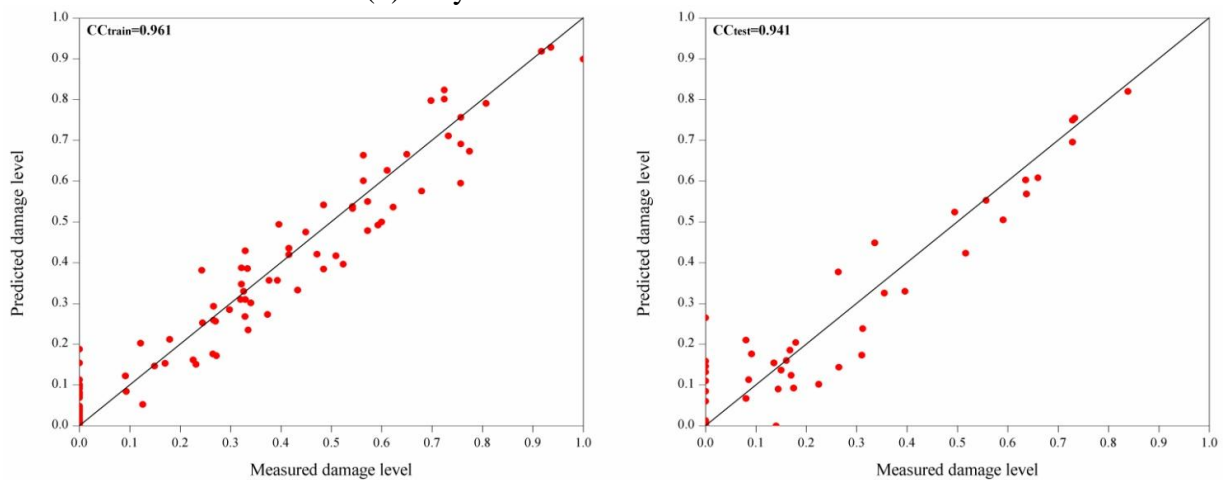
with $CC = 0.941$, $RMSE = 0.088$, $SI = 0.669$ and $NSE = 0.843$ testing, when compared to the rest of the kernel functions. The scatter diagram showing CC of PSO-SVM models for the training and testing data are shown in Fig. 6.22



(a) Linear kernel function



(b) Polynomial kernel function



(c) RBF kernel function

Fig. 6.22 Scatter plots of damage level (S) prediction using SVM model with different kernel functions

From the scatter plots, it is clear that, PSO-SVM model using RBF kernel function gives the best data fitting between predicted data and observed data. The box plot statistics is also used to measure the performance of the PSO-SVM model with different kernel. In terms of box plot assessment of predicted S in respect to observed data points is shown in Fig. 6.23. In the plots spread of predicted values by RBF shows the similar pattern and closely related to the observed values in terms of upper and lower quartile distribution of RBF prediction. Based on the scatter and box plots statistics, PSO-SVM model with polynomial and RBF kernel functions predicts successfully with high accuracy compared to the all other models, can be used as best alternate to predict the wave transmission over submerged reef and damage level of main breakwater of tandem breakwater respectively.

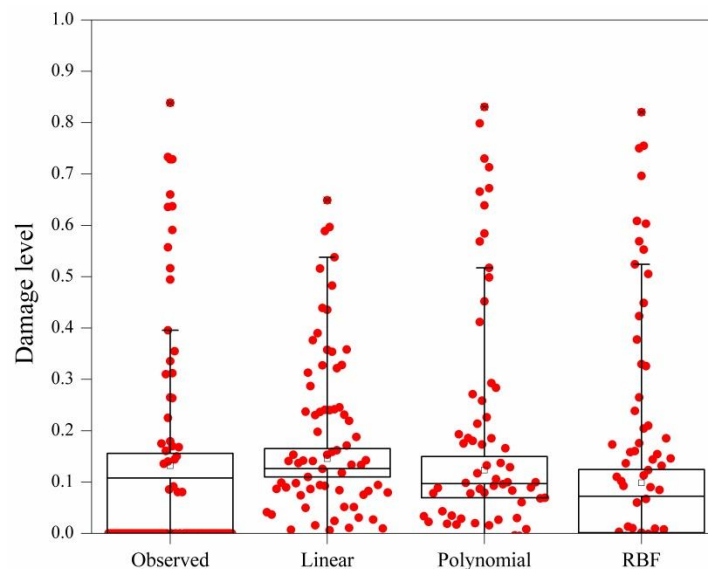


Fig. 6.23 Box-Whiskers plots of damage level (S) for PSO-SVM model

The model developed using linear kernel function gives the least correlation ($CC = 0.741$ for testing) which indicates that the data cannot be separated by a linear hyperplane in a low dimensional space. Fig. 6.24 shows the performance of observed and predicted damage level by PSO-SVM for RBF kernel function. Observing the graph, the PSO-SVM model with RBF kernel function is showing similar pattern compared to actual data with fluctuations are comparatively more around values of $S = 0$. Even though models developed with polynomial kernel function provides results with 83% correlation for both training and testing, the PSO-SVM model using RBF kernel function with 88% correlation, minimum RMSE, SI and maximum NSE value is found to be the best model in prediction of damage level of emergent main breakwater of tandem breakwater.

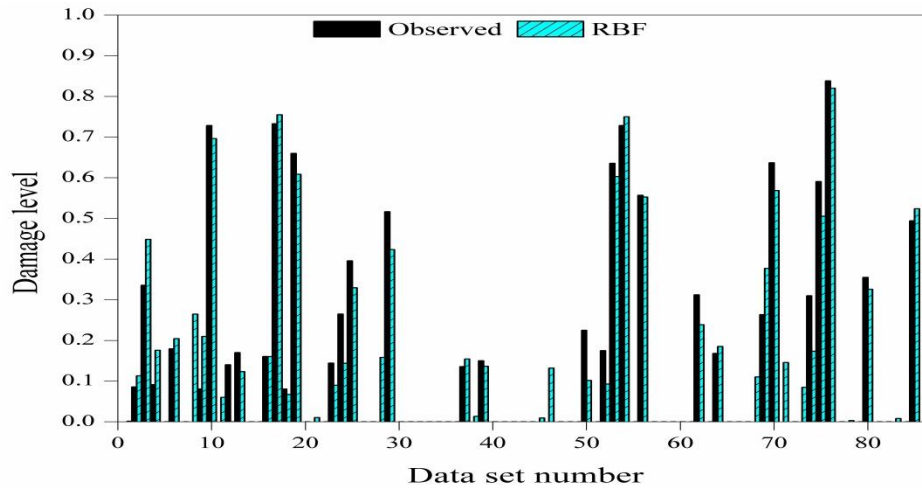


Fig. 6.24 Comparison of damage level predicted by PSO-SVM model (RBF) with observed values

6.4.3 Summary of PSO-SVM model results

Soft computing techniques provide results within a smaller time frame compared to mathematical and physical modeling. The complex nature of mathematical modeling and more expense involved in physical modeling makes soft computing technique a better alternate option for the prediction of transmitted wave height and damage level. As soft computing models are developed based on experimental data, it is essential to have physical model study so as to quantitatively determine the parameters influencing the performance of breakwaters. Therefore, physical model study along with the application of soft computing techniques employed to have effective and faster results. Different soft computing techniques such as ANN, SVM, ANFIS, etc. are successfully used for the prediction of wave parameters as discussed earlier. In this context, effectiveness of model developed for prediction depends on the proper selection of parameters. In this study, an effort is made to check the applicability of PSO-ANN and PSO- SVM model for predicting transmitted wave height and damage level of a tandem and the results are found to be satisfactory and reliable.

6.5 COMPARISON OF PERFORMANCE OF BEST ANN, SVM, ANFIS, PSO-ANN AND PSO-SVM MODELS

The results obtained using individual models have been discussed in previous sections. In this section a comparison of all the selected models have been made to know the best model that could predict wave transmission and damage level of tandem breakwater

accurately. For the given data set, ANN, ANFIS, SVM, PSO-ANN and PSO-SVM models are trained and tested to predict the wave transmission and damage level of tandem breakwater. The ANN (8-3-1), SVM (RBF), ANFIS (Gaussmf), PSO-ANN (8-3-1) and PSO-SVM (polynomial) models performed better among all the soft computing models considered for predicting wave transmission over a submerged reef of tandem breakwater in terms of statistical measures with respect to experimental values are listed in Table 6.9. Similarly, ANN (8-5-1), SVM (RBF), ANFIS (Gaussmf), PSO-ANN (8-2-1) and PSO-SVM (RBF) models performed better among all the soft computing models considered for predicting damage levels of conventional rubble mound breakwater of tandem breakwater in terms of statistical measures with respect to experimental values are listed in the Table 6.10.

Figs. 6.25 and 6.26 illustrate the comparison of wave transmission predicted by ANN with (8-3-1) and SVM with RBF kernel function with respect to experimental values of individual models. Similarly, Figs. 6.27 and 6.28 represent PSO-ANN with (8-3-1) and PSO-SVM with polynomial kernel function with respect to experimental values of hybrid models. ANN with (8-3-1) network outperformed all other soft computing techniques for predicting wave transmission with high CC of 0.989 and high efficiency of 0.978 with least error of 0.031 and small scatter of 0.086. Therefore, ANN with (8-3-1) network can be used as an efficient and reliable soft computing technique for predicting wave transmission over a submerged reef of a tandem breakwater.

Table 6.9 Comparison of Statistical Measures of ANN, SVM, ANFIS, PSO-ANN and PSO-SVM Models for wave transmission (H_t/H_{tmax})

Model	Training Data				Testing Data			
	CC	RMSE	SI	NSE	CC	RMSE	SI	NSE
ANN(8-3-1)	0.988	0.029	0.078	0.976	0.989	0.031	0.086	0.978
SVM (RBF)	0.977	0.055	0.151	0.92	0.965	0.056	0.150	0.911
ANFIS (Gaussmf)	0.99	0.0017	0.006	0.99	0.935	0.075	0.002	0.869
PSO-ANN (8-3-1)	0.940	0.065	0.176	0.88	0.941	0.072	0.199	0.879
PSO-SVM (Polynomial)	0.969	0.051	0.138	0.926	0.960	0.068	0.184	0.894

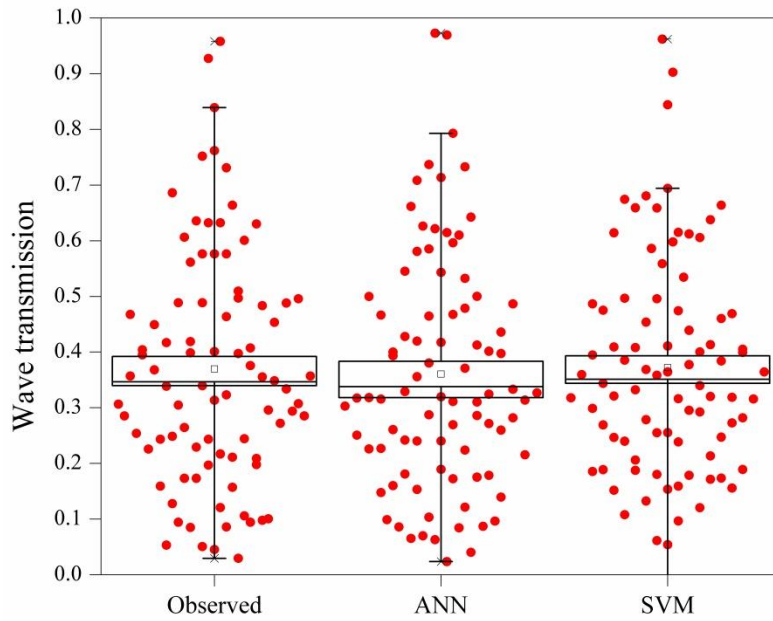


Fig. 6.25 Box-Whisker plot for wave transmission comparison of individual models

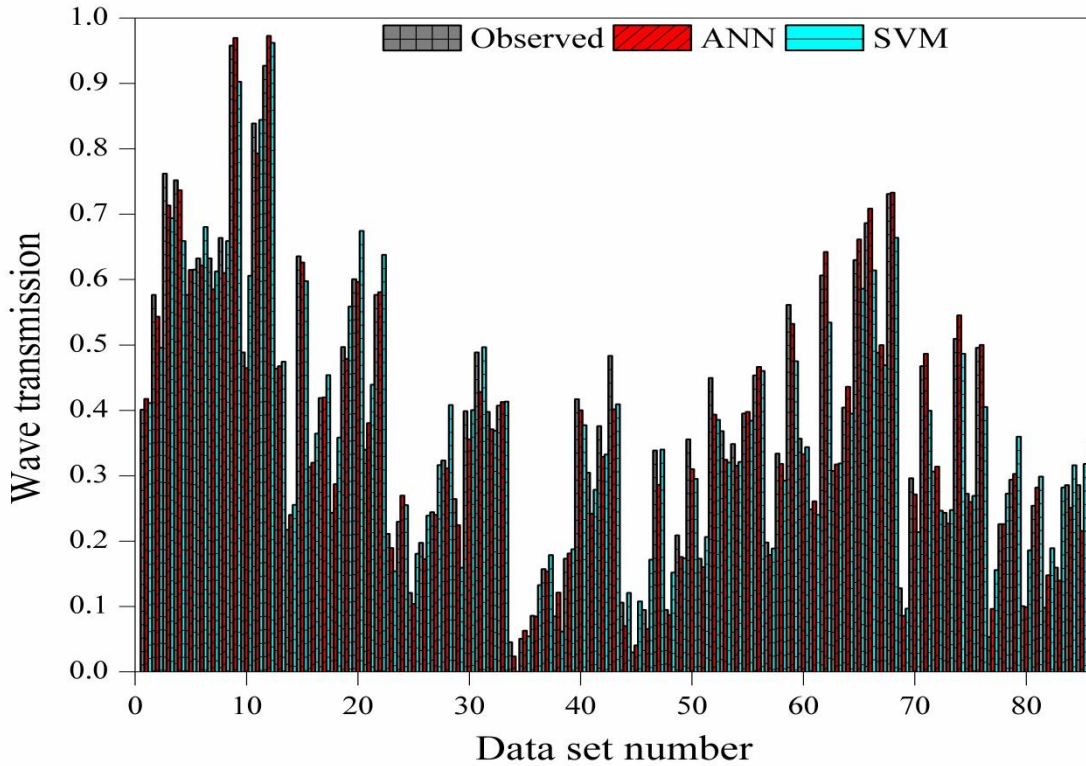


Fig. 6.26 Comparison of ANN (8-3-1) and SVM (RBF) models for wave transmission

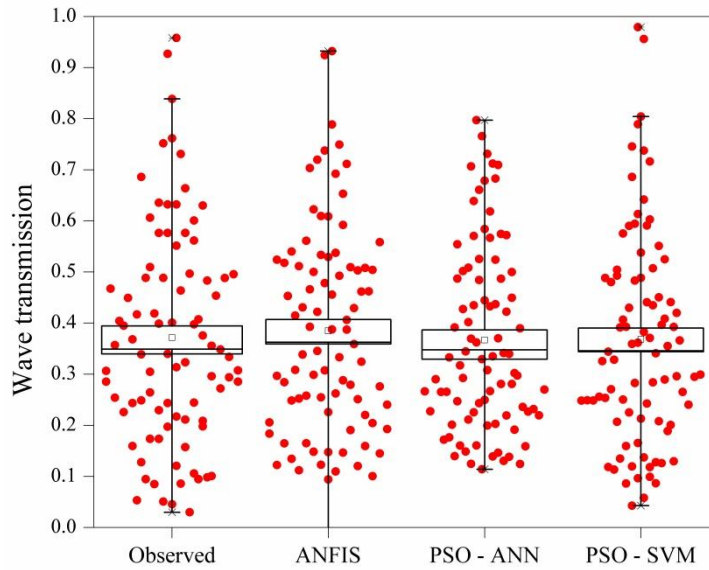


Fig. 6.27 Box-Whisker plot for wave transmission comparison of hybrid models

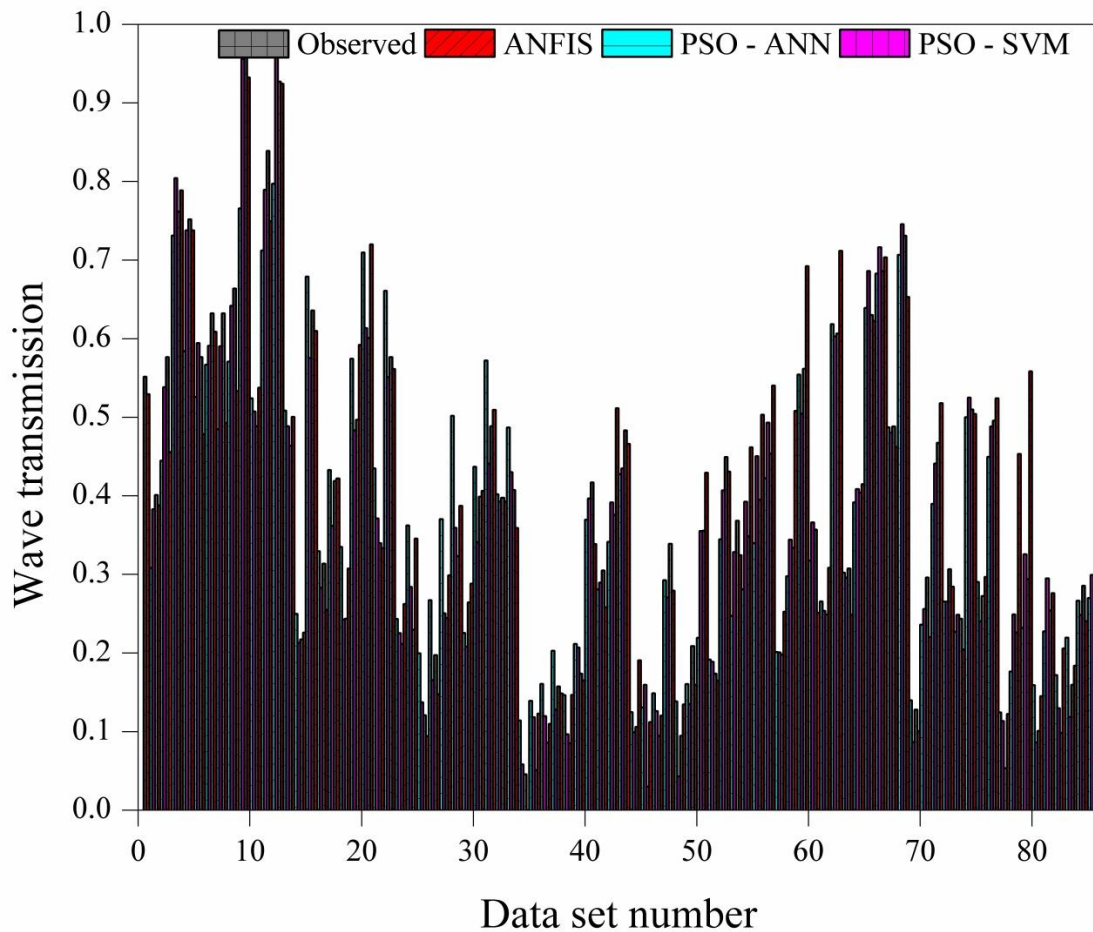


Fig. 6.28 Comparison of ANFIS (Gaussmf), PSO-ANN (8-3-1) and PSO-SVM (Polynomial) models for wave transmission

Table 6.10 Comparison of Statistical Measures of ANN, SVM, ANFIS, PSO-ANN and PSO-SVM Models for damage level (S)

Model	Training Data				Testing Data			
	CC	RMSE	SI	NSE	CC	RMSE	SI	NSE
ANN(8-5-1)	0.974	0.055	0.382	0.949	0.956	0.066	0.515	0.908
SVM (RBF)	0.954	0.0910	0.690	0.903	0.935	0.0765	0.529	0.833
ANFIS (Gaussmf)	0.99	0.0001	0.0012	0.99	0.875	0.123	0.011	0.70
PSO-ANN (8-2-1)	0.767	0.158	1.096	0.584	0.769	0.141	1.093	0.589
PSO-SVM (Polynomial)	0.961	0.071	0.493	0.916	0.941	0.088	0.669	0.843

Similarly, Figs. 6.29 and 6.30 illustrate the comparison of damage levels predicted by ANN with (8-5-1) with respect to experimental values of individual models. Similarly, Figs. 6.31 and 6.32 shows SVM with RBF kernel function, PSO-ANN with (8-2-1) and PSO-SVM with RBF kernel function with respect to experimental values and hybrid models.

ANN with (8-5-1) network outperformed all other soft computing techniques for predicting wave transmission with high CC of 0.956 and high efficiency of 0.908 with least error of 0.066 and small scatter of 0.515. Therefore, ANN with (8-5-1) network can be used as an efficient and reliable soft computing technique for predicting damage level conventional rubble mound breakwater of a tandem breakwater.

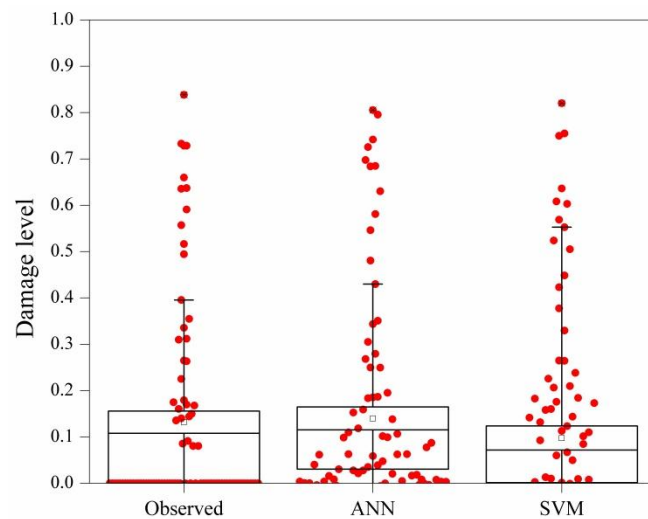


Fig. 6.29 Box-Whisker plot of damage levels comparison for individual models

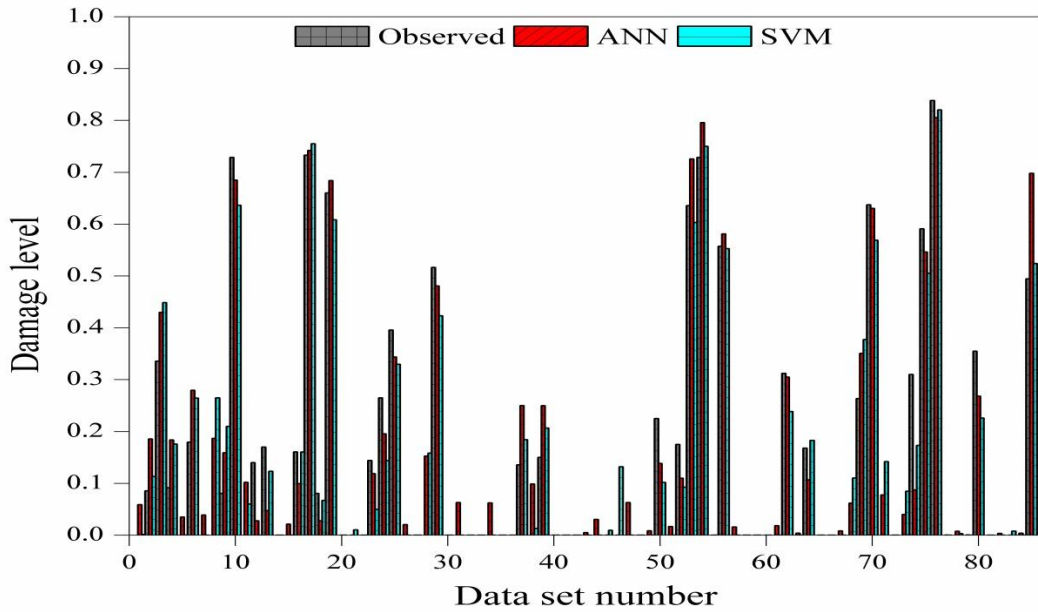


Fig. 6.30 Comparison of ANN (8-5-1) and SVM (RBF) models for damage levels

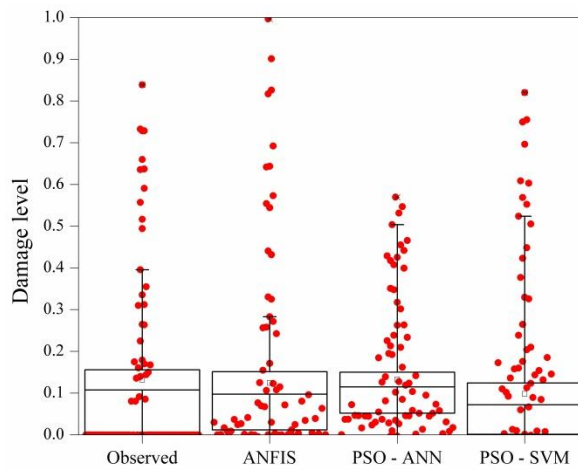


Fig. 6.31 Box-Whisker plot of damage levels comparison of hybrid models

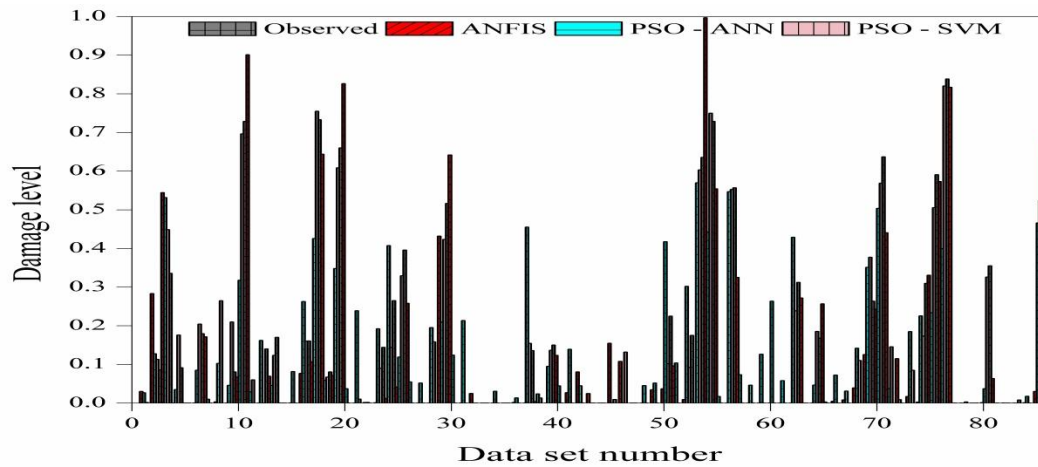


Fig. 6.32 Comparison of ANFIS (Gaussmf), PSO-ANN (8-2-1) and PSO-SVM (RBF) models for damage levels

It is observed that among the individual models ANN (8-3-1) network with high CC of 0.989 and high efficiency NSE of 0.978 and ANN (8-5-1) network with high CC of 0.956 and high efficiency NSE of 0.908 outperformed SVM with RBF in both cases. Similarly, among the hybrid soft computing techniques employed in the present study it is found that the PSO-SVM with polynomial kernel function with high CC of 0.984 and high efficiency NSE of 0.894 outperformed other hybrid techniques ANFIS (Gaussmf) and PSO-ANN with (8-3-1) network with high in case of wave transmission and PSO-SVM with RBF kernel function CC of 0.960 and high efficiency NSE of 0.843 in case of damage level of tandem breakwater. ANN and PSO-SVM models can be used as efficient and reliable techniques for prediction of wave transmission and damage level of tandem breakwater. Among all the individual and hybrid models ANN outperformed with high CC and least RMSE and less scatter and high efficiency for both the cases.

6.5.1 Summary of best model results

It is observed that ANN with 3 hidden layers with 100 epochs are sufficient to get better results from the different models. Firstly, the individual models of the ANN and SVM are tested with eight input parameters. It is observed that ANN with LM algorithm performed better compared to SVM with RBF kernel function.

The individual ANN with LM algorithm and SVM with RBF kernel function are compared to know their respective performance. ANN with LM algorithm showed best performance compared to SVM but a chance for clarification and comparison is available. Hence, in continuation hybrid models are considered for the further study. The different membership functions of the ANFIS and various numbers of hidden nodes of PSO-ANN and also different Kernel functions of PSO-SVM are compared before selecting the best technique. In case of PSO-ANN model, the number of hidden layers and epochs are optimized further before using them in the model. ANN with (8-3-1) and ANN with (8-5-1) shows better results compared to SVM with RBF kernel function. Comparing the different hybrid models, PSO-SVM with polynomial and RBF kernel function performed better than ANFIS (Gaussmf) and PSO-ANN (8-3-1) and PSO-ANN (8-2-1) models. After observing the statistical results of all the individual and hybrid soft computing techniques adopted in the present study ANN with 3 and 5 hidden neurons is found to best model for the prediction of wave transmission and damage levels of tandem breakwater.

SUMMARY AND CONCLUSIONS

7.1 SUMMARY

The development of a mathematical model to determine the transmitted wave height over a submerged reef of tandem breakwater is complex. Therefore, it is necessary for researchers to adopt the physical model study to quantitatively determine the influence of parameters on the performance of breakwaters. Physical modeling is a time consuming process, laborious, expensive and it is inconvenient for immediate needs. Hence, the soft computing techniques are adopted based on the experimental data of tandem breakwater and same are utilized for the validation of the developed AI models.

The soft computing models are built based on the data collected from the physical model study conducted on tandem breakwater in a two dimensional wave flume by Rao and Shirlal in 2004. Non-dimensional input parameters that influence the transmitted wave height (H_t/H_{tmax}) over submerged reef and damage level (S) of conventional rubble mound breakwater of tandem breakwater namely, deepwater wave steepness (H_i/gT^2), relative reef spacing (X/d), Hudson's stability number ($H_i/\Delta D_{n50}$), relative reef crest width (B/d), (B/L_o), relative reef submergence (F/H_i), relative reef crest height (h/d), relative depth (d/gT^2) are used for developing soft computing techniques.

Initially ANN (8-1-1) to ANN (8-5-1) models are developed with different algorithms using eight parameters. ANN models are developed by varying the number of hidden neurons. Here, the numbers of hidden layers are optimized to get better results. Further, SVM models with different kernel functions are developed. The individual ANN and SVM are compared to know their performance. ANN showed better performance compared to SVM but there is scope for improvement in the performance. Hence, in some hybrid models, namely ANFIS and PSO-ANN, PSO-SVM are developed and the best networks are found out. All the AI models are assessed and evaluated using model performance indicators in terms of statistical measures such as RMSE, CC, SI and NSE to find the best network.

The efficiency of the ANFIS models depend on the number of membership functions associated with each input and output data. The efficiency of the SVM model relies on the selection of best kernel function parameters (γ , d) and proper SVM parameters (C, ϵ).

It is observed from literature that there are hardly any applications of ANN, SVM, ANFIS, PSO-ANN and PSO-SVM models to study the stability of tandem breakwaters. Hence, it is decided to investigate of the applicability of ANN, SVM, ANFIS, PSO-ANN and PSO-SVM modeling approach for predicting the transmitted wave height (H_t/H_{tmax}) over a submerged reef and damage level (S) of conventional rubble mound breakwater of tandem breakwater. For this purpose the experimental data set obtained by Rao and Shirlal in 2004 on tandem breakwater using two dimensional wave flume of the Marine Structure laboratory, NITK Surathkal. The performance of the ANN, SVM, ANFIS, PSO-ANN and PSO-SVM are compared and the best model is selected based on statistical parameters.

An application of ANN, SVM, ANFIS, PSO-ANN and PSO-SVM for prediction of wave transmission over the outer submerged reef and damage level of inner conventional rubble mound breakwater are presented in the present study and the following conclusions are drawn.

7.2 CONCLUSIONS

Based on the results of the present investigations and discussion thereon, following conclusions are arrived at:

1. ANN is very successful in predicting transmitted wave height H_t/H_{tmax} . The prediction of ANN (8-3-1) model is very close to the experimental results with CC as 0.99 and the SI as 0.086 for the given data set compared to other models.
2. ANN (8-5-1) model for predicting damage level S has CC as 0.96 and SI as 0.52. Even though the CC value is good, SI value is not as good as in case of H_t/H_{tmax} prediction. This wide scatter of points is observed in the scattered plots due to the presence of more number of zero damage levels.
3. SVM with RBF kernel function gives 0.965 coefficient of correlations in the prediction of transmitted wave height over a submerged reef of tandem breakwater during testing phase with RMSE = 0.06, NSE = 0.911, SI = 0.16.

4. The SVM with RBF kernel gives CC of 0.935 in damage level prediction of conventional rubble mound breakwater of tandem breakwater during testing phase with RMSE = 0.0765, NSE = 0.83, SI = 0.529.
5. From the results obtained, it is evident that SVM with RBF kernel function gives a marginal increase in CC = 0.965 for testing and improved results, when compared to ANFIS model with Gaussian membership function for which CC=0.935 for testing data in the prediction of wave transmission (H_t/H_{tmax}) and 0.875 for damage level prediction.
6. PSO-ANN hybrid model with (8-3-1) network architecture can be considered as best network among other PSO-ANN models for predicting H_t/H_{tmax} with RMSE = 0.07, CC = 0.94, SI = 0.20 and NSE = 0.88 for testing.
7. PSO-ANN hybrid model with (8-2-1) network architecture can be considered as best network among other PSO-ANN models for predicting damage levels with RMSE = 0.14, CC = 0.77, SI = 1.10 and NSE = 0.59 for testing.
8. For the prediction of wave transmission, PSO-SVM model with polynomial kernel function gives best results with CC = 0.984, NSE = 0.968, RMSE = 0.038 and SI = 0.102 for testing. The hybrid PSO-SVM model with polynomial kernel function gives the best results for prediction of the wave transmission compared to other PSO-SVM models.
9. The best values of statistical parameters such as CC = 0.941, NSE = 0.843, RMSE = 0.088 and SI = 0.67, for testing are obtained in the case of PSO-SVM model with RBF kernel function for damage level prediction. The hybrid PSO-SVM model with RBF kernel gives the best result for damage level prediction compared to other PSO-SVM models.
10. The predicted values of the PSO-SVM model shows more proximity to actual data compared to the results of individual SVM model study, for the same data, with about 5% increase in correlation, 30% reduction in RMSE for wave transmission prediction. But the statistical parameter values do not show much variation in case of damage level prediction by PSO-SVM compared to SVM, this is due to the presence of more zero damage levels.

7.3 RECOMMENDATIONS

1. The present study recommends that ANN with (8-3-1) network can be used as efficient and reliable model and network for the prediction of wave transmission over a submerged reef and ANN with (8-5-1) network for damage level of conventional rubble mound breakwater of tandem breakwater among other individual models of SVM.
2. The present study recommends PSO-SVM with polynomial kernel function as an efficient and reliable technique to predict wave transmission over submerged reef and PSO-SVM with RBF kernel function for prediction of damage level of conventional rubble mound breakwater of tandem breakwater among other hybrid models such as ANFIS and PSO-ANN.
3. Overall recommendation of the present study is that the classical model ANN with different networks gave best results compared to all other individual and hybrid models considered in the present study. Therefore, ANN model can be used as efficient and reliable technique to predict wave transmission over a submerged reef and damage level of conventional rubble mound breakwater of tandem breakwater accurately.

7.4 LIMITATIONS OF PRESENT STUDY

- Soft computing techniques are data driven and will give the best results when sufficient experimental data is available beforehand.
- The models cannot be generalized unless similar field conditions are available. These are site specific models

7.5 SUGGESTIONS FOR FUTURE WORK

There is a scope for carrying out further research. The following suggestion may be considered for further study:

- The study can be extended to other evolutionary optimization techniques like ACO and any improvement in the efficiency of predictions can be checked.
- Alternate solver algorithms, such as ISDA and L1QP can be used in finding the initial values of parameters of the SVM model.
- Using emerging alternate novel optimization techniques like differential evolution scatter search etc., in hybridizing the SVM model.

PERFORMANCE OF ANFIS, PSO-ANN AND PSO-SVM MODELS**6.1 GENERAL**

By observing the results discussed in chapter 5, the capacity of the ANN and SVM models can be further cross checked or improve the efficiency of the model by hybridizing the model with other optimization techniques such as Fuzzy and PSO. From the literature, it is also observed that hybrid models give better results than the single models (Patil et al., 2012; Harish et al., 2014) in most of the cases. To improve the results, hybridizing technique such as ANN with Fuzzy Inference System and PSO and SVM with PSO are implemented and analysis is carried out. The obtained results are discussed in this chapter.

6.2 PERFORMANCE OF ADAPTIVE-NEURO FUZZY INFERENCE SYSTEM (ANFIS) MODEL

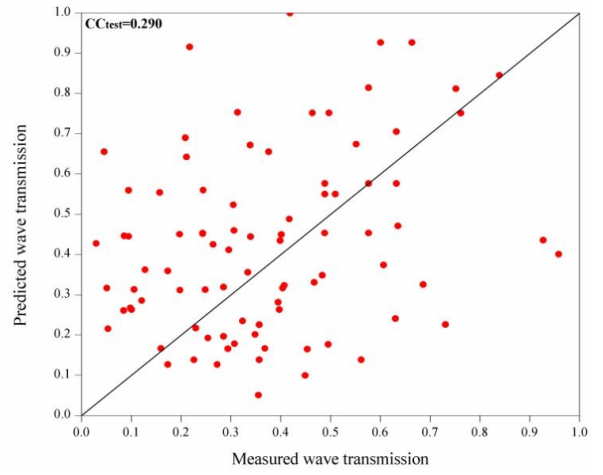
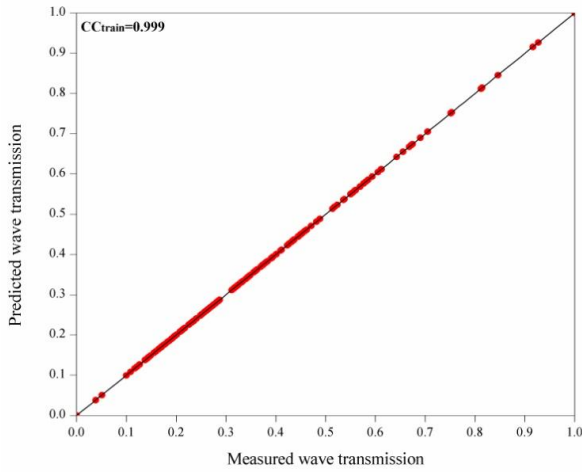
The ANFIS model with eight input parameters and one output parameter is built with different membership functions, fuzzy rules and epoch numbers. The various membership functions considered are Triangular-shaped built-in membership function (TRIMF), Trapezoidal-shaped built-in membership function (TRAPMF), Generalized bell-shaped built-in membership function (GBELLMF), and Gaussian curve built-in membership function (GAUSSMF). An ANFIS model with built-in 2 membership functions for each variable, and 100 epoch numbers are selected and trained using the Levenberg-Marquardt algorithm with tangent sigmoid and linear transfer functions in the hidden and output layers, respectively. In the present chapter ANFIS models are developed for the prediction of wave transmission over submerged reef and damage level of main conventional rubble mound breakwater of tandem breakwater. The performances of these models are evaluated based on statistical measures, namely RMSE, CC, SI and NSE. The CC between desired output and network predicted outputs are calculated by using Equation (4.30). The RMSE, SI and NSE between target output and network predicted output is determined by using Equations (4.31), (4.32), and (4.33) respectively. Each model is developed and results are discussed in the following section.

6.2.1 Simulation results of ANFIS Model for predicting wave transmission (H_t/H_{tmax})

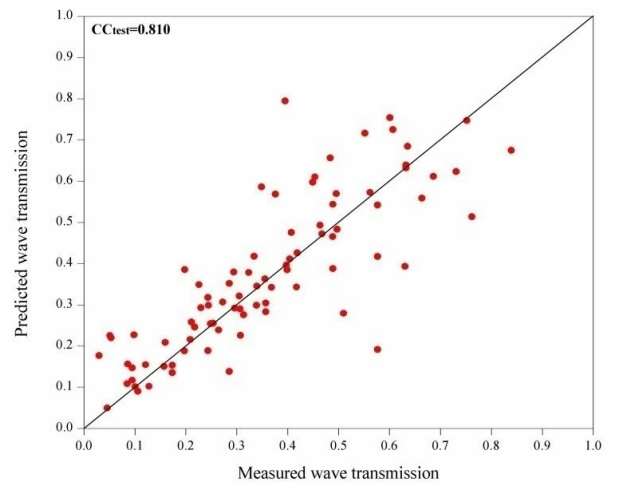
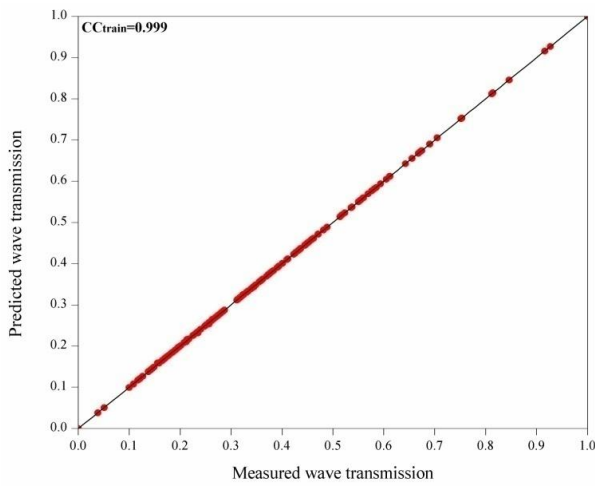
Fuzzy models are developed to predict the wave transmission over submerged reef of tandem breakwater. The proper selection of ANFIS and its membership functions and their number decides the performance of these models. The different membership functions with their performances in the form of scatter plots are shown in Fig. 6.1 and the values of statistical measures are tabulated in Table 6.1. In the present study, with 8 input parameters and 1 output, using Sugeno first order with (2^8) 256 fuzzy rules and 2 generalized ‘Triangular (trimf)’, ‘Trapezoidal (trapmf)’, ‘Gbell (gbellmf)’ and ‘Gaussian (Gaussmf)’ membership functions and 100 epochs the model is trained. Among all the membership functions, the ANFIS model with Gaussian membership function performs better than the other membership functions. It is believed that Gaussian membership function has the capacity to handle higher degree of error tolerance compared to other membership functions. The statistical measures obtained for ANFIS model with Gaussian membership function are RMSE= 0.0754, CC= 0.935. It is also observed that, there is good correlation between the observed and predicted wave transmission in this model with less scatter, SI= 0.0023. Good efficiency, NSE = 0.869 is obtained for testing. The ANFIS model, with a combination of gradient descent algorithm and least squares algorithm, is used in an effective search for the optimal parameters to yield good results. Based on this hybrid approach, correlations of training and testing are increased as presented in Fig. 6.1.

Table 6.1 Statistical measure of ANFIS models for predicting wave transmission

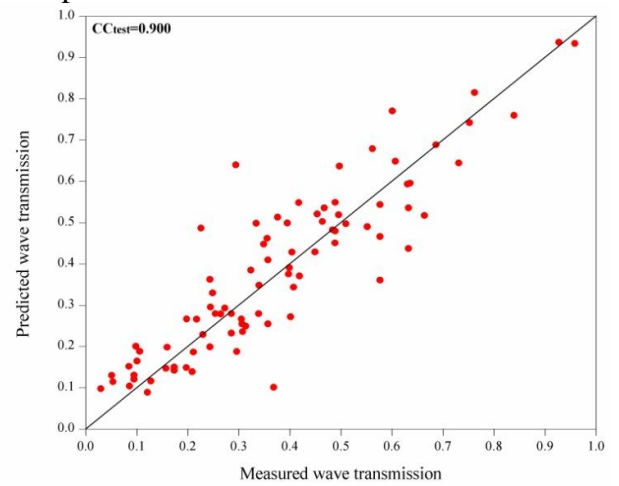
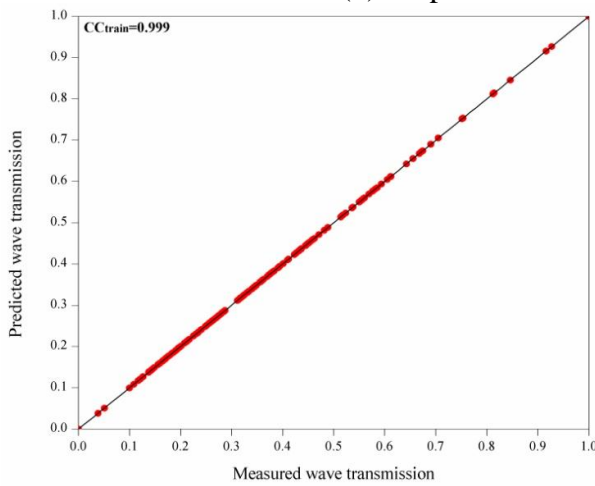
Statistical measures	Membership Functions							
	Triangular		Trapezoidal		Gbell		Gaussian	
	Train	Test	Train	Test	Train	Test	Train	Test
RMSE	0.0003	0.263	0.0004	0.136	0.00021	0.0935	0.0002	0.0754
NSE	0.999	0.588	0.999	0.576	0.999	0.799	0.999	0.869
CC	0.999	0.290	0.999	0.810	0.999	0.900	0.999	0.935
SI	0.0001	0.0081	0.0002	0.004	0.0007	0.0029	0.0006	0.0023



(a) Triangular membership function



(b) Trapezoidal membership function



(c) Gbell membership function

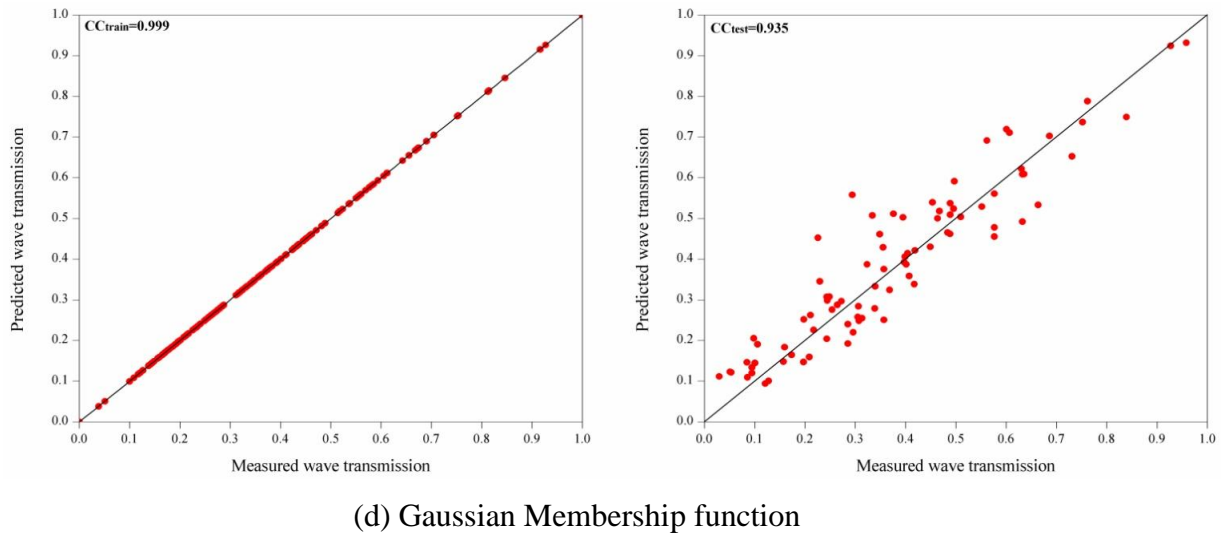


Fig. 6.1 Scatter plots of predicted and observed H_t/H_{tmax} by ANFIS for different membership functions

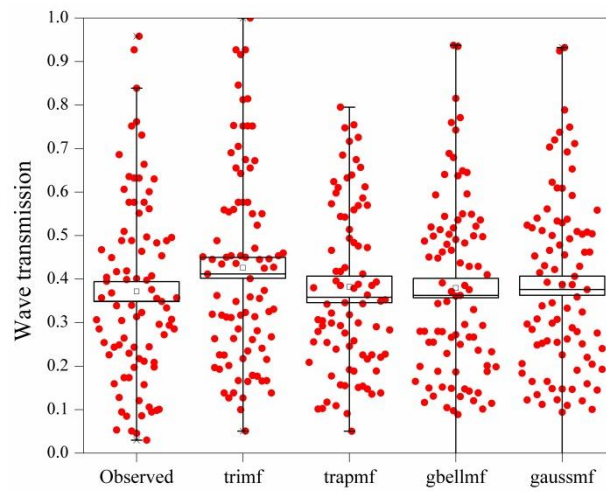


Fig. 6.2 Box-Whiskers plots of H_t/H_{tmax} for ANFIS model with different membership functions

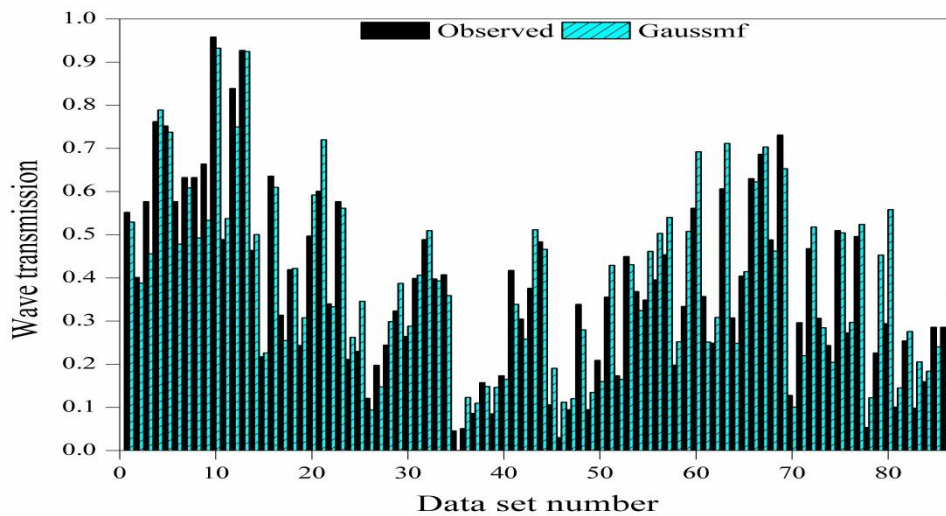


Fig. 6.3 Comparison of H_t/H_{tmax} predicted by ANFIS model with observed values

The box plot statistics are also used to check the variability of the predicted wave transmission by ANFIS model with different membership functions as shown in Fig. 6.2. Distribution of the predicted H_t/H_{tmax} values by Gaussmf is close to the observed one in the upper quartile and lower quartile of the box. The performance of the best model out of all the ANFIS models with various membership functions is assessed by plotting the predicted data with observed data points. Therefore, H_t/H_{tmax} predicting efficiency by ANFIS model with Gaussian membership function is compared with observed data for its validation as shown in Fig. 6.3. From the above figure, it is observed that the predicted results are in good agreement with the observed values and is concluded as a reliable model to predict H_t/H_{tmax} .

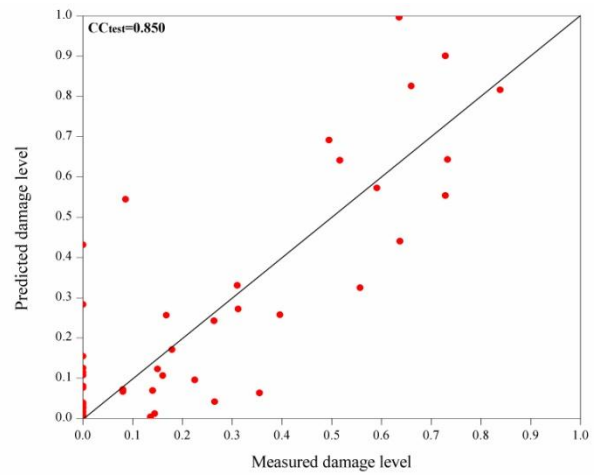
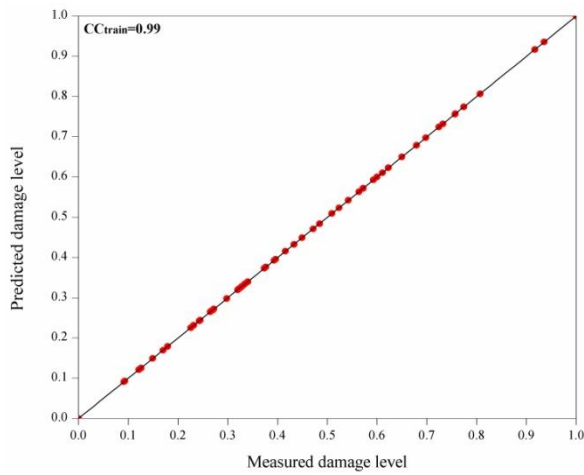
6.2.2 Simulation results of ANFIS Model in predicting the damage level (S)

The performance of different membership functions in terms of statistical measures is presented in the Table 6.2. In the present study, Sugeno first order method is used to trained the model by generating (2^8) 256 fuzzy rules with 2 generalized ‘Triangular (trimf)’, ‘Trapezoidal (trapmf)’, ‘Gbell (gbellmf)’ and ‘Gaussian (Gaussmf)’ membership functions for 100 epochs. To predict damage level, ANFIS model with Gaussmf is chosen as the best ANFIS model based on the model performance indicators, as RMSE = 0.123, CC = 0.875, SI = 0.011, NSE = 0.710 for testing. The ANFIS model is used, with a combination of gradient descent and least squares algorithm for an effective search of the optimal parameters to yield good results. Based on this hybrid approach of feed forward-back propagation neural network (FFBP) and decent gradient-least square principal fuzzy inference system (FIS) correlations of training and testing are increased.

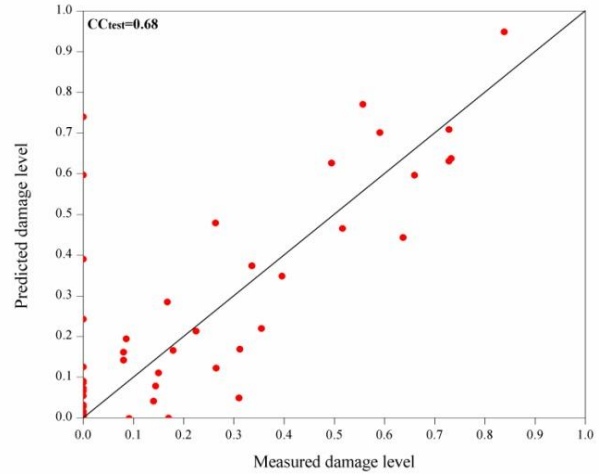
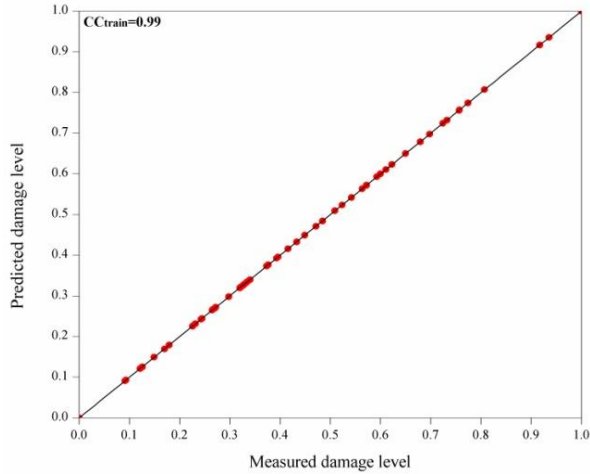
The scatter plots of predicted and observed damage level for ANFIS model with different membership functions are shown in Fig. 6.4. Among all the membership functions, Gaussian membership function is observed to be the best membership function. ANFIS model with Gaussmf outperformed other models with CC=0.875 providing better correlation with measured values and RMSE = 0.123.

Table 6.2 Statistical measure of ANFIS models for prediction of damage level

Statistical	Membership functions							
	Triangular		Trapezoidal		Gbell		Gaussian	
	Train	Test	Train	Test	Train	Test	Train	Test
RMSE	0.0001	0.132	0.0096	0.21	0.0002	0.129	0.002	0.123
NSE	0.99	0.64	0.99	0.575	0.99	0.682	0.99	0.710
CC	0.99	0.850	0.99	0.68	0.99	0.855	0.99	0.875
SI	0.0001	0.012	0.0009	0.018	0.00013	0.011	0.0012	0.011



(a) Triangular Membership function



(b) Trapezoidal Membership function

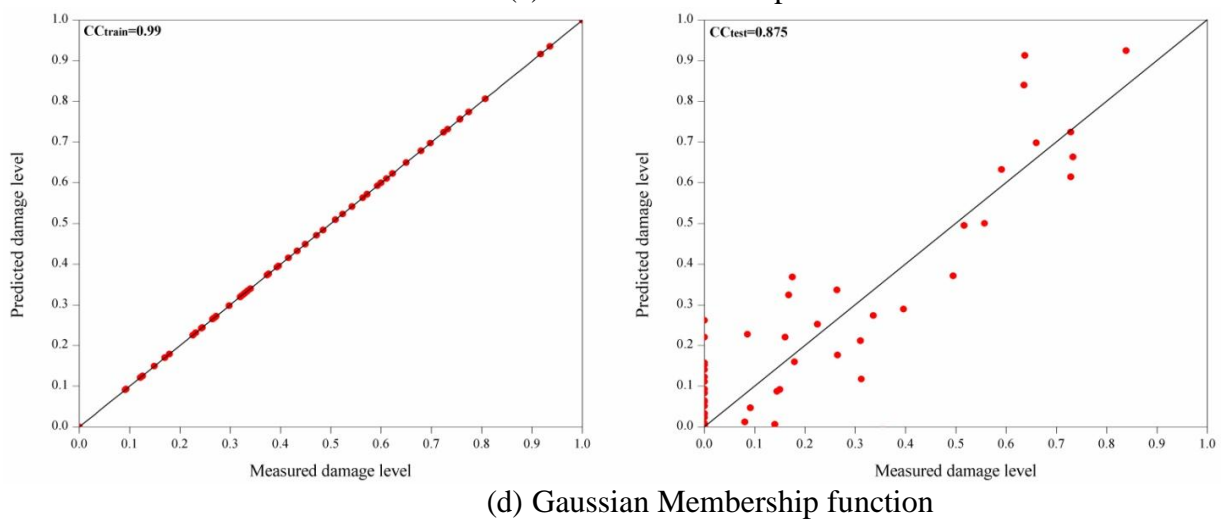
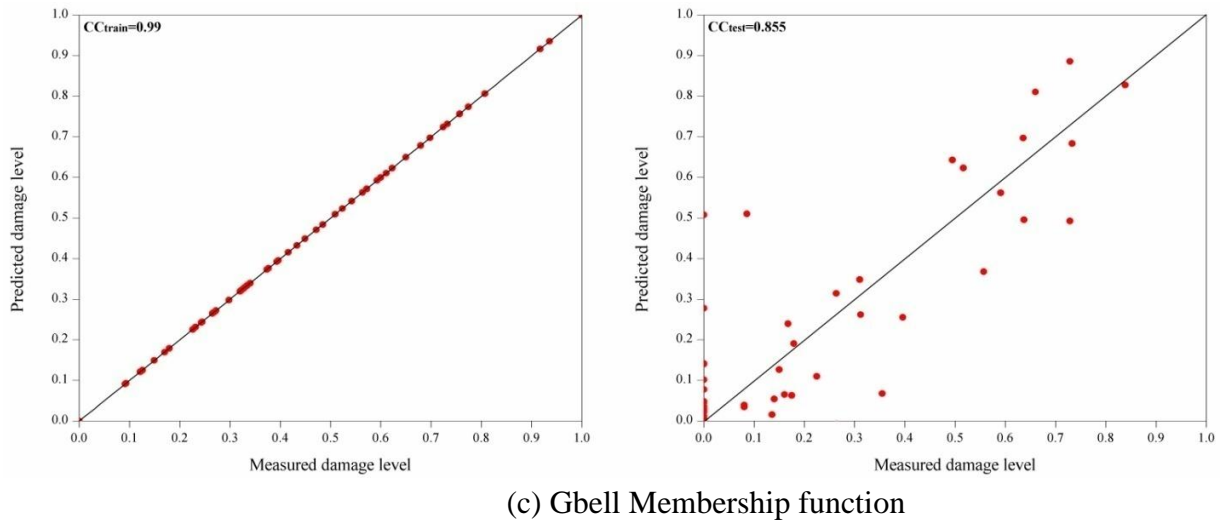


Fig. 6.4 Scatter plots of predicted and observed S for ANFIS model with different membership functions

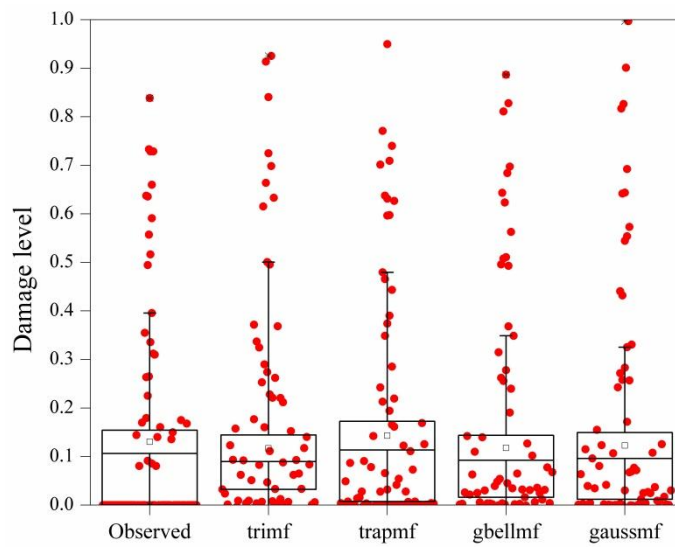


Fig. 6.5 Box-Whisker plots of S for ANFIS model with different membership functions

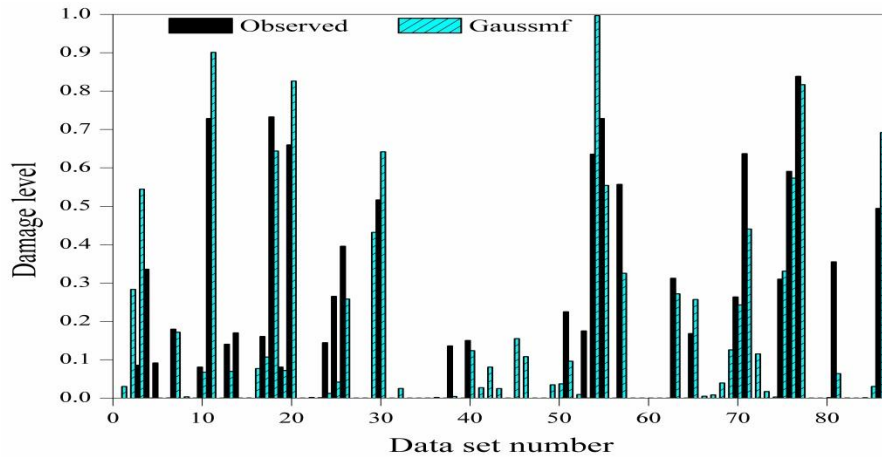


Fig. 6.6 Comparison of damage level prediction by SVM (RBF) with observed values

In terms of box plot statistics, the spread of data at lower and upper quartile of the box are predicted well in comparison with the observed. From Fig. 6.5, it is noticed that, Gbell and Gaussmf predictions match well with observed damage level among other membership functions where many outliers are found. Both box plot and scatter plots illustrations agree that, ANFIS model with Gaussmf is the best model. The efficiency of the best model is validated by presenting the findings in the form of comparison plot and is shown in Fig. 6.6. Out of all, the Gaussmf showed better results in predicting both the H_t/H_{tmax} and damage level. The predicted results of damage level by ANFIS model are scattered more compared to wave transmission, which is due to presence of more number of zero damage levels in the observed data set.

6.2.3 Summary of ANFIS model results

The performance of the ANFIS model in predicting H_t/H_{tmax} and damage level seems to be highly affected by hybridization of FIS with NN. The efficiency of the ANFIS model depends on the type and number of membership functions associated with each input data. The Gaussmf trains the model well before predicting the outputs in the testing phase. Even though results are not exactly matching the observed ones, but can be concluded as tool is efficient and reliable from the obtained results. Therefore, ANFIS can be used to predict the wave transmission and damage level with good correlation.

6.3 PERFORMANCE OF PSO-ANN MODEL FOR PREDICTING WAVE TRANSMISSION (H_t/H_{tmax}) AND DAMAGE LEVEL (S)

Regression analysis is conducted to predict both H_t/H_{tmax} and S by using PSO-ANN and

results are evaluated using different statistical measures such as RMSE, NSE, SI, CC, and box-whiskers plots. Based on the statistical parameters, accuracy of the model is tested. The predicted values are compared with the observed values by plotting the performance variation graph. The prediction will be considered as good when RMSE and SI is minimum ('0') while NSE and CC are maximum ('1').

In case of ANN hybrid model prediction, PSO function is called in place of an LM function by using PSORT and NN in the MATLAB software. The statistical parameters are calculated for various ANN hybrid models with varying size of the hidden neurons and the network with best predictions are considered as optimum. Table 6.3, shows the results of different statistical measures obtained by various ANN hybrid models for predicting transmitted wave heights (H_t/H_{tmax}) and damage level (S).

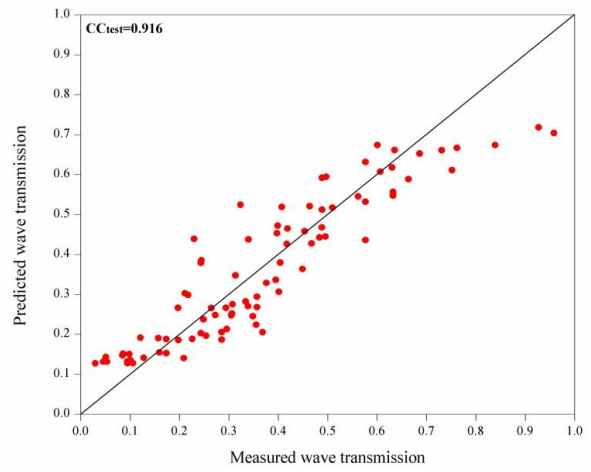
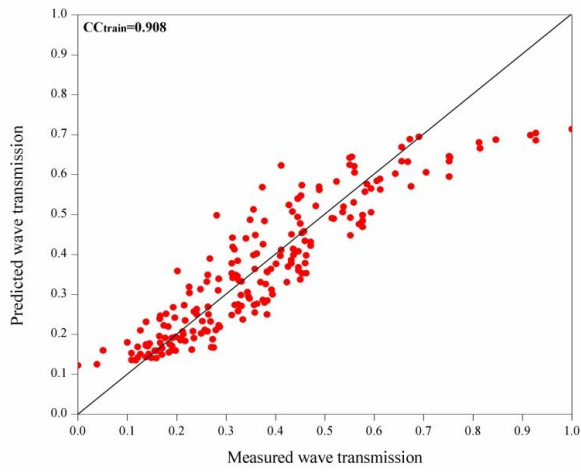
Table 6.3 Statistical parameters of PSO-ANN model predictions for H_t/H_{tmax}

Output	Models	Network	RMSE		C		SI		NSE	
			Train	Test	Train	Test	Train	Test	Train	Test
H_t/H_{tmax}	PSO-ANN1	8-1-1	0.079	0.084	0.908	0.916	0.213	0.232	0.821	0.835
	PSO-ANN2	8-2-1	0.080	0.081	0.904	0.921	0.216	0.224	0.817	0.846
	PSO-ANN3	8-3-1	0.065	0.072	0.940	0.941	0.176	0.199	0.879	0.879
	PSO-ANN4	8-4-1	0.081	0.082	0.903	0.918	0.218	0.228	0.814	0.841
	PSO-ANN5	8-5-1	0.077	0.080	0.912	0.925	0.207	0.222	0.832	0.849

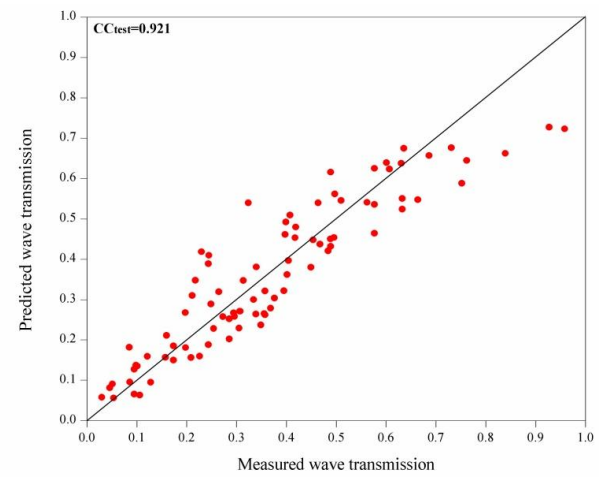
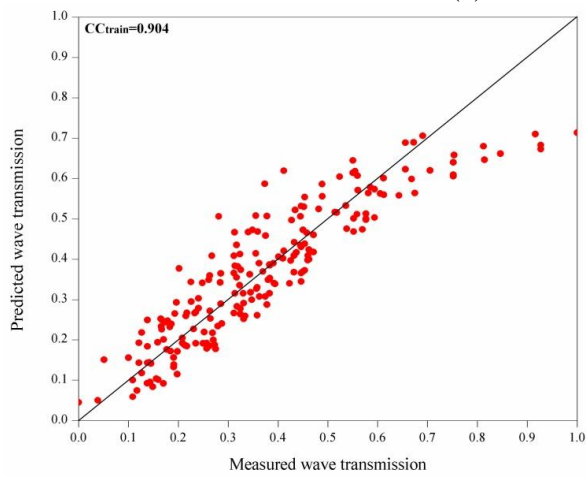
Table 6.4 Statistical parameters of PSO-ANN model predictions for damage level (S)

Output	Models	Network	RMSE		C		SI		NSE	
			Train	Test	Train	Test	Train	Test	Train	Test
S	PSO-ANN1	8-1-1	0.157	0.144	0.772	0.755	1.083	1.119	0.594	0.570
	PSO-ANN2	8-2-1	0.158	0.141	0.767	0.769	1.096	1.093	0.584	0.589
	PSO-ANN3	8-3-1	0.159	0.145	0.763	0.756	1.102	1.125	0.579	0.565
	PSO-ANN4	8-4-1	0.160	0.147	0.761	0.744	1.103	1.142	0.579	0.552
	PSO-ANN5	8-5-1	0.165	0.141	0.740	0.769	1.143	1.094	0.548	0.589

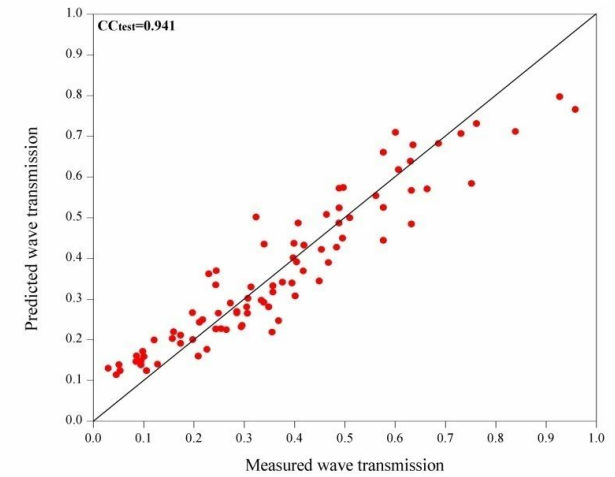
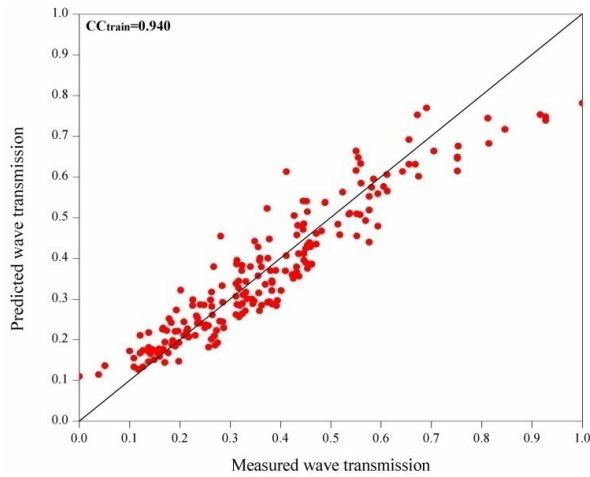
From Table 6.3, it can be seen that PSO-ANN3 model predicts the transmitted wave height better with $CC = 0.941$, $RMSE = 0.072$, $SI = 0.199$ and $NSE = 0.879$ for testing data. In case of damage level prediction PSO-ANN2 performs better with $CC = 0.769$, $RMSE = 0.141$, $SI = 1.093$ and $NSE = 0.589$ for testing data points as listed Table 6.4. It is observed that, damage levels obtained by PSO-ANN2 are poor compared wave transmission results by PSO-ANN3. This is due to the presence of more number of zero's in the data of damage levels. This represents that there is zero damage during physical model testing. Therefore, simulation results are displayed in the graphical form as a scatter plots between predicted and observed values of H_t/H_{tmax} in the Fig. 6.7.



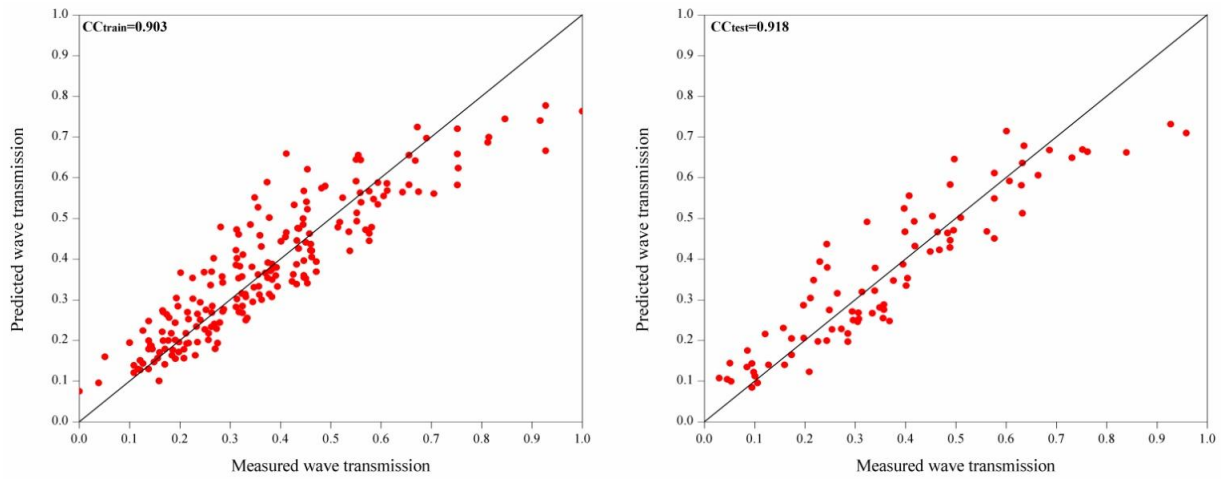
(a) PSO-ANN model with 8-1-1



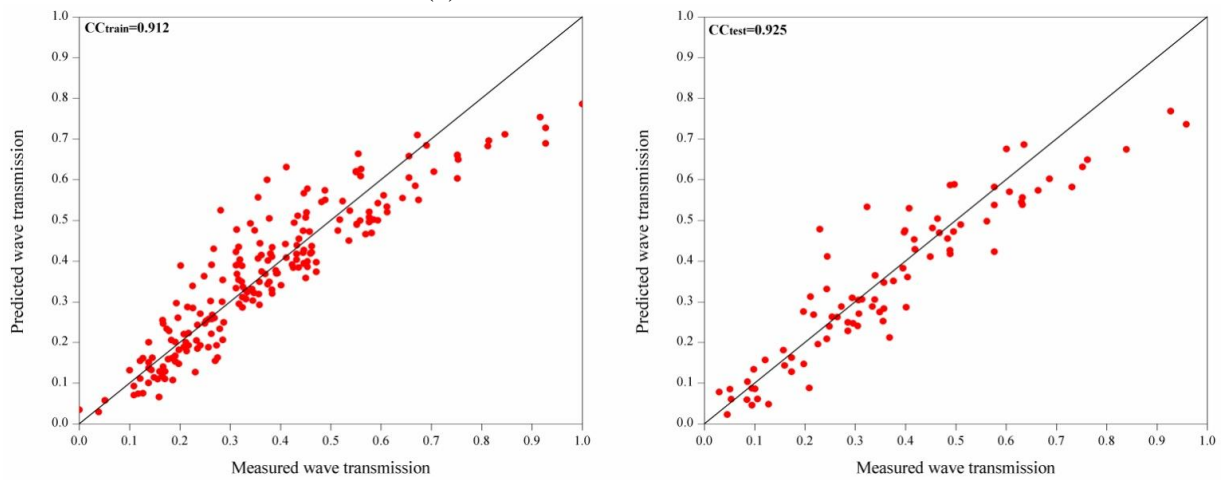
(b) PSO-ANN model with 8-2-1



(c) PSO-ANN model with 8-3-1



(c) PSO- ANN model with 8-4-1



(c) PSO- ANN model with 8-5-1

Fig. 6.7 Scatter plots of H_t/H_{tmax} by PSO-ANN model

It is observed that the scatter is less in Fig. 6.7(c) compared to Fig. 6.7(a), (b), (d) and (e). Similarly, in the prediction of damage level in the Fig. 6.10(b) showed good correlation with observed values whereas, Fig. 6.10(a), (c), (d) and (e) showed more scatter and poor correlation compared to Fig. 6.10(b). It can be summarized that, PSO-ANN3 with (8-3-1) network for H_t/H_{tmax} and PSO-ANN2 with (8-2-1) network for damage level gives the best results. These models can be used efficiently to predict the parameters effecting tandem breakwater stability.

The box plots statistics, is also a kind of measuring tool through which the variability of the predicted values with respect to observed data points, is identified to asses best model. In the Fig. 6.8, the ANN hybrid model with 2 and 4 hidden neurons show almost similar distribution of the predicted values of wave transmission of submerged reef with the observed values in both the lower and upper quartiles of the box plot. Similarly, the ANN

hybrid with 2 hidden neurons predicted damage level of the main breakwater successfully and are depicted in the Fig. 6.11.

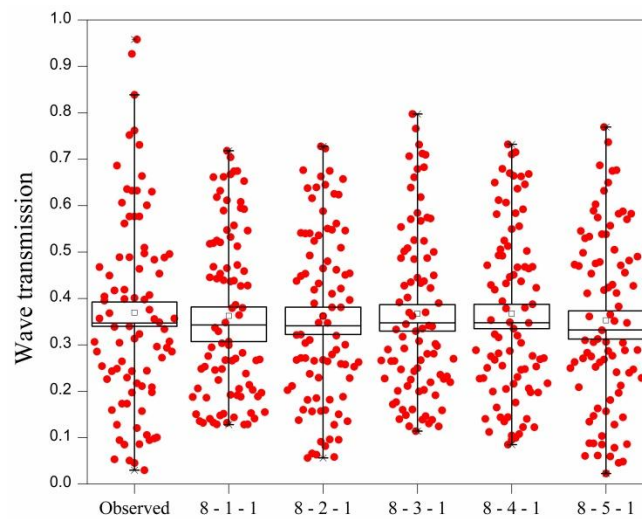


Fig. 6.8 Box-Whisker plots of wave transmission prediction by PSO-ANN with observed values

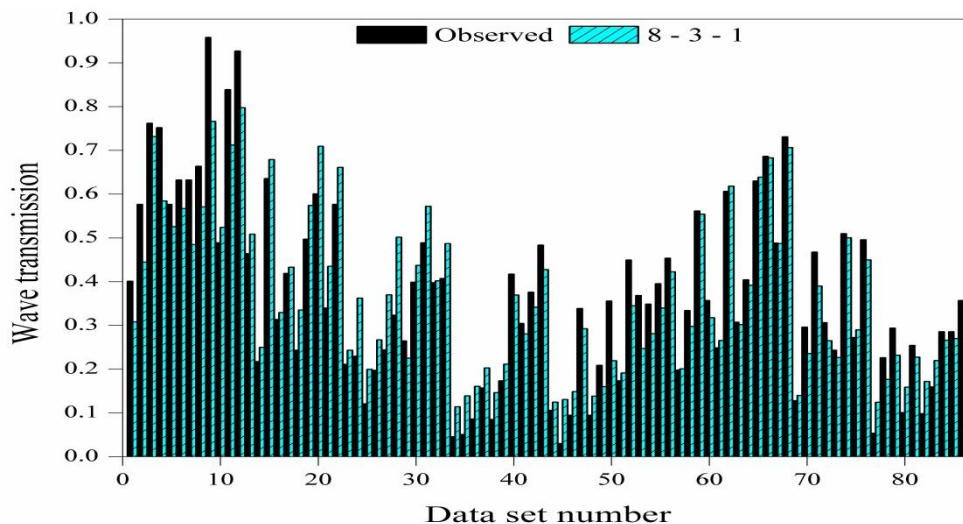
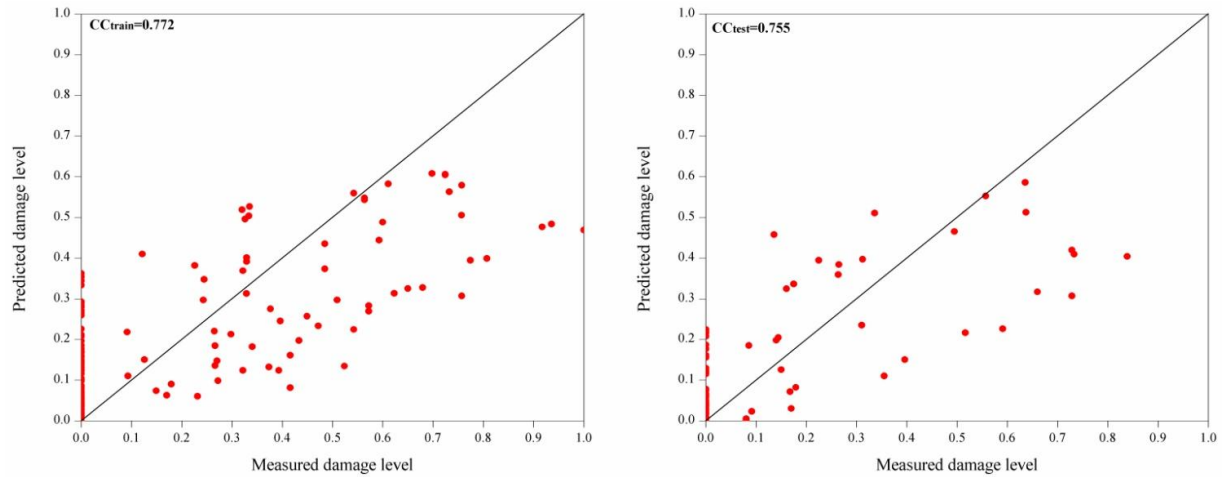


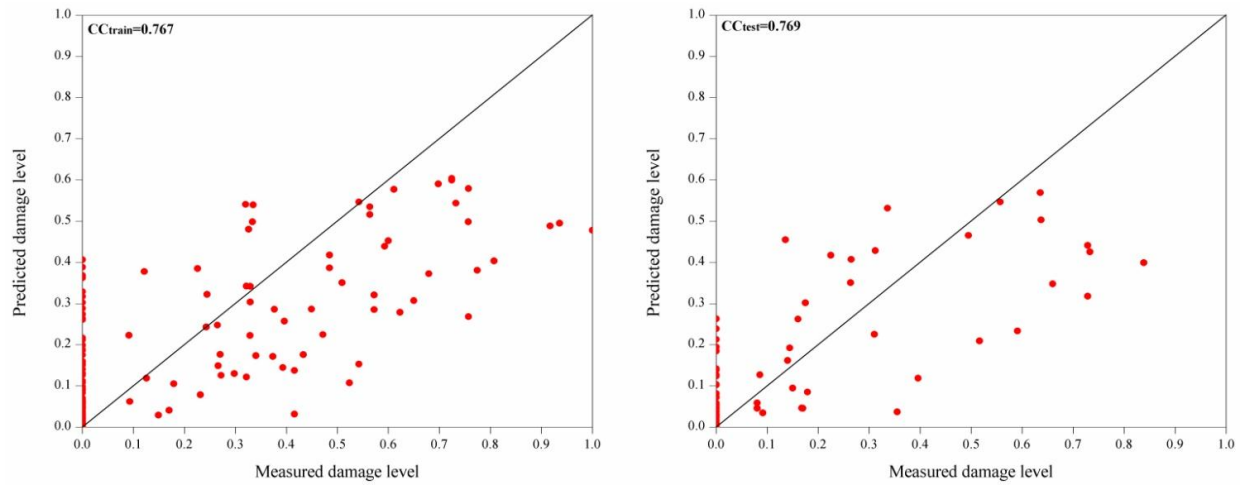
Fig. 6.9 Comparison of wave transmission predicted by PSO-ANN3 with observed values

Fig. 6.9 shows, the validation of PSO-ANN3 model for predicting wave transmission with respect to observed values in the form of comparison graph. Similarly, Fig. 6.12 shows the validation of PSO-ANN2 model performance in predicting damage level with respect to observed values in the form of comparison graph. It is observed that the prediction of PSO-ANN values match well with the observed values of wave transmission and damage level of tandem breakwater. Based on all the statistical measures and different plots, PSO-ANN3 technique can be considered as better model

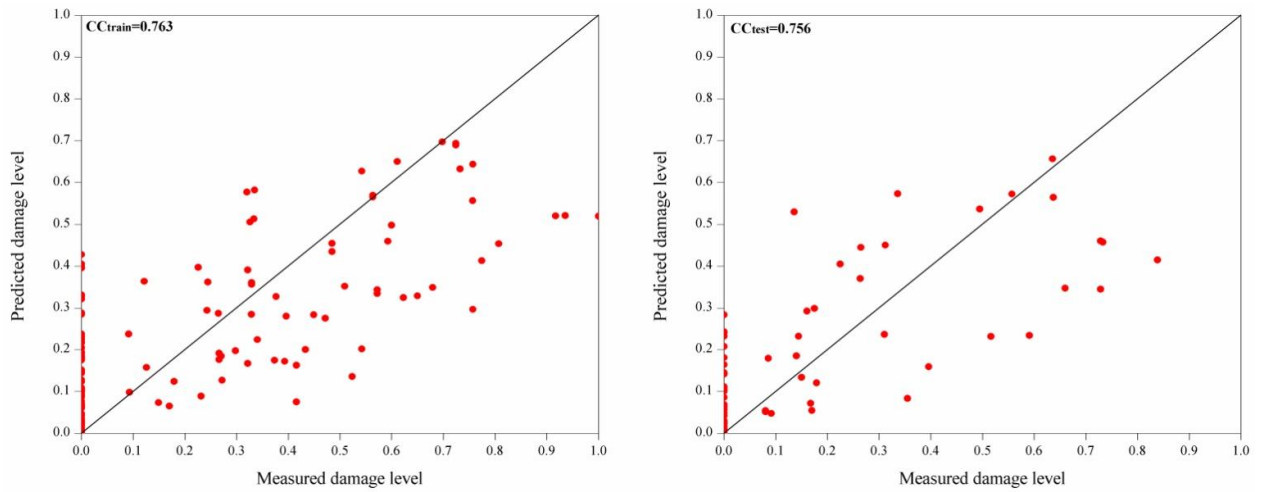
and can be used as an alternate method for prediction of wave transmission successfully for the immediate need or requirement for analysis if the sufficient or a large set of data is available. ANFIS with Gaussmf predicts the damage level better than PSO-ANN2. Hence, ANFIS with Gaussmf can be used as an alternate and reliable tool for damage level prediction.



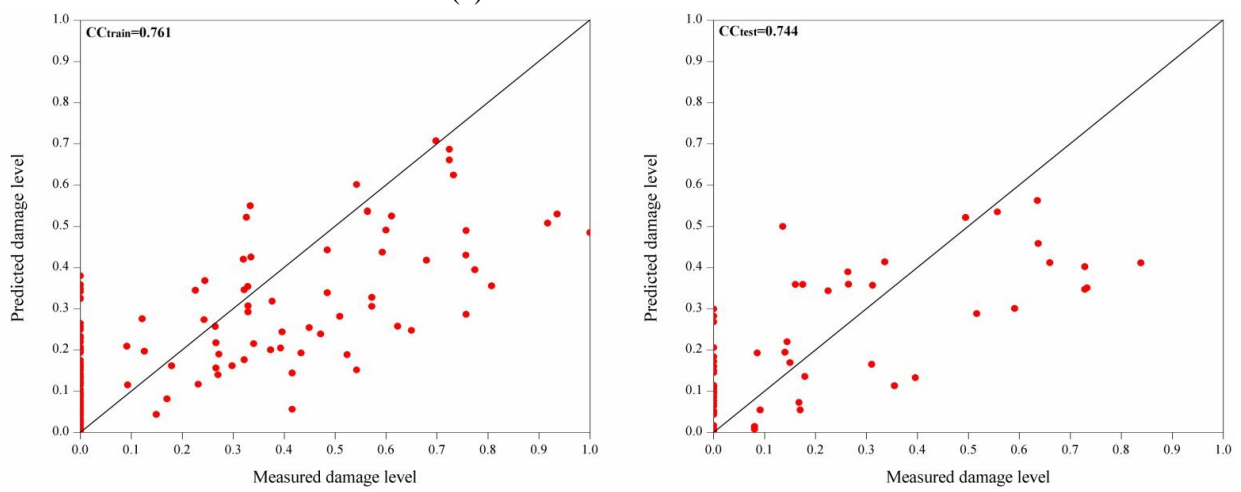
(a) PSO-ANN model with 8-1-1



(b) PSO-ANN model with 8-2-1



(c) PSO-ANN model with 8-3-1



(d) PSO-ANN model with 8-4-1

Fig. 6.10 Scatter plots for S for PSO-ANN hybrid models

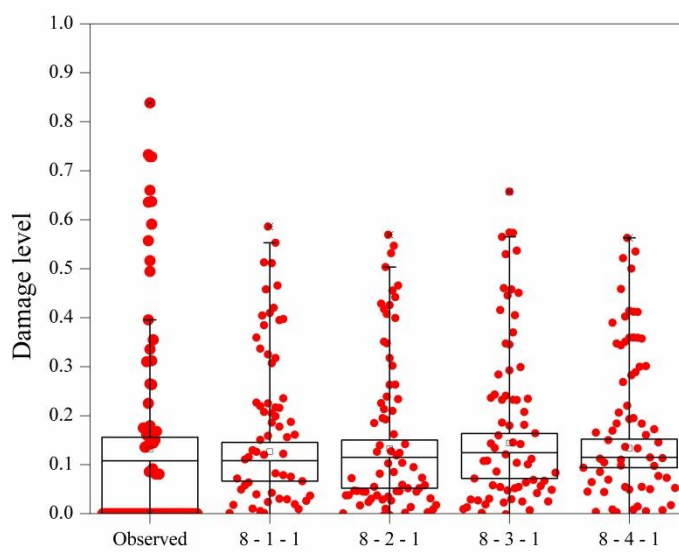


Fig. 6.11 Box-Whisker plots of damage level prediction for different PSO-ANN models

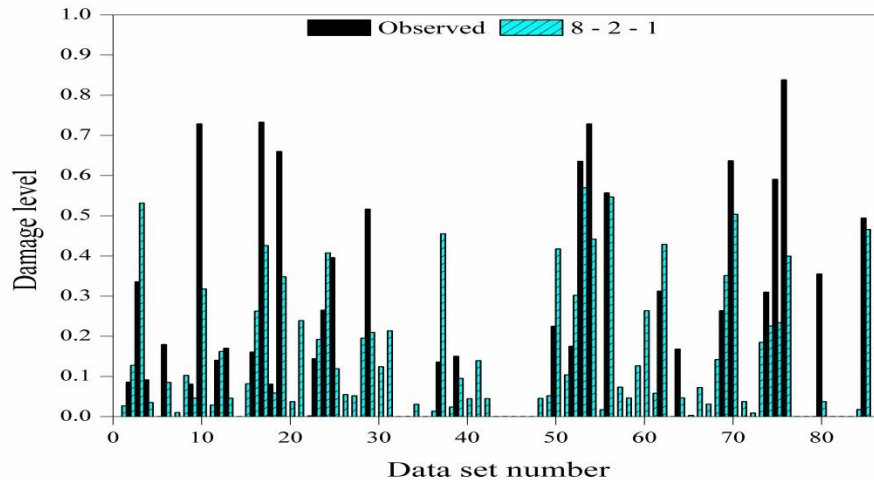


Fig. 6.12 Comparison of damage level predicted by PSO-ANN2 with observed values

6.3.1 Summary of PSO-ANN model results

PSO-ANN with various numbers of hidden neurons is attempted, for selecting the efficient ANN hybrid model using different statistical measures. The results obtained by PSO-ANN3 and PSO-ANN2 models show that, the soft computing techniques can be applied successfully for the prediction of wave transmission over submerged reef and damage level of conventional rubble mound breakwater of tandem breakwater.

6.4 PERFORMANCE OF PSO-SVM MODEL FOR PREDICTION OF WAVE TRANSMISSION AND DAMAGE LEVEL OF TANDEM BREAKWATER

The performance of PSO-SVM model depends on the good setting of SVM parameters such as regularization parameter C and ε with kernel parameters γ and d . Initially the upper and lower bound values of SVM parameters and kernel widths are given as input (i.e. for $C \in [1, 5000]$; $\varepsilon \in [0.000001, 1]$; $\gamma \in [0.01, 5]$ and $d \in [2, 5]$). In the next stage, the marginal difference in range between upper and lower bound values of the SVM parameters are reduced such that both should have in close proximity to the optimal parameter value obtained initially (i.e. for $C \in [(1, 500), (500, 1000), \dots, (4500, 5000)]$; $\varepsilon \in [(0.000001, 0.00001), (0.00001, 0.0001), \dots, (0.1, 1)]$; $\gamma \in [(0.01, 1), (1, 2), \dots, (4, 5)]$ and $d \in [(2, 3), \dots, (4, 5)]$). In associated with such various trials the optimal parameters are obtained and corresponding to that models are developed using linear, polynomial and RBF kernel functions. For each model developed, statistical indicator values such as CC, RMSE, NSE and SI are calculated as evaluation criteria. The kernel function

best suited for the SVM hybrid model is finally determined by evaluating the values of statistical measures obtained as model performance indicators.

The effectiveness and efficiency of the model results obtained during simulation depends upon the proper selection of SVM parameters (C , ϵ) and kernel parameters (γ , d), which can be obtained using particle swarm optimization. Initially, random range of values is provided for the parameters within the range given by software documentation. From the range given the parameter values corresponding to that the best fitness is achieved, and is found by particle searching. If the value selected at random from the range provided does not satisfy the fitness function, then the loop continues with the next available value in the given input.

6.4.1 Simulation results of PSO-SVM model for predicting wave transmission (H_t/H_{tmax}) over submerged reef and damage level (S) of emerged breakwater of tandem breakwater

The prediction of transmitted wave heights over a submerged reef of the tandem breakwater is conducted by considering the 8 inputs variables H_i/gT^2 , X/d , $H_i/\Delta D_{n50}$, B/d , B/L_o , F/H_i , h/d , d/gT^2 which influence the output H_t/H_{tmax} . The training of the model is carried out for 201 data points (70%) and then testing is done by considering 87 data points (30%), for validation of the model prediction.

Initially, for a particular kernel type, PSO-SVM model is developed and among them the one which shows best data fitting is adopted as the best model for the corresponding kernel function. The model that shows the best data fitting is found out by evaluating the statistical parameters. Figs. 6.13, 6.14 and 6.15 depicts the data fitting curves for PSO-SVM models developed using linear, polynomial and RBF kernel functions, respectively using set of testing data. In each figure, it can be observed that predicted value fits better with actual value for specific values of C , ϵ , γ and d . From Fig.6.13, the best fitting curve corresponds to the model having $C = 1500$ and $\epsilon = 0.0885$ which shows the data fitting the predicted values with observed values. Similarly, $C = 183.78$, $\epsilon = 0.0000538$, $d = 3$ and $C = 18.7$, $\epsilon = 0.0827$, $\gamma = 2.6$ are parameter values corresponding to the best fitting curves for Figs. 6.14 and 6.15 respectively obtained by proposed SVM algorithm.

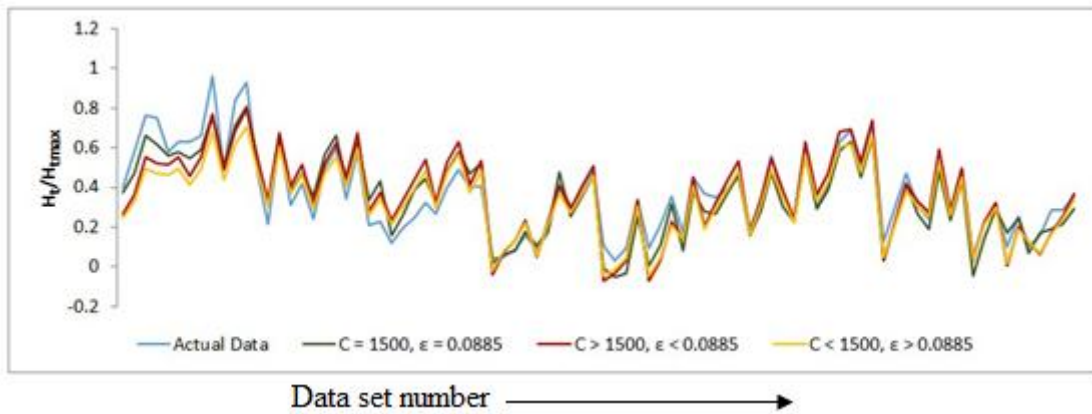


Fig. 6.13 Data fitting of models developed (linear kernel) for prediction of H_t/H_{tmax}

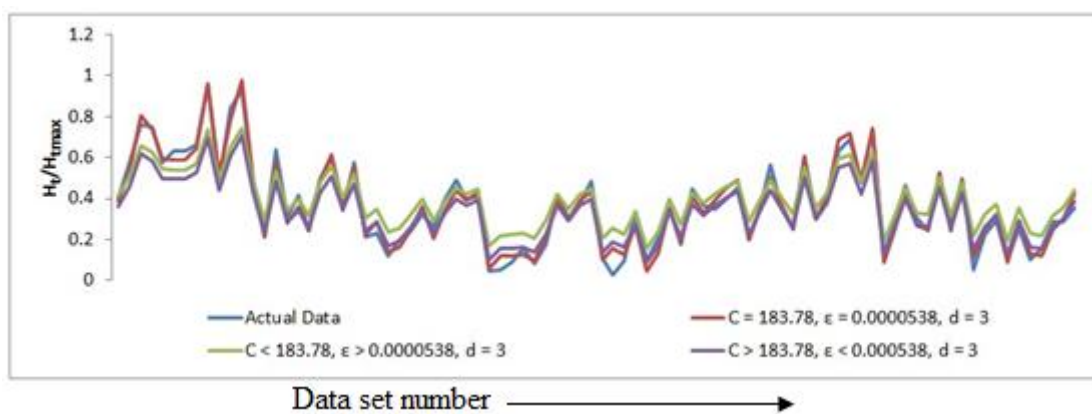


Fig. 6.14 Data fitting of models developed (polynomial) for prediction of H_t/H_{tmax}

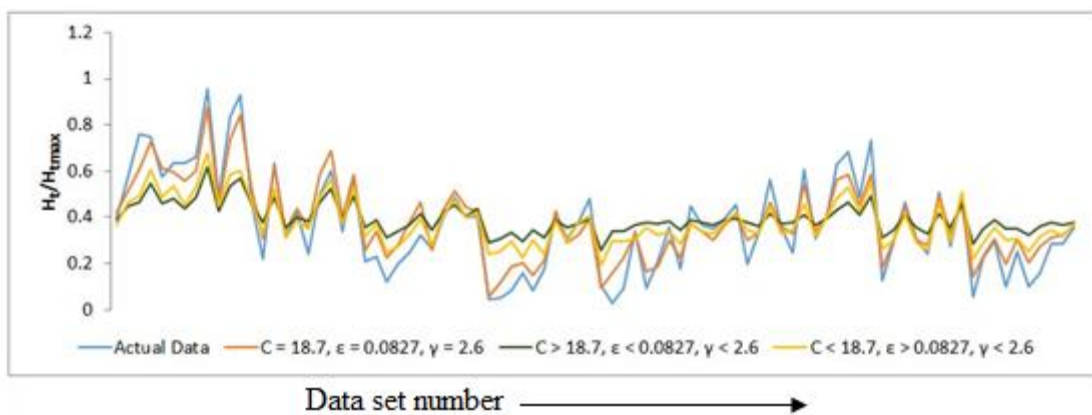


Fig. 6.15 Data fitting of models developed (RBF kernel) for prediction of H_t/H_{tmax}

For the prediction of transmitted wave height, optimal parameters of SVM with linear, polynomial and RBF kernel parameters are obtained using PSO as an optimization searching algorithm. In case of RBF kernel function, the optimal width (γ) is found to be 2.6 and the optimal values of d (degree) in case of polynomial kernel function is 3, as listed in Table 6.5. The optimal parameters obtained are used by the SVM model to predict the transmitted wave height. Thus, the effectiveness, reliability and accuracy of

the model developed are evaluated by calculating the statistical measures as presented in the Table 6.6.

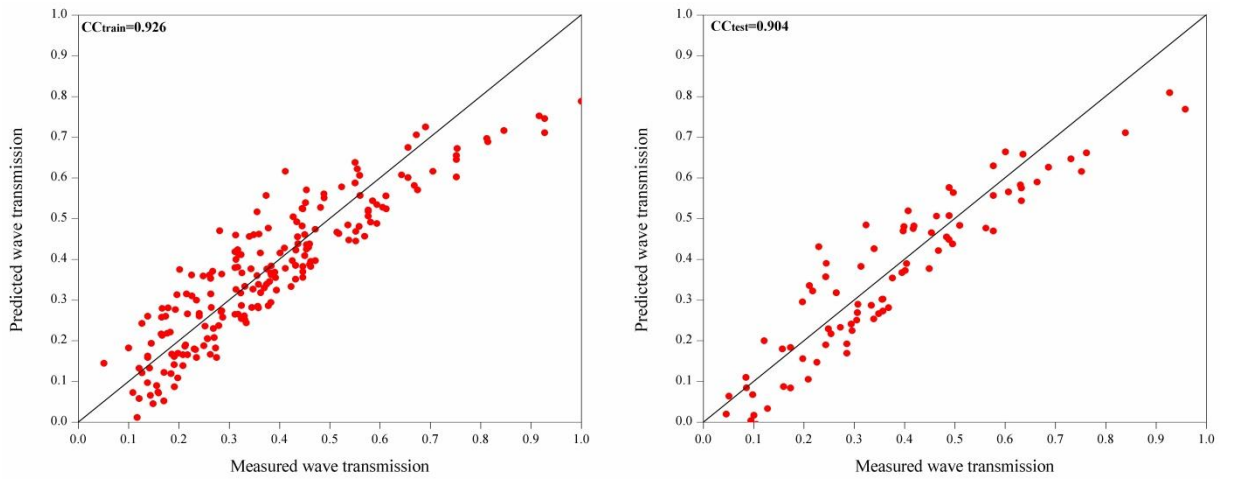
Table 6.5 Optimal parameters for PSO-SVM models for predicting H_t/H_{tmax}

Kernel type	Linear	Polynomial	RBF
C	1500	183.78	18.7
ϵ	0.0885	0.0000538	0.0827
γ	-	-	2.6
d	-	3	-

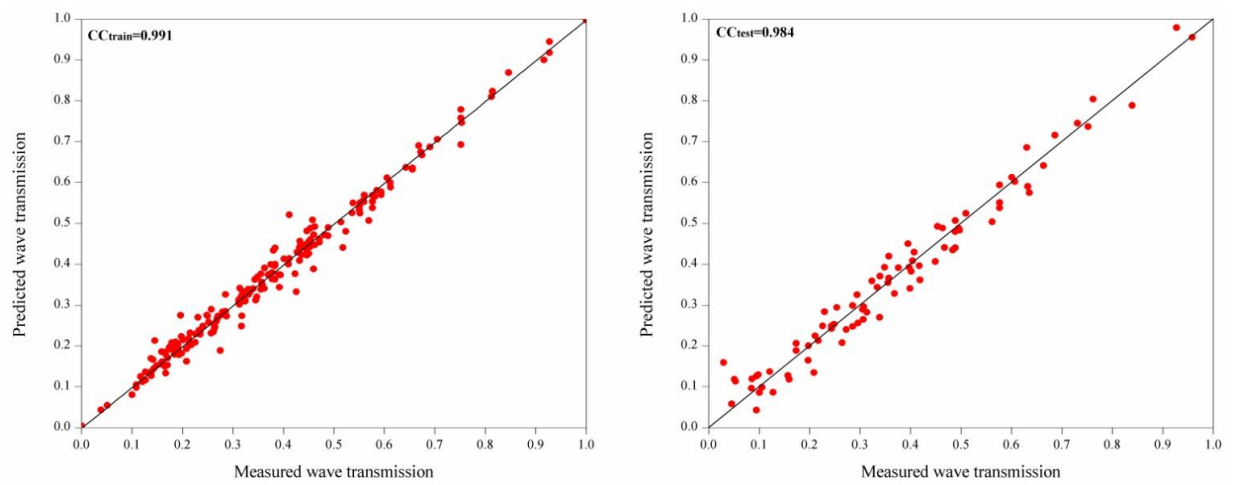
Table 6.6 Statistical parameters for PSO-SVM models for predicting H_t/H_{tmax}

Kernel type	Linear		Polynomial		RBF	
	Train	Test	Train	Test	Train	Test
CC	0.926	0.904	0.991	0.984	0.969	0.960
RMSE	0.077	0.081	0.025	0.037	0.051	0.068
SI	0.217	0.217	0.088	0.102	0.138	0.184
NSE	0.853	0.819	0.982	0.968	0.926	0.894

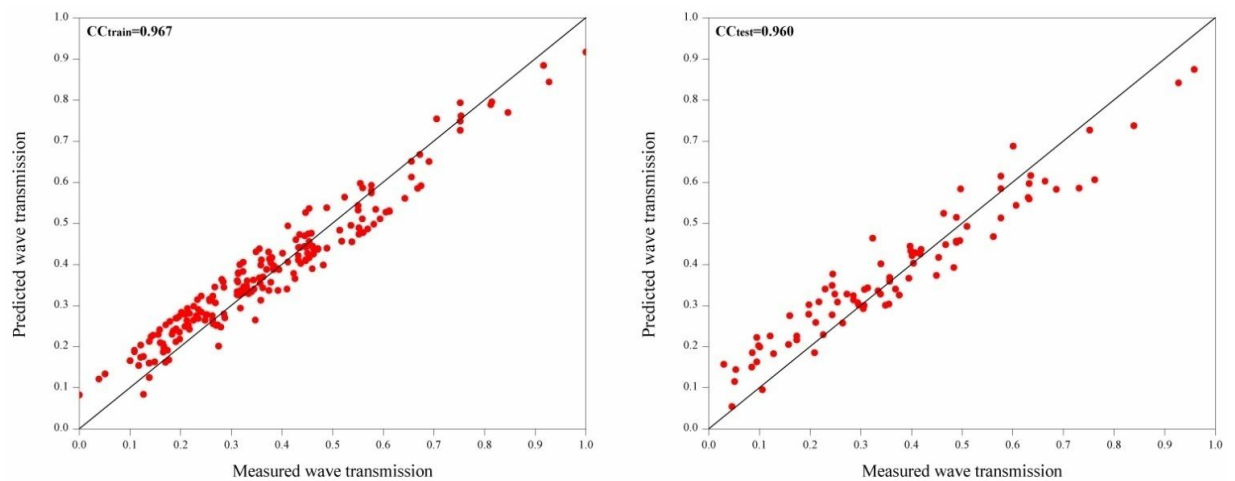
The RMSE=0.037 obtained for testing model for polynomial kernel function is comparatively less than other kernel functions. SI=0.102 value for polynomial kernel function indicates the good correlation and least scattering from actual fitted data. NSE=0.968 for polynomial kernel function indicates the predictive efficiency of PSO-SVM. From all the results obtained, it is observed that PSO-SVM model with polynomial kernel function shows better generalization performance with values of CC=0.984, RMSE=0.037, SI=0.102, NSE=0.968 testing data points, when compared with other kernel functions. The scatter diagram which shows the CC of the models for the training and testing data using various kernels are shown in Fig. 6.16.



a) Linear kernel



b) Polynomial kernel function



(c) RBF kernel function

Fig. 6.16 Scatter plots of PSO-SVM model for H_t/H_{tmax} with observed data

From the scatter plots, it is noticed that, PSO-SVM model using polynomial kernel function gives the best data fitting between predicted and observed data. The box plots

are another type of statistical measures in which the variability of the predicted data is found with reference to observed data and is depicted in the discussion. Fig. 6.17 indicates box plot with the upper and lower quartile values predicted is matching well with the observed wave transmission over submerged reef. SVM model with polynomial kernel, predicted data points are distributed well in the lower quartile of the box plot with reference to the observed values.

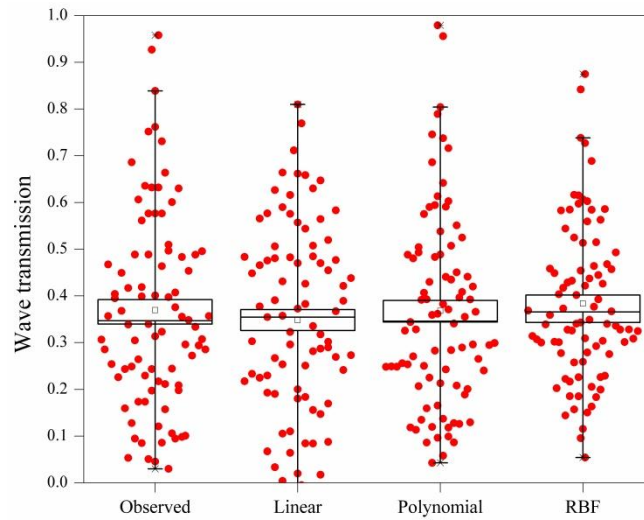


Fig. 6.17 Box-Whiskers plot of H_t/H_{tmax} for PSO-SVM model

The validation of PSO-SVM model using polynomial kernel function for the prediction of wave transmission is shown in Fig. 6.18, using the comparison graph. From the graph, it is clearly noticed that, the predicted data follows similar trend compared to observed data. Even though model developed with RBF kernel function provides results with high correlation, for both training and testing. PSO-SVM model using polynomial kernel function gives 4.36% improved correlation, 48.61% reduced RMSE, SI and maximum NSE value is found to be the best model for prediction of transmitted wave height over submerged reef of a tandem breakwater.

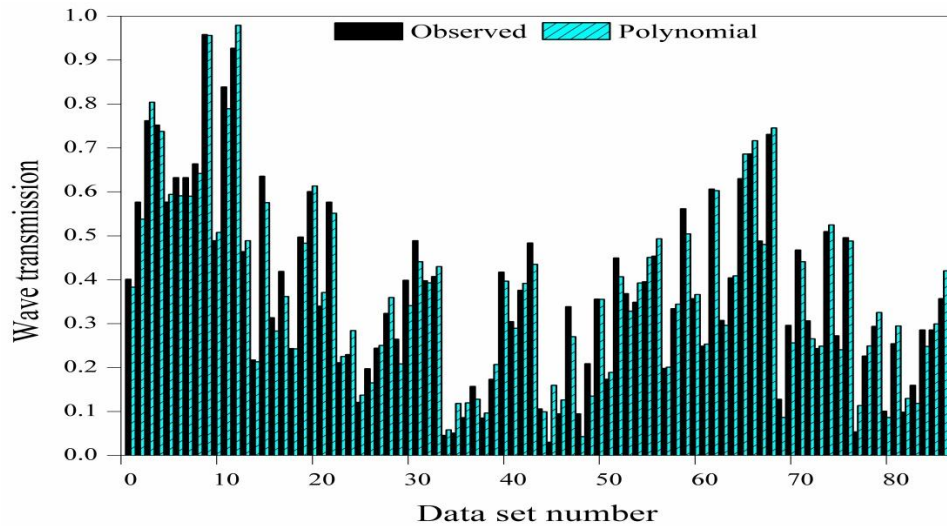


Fig. 6.18 Comparison of PSO-SVM model (polynomial kernel) for H_t/H_{tmax} with observed values

6.4.2 Simulation results of PSO-SVM model for predicting damage level (S) of Conventional rubble mound breakwater of tandem breakwater

The prediction of damage level of the emergent conventional rubble mound breakwater of the tandem breakwater is performed by considering the 8 inputs H_i/gT^2 , X/d , $H_i/\Delta D_{n50}$, B/d , B/L_o , F/H_i , h/d , d/gT^2 influencing the dependent variable damage level (S). The training is carried out using 202 data points (70%) and testing is done for 86 data points (30%). Figs. 6.19, 6.20 and 6.21 depicts the data fitting curves of PSO-SVM models developed for damage level prediction using linear, polynomial and RBF kernel functions, respectively, for testing. In each figure, it is observed that predicted value fits better with actual value for specific values of C , ϵ , γ and d . From the Fig. 6.19, the best fit curve corresponds to the model having (linear kernel) $C = 1327.67$ and $\epsilon = 0.0069$. Similarly, $C = 547$, $\epsilon = 0.0356$, $d = 3$ and $C = 363.83$, $\epsilon = 0.0000228$, $\gamma = 3.2$ are parameter values corresponding to the best fitting curves for Figs. 6.20 and 6.21 respectively.

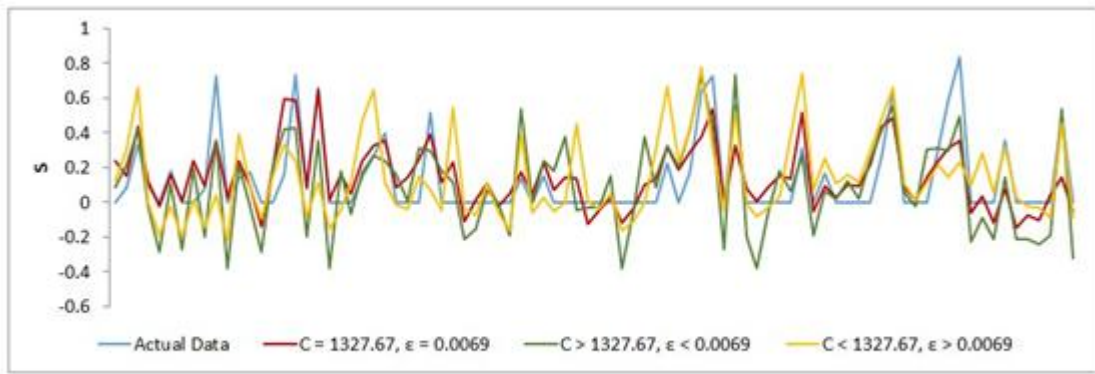


Fig. 6.19 Data fitting of models developed (linear) for prediction of Damage level

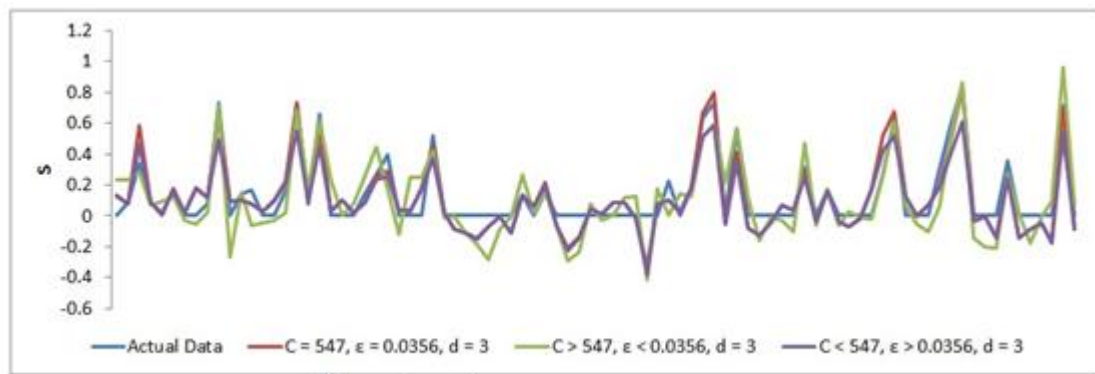


Fig. 6.20 Data fitting of models developed (polynomial) for prediction of damage level

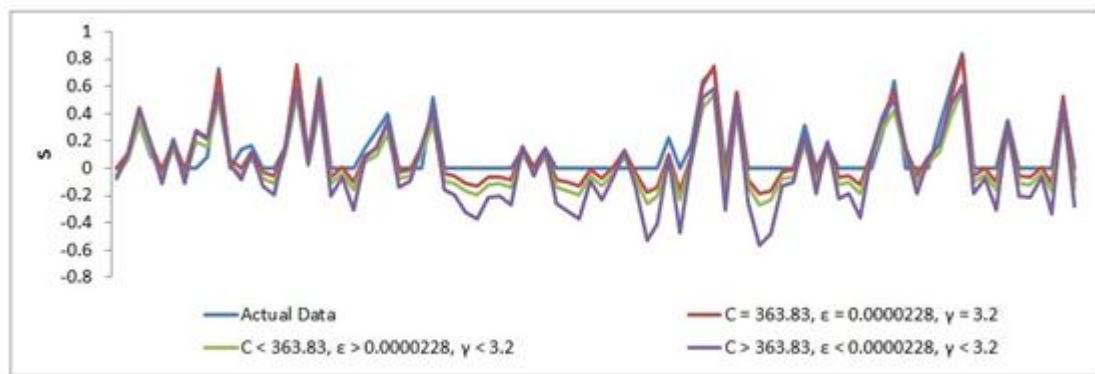


Fig. 6.21 Data fitting of models developed (RBF) for prediction of damage level

Optimal values of SVM and kernel function parameters, obtained using PSO for damage level prediction using linear, polynomial and RBF kernel based models are shown in Table 6.7. The optimal values of the parameters are used by the model in

prediction of damage level of conventional rubble mound breakwater of tandem breakwater. In case of RBF kernel, the optimal width (γ) is found to be 3.2 and the optimal values of d (degree) in case of polynomial kernel function is 3 and effectiveness of the model developed in prediction of damage level is evaluated by calculating the value of statistical parameters.

Table 6.7 Optimal parameters for PSO-SVM models for predicting Damage levels

Kernel type	Linear	Polynomial	RBF
C	1327.6	547	363.83
ϵ	0.0069	0.0356	0.000022
γ	-	-	3.2
d	-	3	-

Model performance indicators of models developed using linear, polynomial and RBF kernels for training and testing are given in Table 6.7. The PSO-SVM model with RBF kernel function gives better correlation of CC = 0.941 for testing compared to all other kernel functions.

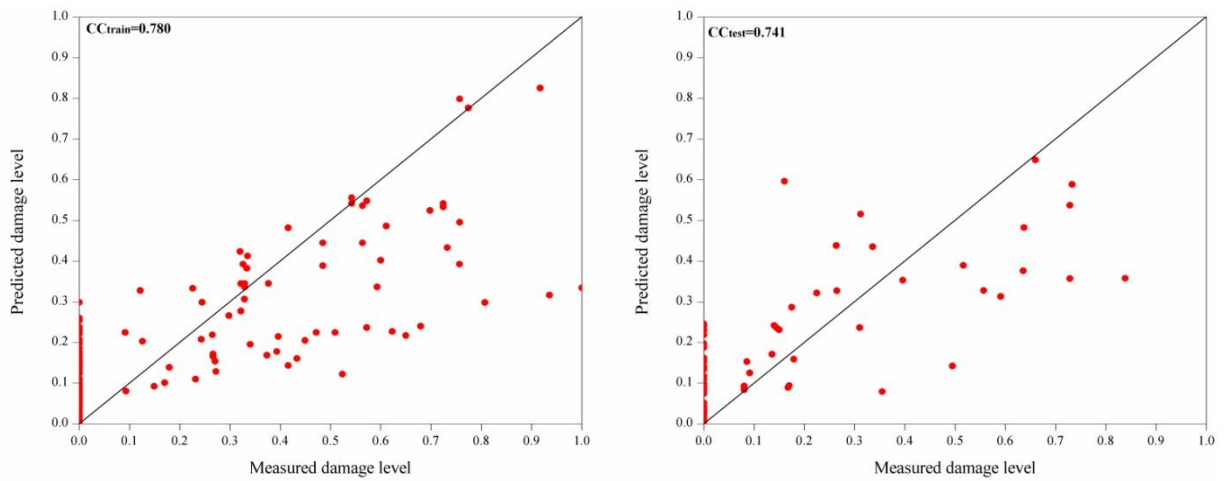
The value of RMSE=0.088 for testing is comparatively lower for developed model using RBF kernel function compared to rest of the kernel functions. This indicates that the predicted data is closer to actual data for RBF kernel function.

Table 6.7 Statistical parameters for PSO-SVM models for predicting Damage levels

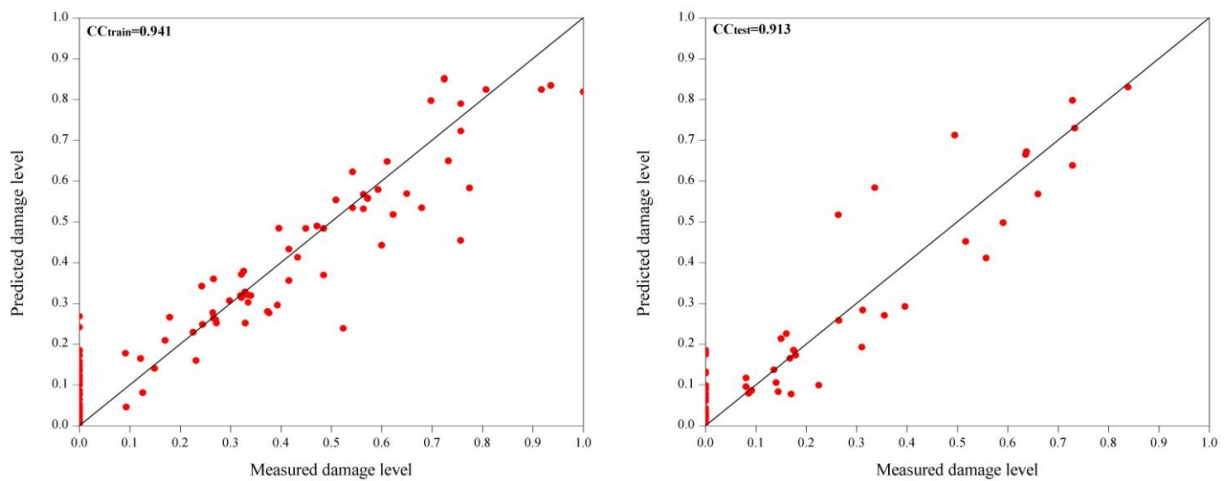
Kernel type	Linear		Polynomial		RBF	
	Train	Test	Train	Test	Train	Test
CC	0.780	0.741	0.941	0.913	0.961	0.941
RMSE	0.154	0.161	0.085	0.099	0.071	0.088
SI	1.067	1.143	0.584	0.756	0.493	0.669
NSE	0.605	0.541	0.882	0.799	0.916	0.843

SI = 0.669 for RBF kernel function indicates the least scattering from actual fitted data compared to 1.143 and 0.756 during testing phase for linear and polynomial kernel functions respectively. NSE value of 0.843 for RBF kernel function compared to 0.541 and 0.799 during testing for linear and polynomial kernels, respectively, indicates the predictive efficiency of model developed using RBF kernel function. Finally, PSO-SVM model with RBF kernel function shows better error generalization performance

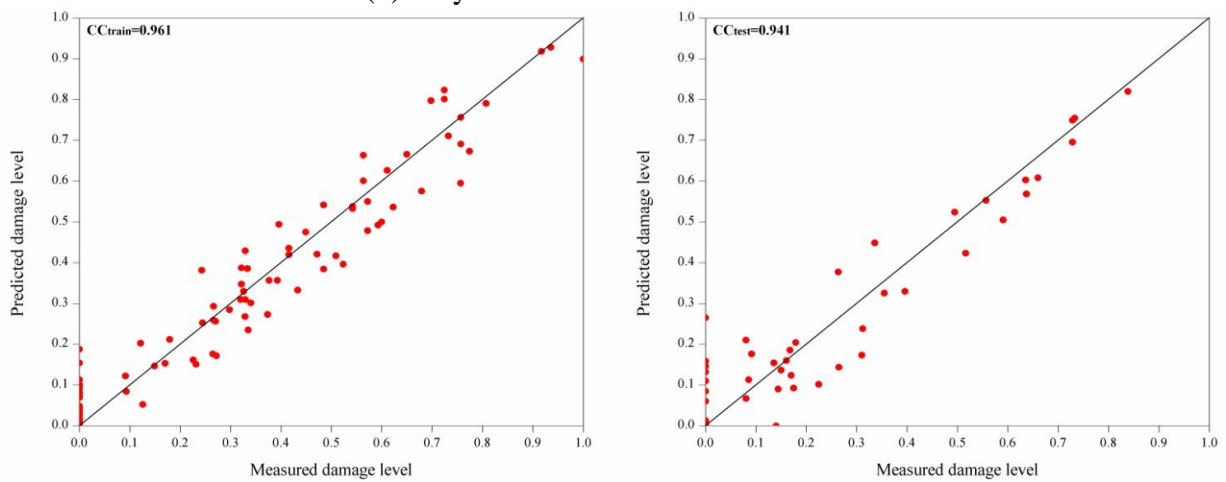
with $CC = 0.941$, $RMSE = 0.088$, $SI = 0.669$ and $NSE = 0.843$ testing, when compared to the rest of the kernel functions. The scatter diagram showing CC of PSO-SVM models for the training and testing data are shown in Fig. 6.22



(a) Linear kernel function



(b) Polynomial kernel function



(c) RBF kernel function

Fig. 6.22 Scatter plots of damage level (S) prediction using SVM model with different kernel functions

From the scatter plots, it is clear that, PSO-SVM model using RBF kernel function gives the best data fitting between predicted data and observed data. The box plot statistics is also used to measure the performance of the PSO-SVM model with different kernel. In terms of box plot assessment of predicted S in respect to observed data points is shown in Fig. 6.23. In the plots spread of predicted values by RBF shows the similar pattern and closely related to the observed values in terms of upper and lower quartile distribution of RBF prediction. Based on the scatter and box plots statistics, PSO-SVM model with polynomial and RBF kernel functions predicts successfully with high accuracy compared to the all other models, can be used as best alternate to predict the wave transmission over submerged reef and damage level of main breakwater of tandem breakwater respectively.

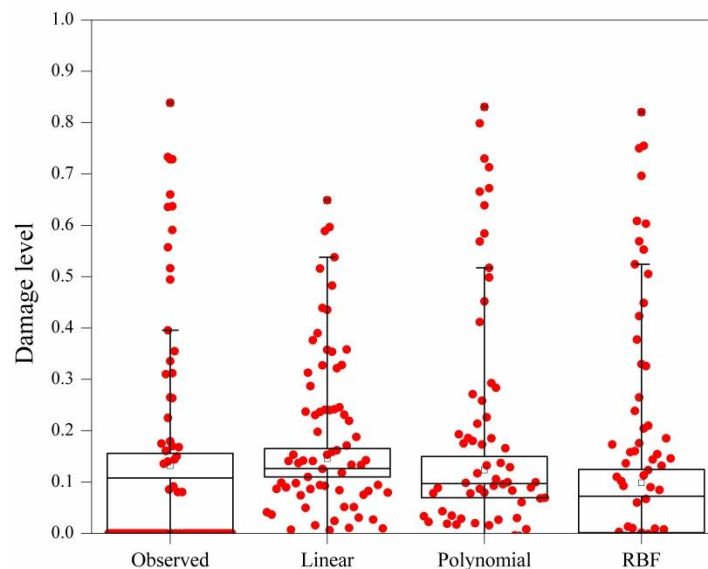


Fig. 6.23 Box-Whiskers plots of damage level (S) for PSO-SVM model

The model developed using linear kernel function gives the least correlation ($CC = 0.741$ for testing) which indicates that the data cannot be separated by a linear hyperplane in a low dimensional space. Fig. 6.24 shows the performance of observed and predicted damage level by PSO-SVM for RBF kernel function. Observing the graph, the PSO-SVM model with RBF kernel function is showing similar pattern compared to actual data with fluctuations are comparatively more around values of $S = 0$. Even though models developed with polynomial kernel function provides results with 83% correlation for both training and testing, the PSO-SVM model using RBF kernel function with 88% correlation, minimum RMSE, SI and maximum NSE value is found to be the best model in prediction of damage level of emergent main breakwater of tandem breakwater.

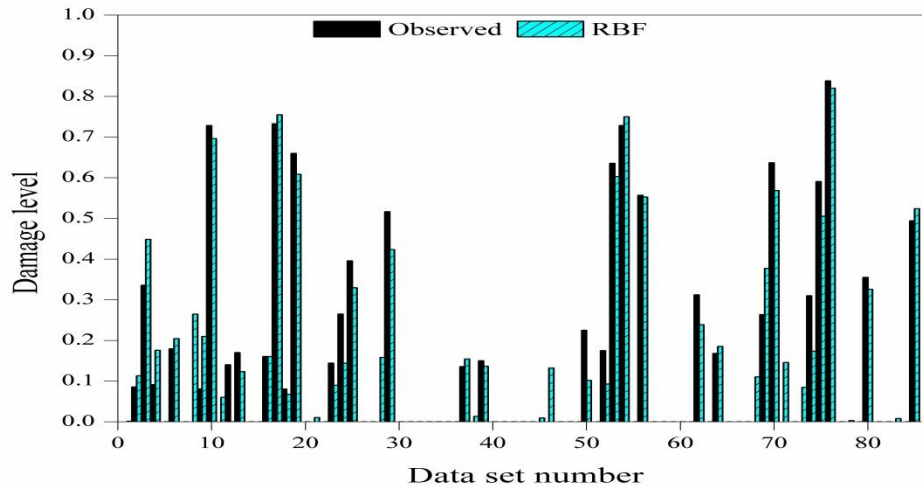


Fig. 6.24 Comparison of damage level predicted by PSO-SVM model (RBF) with observed values

6.4.3 Summary of PSO-SVM model results

Soft computing techniques provide results within a smaller time frame compared to mathematical and physical modeling. The complex nature of mathematical modeling and more expense involved in physical modeling makes soft computing technique a better alternate option for the prediction of transmitted wave height and damage level. As soft computing models are developed based on experimental data, it is essential to have physical model study so as to quantitatively determine the parameters influencing the performance of breakwaters. Therefore, physical model study along with the application of soft computing techniques employed to have effective and faster results. Different soft computing techniques such as ANN, SVM, ANFIS, etc. are successfully used for the prediction of wave parameters as discussed earlier. In this context, effectiveness of model developed for prediction depends on the proper selection of parameters. In this study, an effort is made to check the applicability of PSO-ANN and PSO- SVM model for predicting transmitted wave height and damage level of a tandem and the results are found to be satisfactory and reliable.

6.5 COMPARISON OF PERFORMANCE OF BEST ANN, SVM, ANFIS, PSO-ANN AND PSO-SVM MODELS

The results obtained using individual models have been discussed in previous sections. In this section a comparison of all the selected models have been made to know the best model that could predict wave transmission and damage level of tandem breakwater

accurately. For the given data set, ANN, ANFIS, SVM, PSO-ANN and PSO-SVM models are trained and tested to predict the wave transmission and damage level of tandem breakwater. The ANN (8-3-1), SVM (RBF), ANFIS (Gaussmf), PSO-ANN (8-3-1) and PSO-SVM (polynomial) models performed better among all the soft computing models considered for predicting wave transmission over a submerged reef of tandem breakwater in terms of statistical measures with respect to experimental values are listed in Table 6.9. Similarly, ANN (8-5-1), SVM (RBF), ANFIS (Gaussmf), PSO-ANN (8-2-1) and PSO-SVM (RBF) models performed better among all the soft computing models considered for predicting damage levels of conventional rubble mound breakwater of tandem breakwater in terms of statistical measures with respect to experimental values are listed in the Table 6.10.

Figs. 6.25 and 6.26 illustrate the comparison of wave transmission predicted by ANN with (8-3-1) and SVM with RBF kernel function with respect to experimental values of individual models. Similarly, Figs. 6.27 and 6.28 represent PSO-ANN with (8-3-1) and PSO-SVM with polynomial kernel function with respect to experimental values of hybrid models. ANN with (8-3-1) network outperformed all other soft computing techniques for predicting wave transmission with high CC of 0.989 and high efficiency of 0.978 with least error of 0.031 and small scatter of 0.086. Therefore, ANN with (8-3-1) network can be used as an efficient and reliable soft computing technique for predicting wave transmission over a submerged reef of a tandem breakwater.

Table 6.9 Comparison of Statistical Measures of ANN, SVM, ANFIS, PSO-ANN and PSO-SVM Models for wave transmission (H_t/H_{tmax})

Model	Training Data				Testing Data			
	CC	RMSE	SI	NSE	CC	RMSE	SI	NSE
ANN(8-3-1)	0.988	0.029	0.078	0.976	0.989	0.031	0.086	0.978
SVM (RBF)	0.977	0.055	0.151	0.92	0.965	0.056	0.150	0.911
ANFIS (Gaussmf)	0.99	0.0017	0.006	0.99	0.935	0.075	0.002	0.869
PSO-ANN (8-3-1)	0.940	0.065	0.176	0.88	0.941	0.072	0.199	0.879
PSO-SVM (Polynomial)	0.969	0.051	0.138	0.926	0.960	0.068	0.184	0.894

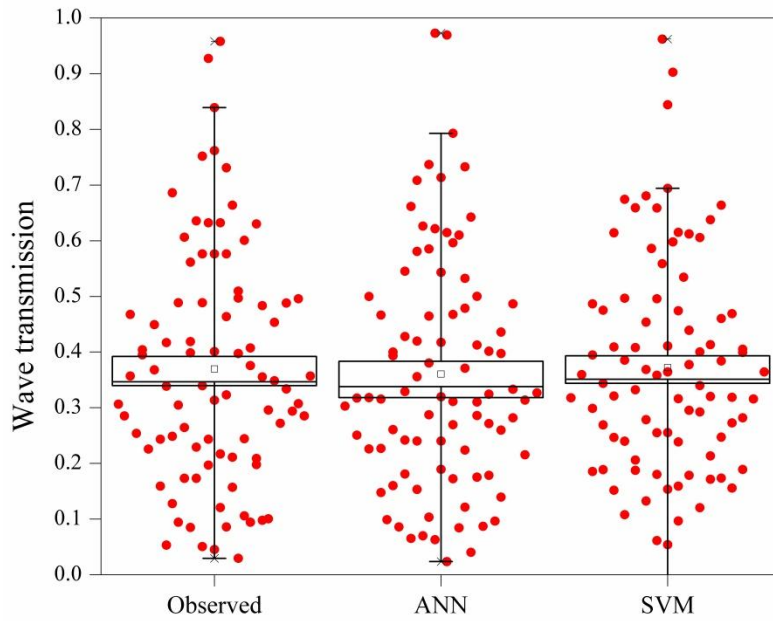


Fig. 6.25 Box-Whisker plot for wave transmission comparison of individual models

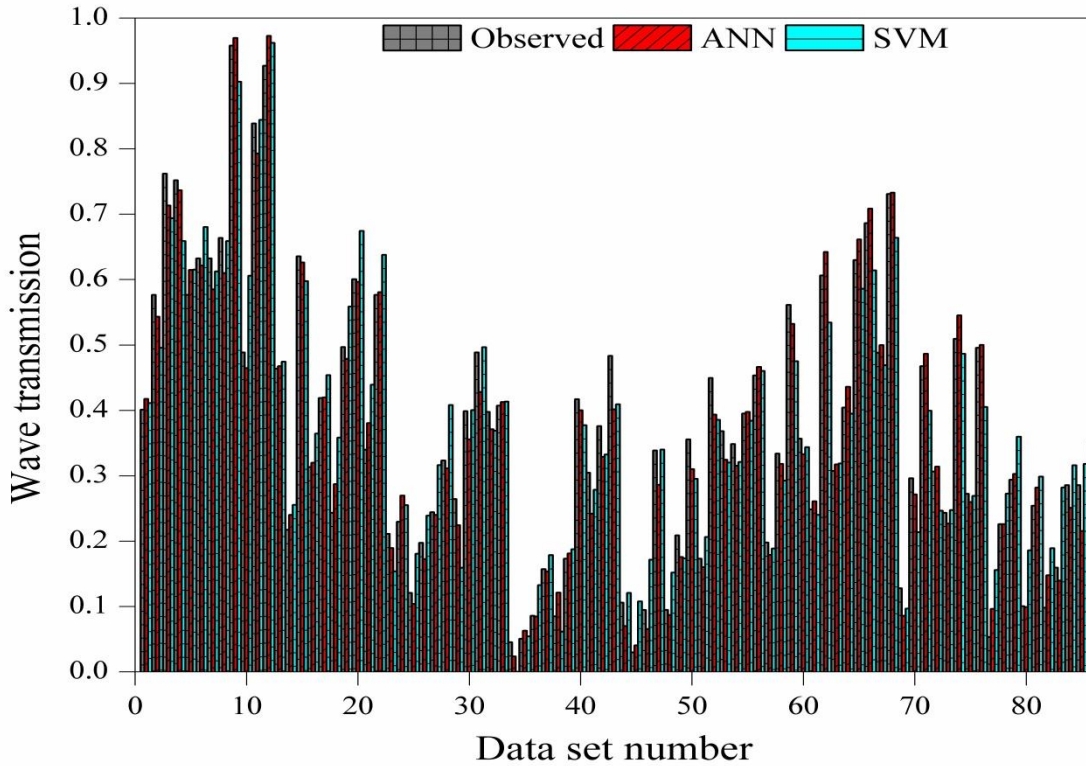


Fig. 6.26 Comparison of ANN (8-3-1) and SVM (RBF) models for wave transmission

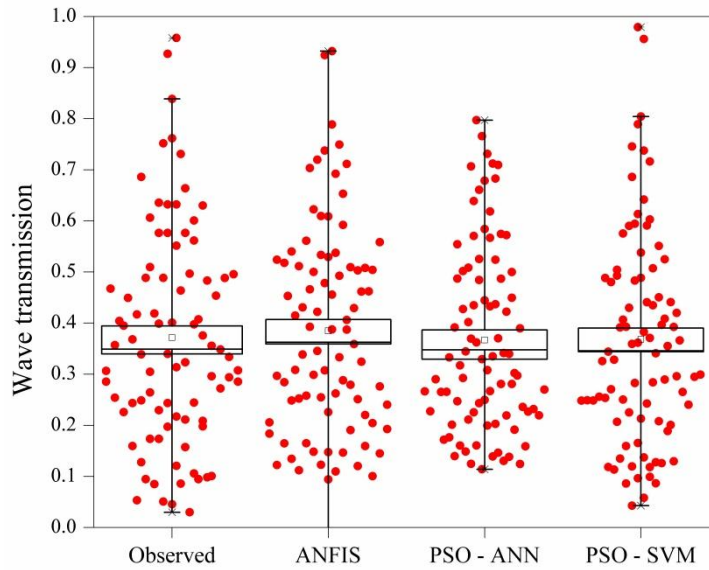


Fig. 6.27 Box-Whisker plot for wave transmission comparison of hybrid models

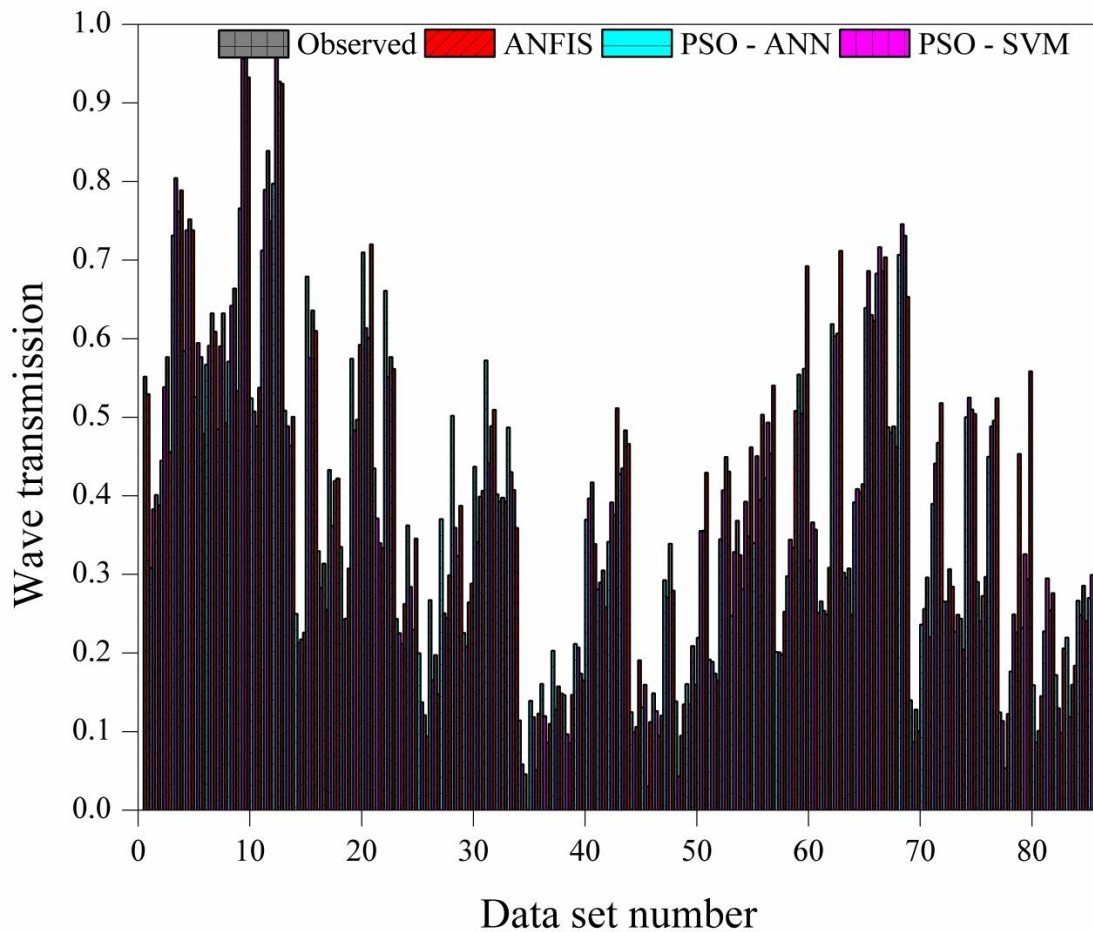


Fig. 6.28 Comparison of ANFIS (Gaussmf), PSO-ANN (8-3-1) and PSO-SVM (Polynomial) models for wave transmission

Table 6.10 Comparison of Statistical Measures of ANN, SVM, ANFIS, PSO-ANN and PSO-SVM Models for damage level (S)

Model	Training Data				Testing Data			
	CC	RMSE	SI	NSE	CC	RMSE	SI	NSE
ANN(8-5-1)	0.974	0.055	0.382	0.949	0.956	0.066	0.515	0.908
SVM (RBF)	0.954	0.0910	0.690	0.903	0.935	0.0765	0.529	0.833
ANFIS (Gaussmf)	0.99	0.0001	0.0012	0.99	0.875	0.123	0.011	0.70
PSO-ANN (8-2-1)	0.767	0.158	1.096	0.584	0.769	0.141	1.093	0.589
PSO-SVM (Polynomial)	0.961	0.071	0.493	0.916	0.941	0.088	0.669	0.843

Similarly, Figs. 6.29 and 6.30 illustrate the comparison of damage levels predicted by ANN with (8-5-1) with respect to experimental values of individual models. Similarly, Figs. 6.31 and 6.32 shows SVM with RBF kernel function, PSO-ANN with (8-2-1) and PSO-SVM with RBF kernel function with respect to experimental values and hybrid models.

ANN with (8-5-1) network outperformed all other soft computing techniques for predicting wave transmission with high CC of 0.956 and high efficiency of 0.908 with least error of 0.066 and small scatter of 0.515. Therefore, ANN with (8-5-1) network can be used as an efficient and reliable soft computing technique for predicting damage level conventional rubble mound breakwater of a tandem breakwater.

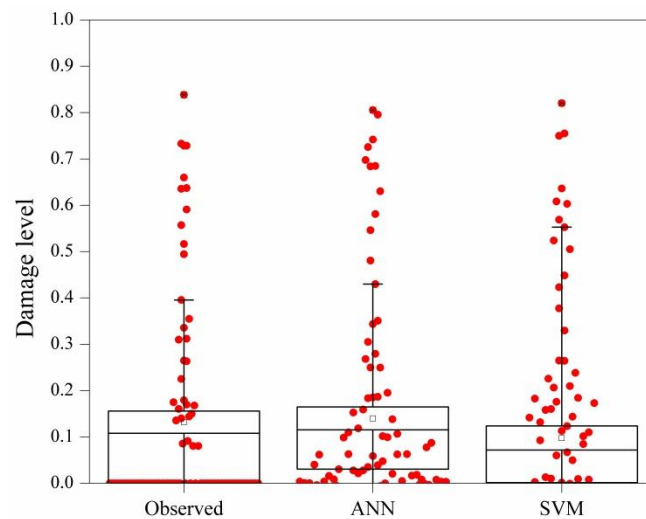


Fig. 6.29 Box-Whisker plot of damage levels comparison for individual models

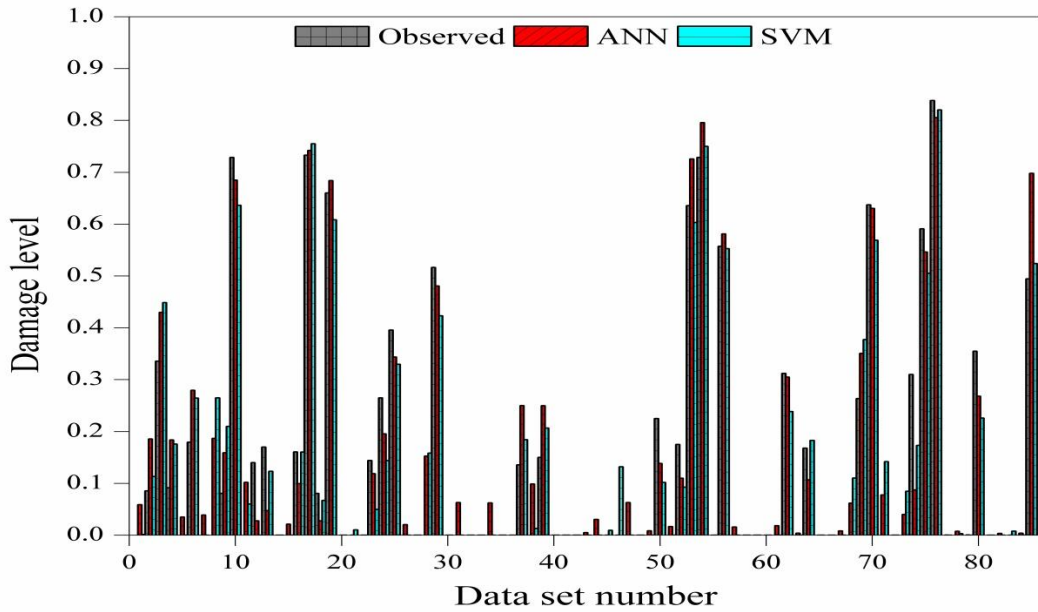


Fig. 6.30 Comparison of ANN (8-5-1) and SVM (RBF) models for damage levels

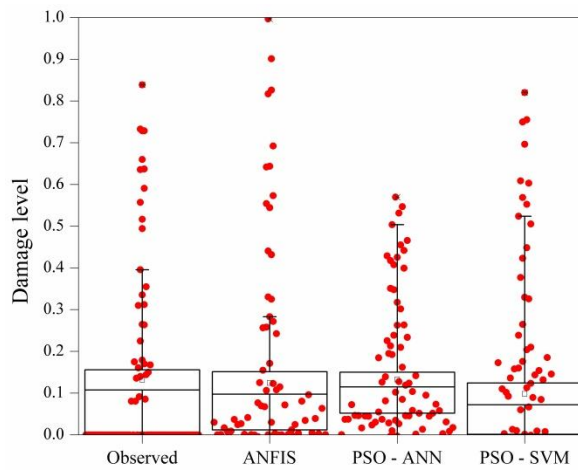


Fig. 6.31 Box-Whisker plot of damage levels comparison of hybrid models

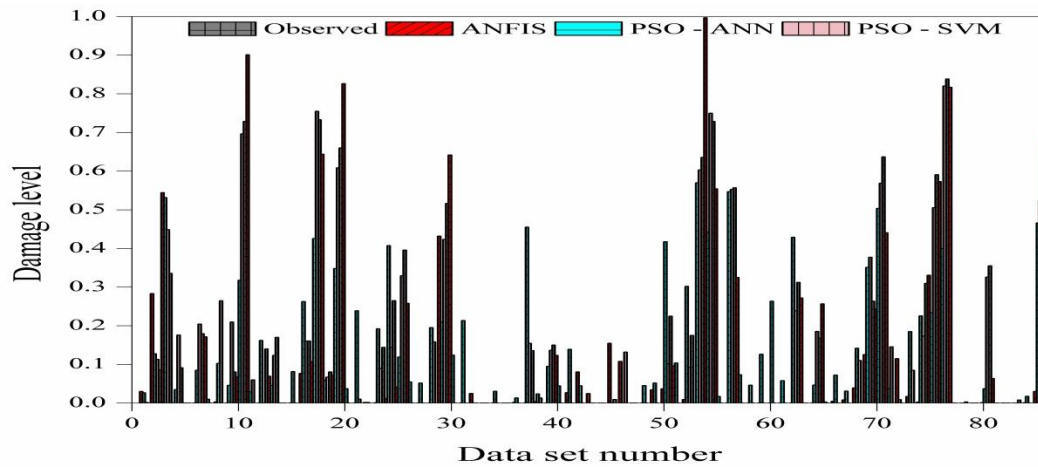


Fig. 6.32 Comparison of ANFIS (Gaussmf), PSO-ANN (8-2-1) and PSO-SVM (RBF) models for damage levels

It is observed that among the individual models ANN (8-3-1) network with high CC of 0.989 and high efficiency NSE of 0.978 and ANN (8-5-1) network with high CC of 0.956 and high efficiency NSE of 0.908 outperformed SVM with RBF in both cases. Similarly, among the hybrid soft computing techniques employed in the present study it is found that the PSO-SVM with polynomial kernel function with high CC of 0.984 and high efficiency NSE of 0.894 outperformed other hybrid techniques ANFIS (Gaussmf) and PSO-ANN with (8-3-1) network with high in case of wave transmission and PSO-SVM with RBF kernel function CC of 0.960 and high efficiency NSE of 0.843 in case of damage level of tandem breakwater. ANN and PSO-SVM models can be used as efficient and reliable techniques for prediction of wave transmission and damage level of tandem breakwater. Among all the individual and hybrid models ANN outperformed with high CC and least RMSE and less scatter and high efficiency for both the cases.

6.5.1 Summary of best model results

It is observed that ANN with 3 hidden layers with 100 epochs are sufficient to get better results from the different models. Firstly, the individual models of the ANN and SVM are tested with eight input parameters. It is observed that ANN with LM algorithm performed better compared to SVM with RBF kernel function.

The individual ANN with LM algorithm and SVM with RBF kernel function are compared to know their respective performance. ANN with LM algorithm showed best performance compared to SVM but a chance for clarification and comparison is available. Hence, in continuation hybrid models are considered for the further study. The different membership functions of the ANFIS and various numbers of hidden nodes of PSO-ANN and also different Kernel functions of PSO-SVM are compared before selecting the best technique. In case of PSO-ANN model, the number of hidden layers and epochs are optimized further before using them in the model. ANN with (8-3-1) and ANN with (8-5-1) shows better results compared to SVM with RBF kernel function. Comparing the different hybrid models, PSO-SVM with polynomial and RBF kernel function performed better than ANFIS (Gaussmf) and PSO-ANN (8-3-1) and PSO-ANN (8-2-1) models. After observing the statistical results of all the individual and hybrid soft computing techniques adopted in the present study ANN with 3 and 5 hidden neurons is found to best model for the prediction of wave transmission and damage levels of tandem breakwater.

SUMMARY AND CONCLUSIONS

7.1 SUMMARY

The development of a mathematical model to determine the transmitted wave height over a submerged reef of tandem breakwater is complex. Therefore, it is necessary for researchers to adopt the physical model study to quantitatively determine the influence of parameters on the performance of breakwaters. Physical modeling is a time consuming process, laborious, expensive and it is inconvenient for immediate needs. Hence, the soft computing techniques are adopted based on the experimental data of tandem breakwater and same are utilized for the validation of the developed AI models.

The soft computing models are built based on the data collected from the physical model study conducted on tandem breakwater in a two dimensional wave flume by Rao and Shirlal in 2004. Non-dimensional input parameters that influence the transmitted wave height (H_t/H_{tmax}) over submerged reef and damage level (S) of conventional rubble mound breakwater of tandem breakwater namely, deepwater wave steepness (H_i/gT^2), relative reef spacing (X/d), Hudson's stability number ($H_i/\Delta D_{n50}$), relative reef crest width (B/d), (B/L_o), relative reef submergence (F/H_i), relative reef crest height (h/d), relative depth (d/gT^2) are used for developing soft computing techniques.

Initially ANN (8-1-1) to ANN (8-5-1) models are developed with different algorithms using eight parameters. ANN models are developed by varying the number of hidden neurons. Here, the numbers of hidden layers are optimized to get better results. Further, SVM models with different kernel functions are developed. The individual ANN and SVM are compared to know their performance. ANN showed better performance compared to SVM but there is scope for improvement in the performance. Hence, in some hybrid models, namely ANFIS and PSO-ANN, PSO-SVM are developed and the best networks are found out. All the AI models are assessed and evaluated using model performance indicators in terms of statistical measures such as RMSE, CC, SI and NSE to find the best network.

The efficiency of the ANFIS models depend on the number of membership functions associated with each input and output data. The efficiency of the SVM model relies on the selection of best kernel function parameters (γ , d) and proper SVM parameters (C, ϵ).

It is observed from literature that there are hardly any applications of ANN, SVM, ANFIS, PSO-ANN and PSO-SVM models to study the stability of tandem breakwaters. Hence, it is decided to investigate of the applicability of ANN, SVM, ANFIS, PSO-ANN and PSO-SVM modeling approach for predicting the transmitted wave height (H_t/H_{tmax}) over a submerged reef and damage level (S) of conventional rubble mound breakwater of tandem breakwater. For this purpose the experimental data set obtained by Rao and Shirlal in 2004 on tandem breakwater using two dimensional wave flume of the Marine Structure laboratory, NITK Surathkal. The performance of the ANN, SVM, ANFIS, PSO-ANN and PSO-SVM are compared and the best model is selected based on statistical parameters.

An application of ANN, SVM, ANFIS, PSO-ANN and PSO-SVM for prediction of wave transmission over the outer submerged reef and damage level of inner conventional rubble mound breakwater are presented in the present study and the following conclusions are drawn.

7.2 CONCLUSIONS

Based on the results of the present investigations and discussion thereon, following conclusions are arrived at:

1. ANN is very successful in predicting transmitted wave height H_t/H_{tmax} . The prediction of ANN (8-3-1) model is very close to the experimental results with CC as 0.99 and the SI as 0.086 for the given data set compared to other models.
2. ANN (8-5-1) model for predicting damage level S has CC as 0.96 and SI as 0.52. Even though the CC value is good, SI value is not as good as in case of H_t/H_{tmax} prediction. This wide scatter of points is observed in the scattered plots due to the presence of more number of zero damage levels.
3. SVM with RBF kernel function gives 0.965 coefficient of correlations in the prediction of transmitted wave height over a submerged reef of tandem breakwater during testing phase with RMSE = 0.06, NSE = 0.911, SI = 0.16.

4. The SVM with RBF kernel gives CC of 0.935 in damage level prediction of conventional rubble mound breakwater of tandem breakwater during testing phase with RMSE = 0.0765, NSE = 0.83, SI = 0.529.
5. From the results obtained, it is evident that SVM with RBF kernel function gives a marginal increase in CC = 0.965 for testing and improved results, when compared to ANFIS model with Gaussian membership function for which CC=0.935 for testing data in the prediction of wave transmission (H_t/H_{tmax}) and 0.875 for damage level prediction.
6. PSO-ANN hybrid model with (8-3-1) network architecture can be considered as best network among other PSO-ANN models for predicting H_t/H_{tmax} with RMSE = 0.07, CC = 0.94, SI = 0.20 and NSE = 0.88 for testing.
7. PSO-ANN hybrid model with (8-2-1) network architecture can be considered as best network among other PSO-ANN models for predicting damage levels with RMSE = 0.14, CC = 0.77, SI = 1.10 and NSE = 0.59 for testing.
8. For the prediction of wave transmission, PSO-SVM model with polynomial kernel function gives best results with CC = 0.984, NSE = 0.968, RMSE = 0.038 and SI = 0.102 for testing. The hybrid PSO-SVM model with polynomial kernel function gives the best results for prediction of the wave transmission compared to other PSO-SVM models.
9. The best values of statistical parameters such as CC = 0.941, NSE = 0.843, RMSE = 0.088 and SI = 0.67, for testing are obtained in the case of PSO-SVM model with RBF kernel function for damage level prediction. The hybrid PSO-SVM model with RBF kernel gives the best result for damage level prediction compared to other PSO-SVM models.
10. The predicted values of the PSO-SVM model shows more proximity to actual data compared to the results of individual SVM model study, for the same data, with about 5% increase in correlation, 30% reduction in RMSE for wave transmission prediction. But the statistical parameter values do not show much variation in case of damage level prediction by PSO-SVM compared to SVM, this is due to the presence of more zero damage levels.

7.3 RECOMMENDATIONS

1. The present study recommends that ANN with (8-3-1) network can be used as efficient and reliable model and network for the prediction of wave transmission over a submerged reef and ANN with (8-5-1) network for damage level of conventional rubble mound breakwater of tandem breakwater among other individual models of SVM.
2. The present study recommends PSO-SVM with polynomial kernel function as an efficient and reliable technique to predict wave transmission over submerged reef and PSO-SVM with RBF kernel function for prediction of damage level of conventional rubble mound breakwater of tandem breakwater among other hybrid models such as ANFIS and PSO-ANN.
3. Overall recommendation of the present study is that the classical model ANN with different networks gave best results compared to all other individual and hybrid models considered in the present study. Therefore, ANN model can be used as efficient and reliable technique to predict wave transmission over a submerged reef and damage level of conventional rubble mound breakwater of tandem breakwater accurately.

7.4 LIMITATIONS OF PRESENT STUDY

- Soft computing techniques are data driven and will give the best results when sufficient experimental data is available beforehand.
- The models cannot be generalized unless similar field conditions are available. These are site specific models

7.5 SUGGESTIONS FOR FUTURE WORK

There is a scope for carrying out further research. The following suggestion may be considered for further study:

- The study can be extended to other evolutionary optimization techniques like ACO and any improvement in the efficiency of predictions can be checked.
- Alternate solver algorithms, such as ISDA and L1QP can be used in finding the initial values of parameters of the SVM model.
- Using emerging alternate novel optimization techniques like differential evolution scatter search etc., in hybridizing the SVM model.

• REFERENCES

- Ahmadi, M. A., Shadizadeh, S. R., & Hasanvand, M. (2011). Neural network based stochastic particle swarm optimization for prediction of minimum miscible pressure. *Int J Comput Appl*, 34(1), 15-19.
- Ahrens, J. P. (1984). "Reef type breakwaters." *Proceedings of Conference on Coastal Engineering*, pp 2648 – 2662.
- Ahrens, J. P. (1987). Technical Report CERC-87-17 Characteristics of Reef Breakwaters. WES Department of the Army, Corps of Engineers. Vicksburg, MS.
- Allsop, N. W. H., Herbert, D. M., & Davis, J. P. (1991, March). Single layer armour units for breakwaters: their design and hydraulic performance. In *Proc Symp Developments in Coastal Engineering*, University of Bristol.
- Allsop, W., & Herbert, D. M. (1991). Single layer armour units for breakwaters. Monograph Technical Report, SR 295, HR Wallingford, UK
- Armono, H. D., & Hall, K. R. (2003, June). Wave transmission on submerged breakwaters made of hollow hemispherical shape artificial reefs. In *Canadian Coastal Conference* (pp. 313-322).
- Baird, W. F., & Hall, K. R. (1985). The design of breakwaters using quarried stones. In *Coastal Engineering 1984* (pp. 2580-2591).
- Balas, C. E., Koç, M. L., & Tür, R. (2010). Artificial neural networks based on principal component analysis, fuzzy systems and fuzzy neural networks for preliminary design of rubble mound breakwaters. *Applied Ocean Research*, 32(4), 425-433.
- Balas, C. E., Koç, M. L., & Tür, R. (2010). Artificial neural networks based on principal component analysis, fuzzy systems and fuzzy neural networks for preliminary design of rubble mound breakwaters. *Applied Ocean Research*, 32(4), 425-433.
- Basheer, I. A., & Hajmeer, M. (2000). Artificial neural networks: fundamentals, computing, design, and application. *Journal of microbiological methods*, 43(1), 3-31.
- Bethani, A., Bevan, A. J., Hays, J., & Stevenson, T. J. (2016, October). Support Vector Machines and Generalisation in HEP. In *Journal of Physics: Conference Series* (Vol. 762, No. 1, p. 012052). IOP Publishing.

- Bruun, P., & Günbak, A. R. (1977). New design principles for rubble mound structures. In *Coastal Engineering*, 2429-2473.
- Burcharth, H. F., & Hughes, S. (2000). *Coastal Engineering Manual, Fundamentals of Design*. Chapter 5, Part VI. To be published by Coastal Engineering Research Center, Waterways Experiment Station. US Army Corps of Engineers, Vicksburg, USA.
- Carver, R. D., & Davidson, D. D. (1982). Breakwater Stability–Breaking Wave Data. In *Coastal Engineering 1982* (pp. 2107-2128).
- Castro, A., Carballo, R., Iglesias, G., & Rabuñal, J. R. (2014). Performance of artificial neural networks in nearshore wave power prediction. *Applied Soft Computing*, 23, 194-201.
- Chakrabarti, S. K. (1996). Experimental techniques in offshore engineering.
- Chang, H. K., & Lin, L. C. (2006). Multi-point tidal prediction using artificial neural network with tide-generating forces. *Coastal Engineering*, 53(10), 857-864.
- Chau, K. W. (2006). Particle swarm optimization training algorithm for ANNs in stage prediction of Shing Mun River. *Journal of hydrology*, 329(3), 363-367.
- Cherkassky, V., & Ma, Y. (2004). Practical selection of SVM parameters and noise estimation for SVM regression. *Neural networks*, 17(1), 113-126.
- Cornett, A., Mansard, E., & Funke, E. (1993). Wave Transformation and Load Reduction Using a Small Tandem Reef Breakwater–Physical Model Tests. In *Ocean Wave Measurement and Analysis* (pp. 1008-1023). ASCE.
- Cortes, C., & Vapnik, V. (1995). Support-vector networks. *Machine learning*, 20(3), 273-297.
- Cox, J. C., & Clark, G. R. (1992). Design Development of a Tandem Breakwater System for Hammond Indiana. *Proceedings of Coastal structures and breakwaters*, Thomas Telford, London, 111-121.
- Cristianini, N., & Shawe-Taylor, J. (2000). *An introduction to support vector machines and other kernel-based learning methods*. Cambridge university press.
- Danel, P. (1953). Tetrapods. *Coastal Engineering Proceedings*, 1(4), 28.
- Dattatri, J., Raman, H., & Shankar, N. J. (1978). Performance characteristics of submerged breakwaters. In *Coastal Engineering 1978* (pp. 2153-2171).

- Deo, M. C., & Jagdale, S. S. (2003). Prediction of breaking waves with neural networks. *Ocean Engineering*, 30(9), 1163-1178.
- Deo, M. C., & Kumar, N. K. (2000). Interpolation of wave heights. *Ocean Engineering*, 27(9), 907-919.
- Deo, M. C., Jha, A., Chaphekar, A. S., & Ravikant, K. (2001). Neural networks for wave forecasting. *Ocean Engineering*, 28(7), 889-898.
- Duan, W. Y., Han, Y., Huang, L. M., Zhao, B. B., & Wang, M. H. (2016). A hybrid EMD-SVR model for the short-term prediction of significant wave height. *Ocean Engineering*, 124, 54-73.
- Edge, B. L., & Magoon, O. T. (1979, March). A review of recent damages to coastal structures. In *Coastal Structures' 79* (pp. 333-349). ASCE.
- Ergin, A., Günbak, A. R., & Yanmaz, A. M. (1989). Rubble-mound breakwaters with S-shape design. *Journal of waterway, port, coastal, and ocean engineering*, 115(5), 579-593.
- Franco, L. (2001). New Italian experience in the design of maritime structures. In *International Workshop on Advanced design of maritime structures in the 21st century* (pp. 76-85).
- Gadre, M. R., Poonawala, I. Z., & Kudale, M. D. (1985). Design of reclamation bunds for Madras port. In *Proceedings of first National Conference on Dock and Harbour Engineering*, Dec, IIT Bombay (pp. B113-B123).
- Gadre, M. R., Poonawala, I. Z., & Kudale, M. D. (1992). Stability of rock armour protection for submarine pipelines. In *Proceedings of 8th Congress of Asian and Pacific Division of IAHR, CWPRS, India* (Vol. 3, pp. D-149).
- Garde, M. R., Poonawala, I. Z., Kale, A. G., & Kudale, M. D. (1989). Rehabilitation of Rubble Mound Breakwaters. In *Proceedings of the Third National Conference on Dock and Harbor Engineering*, KREC, Surathkal (1), 387-394.
- Garg, V., & Jothiprakash, V. (2013). Evaluation of reservoir sedimentation using data driven techniques. *Applied Soft Computing*, 13(8), 3567-3581.
- Gaur, S., & Deo, M. C. (2008). Real-time wave forecasting using genetic programming. *Ocean Engineering*, 35(11), 1166-1172.

- Gaur, S., Ch, S., Graillet, D., Chahar, B. R., & Kumar, D. N. (2013). Application of artificial neural networks and particle swarm optimization for the management of groundwater resources. *Water resources management*, 27(3), 927-941.
- Ghasemi, H., Kollahdoozan, M., Pena, E., Ferreras, J., & Figuero, A. (2017). A new hybrid ANN model for evaluating the efficiency of π -type floating breakwater. *Coastal Engineering Proceedings*, 1(35), 25.
- Ghasemi, H., Kollahdoozan, M., Pena, E., Ferreras, J., & Figuero, A. (2017). A new hybrid ANN model for evaluating the efficiency of π -type floating breakwater. *Coastal Engineering Proceedings*, 1(35), 25.
- Goda, Y. (1996). Wave damping characteristics of longitudinal reef system. *Advances in coastal structures and breakwaters*, 192-207.
- Groeneveld, R. L., Mol, A., & Nieuwenhuys, E. H. (1985). Rehabilitation Methods for Damaged Breakwaters. In *Coastal Engineering 1984* (pp. 2467-2486).
- Günaydın, K. (2008). The estimation of monthly mean significant wave heights by using artificial neural network and regression methods. *Ocean Engineering*, 35(14), 1406-1415.
- Gunn, S. R. (1998). Support vector machines for classification and regression. *ISIS technical report*, 14, 85-86.
- Hagan, M. T., & Menhaj, M. B. (1994). Training feedforward networks with the Marquardt algorithm. *IEEE transactions on Neural Networks*, 5(6), 989-993.
- Hagan, M. T., & Menhaj, M. B. (1994). Training feedforward networks with the Marquardt algorithm. *IEEE transactions on Neural Networks*, 5(6), 989-993.
- Hagra, M. A. (2013). Prediction of Hydrodynamic Coefficients of Permeable Paneled Breakwater using Artificial Neural Networks. *International Journal of Engineering Science and Technology*, 5(8), 1616.
- Han, D., Chan, L., & Zhu, N. (2007). Flood forecasting using support vector machines. *Journal of hydroinformatics*, 9(4), 267-276.
- Harish, N., Mandal, S., Rao, S., & Patil, S. G. (2015). Particle Swarm Optimization based support vector machine for damage level prediction of non-reshaped berm breakwater. *Applied Soft Computing*, 27, 313-321.

- Harris, L. E. (2003). Artificial reef structures for shoreline stabilization and habitat enhancement. In Proceedings of the 3rd International Surfing Reef Symposium, (pp.176-178).
- Hashemi, M. R., Ghadampour, Z., & Neill, S. P. (2010). Using an artificial neural network to model seasonal changes in beach profiles. *Ocean Engineering*, 37(14), 1345-1356.
- Hegde, A. V., & Samaga, B. R. (1996). Study on the Effect of Core Porosity on Rubble Mound Breakwater'. In Proceedings of Tenth Congress of the Asian and Pacific Regional Division of the International Association for Hydraulic Research, IAHR, 287.
- Hettiarachchi, S., Franco, L., & Materazzi, A. L. (1991). Wave induced loads on single layer hollow block armour units.
- Hornik, K., Meyer, D., & Karatzoglou, A. (2006). Support vector machines in R. *Journal of statistical software*, 15(9), 1-28.
- Hudson, R. Y. (1959). Laboratory investigation of rubble-mound breakwaters. Reprint of the original paper as published in the *Journal of the Waterways and Harbors Division of ASCE*, proceedings paper 2171.
- Hughes, S. A. (1993). *Physical models and laboratory techniques in coastal engineering* (Vol. 7). World Scientific.
- Iglesias, G., Castro, A., & Fraguera, J. A. (2010). Artificial intelligence applied to floating boom behavior under waves and currents. *Ocean Engineering*, 37(17), 1513-1521.
- Isaacson, M. (1991). "Measurement of regular wave reflection." *Journal Waterways, Port, Coastal and Ocean Engineering*, ASCE, 117, 553-569.
- Jang, J. S. (1993). ANFIS: adaptive-network-based fuzzy inference system. *IEEE transactions on systems, man, and cybernetics*, 23(3), 665-685.
- Johnson, R. R., Mansard, E. P. D., & Ploeg, J. (1978). Effects of wave grouping on breakwater stability. In *Coastal Engineering*, 2228-2243.
- Johnson, R. R., Mansard, E. P. D., & Ploeg, J. (1978). Effects of wave grouping on breakwater stability. In *Coastal Engineering 1978* (pp. 2228-2243).
- Kakinuma, T. (2003). Nonlinear interaction of surface and internal waves with very large floating or submerged structures. In *Proceedings of Civil Engineering in the Ocean* (Vol. 19, pp. 583-588). Japan Society of Civil Engineers.

- Kalanaki, M., & Soltani, J. (2013). Performance assessment among hybrid algorithms in tuning SVR parameters to predict pipe failure rates. *Advances in Computer Science: an International Journal*, 2(5), 40-46.
- Kao, J. S., & Hall, K. R. (1991). Trends in stability of dynamically stable breakwaters. In *Coastal Engineering 1990*(pp. 1730-1741).
- Kazeminezhad, M. H., Etemad-Shahidi, A., & Mousavi, S. J. (2005). Application of fuzzy inference system in the prediction of wave parameters. *Ocean Engineering*, 32(14), 1709-1725.
- Kecman, V. (2001). *Learning and soft computing: support vector machines, neural networks, and fuzzy logic models*. MIT press.
- Kennedy, R. C. (1942). Eberha~ Particle swarm optimization. In *Proc, IEEE Inf1 Conf on Neural Networks. IV (Vol. 1948)*.
- Kim, D. H., & Park, W. S. (2005). Neural network for design and reliability analysis of rubble mound breakwaters. *Ocean engineering*, 32(11), 1332-1349.
- Kim, D. H., Kim, Y. J., & Hur, D. S. (2014). Artificial neural network based breakwater damage estimation considering tidal level variation. *Ocean Engineering*, 87, 185-190.
- Kim, D., Kim, D. H., Chang, S., Lee, J. J., & Lee, D. H. (2011). Stability number prediction for breakwater armor blocks using Support Vector Regression. *KSCE Journal of Civil Engineering*, 15(2), 225-230.
- Kobayashi, N., & Jacobs, B. K. (1985). Riprap stability under wave action. *Journal of waterway, port, coastal, and ocean engineering*, 111(3), 552-566.
- Koç, M. L., & Balas, C. E. (2013). Reliability analysis of a rubble mound breakwater using the theory of fuzzy random variables. *Applied Ocean Research*, 39, 83-88.
- Kosko, B., & Mitaim, S. (2003). Stochastic resonance in noisy threshold neurons. *Neural networks*, 16(5), 755-761.
- Lee, T. L., Tsai, C. P., Lin, H. M., & Fang, C. J. (2009). A combined thermographic analysis—Neural network methodology for eroded caves in a seawall. *Ocean engineering*, 36(15), 1251-1257.
- Liang, S. X., Li, M. C., & Sun, Z. C. (2008). Prediction models for tidal level including strong meteorologic effects using a neural network. *Ocean Engineering*, 35(7), 666-675.

- Londhe, S. N. (2008). Soft computing approach for real-time estimation of missing wave heights. *Ocean Engineering*, 35(11), 1080-1089.
- Londhe, S. N., & Deo, M. C. (2003). Wave tranquility studies using neural networks. *Marine Structures*, 16(6), 419-436.
- Mahjoobi, J., & Mosabbeb, E. A. (2009). Prediction of significant wave height using regressive support vector machines. *Ocean Engineering*, 36(5), 339-347.
- Makarynskyy, O. (2004). Improving wave predictions with artificial neural networks. *Ocean Engineering*, 31(5), 709-724.
- Makarynskyy, O., Pires-Silva, A. A., Makarynska, D., & Ventura-Soares, C. (2005). Artificial neural networks in wave predictions at the west coast of Portugal. *Computers & Geosciences*, 31(4), 415-424.
- Makris, C. V., & Memos, C. D. (2007, January). Wave transmission over submerged breakwaters: Performance of formulae and models. In *The Seventeenth International Offshore and Polar Engineering Conference*. International Society of Offshore and Polar Engineers.
- Malekmohamadi, I., Bazargan-Lari, M. R., Kerachian, R., Nikoo, M. R., & Fallahnia, M. (2011). Evaluating the efficacy of SVMs, BNs, ANNs and ANFIS in wave height prediction. *Ocean Engineering*, 38(2), 487-497.
- Mandal, S., & Prabakaran, N. (2006). Ocean wave forecasting using recurrent neural networks. *Ocean engineering*, 33(10), 1401-1410.
- Mandal, S., Rao, S., & Harish, N. (2012). Damage level prediction of non-reshaped berm breakwater using ANN, SVM and ANFIS models. *International Journal of Naval Architecture and Ocean Engineering*, 4(2), 112-122.
- Mandal, S., Rao, S., Manjunath, Y. R., & Kim, D. H. (2007). Stability analysis of rubblemound breakwater using ANN. *Proc., Indian National Conference on Harbour and Ocean Engineering, INCHOE, National Institute of Technology Karnataka, Surathkal, India*, 551-560.
- Mandal, S., Rao, S., Manjunath, Y. R., & Kim, D. H. (2007). Stability analysis of rubblemound breakwater using ANN.
- Mani, J. S., & Jayakumar, S. (1995). Wave transmission by suspended pipe breakwater. *Journal of waterway, port, coastal, and ocean engineering*, 121(6), 335-338.

- Manu, Rao, S., Shirlal, K. G., Prashanth, J., & Rao, K. B. (2011). Physical Model Studies on Stability of Concrete Armoured Breakwaters. *ISH Journal of Hydraulic Engineering*, 17(sup1), 51-60.
- Mase, H., & Kitano, T. (1999). Prediction model for occurrence of impact wave force. *Ocean Engineering*, 26(10), 949-961.
- Mase, H., Sakamoto, M., & Sakai, T. (1995). Neural network for stability analysis of rubble-mound breakwaters. *Journal of waterway, port, coastal, and ocean engineering*, 121(6), 294-299.
- Masters, T. (1995). *Advanced algorithms for neural networks: a C++ sourcebook* (Vol. 97). New York: Wiley.
- Minqiang, P., Dehuai, Z., & Gang, X. U. (2010). Temperature prediction of hydrogen producing reactor using SVM regression with PSO. *Journal of computers*, 5(3), 388-393.
- Mlybari, E. A., Elbisy, M. S., Alshahri, A. H., & Albarakati, O. M. The Use Support Vector Machine and Back Propagation Neural Network for Prediction of Daily Tidal Levels along the Jeddah Coast, Saudi Arabia. *World Academy of Science, Engineering and Technology, International Journal of Mathematical, Computational, Physical, Electrical and Computer Engineering*, 8(1), 13-18.
- Msiza, I. S., Nelwamondo, F. V., & Marwala, T. (2008). Water demand prediction using artificial neural networks and support vector regression.
- Munireddy, M. G. (2004). Wave pressure reduction on vertical seawalls/caissons due to an offshore breakwater.
- Muni-Reddy, M. G., & Neelamani, S. (2006). Wave interaction with caisson defenced by an offshore low-crested breakwater. *Journal of Coastal Research*, 1767-1770.
- Naithani, R., & Deo, M. C. (2005). Estimation of wave spectral shapes using ANN. *Advances in Engineering Software*, 36(11), 750-756.
- Neelamani, S., Sumalatha, B. V., & Rao Narasimhan, S. (2002). Hydrodynamics of seaward defenced by a detached breakwater. In *Conference on Hydraulics, Water resources, and Ocean Engineering, HYDRO* (pp. 244-249).
- Nikelshpur, D., & Tappert, C. (2013). Using particle swarm optimization to pre-train artificial neural networks: selecting initial training weights for feed-forward

back-propagation neural networks. Proceedings of the Student-Faculty Research Day, CSIS, Pace University, New York, NY, USA, 3.

- Nizam, Y. N. (1996). Artificial reef as an alternative beach protection. In Proceedings of Tenth Congress of Asian and Pacific Division of IAHR, Langkawi, Malaysia, (pp.422-430).
- Owen, M. W., & Briggs, M. G. (1986). Limitations of modelling. In Developments in Breakwaters (pp. 91-101). Thomas Telford Publishing.
- Özger, M. (2011). Prediction of ocean wave energy from meteorological variables by fuzzy logic modeling. *Expert systems with applications*, 38(5), 6269-6274.
- Park, S. H., Lee, S. O., Jung, T. H., & Cho, Y. S. (2007). Effects of submerged structure on rubble-mound breakwater: Experimental study. *KSCE Journal of Civil Engineering*, 11(6), 277-284.
- Park, S. H., Lee, S. O., Jung, T. H., & Cho, Y. S. (2007). Effects of submerged structure on rubble-mound breakwater: Experimental study. *KSCE Journal of Civil Engineering*, 11(6), 277-284.
- Patil, S. G., Mandal, S., Hegde, A. V., & Alavandar, S. (2011). Neuro-fuzzy based approach for wave transmission prediction of horizontally interlaced multilayer moored floating pipe breakwater. *Ocean Engineering*, 38(1), 186-196.
- Patil, S. G., Mandal, S., Hegde, A. V., & Alavandar, S. (2011). Neuro-fuzzy based approach for wave transmission prediction of horizontally interlaced multilayer moored floating pipe breakwater. *Ocean Engineering*, 38(1), 186-196.
- Pilarczyk, K. W., & Zeidler, R. B. (1996). Offshore breakwaters and shore evolution control.
- Poonawala, I. Z., Kudale, M. D., & Purohit, A. (2001, December). Wave transmission through rubble-mound breakwater. In *International Conference in Ocean Engineering- 2001* (p. 5).
- Priest, M. S., Pugh, J. W., & Singh, R. (1965). Seaward profile for rubble mound breakwaters. In *Coastal Engineering 1964*(pp. 553-559).
- Radhika, Y., & Shashi, M. (2009). Atmospheric temperature prediction using support vector machines. *International journal of computer theory and engineering*, 1(1), 55.

- Rajasekaran, S., Gayathri, S., & Lee, T. L. (2008). Support vector regression methodology for storm surge predictions. *Ocean Engineering*, 35(16), 1578-1587.
- Rao, S & Shirlal, K. G. (2004). Studies on the stability of conventional rubble mound breakwater defenced by a seaward submerged reef. R&D project report, INCHMinistry of Water Resources, GOI, New Delhi, pp.250.
- Rao, S., & Mandal, S. (2005). Hindcasting of storm waves using neural networks. *Ocean Engineering*, 32(5), 667-684.
- Rao, S., Mandal, S., & Prabakaran, N. (2001). Wave forecasting in near real time basis by neural network.
- Reynolds, C. W. (1987). Flocks, herds and schools: A distributed behavioral model. *ACM SIGGRAPH computer graphics*, 21(4), 25-34.
- Roy, A., Dutta, D., & Choudhury, K. (2013). Training artificial neural network using particle swarm optimization algorithm. *International Journal of Advanced Research in Computer Science and Software Engineering*, 3(3).
- Seelig, W. N. (1979). Effects of breakwaters on waves: Laboratory test of wave transmission by overtopping. In *Proc. Conf. Coastal Structures, 1979 (Vol. 79, No. 2, pp. 941-961)*.
- Shirlal, K. G., & Rao, S. (2003). Laboratory studies on the stability of tandem breakwater. *ISH Journal of Hydraulic Engineering*, 9(1), 36-45.D
- Shirlal, K. G., & Rao, S. (2007). Ocean wave transmission by submerged reef-A physical model study. *Ocean engineering*, 34(14), 2093-2099.
- Shirlal, K. G., & Rao, S. (2008). Performance of a submerged reef--a physical model study. *International Journal of Ecology & Development*, 11, 90-99.
- Shirlal, K. G., & Rao, S. (2008). Performance of a submerged reef--a physical model study. *International Journal of Ecology & Development*, 11, 90-99.
- Smith, D. A. X., Warner, P. S., Sorensen, R. M., Nurse, L. A., & Atherley, K. A. (1996). Submerged-crest breakwater design. In *Advances in coastal structures and breakwaters (pp. 208-219)*. Thomas Telford Publishing.
- Smola, A. J. (1996). Regression estimation with support vector learning machines (Doctoral dissertation, Master's thesis, Technische Universität München).

- Smola, A. J., & Schölkopf, B. (2004). A tutorial on support vector regression. *Statistics and computing*, 14(3), 199-222.
- Sudheer, K. P., & Jain, S. K. (2003). Radial basis function neural network for modeling rating curves. *Journal of Hydrologic Engineering*, 8(3), 161-164.
- Swingler, K. (1996). *Applying neural networks: a practical guide*. Morgan Kaufmann.
- Sylaios, G., Bouchette, F., Tsihrintzis, V. A., & Denamiel, C. (2009). A fuzzy inference system for wind-wave modeling. *Ocean Engineering*, 36(17), 1358-1365.
- Takinuma, T. (2003). "Nonlinear interaction of surface and internal waves with very large floating or submerged structures", *Scientific Journal of Japan Science & Technology information Aggregator, Electronic*, 117-126.
- Tomasicchio, G. R., & D'Alessandro, F. (2013). Wave energy transmission through and over low crested breakwaters. *Journal of Coastal Research*, 65(sp1), 398-403.
- Tripathy, A. K., Mohapatra, S., Beura, S., & Pradhan, G. (2011). Weather Forecasting using ANN and PSO. *International J. Scientific & Eng. Res*, 2, 1-5.
- Tsai, C. P., Chen, H. B., & Yu, C. H. (2010, January). Wave Transformation between a Submerged Breakwater and a Seawall. In *The Twentieth International Offshore and Polar Engineering Conference*. International Society of Offshore and Polar Engineers.
- Tseng, C. M., Jan, C. D., Wang, J. S., & Wang, C. M. (2007). Application of artificial neural networks in typhoon surge forecasting. *Ocean Engineering*, 34(11), 1757-1768.
- Türker, U. (2014). Excess energy approach for wave energy dissipation at submerged structures. *Ocean Engineering*, 88, 194-203.
- Vairappan, C., Tamura, H., Gao, S., & Tang, Z. (2009). Batch type local search-based adaptive neuro-fuzzy inference system (ANFIS) with self-feedbacks for time-series prediction. *Neurocomputing*, 72(7), 1870-1877.
- Van de Kreeke, J. (1969). Damage function of rubble-mound breakwaters. *Journal of Waterways and Harbors Division*. 95 Aug.

- Van der Meer, J. W. (1988). Deterministic and probabilistic design of breakwater armor layers. *Journal of Waterway, Port, Coastal, and Ocean Engineering*, 114(1), 66-80.
- Van der Meer, J. W. (1992). Stability of the seaward slope of berm breakwaters. *Coastal Engineering*, 16(2), 205-234.
- Van der Meer, J. W., & Daemen, I. F. (1994). Stability and wave transmission at low-crested rubble-mound structures. *Journal of waterway, port, coastal, and ocean engineering*, 120(1), 1-19.
- Van der Meer, J. W., & Daemen, I. F. (1994). Stability and wave transmission at low-crested rubble-mound structures. *Journal of waterway, port, coastal, and ocean engineering*, 120(1), 1-19.
- Van der Meer, J. W., & Pilarczyk, K. W. (1985). Stability of rubble mound slopes under random wave attack. In *Coastal Engineering 1984* (pp. 2620-2634).
- Van der Meer, J. W., Briganti, R., Zanuttigh, B., & Wang, B. (2005). Wave transmission and reflection at low-crested structures: Design formulae, oblique wave attack and spectral change. *Coastal Engineering*, 52(10), 915-929.
- Van der Meer, J. W., d'Agremond, K., & Gerding, E. (1996). Toe structure stability of rubble mound breakwaters. In *Proceedings of the Advances in Coastal Structures and Breakwaters Conference* (pp. 308-321).
- Van Gent, M. R., van den Boogaard, H. F., Pozueta, B., & Medina, J. R. (2007). Neural network modelling of wave overtopping at coastal structures. *Coastal Engineering*, 54(8), 586-593.
- Vapnik, V. (1995). *The nature of statistical learning theory* Springer New York Google Scholar.
- Vapnik, V. N. (1999). An overview of statistical learning theory. *IEEE transactions on neural networks*, 10(5), 988-999.
- Wilamowski, B. M., Iplikci, S., Kaynak, O., & Efe, M. O. (2001). An algorithm for fast convergence in training neural networks. In *Neural Networks, 2001. Proceedings. IJCNN'01. International Joint Conference on* (Vol. 3, pp. 1778-1782). IEEE.
- Xi, Z., Zhang, Y., & Zhu, C. (2012). Application of PSO-neural network model in prediction of groundwater level in Handan City. *Adv Inf Sci Serv Sci*, 4(6), 177-183.

- Yagci, O., Mercan, D. E., Cigizoglu, H. K., & Kabdasli, M. S. (2005). Artificial intelligence methods in breakwater damage ratio estimation. *Ocean Engineering*, 32(17), 2088-2106.
- Yin, J. C., Wang, N. N., & Hu, J. Q. (2015). A hybrid real-time tidal prediction mechanism based on harmonic method and variable structure neural network. *Engineering Applications of Artificial Intelligence*, 41, 223-231.
- Zamani, A., Solomatine, D., Azimian, A., & Heemink, A. (2008). Learning from data for wind–wave forecasting. *Ocean Engineering*, 35(10), 953-962.
- Zanaganeh, M., Mousavi, S. J., & Shahidi, A. F. E. (2009). A hybrid genetic algorithm–adaptive network-based fuzzy inference system in prediction of wave parameters. *Engineering Applications of Artificial Intelligence*, 22(8), 1194-1202.
- Zanuttigh, B., Formentin, S. M., & Briganti, R. (2013). A neural network for the prediction of wave reflection from coastal and harbor structures. *Coastal engineering*, 80, 49-67.
- Zwamborn, J. A. (1979, March). Analysis of causes of damage to Sines breakwater. In *Coastal Structures' 79* (pp. 422-441). ASCE.

PUBLICATIONS

INTERNATIONAL AND NATIONAL JOURNALS

1. **Kuntoji, G. S.,** Rao, S., Manu & Mandal, S (2017). Performance evaluation of ANFIS and SVM Model in Prediction of Wave Transmission over Submerged Reef of Tandem Breakwater. *International Journal of Ecology & Development*, 32(2), 141-155.
2. **Kuntoji, G. S.,** Rao, S., & Mandal, S (2017). “Application of Support Vector Machine Technique for Damage Level Prediction of Tandem Breakwater”. *International Journal of Earth Sciences and Engineering*, 10(3), 633-638, ISSN 0974-5904.
3. **Geetha Kuntoji,** Subba Rao and Manu (2018). “Prediction of Wave transmission over Submerged Reef of Tandem Breakwater Using PSO-ANN and PSO-SVM Techniques.” *ISH Journal of Hydraulic Engineering, Taylor & Francis Publication*.
4. **Geetha Kuntoji,** Subba Rao, Manu and Eluru Nava Bharath Reddy. (2017). Prediction of damage level of inner conventional rubble mound breakwater of Tandem breakwater using Swarm Intelligence based Neural Network (PSO-ANN) approach. (**Scopus indexed, Springer publication**)

INTERNATIONAL CONFERENCES

1. **Geetha Kuntoji,** Subba Rao and Manu. (2018) “Prediction of Wave transmission over an outer submerged reef of Tandem breakwater using RBF based Support Vector Regression technique.” *4th International Conference in Ocean Engineering (ICOE 2018)*, Chennai, India.
2. **Geetha Kuntoji,** Subba Rao, Manu and Eluru Nava Bharath Reddy. (2017) “Prediction of damage level of inner conventional rubble mound breakwater of Tandem breakwater using Swarm Intelligence based Neural Network (PSO-ANN) approach.” *7th International Conference. Soft Computing for Problem Solving*

(SocProS-2017), held during December 23-24, 2017 at Indian Institute of Technology Bhubaneswar, Bhubaneswar, India (**Received Best paper Award**).

3. **Geetha Kuntoji**, Subba Rao, Manu and Sukomal Mandal. (2016). “Prediction of Wave Transmission over Submerged Reef of Tandem breakwater using Support Vector Machine.” *Proceedings of 21st International Conference on Hydraulics, Water Resources and Coastal Engineering- HYDRO 2016*, CWPRS Khadakwasla, Pune, Maharashtra, 8th -10th December, 2016
4. J. S Jithin, **Geetha Kuntoji**, Manu, Subba Rao and S. Mandal. (2016). “A Study on Submerged Reef using SVM Technique”, *Proceedings of 10th International Symposium on Lowland Technology ISLT-2016*, IALT, NITK Surathkal and ILMR, Japan, NITK Surathkal, Mangalore, India, pp 404 - 408.
5. J. S Jithin, **Geetha Kuntoji**, Subba Rao, Manu and S. Mandal. (2016). “Prediction of Transmitted Wave Height of Tandem Breakwater using Support Vector Regression”, *Proceedings of 20th International Conference on Emerging Trends in Engineering ICETE-2016*, held at NMAM Institute of Technology, NITTE 12th to 13th May 2016.
6. Nava Bharath Reddy, **Geetha Kuntoji**, Subba Rao, Manu and S. Mandal. (2016). “Prediction of Wave Transmission using ANN for Submerged Reef of Tandem Breakwater”, *Proceedings of 20th International Conference on Emerging Trends in Engineering ICETE-2016*, held at NMAM Institute of Technology, NITTE 12th to 13th May 2016.
7. **Geetha Kuntoji**, Subba Rao and Manu. (2015). “Prediction of Wave Transmission over Submerged Breakwater using Soft computing Techniques.” *Proceedings of 20th International Conference on “Hydraulics, Water Resources, Coastal and Environmental Engineering”- HYDRO-2015*, 17st to 19th December, 2015 IIT Roorkee, India.

RESUME

Name : Geetha S Kuntoji
Date of Birth : 05.03.1987
Address : C/o, S. B. Kuntoji
(Retd KSRTC Conductor)
Sangameshwarnagar,
Muddebihal Post,
Bijapur Dist-586212



Mobile : +91-7204858053
E-mail : geeta.kuntoji@gmail.com
Qualifications : B.E (Civil Engineering),
M.Tech (Marine Structures)
Publications :
International journals : 4
International conferences : 7